MATHEMATICAL MODEL AND OPTIMAL CONTROL ANALYSIS OF COFFEE BERRY DISEASE

Abdisa Shiferaw Melese

A Dissertation Submitted to the Department of Applied Mathematics,
School of Applied Natural Science

Presented in Partial Fulfillment of the Requirements for the Degree of Doctor of Philosophy
in Applied Mathematics

Office of Graduate Studies
Adama Science and Technology University

June, 2022
Adama, Ethiopia

MATHEMATICAL MODEL AND OPTIMAL CONTROL ANALYSIS OF COFFEE BERRY DISEASE

Abdisa Shiferaw Melese
Main Supervisor: Prof. Oluwole Daniel Makinde
Co-Supervisor: Dr. Legesse Lemecha Obsu

A Dissertation Submitted to the Department of Applied Mathematics,
School of Applied Natural Science

Presented in Partial Fulfillment of the Requirements for the Degree of Doctor of Philosophy
in Applied Mathematics

Office of Graduate Studies
Adama Science and Technology University

June, 2022
Adama, Ethiopia

Declaration

I hereby declare that this dissertation entitled **"Mathematical model and optimal control analysis of coffee berry disease"** is my own work. That is, it has not been submitted for the award of any academic degree, diploma or certificate in any other university. All sources of materials used for this thesis have been duly acknowledged through appropriate citations.

Abdisa Shiferaw Melese	_____	_____
Name of Student	Signature	Date

Approval page

We hereby certify that the recommendations and suggestions made by the board of examiners are appropriately incorporated into the final version of the dissertation entitled **"Mathematical model and optimal control analysis of coffee berry disease"** by Abdisa Shiferaw.

Prof. Oluwole Daniel Makinde	_____	_____
Main Supervisor	Signature	Date
Dr. Legesse Lemecha Obsu	_____	_____
Co-supervisor	Signature	Date

We, the undersigned, members of the Board of Examiners of the dissertation open defense by Abdisa Shiferaw have read and evaluated the dissertation entitled **"Mathematical model and optimal control analysis of coffee berry disease"** and examined the candidate during open defense. This is, therefore, to certify that the dissertation is accepted for partial fulfillment of the requirement of the degree of Doctor of Philosophy in Applied Mathematics.

_____	_____	_____
Chairperson	Signature	Date
_____	_____	_____
Internal Examiner 1	Signature	Date
_____	_____	_____
Internal Examiner 2	Signature	Date
_____	_____	_____
External Examiner 1	Signature	Date
_____	_____	_____
External Examiner 2	Signature	Date

Finally, approval and acceptance of the dissertation is contingent upon submission of its final copy to the Office of Postgraduate Studies (OPGS) through the candidate's Department Graduate Council (DGC) and School Graduate Committee (SGC).

Department Head	Signature	Date
School Dean	Signature	Date
Office of Postgraduate Studies, Dean	Signature	Date

Recommendation

We, the supervisors of this dissertation, hereby certify that we have read and revised the dissertation entitled "Mathematical model and optimal control analysis of coffee berry disease" prepared under our guidance by Abdisa Shiferaw submitted in partial fulfillment of the requirements for the degree of Doctor of Philosophy in Applied Mathematics. Therefore, we recommend the submission of the dissertation to the department for further review and defense.

Prof. Oluwole Daniel Makinde	_____	_____
Main Supervisor	Signature	Date

Dr. Legesse Lemecha Obsu	_____	_____
Co-supervisor	Signature	Date

ACKNOWLEDGMENTS

First of all, I give honor and glory to almighty God for his grace and for giving me, strength, direction and wisdom to undertake this research. Next, I would like to express my sincere gratitude and appreciation to my supervisor Prof. Oluwole Daniel Makinde and my co-supervisor Dr. Legesse Lemecha Obsu for their great effort in encouraging and providing me with valuable advice. Their support, guidance and constructive criticism, particularly for reading this research thoroughly for the better improvement were of great help to my progress. Additionally, I would like to thank Dr. Kassaye Gutema for his support, specially to check typos and grammatically errors throughout the dissertation. I would like to express my appreciation to my wife Workinesh Tufa for her wise counsel and moral encouragement. My appreciation also goes to all my brothers and classmates that supported me during writing up of this dissertation. Last but not least, I would like to thank department of Applied Mathematics, School of Applied Natural Science, and Adama science and Technology University for providing me all the necessary facilities for this research work.

Dedication

This work is dedicated for the Jesus Christ who is the source of life and wisdom.

Abstract

Coffee berry disease (CBD) caused by Colletotrichum kahawae is a major challenge to Arabica coffee production in African countries. In this dissertation, we studied mathematical models designed to describe the dynamics of plant pathogen and CBD infection to forecast the possible features and establish mitigation strategies for its spread. First, we showed the positivity, existence, uniqueness and positivity of solution, feasible region, equilibria and basic reproduction numbers of the models. Thus, the models turned out to be both biologically meaningful and mathematically well-posed. The local stability of the equilibria is shown via Routh-Hurwitz criteria, while the global stability of the equilibria is proved by using a Lyapunov function. Using center manifold theory, we proved that the model exhibits forward bifurcation. Sensitivity indices of basic reproduction numbers at minimum temperature and rainfall, and maximum temperature and rainfall are determined. The first model is extended to the optimal control problem using quarantine and chemical controls. The next models are extended to the optimal control problem with cost-effectiveness using genetic resistance, chemical control, and cultural practice in the presence of temperature and rainfall variability. The optimal control problem was analyzed with Pontryagin's Minimum Principle (PMP). Numerical simulations were performed at minimum temperature and rainfall, and maximum temperature and rainfall. Furthermore, we studied the cost-effectiveness of strategies to determine the best approach to minimize the burden of the disease and the cost of interventions. The simulation resuls of the first model shows that a combination of quarantine and chemical controls strategies are very effective to eradicate the disease. The simulation resuls of the remaining models show that a combination of genetic resistance, chemical, and cultural control strategies are very effective to eradicate the disease.

Keywords: *Colletotrichum Kahawae; Coffee Berry; Deterministic Model; Temperature Variability, Rainfall Variability; Stability Analysis; Optimal Control; Cost-Effectiveness.*

Contribution of Dissertation

This PhD dissertation reports original results that contribute knowledge to scientific development of Mathematics. The main contribution of this dissertation have been listed as follows:

1. A. S. Melese, O. D. Makinde and L. L. Obsu (2022). Modelling and analysis of pathogens impact on the plant disease transmission with optimal control, *Journal of Applied Nonlinear Dynamics*, Vol. 11, No. 3, pp. 499-521, doi:10.5890/JAND.2022.09.001.

2. A. S. Melese, O. D. Makinde and L. L. Obsu (2022). Mathematical modelling and analysis of coffee berry disease dynamics on a coffee farm, *Mathematical Bioscience and Engineering*, Vol. 19, No. 7, pp. 7349-7373, doi: 10.3934/mbe.2022347.

3. A. S. Melese, O. D. Makinde and L. L. Obsu (2020). Modelling and optimal control analysis of coffee berry disease with cost-effectiveness in the presence of temperature variability, *International Journal of Computing Science and Mathematics* (Accepted and in production).

4. A. S. Melese, O. D. Makinde and L. L. Obsu (2021). Optimal control strategies for coffee berry disease with cost-effectiveness analysis in the presence of temperature and rainfall variability, *Journal of Applied Nonlinear Dynamics*, Vol. 12, No. 2, (Accepted).

5. A. S. Melese, O. D. Makinde and L. L. Obsu (2021). Mathematical model for the dynamics of coffee berry disease infestation in the presence of temperature and rainfall variability, *Journal of Biological Dynamics* (Revised).

6. A. S. Melese, O. D. Makinde and L. L. Obsu (2022). Modeling and optimal control strategies for coffee berry disease with cost-effectiveness analysis, *Plos One* (Under review).

TABLE OF CONTENTS

LIST OF TABLES

LIST OF FIGURES

Acronyms

CBD	.....	Coffee Berry Disease
CWD	.....	Coffee Wilt Disease
CRD	.....	Coffee Rust Disease
PMP	.....	Pontryagin's Minimum Principle
CEA	.....	Cost Effectiveness Analysis
ACER	.....	Average Cost Effectiveness Ratio
ICER	.....	Incremental Cost Effectiveness Ratio
PFEP	.....	Pathogen Free Equilibrium Point
LHS	.....	Latin Hypercube Sampling
PRCC	.....	Partial Rank Correlation Coefficients
CEP	.....	Coexistence Equilibrium Point
DFEP	.....	Disease Free Equilibrium Point
EEP	.....	Endemic Equilibrium Point
ODEs	.....	Ordinary Differential Equations
PDE	.....	Partial Differential Equation
CBSD	.....	Cassava Brown Streak Virus Disease
TYLCV	.....	Tomato Yellow Leaf Curl Virus
MVS	.....	Maize Streak Virus
BXW	.....	Banana Xanthomonas Wilt
JARC	.....	Jimma Agricultural Research Center
FAO	.....	Food and Agriculture Organization

CHAPTER 1

INTRODUCTION

Coffee is a cash crop supporting the livelihoods of millions of individuals who are participating in its cultivation, processing, marketing, and exporting (Rutherford, 2006). It (coffee) is one of the most important commercial commodities and foreign currency earnings in more than 80 developing countries. The worldwide exports of coffee currently go beyond 12 billion dollars, and the sector employs millions of people around the world (Tesfaye, 2010). Due to the global climate change the fungal pathogens are the most harmful pathogens in global coffee production. In this chapter, we give a brief discussion on the background of plant pathogens, coffee berry disease, and their control mechanisms.

1.1 Background of the Study

Plants form the critical base of food chains in nearly all ecosystems. Sometimes they can get infected by various kinds of diseases which are caused by pathogens that spread through media such as water, wind, and other intermediary carriers called vectors (Agrios, 2010). These diseases can be the major threats to crops around the world because they carry healthy, economic, environmental, and social problems (Contreras-Medina et al., 2009).

A plant pathogen is an organism that can inhabit and survive on plants and thereby compromise the health of plants causing disease symptoms. Therefore, plant pathogens are important ecological agents that can influence the composition of plant populations (Gilbert, 2002) and in extreme cases, cause the local extinction of host species (Alexander et al., 2014). In addition, plant pathogens are responsible for yield reductions in crops. It has been estimated that 13-16% of crop production worldwide is lost directly (yield, quality, etc.) every year due to pathogens (Oerke, 2006).

The food and agriculture organization (FAO) estimates that indirect losses (effect, rural communities, environment, etc.) may increase up to 20-40% (Pests, 2015), with subsequent economic and social impacts (Oerke, 2006). To survive with pathogens, hosts have developed a variety of defense mechanisms to avoid/limit infection and their negative effects (Pests, 2015). The two main defense mechanisms of plants against pathogens are resistance, i.e., the host's ability to limit pathogen multiplication (Agnew et al., 2000), and tolerance, i.e., the host's ability to reduce the effect of infection on its fitness regardless of the level of

pathogen multiplication (Agnew et al., 2000).

Infectious diseases are very destructive diseases that spread from one host to another plant (Murwayi et al., 2017). They are the result of a conflicting ecological interaction between a microbial infectious agent (bacteria, fungi, parasites, or viruses) and a host, where the dynamics in this interaction are subjected to the modulator influence of several factors. The factors are the environment, the biological properties of the pathogens, and the host's susceptibilities to disease, as well as the influence of behavioral, cultural, and social patterns that can enhance or mitigate the host's exposure to the disease sources and consequently its transmission in the population (Da Costal et al., 2019).

Mathematical modelling is the representation of a system in relation to mathematical terminologies which are used to answer the questions: how many plants will be infected, how many infected plants will require treatment, what is the expected maximum number of plants infected at any given time and what is the estimated duration of the epidemic? These models are used to aid policymakers in decision making, so as to test the effects of introducing changes in a system and develop a scientific understanding of systems (Murray, 2002).

In the epidemiology of infectious diseases, mathematical modelling is a tool of great versatility, that allows the identification of patterns in epidemics, extrapolations of epidemic behaviors along with the effect of control interventions (Opatowski et al., 2011).

In general terms, the mathematical models applied to the epidemiology of infectious diseases can be classified into two, namely: deterministic and stochastic models. In the deterministic model output variables are determined by parameter values and initial conditions while stochastic models consider random variables in the movements between the compartments of the model such as the probability of a susceptible individual being infected and the probability of transmitting the disease in the population (Siettos and Russo, 2013). In mathematical epidemiology, these mathematical models have three aims: understanding disease propagation processes, forecasting, and control of infectious disease epidemics.

There are numerous plant diseases caused by pathogens like fungi, bacteria, nematodes, viruses, insects, etc that live on/in plants and natural environments (Mikkelsen et al., 2006). Plant pathogenic fungi and bacteria live within their plant hosts (Schaechter, 2009) and the rest live in the soil.

Fungi pathogen

Fungi reproduce both sexually and asexually through the production of spores. Spores can be spread over long distances by air or water, or they can be carried by soil. Fungal plant

pathogens are among the major biotic factors causing devastating diseases in crops (Doehlemann et al., 2017). About 8,000 species of fungi and oomycetes are linked with diseases in plants (Fisher et al., 2020). Pathogenic fungi infect plants at any stage, from sowing to seed ripening under natural environmental conditions. The most common diseases caused by phytopathogenic fungi are anthracnose, mildew, cancer, moldoff, dieback, gall, leaf spot, powdery mildew, rust, root rot, scab, and wilt (Hussain and Usman, 2019).

Anthracnose is a phytopathology which attacks a wide range of commercial crops, including coffee, mango, banana, blueberry, cherry, citrus and strawberry. The Anthracnose pathogen belongs to the *Colletotrichum* species (*acutatum, capsici, gloeosporioides, kahawae, lindemuthianum, musae*, etc). *Colletotrichum* is an ascomycete fungus pathogen. It can reproduce either asexually or sexually, but sexual reproduction is rare in nature (Grahovac et al., 2012). Understanding the complex life style patterns of Colletotrichum spp. (see Figure 1.1) and the dynamic state of their interaction with their host has important implication for management.

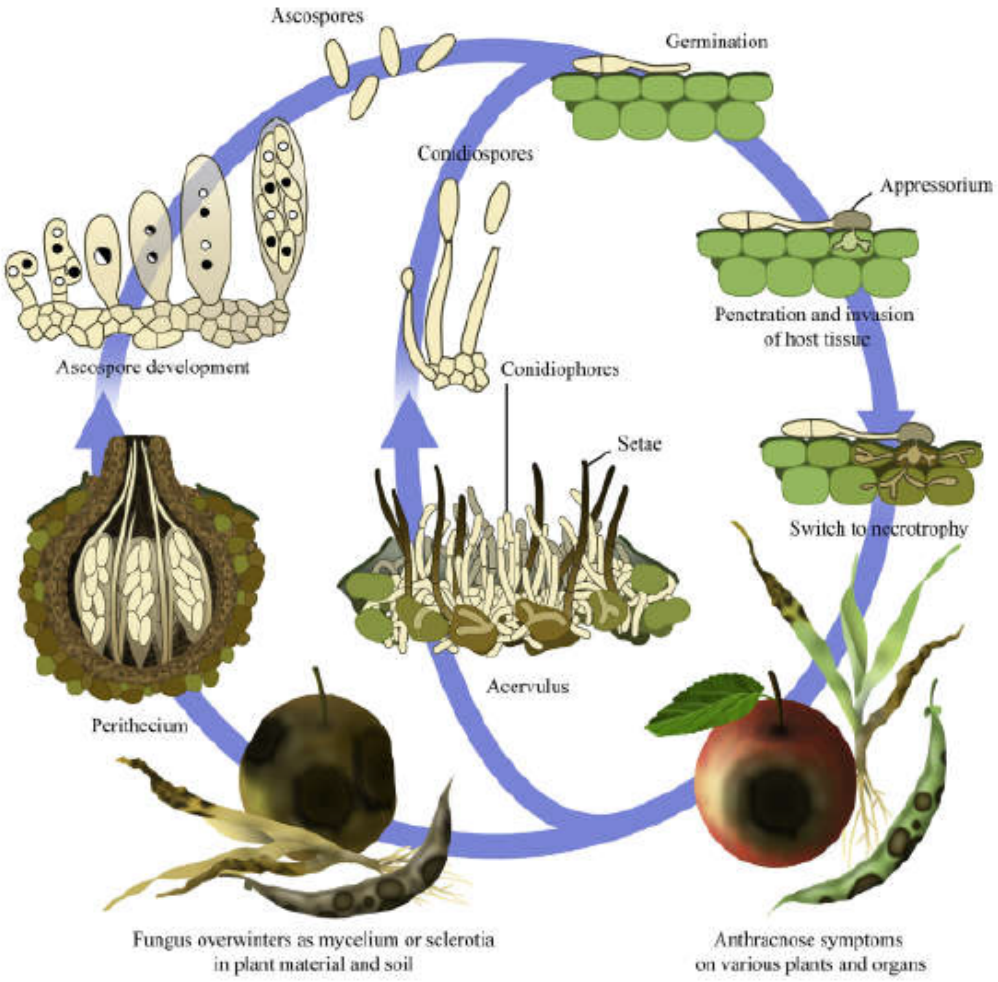

Figure 1.1: General life cycle of Colletotrichum species (Hordofa, 2019).

Bacteria pathogen

Bacteria are single-celled microorganisms, generally ranging from 1-2 μm in size and cannot be seen without microscope. Plant pathogenic bacteria cause many serious plant diseases in tropical and subtropical regions of theworld, but fewer than fungi or viruses, and they cause relatively less damage and economic cost (Kennedy et al., 1980).

Nematodes

Nematodes are small, multicellular worm-like animals. Many nematodes are free-living in the soil, but some species parasitize plant roots. They are a problem in tropical and subtropical regions of the world, where they can infect crops. Potato cyst nematodes (Globodera pallida and G.rostochiensis) are widely distributed in Europe and America and cause damage worth 300 million dollars in Europe every year. Root-knot nematodes have a fairly wide host range, parasitize the root systems of plants and thus directly affect water uptake andnutrients needed for normal plant growth and reproduction (Huynh et al., 2016), whereas cyst nematodes tend to be able to infect only a few species.

Viruses pathogen

Plant viruses are viruses that affect plants. Viruses are extremely small and can only be observed under an electron microscope (Gergerich and Dolja, 2006). Like all other viruses, plant viruses are obligate intracellular parasites that lack the molecular machinery to replicate without a host. Plant viruses can be pathogenic to higher plants. Most plant viruses are actively transmitted from infected plants to healthy plants by a living organism called a vector. Arthropods, nematodes and plant-parasitic fungi are the main types of vector organisms for plant viruses (Walkey, 2012). Among these, aphids and whiteflies are capable of transmitting the largest number of virus species.

Insects

Purcell and Almeida (2005) identified that some plant diseases like CBD pathogens require dynamic vectors. The most common vectors are insects such as aphids, whiteflies, planthoppers and leafhoppers. Whiteflies (Hemiptera Aleyrodidae) occur as a diverse group of about 1500 species throughout the tropics, and to a lesser degree in warmer temperate environments, roughly a quarter of the total number being reported from Africa (Martin et al., 2000). Whitefly was usually able to complete development from egg to adult in the temperature range of 15-30 $^{\circ}C$ (Honěk et al., 1990).

1.2 Coffee Berry Disease

Coffee production faced with many factors primarily due to shortage of adaptive cultivar and soil fertility status, diseases, insects, pests and weeds. Among these factors, coffee berry disease (CBD) which is caused by *Colletotrichum kahawae* is a major challenge to Arabica

coffee production in African countries (Mulinge, 1973) and a dangerous threat to coffee production elsewhere. This pathogen is an ascomycete that reproduces sexually and asexually. The asexual spores (conidia) are stored within acervuli (Waller et al., 1993; Mouen Bedimo et al., 2010). CBD infects all stages of the crop and occasionally leaves, but highest crop losses occur among green berries between 4-14 weeks after flowering (Silva et al., 1999). This disease does not kill trees, but causes production loss in quality and quantity. For instance, the overall national average loss due to CBD in Ethiopia is estimated to range 25-30% per year. Losses may be more than 30% based on high rainfall, humidity and altitude areas (Zeru, 2006; Belachew et al., 2015).

The CBD is first reported in western Kenya (1922) when it led to the destruction and abandoning of coffee Arabica plantations in some regions (McDonald et al., 1926). Soon after, the fungus has quickly spread throughout most African countries (see Figure 1.2). According to the survey results, CBD was the most widespread coffee disease.

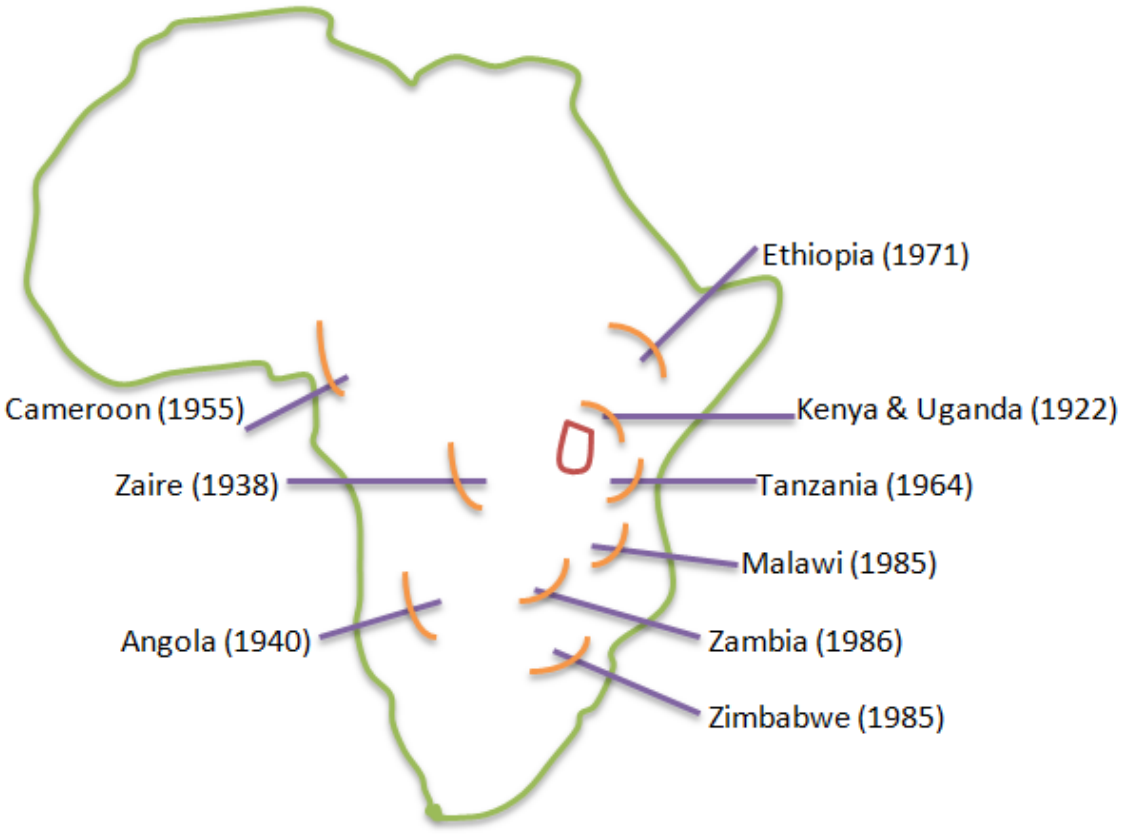

Figure 1.2: The spread of coffee berry disease (CBD) across Africa (Waller et al., 2007).

1.2.1 Cause and Symptom of Coffee Berry Disease

Precipitation, high humidity, moderately warm temperatures, and high altitude are the most important factors determining CBD outbreaks (Chitnis et al., 2006). Favorable climatic con-

ditions to *Colletotrichum kahawae* occurs at high elevations greater than 1,600 m (Phiri et al., 2001). The optimum temperatures for *Colletotrichum kahawae* germination and mycelium growth are about 20 to 22°*C* (Griffiths et al., 1971). Infections can occur at any stage of the plant, from unopened inflorescences to ripe berries and, occasionally, leaves (see Figure 1.3). Figure 1.4 shows the coffee plants with healthy berries (Jeffrey, 2017).

Based on the susceptible response of coffee genotypes, there are two types of symptoms: scab and active lesions. Scab lesions are plants' resistance response that restricts fungal development which allows only the formation of small black spots. The deeper layers of the fruit are not invaded and the lesion appears stationary not affecting the normal development of the green berry. While, among susceptible plants' active lesions development is observed starting as little black spots, in the presence of good conditions can form dark, sunken, active lesions that rapidly expand and destroy the entire fruit (Masaba and Van Der Vossen, 1982; Manuel et al., 2010).

The primary and secondary inoculum pathogen cause primary and secondary infection, respectively. The primary infection is the first time plant is exposed to and arises from a free-living inoculum pathogen. The secondary inoculum is formed from primary infections during or after treatment for another infection (Belachew et al., 2015; Abdulkhair and Alghuthaymi, 2016). It may be produced by the pathogen as seen by concentric rings that are surrounded by emerging black acervuli within the lesion.

Figure 1.3: Coffee berries infected with coffee berry disease (Silva et al., 2006).

Figure 1.4: Coffee plants with healthy berries (Jeffrey, 2017).

1.2.2 Way of Transmission of Coffee Berry Disease

Pathogens can be spread to host plants in many ways. Locally, the disease spreads between coffee trees and branches by wind and rainfall. This disease is heavily dependent on rainfall for conidial production, dispersion, germination, and infection (Waller, 1972). Its infection begins with the germination of conidia (asexual spore) which can happen within 24 hours after contact with the host plant tissue. Most conidia of *Colletotrichum kahawae* can be effectively dispersed by an optimum rainfall of 10 mm but heavy rainfall (more than 700 mm) leads more to their leaching from the coffee tree canopy to the soil (Waller, 1972). This follows when elongation of the germ tube in the apical selection is differentiated into melanized appressorium which functions to penetrate the plant cell cuticle (See Figure 1.5) directly via turgor pressure, secretion of cutin degrading enzymes, or the combination of the two processes (Silva et al., 2006; Mouen Bedimo et al., 2007). However, the common vectors of long and medium-distance dispersals are insects, birds, and coffee harvesters (Gaitan et al., 2015). Thus, in this study, we consider any insects, birds, and harvesters that, after contacting pathogens from either the environment or already CBD infected coffee berries, then contact healthy coffee berries as responsible vectors for the spread of CBD.

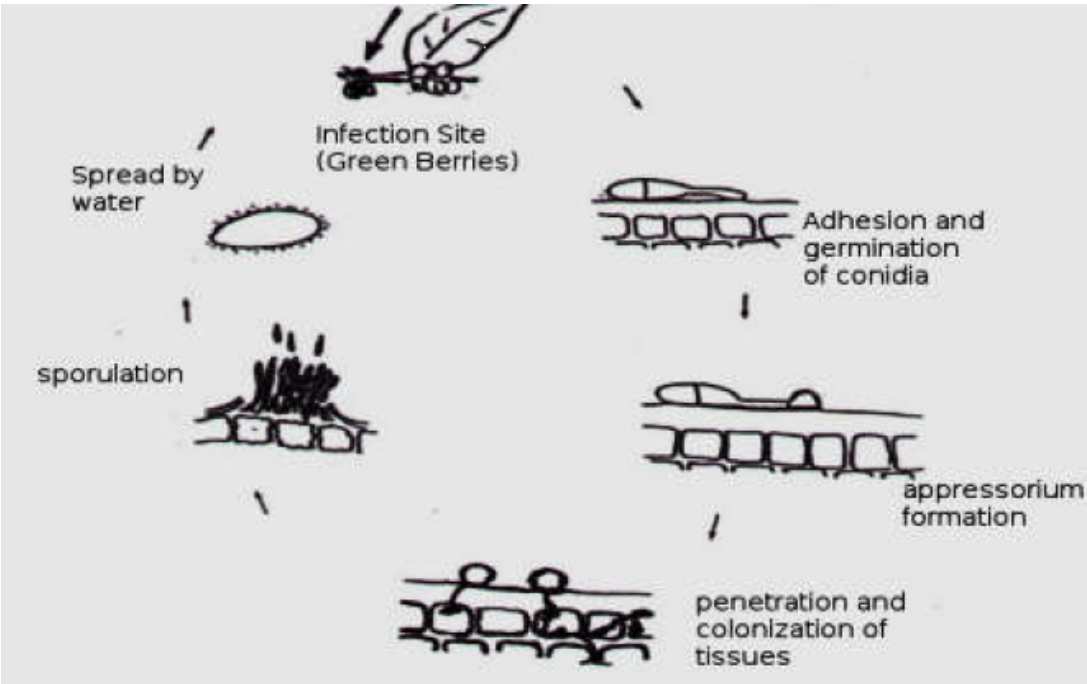

Figure 1.5: The systemic infection process of Colletotrichum kahawae (Hordofa, 2019).

1.2.3 Control Measures of Coffee Berry Disease

1.2.3.1 Agricultural Perspective

Disease-causing organisms cannot be eliminated from the environment and therefore management measures need to be undertaken to reduce their impact. For the disease control measures, numerous options have been recommended. These recommendations fall into five categories. These are quarantine, chemical methods, cultural practices, selection breeding for resistance, and biological control. Each of these control options has its own advantages and disadvantages.

1.2.3.1.1 Quarantine

A legal restriction to prevent the entrance and establishment of a plant disease/pest/pathogen in a country where the pest/pathogen/disease does not exist.

1.2.3.1.2 Chemical Control

Fungicides screening program was started one year after the occurrence of CBD in 1972 (Ejeta, 1986). The success of chemical control depends on the disease pathogenesis stage at the moment when the fungicide is applied (Balardin et al., 2010).

Major advances have been made in the type of molecules, concentrations, formulations, rates as well as spray intervals. All are done with the concern of environmental impact. Various

categories of fungicides have therefore been developed for the agricultural sector. Different copper-based fungicides, organic fungicides, and mixtures of the two are recommended to control the disease (Yemo et al., 2017). The use of organic fungicides began in 1934 and has since played a major role in the worldwide control of plant diseases (Alwora and Gichuru, 2014). They are more effective and less toxic than inorganic ones.

Furthermore, fungicide screening programs have been continued and twenty-one fungicides were tested against the disease from 1987 to 1997 in Ethiopia at Gera. As a result, six fungicides are identified and were recommended to control CBD in Ethiopia (Derso et al., 2000). These are Daconil '2787' 75% WP, Daconil 75% WDG, Shirlan 50% SC, Nordox 50% WP, Octave super 50% WP and a tank mixture of Daconil '2787' and Nordox.

Formulations, application rate, and spray intervals of fungicide in Ethiopia have been identified. In this county fungicide spray against CBD starts six weeks after the main flowering for six rounds at 4 week (28 days) interval in a crop season was recommended (Derso et al., 2000). In areas where a shortage of water does not occur, a high volume of 750 - 1000 ml per tree can be used depending on the size of the tree (Derso et al., 2000). The regions where water is scarce for spraying, low volume application, 200 - 250 ml per tree, using a motorized knapsack sprayer was effective in controlling CBD. It is also advisable to repeat the spraying if heavy rains (>10 mm) fell immediately within six hours after spraying since the initial fungicide deposit could be washed away from the tree (Derso et al., 2000). Chemical control seems the most effective method but incorrect user causes ecological risks.

1.2.3.1.3 Cultural Practices

Cultural practices are a variety of management techniques that may be manipulated by farmers to attain their crop production goals (Bedimo et al., 2007). They are suggested to be interwoven in conventional management tactics. They include mixed cropping with shade plants, pruning infected branches, destruction of infected material, and removal of mummified berries, which create environmental conditions that limit CBD development (Bedimo et al., 2007).

1.2.3.1.4 Resistant Varieties

The Arabica coffee in Ethiopia is diverse and variations in susceptibility were obvious from the first CBD outbreaks (Robinson, 1974). Resistance variety is the best option to protect the crop from damage due to biotic factors. It is only the use of cultivars with durable resistance that provides a permanent solution and guarantees stable cash income to the growers. Realizing these circumstances a breeding program was launched by the Ethiopian Institute of Agricultural Research, Jimma Agricultural Research Center (JARC).

Since Ethiopia is the center of origin and genetic diversity for coffee Arabica, the coffee population provides immense opportunities to make selections for any desirable trait for high-yielding and diseases resistant varieties. The CBD resistant selection program in Ethiopia basically consisted of four steps: mother tree selection, testing of mother trees, multiplication, and progeny testing (Ejeta, 1986).

Among the selections most have been under evaluation. As a result, some were, discarded after appropriate evaluations, and some mother trees' progenies were established for further tests in their respective locality. Since the inception of the CBD resistant selection and breeding program at JARC, nineteen CBD resistant selections having reasonable yield and resistance to other diseases and pests were released to growers (Bellachew, 2001). Based on regular field observations on the farms, six of them were withdrawn from production from time to time due to their manifestation of either high CBD, rust, or wilt diseases and/or low yield performance.

1.2.3.1.5 Biological Controls

Biological control (biocontrol) is the use of living organisms to control disease-causing organisms (Pal and Gardener, 2006). There has been a shift in the control of plant diseases from the regular use of pesticides to alternative and more eco-friendly biopesticides and plant-based products over the recent years (Pal and Gardener, 2006). Many fungi and bacteria have the potential to act as biological control agents.

1.2.3.2 Mathematical Modelling Perspective

A mathematical model is a simplification of reality and attempts to summarize the main processes, put forward hypotheses, and verify their coherence and consequences. It also represents a test to determine the minimum assumptions that would allow a minimum mathematical representation of real processes.

In mathematics, modelling plays a crucial role in better understanding the dynamics of plant disease in order to establish sustainable approaches for strategic and tactical disease management. See, for example, the following mathematical models.

Fotsa et al. (2013) introduced the mathematical modelling and optimal control of Anthracnose disease. Anthracnose is another name for CBD. It attacks a wide range of commercial crops, including coffee, mango, banana, blueberry, cherry, strawberry, etc. This model seems quite theoretical but could be used for practical applications if the needed parameters were provided. Indeed, in the literature (Danneberger et al., 1984; Mouen Bedimo et al., 2007)

there are several attempts to estimate these parameters. The main advantage of this model is that it can be used to set up automatic means to control the disease which are able to adapt themselves with respect to the host plant and to the parameters' values. In practice, most parameters are piecewise continuous, and some control strategies are discontinuous. For instance, cultural interventions and application of antifungal treatments are pulses with respect to a certain calendar, and the effects of these treatments though continuous are of limited duration. Thus, the authors investigated a more general model that takes into account those irregularities. The authors also showed how to optimize the use of chemical control with respect to a given cost function. Later, this study was generalized by incorporating an impulsive control strategy that represents cultivation practices (Mbogne and Thron, 2015).

In this dissertation, we focused on a nonlinear deterministic model with an optimal control mechanism. We developed mathematical models in which the analysis of the models may assist decision-makers in identifying and estimating the risk and the potential future growth of the disease in the plant population. For this, six mathematical models were developed to study the dynamics of plant pathogen, CBD infection and their controls.

1.3 Statement of the Problem

Coffee berry disease (CBD) is a critical problem that affects the production of coffee in many African countries in general and Ethiopia in particular. For instance, in Ethiopia, the overall national average loss due to CBD is estimated to range 25-30% per annual (Garedew et al., 2017). Losses may be more than 30% in high humidity, relatively warm temperatures, and high altitude areas. These infections can be disturbing to not only the plants themselves but also the ecosystem that depends on them (Jackson and Chen-Charpentier, 2018).

There are few studies on coffee disease transmission based on mathematical modelling with optimal control. For example, Fotsa et al. (2013) developed the mathematical modelling and optimal control of Anthracnose disease. Cunniffe and Gilligan (2010) investigated epidemiological models for plant pathogens. The authors compare the effects of using two commonly used formulations for host growth, one linear and the other nonlinear, upon the outcomes for invasion, persistence, and control of pathogens in a widely used, generic model for botanical epidemics. Djuikem et al. (2021) proposed and analysed a PDE model that describes the dispersal of CLR in a coffee plantation during the rainy and dry seasons.

However, studies on CBD infection based on mathemaical model are rare. Hence, it is important to study the dynamics of CBD model with optimal control in the presence of temperature and rainfall variability. Also, apply cost-effective analysis to determine the most effective strategy for controlling infectious diseases in limit resources. Therefore, we iden-

tified the best among the control strategies considered in this study to protect coffee berries from the disease and to increase the farmers' coffee yield production for beverage, income generation, and as a source of livelihood.

1.4 Objectives of the Study

1.4.1 General Objective

The general objective of this study is developing a mathematical model and investigating the dynamics of CBD and its controls.

1.4.2 Specific Objectives

The specific objectives are to:

1. formulate SIR-X mathematical model to investigate the impact of pathogens on plant disease dynamics and its control.
2. develop a deterministic mathematical model that describe the dynamics of CBD on a coffee farm.
3. formulate a mathematical model of CBD infection considering temperature and rainfall variability.
4. analysis all developed mathematical models qualitatively and quantatively.
5. predict the long term trends the disease and recommend intervention strategies.

1.5 Significance of the Study

The study is significant in many ways. It provides reliable information on how one can use mathematical modeling to improve the roles of control strategies and prevention in CBD transmission in a coffee farm. The outcome of the study may guide public agriculture policymakers on optimal control strategies to control the CBD with minimal cost. In addition, it may serve as a springboard for other researchers.

1.6 Structure of the Dissertation

The dissertation is organized as follows. In Chapter 2, relevant related literature is presented. Chapter 3 presents the methodology part of the study. In Chapter 4, optimal control analysis of the plant-pathogen model is proposed and discussed. Chapter 5 is devoted to mathematical

modelling of coffee berry disease and its control. Modelling the dynamics of coffee berry disease in the presence of temperature variability is considered in Chapter 6. Optimal control analysis of coffee berry disease in the presence of temperature and rainfall variability is presented in Chapter 7. Summary, conclusions, and recommendations are drawn in the last Section 8.

CHAPTER 2

LITERATURE REVIEW

CBD is the main factor that seriously affects the coffee berry (Zeru et al., 2012). It brings every year to a sharp decline in coffee production in tropical and subtropical highlands of Africa. Therefore, some researchers have focused their attention on understanding how to control this disease. A number of studies have been conducted from the agricultural perspective to control CBD. However, mathematical modelling on CBD is rare. Thus, in this chapter, we review some mathematical modelling of infectious diseases particularly related to CBD. In addition, we review some models that use the optimal control theory and cost-effective analysis.

2.1 Mathematical Modelling of Plant Infectious Diseases

A mathematical modelling of maize streak virus (MSV) pathogen interaction with a pest invasion on maize plant has been developed (Alemneh et al., 2019). The model consists of two populations (maize and the leafhopper vector) with the interaction of the MSV pathogen. Analysis of the model showed that there exists a domain where the model is epidemiologically and mathematically well-posed. The basic reproduction number of the model was computed using the next-generation matrix method. The model was then qualitatively analyzed for the existence and stability (local and global) of their associated equilibria. Sensitivity and bifurcation analysis of the model are investigated. Numerical simulations are performed and displayed graphically to justify the analytical results.

Kermack and McKendrick's (1932) published work on epidemic models has greatly influenced the development of compartmental mathematical modelling. These models are still widely used in some epidemic situations (Murray, 2002). Specific models have been developed for plant diseases like cassava brown streak virus disease (CBSD), potato late blight, Tomato yellow leaf curl virus (TYLCV), Cotton leaf curl viruses (CLCuV), maize streak virus (MVS), blueberry plant diseases, cherry tree diseases, banana xanthomonas wilt (BXW) and co-infections of those diseases, etc.

2.2 Optimal Control Analysis of Plant Diseases

Cunniffe and Gilligan (2010) investigated epidemiological models for plant pathogens: the

effect of host demography. The authors compare the effects of using two commonly used formulations for host growth, one linear and the other nonlinear, upon the outcomes for invasion, persistence, and control of pathogens in a widely used, generic model for botanical epidemics. The criterion for invasion, reflected in the basic reproductive number is unaffected by host demography: it is simply a function of epidemiological parameters alone. When, however, host growth is intrinsically nonlinear, unexpected results arise for persistence and the control of the disease. This model ensured maximum transferability across the widest range of host-pathogen systems by using the common currency of the field and has illustrated the results in a class of models that has been experimentally tested for plant disease.

Djuikem et al. (2021) proposed and analyzed a partial differential equation (PDE) model that describes the dispersal of coffee leaf rust (CLR) in a coffee plantation during the rainy and dry seasons. The model includes coffee branches, leafless coffee branches, urediniospores, and coffee berries. In this model, the disease-free and endemic equilibria, and dry and rainy basic reproduction numbers are computed. To illustrate the theoretical results of the model, numerical simulations are performed.

Kinene et al. (2015) proposed a mathematical model for the dynamics and cost-effectiveness of the current controls of cassava brown streak disease (CBSD) in Uganda. In this model, the authors introduced two time-dependent controls. The first control aimed at reducing the transmission from the vector to the cassava plant. This involves killing the vector through spraying pesticides. The second control is aimed at stopping infection to the vector by the plant.

A mathematical model for the vector transmission and control of banana Xanthomonas wilt was discussed in (Horub et al., 2017). A novel theoretical model for the transmission of banana xanthomonas wilt (BXW) by insect vectors is formulated and analyzed. The model incorporates roguing infected plants and replanting using healthy suckers. The model is analyzed for the existence and stability of the equilibrium points. It was established that if the basic reproduction number satisfies $R_0 < 1$, the disease-free equilibrium point is globally stable and the disease will be wiped out, and if $R_0 \geq 1$, the endemic equilibrium is stable and the disease persists. Disease management involves reducing the contact rates between the banana plants and the vectors and reducing the vector-plant ratio. Contact between the vector and the banana plant is made at the male buds and therefore removal of the male buds is key. Removal of male buds also ensures that the number of insect vectors visiting the plant is also reduced thereby reducing the vector-plant ratio. A numerical simulation of the model was also carried out.

The optimal control and cost-effectiveness analysis of tomato yellow leaf curl virus (TYLCV)

disease epidemic model was discussed in (Hugo et al., 2019). The formulated dynamics include tomato plants and vectors that spread the disease in tomatoes. The boundedness of the model has been analytically examined. The preferable optimal level of the intervention strategy to reduce the spreads and the cost of implementing control strategies were determined by introducing the time-dependent control. The Pontryagin's maximum principle was used in deriving and analyzing the conditions for optimal control of the tomato yellow leaf curl disease with control strategies such as protective netting, insecticide control, and removal of the infected plant. Cost-effectiveness analysis indicates that the use of protective netting and removal of the infected plant is the cost-effective optimal control strategy and is sufficient to combat the epidemic of tomato disease with limited resources.

A mathematical analysis of plant disease dispersion model that incorporates wind strength and insect vector at equilibrium is discussed in (Murwayi et al., 2017). The model formulates and analyzes a dynamical nonlinear plant vector-borne dispersion disease model that incorporates insect and plant populations at equilibrium and wind as a parameter of climate change. Local and global stability of equilibria is performed. And also, sensitivity at basic reproduction number is analyzed.

An epidemiology of insect-transmitted plant viruses: modelling disease dynamics and control interventions were discussed in (Jeger et al., 2004). The modelling approaches have been vector-based dealing with empirical forecasting systems or simulation of vector population dynamics. The theoretical bases for these models and their use in evaluating control strategies in terms of the interactions between host, virus, and vector are considered here. Vector activity and behavior, especially in relation to virus transmission, are important determinants of the rate and extent of epidemic development.

An optimal control issue in a plant disease with host demographic factor and botanical fungicides was discussed in (Anggriani et al., 2018). The fungicide is given as a preventive treatment for infectious plants. The model is constructed based on the development of the disease in which the monomolecular is monocyclic. The dynamics of the model are highly sensitive to changes in contact rate and infectious period. And also the optimal control of the infected plant host by considering a preventive treatment aimed at reducing the infected host plant was discussed. The obtained optimal control shows that it can reduce the number of infected hosts compared to that without control.

Alemneh et al. (2020) developed an optimal control model and cost-effectiveness analysis of maize streak virus (MSV) pathogen interaction with pest invasion in maize plant. The model consists of maize host and leafhopper vector populations with the interaction of MSV pathogen in the environment. For minimizing the spread of maize streak disease, three con-

trols namely prevention, quarantine and chemical control were incorporated. In this model, Pontryagin's maximum principle is applied to derive and study the conditions necessary for optimal control strategies. The authors investigated cost-effectiveness using ICER to determine the best strategy. They found that the combination of prevention and quarantine is the best effective strategies in terms of cost as well as health benefits.

In general, the mathematical models presented in the CBD are rare in the literature and the existing ones also do not take into account the relevance of vector population, temperature, and rainfall variability in the CBD dynamics. Therefore, by considering previous limited works and no work has been done to investigate the mathematical model of CBD with the application of optimal control and cost-effective strategies in the presence of temperature and rainfall variability.

CHAPTER 3

RESEARCH METHODOLOGY

In this chapter, we briefly discuss the model formulation, method of analysis and mathematical procedures that are used to attain the general and specific objectives of the dissertion.

3.1 Formulation of Mathematical Models

We developed an SIR-X type mathematical model for the transmission dynamics of plant pathogen and CBD. Indeed, we formulated six mathemaical models based on coffee berry and vector populations, fungal pathogen, temperature and rainfall variability.

In our models, we consider some basic assumptions. For the dynamics of plant pathogen, we subdivide the population into four compartments, namely susceptible (S), infected (I), removed (R) and inoculum pathogen (X). For the dynamics of CBD infection, we subdivide the population into five compartments, namely susceptible coffee berry (S_c), infected coffee berry (I_c), susceptible vector (S_v), infected vector (I_v), and fungal pathogen (B). This CBD model extended into six compartments by including temperature variability (T) compartment. Furthermore, CBD model extended into seven compartments by including temperature variability (T) and rainfall variability (R) compartments.

3.2 Method of Analysis

Our mathematical models are deterministic and its output variables are determined by parameter values and initial condition. Some of the parameter values employed in the numerical simulations were assumed based on qualitative results obtained from the model analysis. Some of them were obtained from literature. In addition to these parameter values, the initial condition was assumed.

3.3 Mathematical Procedures

Mathematical models begin with a clear description of the processes based on the understanding of the system. Then translation into mathematical equations should be made with a specific goal. We present a mathematical model describing the impact of temperature and precipitation variability on CBD infection using a logistic model with respect to pathegen

multiplication and vector breeding rate. The study involved qualitative analysis such as analytical and numerical simulations, then its results are displayed in the form of figures.

Firstly, well-possedness of the models were determined in the mathematical and epidemiological sense. In analytical methods, both local and global stability analysis of the equilibrium points of the model have been performed using Jacobian matrix and Lyapunov functions, respectively. The model bifurcation is also identified using the method described by (Castillo-Chavez and Song, 2004). Sensitivity analyses of basic reproduction numbers have been studied to determine which parameter plays greater role in the transmission of the disease.

Furthermore, a CBD transmission model is extended to the optimal control problem to examine possible control strategies for decreasing the prevalence of disease. The existence of the optimal controls is illustrated. Then the necessary conditions of the optimal control have been derived by using the Pontryagin's minimum principle. Numerical methods for solving ordinary differential equations and boundary value problems have then be employed to solve the resulting two-point boundary value problem. The method called fourth order forward-backward Runge-Kutta sweep is used to solve the optimality system.

Lastly, numerical simulations of the models are done using the MATLAB software to supplement the analytical solution of the model. The cost-effectiveness analysis is described with the purpose of finding the most cost-effective strategy for the prevention of the disease. The most effective and less costly strategy is obtained using the method called incremental cost-effectiveness ratio (ICER).

CHAPTER 4

OPTIMAL CONTROL ANALYSIS OF PLANT PATHOGEN MODEL

In this chapter, a nonlinear deterministic mathematical model for the impact of pathogens on plant disease transmission with optimal control is analyzed. Furthermore, the model is represented with the qualitative and numerical analysis for the system of ordinary differential equations.

4.1 Model Derivation

The model divides the population into four compartments: susceptible, infected, removed plants and inoculum pathogens, to be denoted by $S(t)$, $I(t)$, $R(t)$ and $X(t)$, respectively. The susceptible plant is produced by replanting at rate $g(S)$ and the natural death rate of plant hosts is h. The removal rate for an infected plant is m. The susceptible plant can be infected in two ways: through contact with inoculum pathogen from the environment at rate β_p and from inoculum infected plant at rate β_s. The inoculum pathogen is produced by the infected plant at rate a and decay at rate c. The schematic diagram of the model is shown in Figure 4.1. For further information, the description of the model parameters is given in Table 4.1.

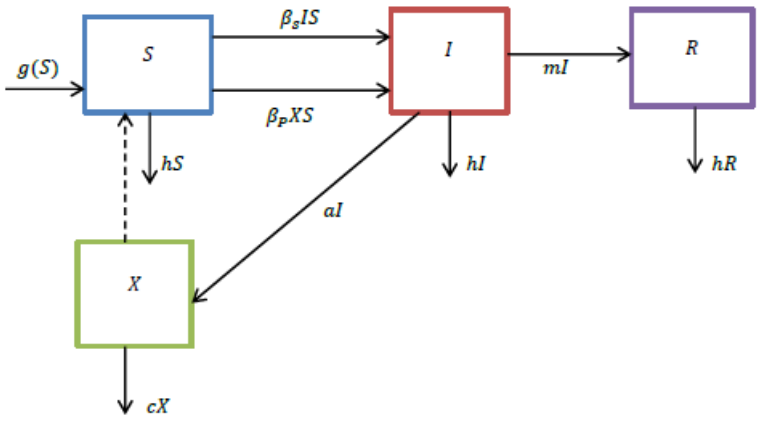

Figure 4.1: Schematic diagram for the plant pathogen dynamics

Table 4.1: Explanation of parameters

Parameters	Explanation
β_p	Primary infection rate
β_s	Secondary infection rate
m	Removal rate of infected plant
h	Natural death rate of hosts
a	Induced rate of inoculum pathogen by infected plant
c	Rate of decay of inoculum pathogen

Based on the above assumptions, the transmission dynamics of plant disease via pathogen is governed by the following system of differential equations:

$$\begin{cases} \dfrac{dS}{dt} = g(S) - (\beta_p X + \beta_s I)S - hS, \\ \dfrac{dI}{dt} = (\beta_p X + \beta_s I)S - (m+a)I - hI, \\ \dfrac{dR}{dt} = mI - hR, \\ \dfrac{dX}{dt} = aI - cX, \end{cases} \tag{4.1}$$

with initial condition: $S(0) = S_0 > 0, I(0) = I_0 \geq 0, R(0) = R_0 \geq 0, X(0) = X_0 \geq 0$.

The infection occurence is decreasing after treatment (chemical spray) for another infection because primary inoculum is more available than secondary inoculum pathogen. Therefore, it is reasonable to assume that $\beta_s < \beta_p$ (Kungaro et al., 2013). Compared to the model introduced in (Cunniffe and Gilligan, 2010), the present study involves the induced rate of inoculum pathogen by the infected plant into the environment. Besides, detailed sensitivity and phase portrait analysis are studied. Furthermore, the model is extended into the control problem by incorporating two control variables as given in Section 4.4.

4.2 Non-Dimensionalization

Non-dimensionalization is used to simplify the model (4.1) by removing free parameters and units using suitable substitution of variables and parameters. The units are eliminated from dimensionless system since they do not affect the dynamical analysis. For simplicity, let us consider $\mu = m + a$ for the total rate of loss of infected host and $dS/dt = f(S) = g(S) - hS$ for the total dynamics of susceptible hosts in the model (4.1). If we consider constant growth rate, with $g(S) = r$, then $f(S) = b(k - S)$, where $b = h$, $k = r/h$, with birth rate b and carrying capacity k (Gilligan, 1990).

Table 4.2: Scaled dimensionless variables and parameters

Scaled dimensionless variables	Dimensionless parameters
$\hat{S} = \frac{S}{k}$	$\hat{\beta}_p = \frac{a}{b}\frac{k\beta_p}{b}$
$\hat{I} = \frac{I}{k}$	$\hat{\beta}_s = \frac{k\beta_s}{b}$
$\hat{R} = \frac{b}{m}\frac{R}{k}$	$\hat{\mu} = \frac{\mu}{b}$
$\hat{X} = \frac{b}{a}\frac{X}{k}$	$\hat{h} = \frac{h}{b}$
$\hat{t} = bt$	$\hat{c} = \frac{c}{b}$

The dimensionless model is formulated by substituting the given terms from Table 4.2 into Eq. (4.1) as follows.

$$\begin{aligned}
\frac{dS}{dt} &= \frac{dS}{d\hat{S}}\frac{d\hat{S}}{d\hat{t}}\frac{d\hat{t}}{dt} = kb\frac{d\hat{S}}{d\hat{t}} = b(k - k\hat{S}) - (\frac{b^2\hat{\beta}_p}{ak}\frac{ak\hat{X}}{b} + \frac{b\hat{\beta}_s}{k}k\hat{I})k\hat{S},\\
\frac{dI}{dt} &= \frac{dI}{d\hat{I}}\frac{d\hat{I}}{d\hat{t}}\frac{d\hat{t}}{dt} = kb\frac{d\hat{I}}{d\hat{t}} = (\frac{b^2\hat{\beta}_p}{ak}\frac{ak\hat{X}}{b} + \frac{b\hat{\beta}_s}{k}k\hat{I})k\hat{S} - bk\hat{\mu}\hat{I} - b\hat{h}k\hat{I},\\
\frac{dR}{dt} &= \frac{dR}{d\hat{R}}\frac{d\hat{R}}{d\hat{t}}\frac{d\hat{t}}{dt} = mk\frac{d\hat{R}}{d\hat{t}} = mk\hat{I} - b\hat{h}\frac{mk\hat{R}}{b},\\
\frac{dX}{dt} &= \frac{dX}{d\hat{X}}\frac{d\hat{X}}{d\hat{t}}\frac{d\hat{t}}{dt} = ak\frac{d\hat{X}}{d\hat{t}} = ak\hat{I} - b\hat{c}\frac{ak\hat{X}}{b}.
\end{aligned} \tag{4.2}$$

After simplification (4.2) becomes

$$\begin{cases}
\frac{d\hat{S}}{d\hat{t}} = 1 - \hat{S} - (\hat{\beta}_p\hat{X} + \hat{\beta}_s\hat{I})\hat{S},\\
\frac{d\hat{I}}{d\hat{t}} = (\hat{\beta}_p\hat{X} + \hat{\beta}_s\hat{I})\hat{S} - (\hat{\mu} + \hat{h})\hat{I},\\
\frac{d\hat{R}}{d\hat{t}} = \hat{I} - \hat{h}\hat{R},\\
\frac{d\hat{X}}{d\hat{t}} = \hat{I} - \hat{c}\hat{X},
\end{cases} \tag{4.3}$$

with initial condition: $\hat{S}(0) = \hat{S}_0 > 0$, $\hat{I}(0) = \hat{I}_0 \geq 0$, $\hat{R}(0) = \hat{R}_0 \geq 0$, $\hat{X}(0) = \hat{X}_0 \geq 0$.

The parameters: a, m, b and k do not have direct analogues in the model (4.3) after scaling. However, the main parameters: $\hat{\beta}_p$, $\hat{\beta}_s$, $\hat{\mu}$, $\hat{c}$ and $\hat{h}$ stay the same. We note that in the above dimensionless formulation, the model (4.1) is reduced into model (4.3) of five parameters.

4.3 Model Analysis

In this section, we study the invariant region, the positivity of solutions, pathogen-free and coexistence equilibrium, basic reproduction number, local and global stability analysis, phase portrait, bifurcation and sensitivity analysis of the model (4.3).

4.3.1 Positivity of Solutions

When dealing with the plant pathogen model, we are aiming at getting non-negative solutions. Thus, the conditions under which the governing system (4.3) has non-negative solutions are very important. This is stated as follows.

Theorem 4.3.1. *Every solution of model* (4.3) *with the prescribed initial condition will remain in* $\mathbb{R}^4_+$ *as* $\hat{t} \geq 0$.

Proof. From the first equation of Eq. (4.3), we obtain the inequality expression

$$\frac{d\hat{S}}{d\hat{t}} \geq -(1+\hat{\beta}_p\hat{X}+\hat{\beta}_s\hat{I})\hat{S},$$

which gives

$$\hat{S}(\hat{t}) \geq \hat{S}_0 e^{-\int(1+\hat{\beta}_p\hat{X}+\hat{\beta}_s\hat{I})d\hat{t}} > 0.$$

By the same procedure, the positivity of the remaining state variables: $\hat{I}$, $\hat{R}$ and $\hat{X}$ becomes

$$\begin{aligned}
\hat{I}(\hat{t}) &\geq \hat{I}_0 e^{-(\hat{\mu}+\hat{h})\hat{t}} \geq 0,\\
\hat{R}(\hat{t}) &\geq \hat{R}_0 e^{-\hat{h}\hat{t}} \geq 0,\\
\hat{X}(\hat{t}) &\geq \hat{X}_0 e^{-\hat{c}\hat{t}} \geq 0.
\end{aligned}$$

Clearly, all the solutions of model (4.3) are non-negative for all $\hat{t} \geq 0$. Thus, the proposed model (4.1) is epidemiologically meaningful in Ω_1 (where Ω_1 is given in Eq. (4.7)). □

4.3.2 Invariant Region

The region where the solution set of model (4.3) bounded is invariant region Ω_1. To compute Ω_1, we first denote total plant population by $\hat{N}$ so that $\hat{N}(\hat{t}) = \hat{S}(\hat{t}) + \hat{I}(\hat{t}) + \hat{R}(\hat{t})$. Then taking derivative of $\hat{N}(\hat{t})$ with respect to time $\hat{t}$, and then adding the first three equations of (4.3), we get

$$\begin{aligned}
\frac{d\hat{N}}{d\hat{t}} &= 1-\hat{S}-(\hat{\mu}+\hat{h}-1)\hat{I}-\hat{h}\hat{R},\\
&\leq 1-\hat{M}\hat{N},
\end{aligned} \tag{4.4}$$

where $\hat{M} = \min\{1, \hat{\mu}+\hat{h}-1, \hat{h}\}$. Integrating the last inequality in Eq. (4.4) by separation of variables one can easily obtain that

$$\hat{N}(\hat{t}) \leq \tfrac{1}{\hat{M}}(1-Ce^{-\hat{M}\hat{t}}),$$

where C is an arbitrary constant. From Eq. (4.4), as $\hat{t} \to \infty$, we obtain $0 \leq \hat{N}(\hat{t}) \leq 1/\hat{M}$. Similarly, from the fourth equation of (4.3), we have

$$\begin{aligned} \frac{d\hat{X}}{d\hat{t}} &= \hat{I} - \hat{c}\hat{X}, \\ &\leq \hat{N} - \hat{c}\hat{X}, \\ &\leq \frac{1}{\hat{M}} - \hat{c}\hat{X}. \end{aligned} \tag{4.5}$$

From Eq. (4.5), we have pathogen

$$\hat{X}(t) \leq \frac{1}{\hat{c}\hat{M}} + (\hat{X}(0) - \frac{1}{\hat{c}\hat{M}})e^{-\hat{c}\hat{t}}. \tag{4.6}$$

From Eq. (4.6), as $\hat{t} \to \infty$, we obtain $0 \leq \hat{X}(\hat{t}) \leq 1/\hat{c}\hat{M}$. Thus, the invariant region for the model (4.3) is given by

$$\Omega_1 = \left\{ (\hat{S}, \hat{I}, \hat{R}, \hat{X}) \in \mathbb{R}^4_+ : 0 \leq \hat{S} + \hat{I} + \hat{R} \leq \frac{1}{\hat{M}}, 0 \leq \hat{X} \leq \frac{1}{\hat{c}\hat{M}} \right\}. \tag{4.7}$$

Therefore, the model (4.3) is well posed epidemiologically. Hence, it is possible to study the dynamics of the model in Ω_1.

4.3.3 Pathogen Free Equilibrium Point (PFEP)

There is no infection in the plant populations at pathogen free. The pathogen free equilibrium E_0 can be computed as follows.

$$\begin{aligned} 1 - \hat{S} - (\hat{\beta}_p\hat{X} + \hat{\beta}_s\hat{I})\hat{S} &= 0, \\ (\hat{\beta}_p\hat{X} + \hat{\beta}_s\hat{I})\hat{S} - (\hat{\mu} + \hat{h})\hat{I} &= 0, \\ \hat{I} - \hat{h}\hat{R} &= 0, \\ \hat{I} - \hat{c}\hat{X} &= 0. \end{aligned} \tag{4.8}$$

We set $\hat{I} = 0$, $\hat{X} = 0$ in Eq. (4.8) and solving for the noninfected state variable, we get $\hat{S} = 1$. Therefore, PFEP is $E_0 = (1,\ 0,\ 0,\ 0)$.

4.3.4 Basic Reproduction Number

The basic reproduction number R_0 is is the average number of secondary infections caused by primary infectious in the given period (Diekmann et al., 1990; Khan et al., 2015). It measures how a disease is transferable to the host. We can calculate R_0 using the next-generation matrix method presented in (Van den Driessche and Watmough, 2002). In epidemiology, the next-generation matrix is a method used to derive R_0 for a compartmental model with

multiple infectious classes discussed in (Heffernan et al., 2005). The model equations are rewritten beginning with newly infective groups:

$$\begin{cases} \dfrac{d\hat{I}}{d\hat{t}} = (\hat{\beta}_p\hat{X} + \hat{\beta}_s\hat{I})\hat{S} - (\hat{\mu} + \hat{h})\hat{I}, \\ \dfrac{d\hat{X}}{d\hat{t}} = \hat{I} - \hat{c}\hat{X}. \end{cases} \tag{4.9}$$

We decompose the right-hand side of system (4.9) as $u - v$ with

$$u = \begin{bmatrix} (\hat{\beta}_p\hat{X} + \hat{\beta}_s\hat{I})\hat{S} \\ 0 \end{bmatrix}, \quad v = \begin{bmatrix} (\hat{\mu} + \hat{h})\hat{I} \\ -\hat{I} + \hat{c}\hat{X} \end{bmatrix}.$$

Next, by linearization approach, the associated matrices of u and v at E_0 are given by

$$U = \begin{bmatrix} \hat{\beta}_s & \hat{\beta}_p \\ 0 & 0 \end{bmatrix}, \quad V = \begin{bmatrix} \hat{\mu} + \hat{h} & 0 \\ -1 & \hat{c} \end{bmatrix}.$$

Then V is an invertible and its inverse is given by

$$V^{-1} = \frac{1}{(\hat{\mu} + \hat{h})\hat{c}} \begin{bmatrix} \hat{c} & 0 \\ 1 & \hat{\mu} + \hat{h} \end{bmatrix}.$$

The product of U and V^{-1} can be computed as follows.

$$UV^{-1} = \frac{1}{(\hat{\mu} + \hat{h})\hat{c}} \begin{bmatrix} \hat{\beta}_s\hat{c} + \hat{\beta}_p & \hat{\beta}_p(\hat{\mu} + \hat{h}) \\ 0 & 0 \end{bmatrix}.$$

Since the basic reproduction number R_0 is the dominant eigenvalue of the matrix UV^{-1}, then we get

$$R_0 = \frac{1}{(\hat{\mu} + \hat{h})} \left(\frac{\hat{\beta}_p}{\hat{c}} + \hat{\beta}_s \right).$$

On the other hand, R_0 can be expressed with respect to primary infection and secondary infection as:

$$R_0 = R_0^p + R_0^s,$$

where $R_0^p = \hat{\beta}_p/(\hat{\mu} + \hat{h})\hat{c}$ and $R_0^s = \hat{\beta}_s/(\hat{\mu} + \hat{h})$.

In terms of the dimensionless parameter, we can see that R_0^p characterizes the average number of new infections produced with a rate $\hat{\beta}_p$ by the free-living inoculum, which survived the latent period of length over the mean lifetime of the inoculum $1/\hat{c}$, over the mean lifetime of the infection $1/(\hat{\mu} + \hat{h})$. Analogously, R_0^s, so that it characterizes the average number of new infections produced with a rate $\hat{\beta}_s$ by the infected host (e.g. through release of spores) over $1/(\hat{\mu} + \hat{h})$.

4.3.5 Sensitivity Analysis

To study the model parameters that most impact the transmission dynamics of the plant-pathogen epidemic, both the local sensitivity of basic reproduction number and global sensitivity analyses of model (4.3) are considered.

(A) Local Sensitivity of R_0

In this subsection, we perform sensitivity analysis in order to determine the relation of model parameters to disease transmission. This helps us to check and classify parameters that extremely affect the R_0 and thus determine appropriate parameter values to minimize disease from plant population. To do this, we used a similar method outlined in (Chitnis et al., 2006). The definition of normalized forward sensitivity index of R_0 with respect to Ψ is given by

$$\Delta_{\Psi}^{R_0} = \frac{\partial R_0}{\partial \Psi} \times \frac{\Psi}{R_0}, \tag{4.10}$$

where R_0 is a given variable, Ψ is a set of parameters in R_0.

Remark 4.3.1. *If the sensitivity index $\Delta_{\Psi}^{R_0}$ is $+ve$, then an increase of Ψ by n% increases R_0 by n% and a decrease of Ψ by n% decreases R_0 by n%. On the other hand, if $\Delta_{\Psi}^{R_0}$ is $-ve$, then an increase of Ψ by n% decreases $\Delta_{\Psi}^{R_0}$ by n% and a decrease of Ψ by n% increases $\Delta_{\Psi}^{R_0}$ by n%.*

By applying the definition, sensitivity indices of R_0 are computed and their sensitivity indeces: $\Delta_{\hat{\beta}_p}^{R_0}$, $\Delta_{\hat{\beta}_s}^{R_0}$, $\Delta_{\hat{\mu}}^{R_0}$, $\Delta_{\hat{h}}^{R_0}$ and $\Delta_{\hat{c}}^{R_0}$ are given in Table 4.3.

Table 4.3: Sensitivity indices of R_0

Parameter	**Sensitivity indices of R_0**
$\hat{\beta}_p$	0.5263
$\hat{\beta}_s$	0.4737
$\hat{\mu}$	-0.1800
$\hat{h}$	-0.7200
$\hat{c}$	-0.5263

Since $\Delta_{\hat{\beta}_p}^{R_0} > 0$ and $\Delta_{\hat{\beta}_s}^{R_0} > 0$ in Table 4.3, then the parameters $\hat{\beta}_p$ and $\hat{\beta}_s$ show that the more impact for spreading disease in the plant population. This result show that as their values increase, the R_0 increases. Conversely, the parameters $\hat{\mu}$, $\hat{h}$ and $\hat{c}$ show that the less impact for spreading disease in the population, since $\Delta_{\hat{\mu}}^{R_0} < 0$, $\Delta_{\hat{h}}^{R_0} < 0$ and $\Delta_{\hat{c}}^{R_0} < 0$ in Table 4.3. In this case, as their values increase, the R_0 decreases. Therefore, we can minimize the disease endemic from plant population by decreasing the values of $\hat{\beta}_p$ and $\hat{\beta}_s$, at the same time, by increasing the values of $\hat{\mu}$, $\hat{h}$ and $\hat{c}$.

(B) Global Sensitivity Analysis

The proposed mathematical model is governed by the input state and parameters of the deterministic type. The sensitivity of R_0 considered in the previous section is used to understand the effect of each parameter involved in the response function R_0. However, global sensitivity analysis takes into account the impact of individual parameters' effects on output variables within their respective range. Furthermore, it is helpful to explore how the initial inputs to the model contribute to the system outputs.

To perform this, we follow the method introduced in (Asamoah et al., 2020; Ullah and Khan, 2020) by applying Latin hypercube sampling (LHS) and partial rank correlation coefficients (PRCC). LHS is a statistical method that follows the stratified sampling without replacement. It helps to efficiently analyze the parameter variations through uncertainty ranges in each parameter simultaneously. In this approach, one must first decide how many sample points to use and for each sample point remember in which row and column the sample point was taken.

PRCC helps to measure the strength of the relationship that exists between the outcome of a model and its input parameters, demonstrating how individual parameters influence the outcome. Consequently, sensitivity analysis indicates the parameters that most significantly impact the outcome via numerical simulations. In order to produce the LHS matrices, it is assumed that all the parameters of model (4.3) are uniformly dispersed. Using R_0 as the response function, the PRCC values for the model parameters are shown in Figure 4.2.

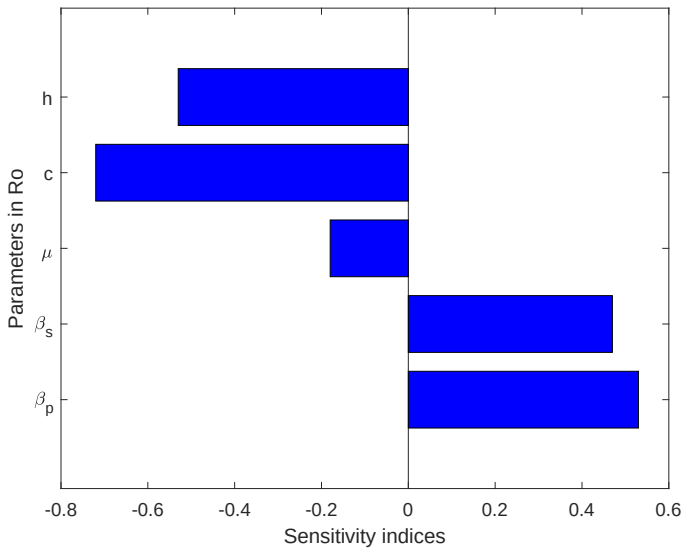

Figure 4.2: Sensitivity indices of basic reproduction number R_0.

Furthermore, this figure clearly shows that the parameters with the highest PRCC values most influence R_0. Hence, the basic parameters that impact R_0 are grouped into those that reduce R_0 when increased (such are the parameters with negative PRCC values for which bars extend to the left), while the others (that have positive PRCC values for which bars extend to the right) make R_0 to increase when increased.

4.3.6 Local Stability of Pathogen Free Equilibrium Point

In this subsection, we investigate the local stability of pathogen free equilibrium point E_0 based on the basic reproduction number R_0.

Theorem 4.3.2. *If $R_0 < 1$, then pathogen free equilibrium $E_0 = (1,0,0,0)$ of the model (4.3) is locally asymptotically stable, and otherwise it is unstable in Ω_1.*

Proof. The Jacobian matrix of the model (4.3) at $(\hat{S},\hat{I},\hat{R},\hat{X})$ is given by

$$J(\hat{S},\hat{I},\hat{R},\hat{X}) = \begin{bmatrix} -1-(\hat{\beta}_p\hat{X}+\hat{\beta}_s\hat{I}) & -\hat{\beta}_s\hat{S} & 0 & -\hat{\beta}_p\hat{S} \\ \hat{\beta}_p\hat{X}+\hat{\beta}_s\hat{I} & \hat{\beta}_s\hat{S}-\hat{\mu}-\hat{h} & 0 & \hat{\beta}_p\hat{S} \\ 0 & 1 & -\hat{h} & 0 \\ 0 & 1 & 0 & -\hat{c} \end{bmatrix}. \tag{4.11}$$

It is clear that an eigenvalue on the third column of Eq. (4.11) is always $-\hat{h}$, and so local stability is controlled by Jacobian matrix J^* corresponding to $\hat{S}$, $\hat{I}$ and $\hat{X}$ components:

$$J^*(\hat{S},\hat{I},\hat{X}) = \begin{bmatrix} -1-(\hat{\beta}_p\hat{X}+\hat{\beta}_s\hat{I}) & -\hat{\beta}_s\hat{S} & -\hat{\beta}_p\hat{S} \\ \hat{\beta}_p\hat{X}+\hat{\beta}_s\hat{I} & \hat{\beta}_s\hat{S}-\hat{\mu}-\hat{h} & \hat{\beta}_p\hat{S} \\ 0 & 1 & -\hat{c} \end{bmatrix}. \tag{4.12}$$

The Jacobian matrix J^* at pathogen free equilibrium E_0 becomes

$$J^*(E_0) = \begin{bmatrix} -1 & -\hat{\beta}_s & -\hat{\beta}_p \\ 0 & \hat{\beta}_s-\hat{\mu}-\hat{h} & \hat{\beta}_p \\ 0 & 1 & -\hat{c} \end{bmatrix}. \tag{4.13}$$

The characteristic polynomial of Eq. (4.13) is given by

$$-(1+\lambda)[\lambda^2+(\hat{\mu}+\hat{h}+\hat{c}+\hat{\beta}_s)\lambda+\hat{c}(\hat{\mu}+\hat{h})-\hat{c}\hat{\beta}_s-\hat{\beta}_p] = 0. \tag{4.14}$$

From Eq. (4.14), $\lambda_1 = -1 < 0$, and the other characteristic polynomial is

$$\lambda^2+a_1\lambda+a_0 = 0, \tag{4.15}$$

where

$$a_1 = \hat{\mu} + \hat{h} + \hat{c} + \hat{\beta}_s,$$
$$a_0 = \hat{c}(\hat{\mu} + \hat{h}) - (\hat{c}\hat{\beta}_s + \hat{\beta}_p) = \hat{c}(\hat{\mu} + \hat{h})(1 - R_0).$$

By Routh-Hurwitz criterion (Martcheva, 2015), Eq. (4.15) has real root that strictly negative if $a_1 > 0, a_0 > 0$ and $a_1 a_0 > 0$. But, $a_0 > 0$ if $R_0 < 1$. Therefore, E_0 is local asymptotically stable for $R_0 < 1$. □

4.3.7 Global Stability of Pathogen Free Equilibrium Point

Theorem 4.3.3. *If $R_0 < 1$, then the pathogen free equilibrium $E_0 = (1,0,0,0)$ of the model (4.3) is globally asymptotically stable in Ω_1.*

Proof. To establish the global stability of pathogen free equilibrium E_0, we consider Lyapunov function:

$$L = \frac{(\hat{S} - \hat{S}^0)^2}{2} + \hat{I} + \hat{R} + \hat{X}. \tag{4.16}$$

The above function L needs to satisfy the conditions: $L(\hat{S},\hat{I},\hat{R},\hat{X}) > 0$ for all $(\hat{S},\hat{I},\hat{R},\hat{X}) \backslash E_0$ and $L(E_0) = 0$. By differentiating L with respect to $\hat{t}$, we get

$$\frac{dL}{d\hat{t}} = (\hat{S} - \hat{S}^0)\frac{d\hat{S}}{d\hat{t}} + \frac{d\hat{I}}{d\hat{t}} + \frac{d\hat{R}}{d\hat{t}} + \frac{d\hat{X}}{d\hat{t}}. \tag{4.17}$$

Substituting expression for $d\hat{S}/d\hat{t}$, $d\hat{I}/d\hat{t}$, $d\hat{R}/d\hat{t}$ and $d\hat{X}/d\hat{t}$ from model (4.3) into Eq. (4.17) leads to

$$\begin{aligned} \frac{dL}{d\hat{t}} &= -(\hat{S} - 1)^2 + 2(\hat{\beta}_p \hat{X}\hat{S} + \hat{\beta}_s - [\hat{\mu}\hat{I} + \hat{h}\hat{I} + \hat{h}\hat{R} + \hat{c}\hat{X} + (\hat{\beta}_p \hat{X} + \hat{\beta}_s \hat{I})\hat{S}^2], \\ &= -(\hat{S} - 1)^2 + \hat{p}_1 - \hat{p}_2. \end{aligned} \tag{4.18}$$

From Eq. (4.18) we have $dL/d\hat{t} \leq 0$ if and only if $\hat{S} = 1$, $\hat{I} = \hat{R} = \hat{X} = 0$, $\hat{p}_1 \leq \hat{p}_2$ and $\hat{p}_1 > 0, \hat{p}_2 > 0$. Therefore, the largest compact invariant set in $\{(\hat{S},\ \hat{I},\ \hat{R},\ \hat{X}) \in \Omega_1 : dL/d\hat{t} = 0\}$ is the singleton $\{E_0\}$. By La Salle (1976) invariant principle, it then implies that E_0 is globally asymptotically stable. □

4.3.8 Coexistence Equilibrium Point (CEP)

We consider a situation in which pathogen persist in the plant population. A coexistence equilibrium point $E^* = (\hat{S}^*, \hat{I}^*, \hat{R}^*, \hat{X}^*)$ can be computed as follows.

$$\begin{aligned} 1 - \hat{S}^* - (\hat{\beta}_p \hat{X}^* + \hat{\beta}_s \hat{I}^*)\hat{S}^* &= 0, \\ (\hat{\beta}_p \hat{X}^* + \hat{\beta}_s \hat{I}^*)\hat{S}^* - (\hat{\mu} + \hat{h})\hat{I}^* &= 0, \\ \hat{I}^* - \hat{h}\hat{R}^* &= 0, \\ \hat{I}^* - \hat{c}\hat{X}^* &= 0. \end{aligned} \tag{4.19}$$

Solving Eq. (4.19), we obtain CEP:

$$E^* = \left(\frac{(\hat{\mu}+\hat{h})\hat{c}}{\hat{\beta}_p + \hat{c}\hat{\beta}_s}, \frac{1}{\hat{\mu}+\hat{h}}\left(1 - \frac{(\hat{\mu}+\hat{h})\hat{c}}{\hat{\beta}_p + \hat{c}\hat{\beta}_s}\right), \frac{1}{\hat{h}(\hat{\mu}+\hat{h})}\left(1 - \frac{(\hat{\mu}+\hat{h})\hat{c}}{\hat{\beta}_p + \hat{c}\hat{\beta}_s}\right), \frac{1}{\hat{c}(\hat{\mu}+\hat{h})}\left(1 - \frac{(\hat{\mu}+\hat{h})\hat{c}}{\hat{\beta}_p + \hat{c}\hat{\beta}_s}\right) \right).$$

On the other hand, we can expressed E^* in terms of R_0 as:

$$E^* = \left(\frac{1}{R_0}, \frac{1}{\hat{\mu}+\hat{h}}\left(1 - \frac{1}{R_0}\right), \frac{1}{\hat{h}(\hat{\mu}+\hat{h})}\left(1 - \frac{1}{R_0}\right), \frac{1}{\hat{c}(\hat{\mu}+\hat{h})}\left(1 - \frac{1}{R_0}\right) \right). \tag{4.20}$$

Remark 4.3.2. *The coexistence equilibrium point E^* in Eq. (4.20) is biologically feasible when $R_0 > 1$.*

4.3.9 Local Stability of Coexistence Equilibrium Point

Theorem 4.3.4. *If $R_0 > 1$, then the coexistence equilibrium point E^* of model (4.3) is locally asymptotically stable, and otherwise it is unstable in Ω_1.*

Proof. From Eq. (4.11) the Jacobian matrix J^* at $E^* = (\hat{S}^*, \hat{I}^*, \hat{X}^*)$ is given by

$$J^*(E^*) = \begin{bmatrix} -R_0 & -\dfrac{\hat{\beta}_s}{R_0} & -\dfrac{\hat{\beta}_p}{R_0} \\ R_0 - 1 & \dfrac{\hat{\beta}_s}{R_0} - \hat{\mu} - \hat{h} & \dfrac{\hat{\beta}_p}{R_0} \\ 0 & 1 & -\hat{c} \end{bmatrix}. \tag{4.21}$$

The characteristic polynomial of Eq. (4.21) is given by

$$\lambda^3 + a_2\lambda^2 + a_1\lambda + a_0 = 0, \tag{4.22}$$

where

$$a_2 = \hat{c} + \hat{\mu} + \hat{h} - \frac{\hat{\beta}_s}{R_0} + R_0 = \hat{c} + \frac{\hat{\beta}_p}{\hat{c}R_0} + R_0,$$

$$a_1 = \hat{c}\left(\hat{\mu} + \hat{h}\right) + (\hat{c} + \hat{\mu} + \hat{h})R_0 - \frac{\hat{c}\hat{\beta}_s + \hat{\beta}_p}{R_0} - \frac{\hat{\beta}_s}{R_0} = \hat{\beta}_s\left(\frac{\hat{c} + \hat{\mu} + \hat{h}}{\hat{\beta}_s}\right)\left(\frac{R_0^2 - 1}{R_0}\right),$$

$$a_0 = \hat{c}(\hat{\mu} + \hat{h})R_0 - \frac{\hat{c}\hat{\beta}_s + \hat{\beta}_p}{R_0} = \hat{c}(\hat{\mu} + \hat{h})(R_0 - 1).$$

Since the characteristic polynomial in Eq.(4.22) is degree $n = 3$, then we can find matrices:

$$M1 = \begin{bmatrix} a_2 \end{bmatrix}, \quad M2 = \begin{bmatrix} a_2 & a_0 \\ 1 & a_1 \end{bmatrix}, \quad M3 = \begin{bmatrix} a_2 & a_0 & 0 \\ 1 & a_1 & 0 \\ 0 & a_2 & a_0 \end{bmatrix}.$$

Applying Routh-Hurwitz criterion (Martcheva, 2015) on Eq. (4.21) shows that all eigenvalues have negative real part, and so E^* is local asymptotically stable if $a_i > 0,\ i = 0, 1, 2$;

$$\det(M1) = \hat{c} + \frac{\hat{\beta}_p}{\hat{c}R_0} + R_0 > 0,$$

$$\det(M2) = \frac{\hat{c}^2(\hat{\mu} + \hat{h}) + \hat{c}^3 + (\hat{\mu} + \hat{h})\hat{\beta}_p}{\hat{c}} + \frac{\hat{c}\hat{\beta}_s + (\hat{c} + \hat{\mu} + \hat{h})R_0^2 + (\hat{\beta}_p + \hat{\beta}_s)R_0}{R_0} > 0,$$

$$\det(M3) = \left(\frac{\hat{c}^2(\hat{\mu} + \hat{h}) + \hat{c}^3 + (\hat{\mu} + \hat{h})\hat{\beta}_p}{\hat{c}}\right)\hat{c}(\hat{\mu} + \hat{h})(R_0 - 1)$$
$$+ \left(\frac{\hat{c}\hat{\beta}_s + (\hat{c} + \hat{\mu} + \hat{h})R_0^2 + (\hat{\beta}_p + \hat{\beta}_s)R_0}{R_0}\right)\hat{c}(\hat{\mu} + \hat{h})(R_0 - 1) > 0.$$

However, $\det(M3) > 0$ if $R_0 > 1$. Therefore, the coexistence equilibrium E^* is locally asymptotically stable for $R_0 > 1$. □

4.3.10 Global Stability of Coexistence Equilibrium Point

Theorem 4.3.5. *If $R_0 > 1$, then the coexistence equilibrium E^* of model (4.3) is globally asymptotically stable in Ω_1.*

Proof. To prove this result, consider the Lyapunov function defined by

$$\ell = \frac{[(\hat{S} - \hat{S}^*) + (\hat{I} - \hat{I}^*) + (\hat{R} - \hat{R}^*)]^2}{2} + \frac{(\hat{X} - \hat{X}^*)^2}{2}. \tag{4.23}$$

Then, applying derivative of ℓ with respect to $\hat{t}$, we find that

$$\frac{d\ell}{d\hat{t}} = [(\hat{S} - \hat{S}^*) + (\hat{I} - \hat{I}^*) + (\hat{R} - \hat{R}^*)][\frac{d\hat{S}}{d\hat{t}} + \frac{d\hat{I}}{d\hat{t}} + \frac{d\hat{R}}{d\hat{t}}] + (\hat{X} - \hat{X}^*)\frac{d\hat{X}}{d\hat{t}}. \tag{4.24}$$

On the other hand, from Eqs. (4.4) and (4.5), we have

$$\frac{d\hat{N}}{d\hat{t}} \leq 1-\hat{M}\hat{N}, \quad \frac{d\hat{X}}{d\hat{t}} \leq \frac{1}{\hat{M}} - \hat{c}\hat{X}. \tag{4.25}$$

By substituting for $d\hat{N}/d\hat{t}$ and $d\hat{X}/d\hat{t}$ from Eq. (4.25) into Eq. (4.24), we obtain

$$\begin{aligned}
\frac{d\ell}{d\hat{t}} &= [(\hat{S}-\hat{S}^*)+(\hat{I}-\hat{I}^*)+(\hat{R}-\hat{R}^*)]\frac{d\hat{N}}{d\hat{t}} + (\hat{X}-\hat{X}^*)\left(\frac{1}{\hat{M}}-\hat{c}\hat{X}\right), \\
&\leq [(\hat{S}+\hat{I}+\hat{R}+\hat{X})-(\hat{S}^*+\hat{I}^*+\hat{R}^*)](1-\hat{M}\hat{N}) + \left(\hat{X}-\frac{1}{\hat{c}\hat{M}}\right)\left(\frac{1}{\hat{M}}-\hat{c}\hat{X}\right), \\
&\leq \left(\hat{N}-\frac{1}{\hat{M}}\right)(1-\hat{M}\hat{N}) + \hat{c}\left(\hat{X}-\frac{1}{\hat{c}\hat{M}}\right)\left(\frac{1}{\hat{c}\hat{M}}-\hat{X}\right).
\end{aligned}$$

Next, rearranging the preceding equation, we obtain

$$\frac{d\ell}{d\hat{t}} \leq -\frac{1}{\hat{M}}(1-\hat{M}\hat{N})^2 - \hat{c}\left(\hat{X}-\frac{1}{\hat{c}\hat{M}}\right)^2.$$

Thus, $d\ell(\hat{S},\hat{I},\hat{R},\hat{X})/d\hat{t} \leq 0$ if and only if $\hat{S}=\hat{S}^*$, $\hat{I}=\hat{I}^*$, $\hat{R}=\hat{R}^*$, $\hat{X}=\hat{X}^*$. Hence, the maximum compact invariant set in $\left\{(\hat{S}^*,\hat{I}^*,\hat{R}^*,\hat{X}^*)\in\Omega_1 : dV/d\hat{t}=0\right\}$ is the singleton $\{E^*\}$. Therefore, by La Salle (1976) invariant principle, as $\hat{t}\to\infty$, all the solutions of the system (4.3) approaches E^* for $R_0>1$ in Ω_1. □

4.3.11 Phase Portrait Analysis

The phase portrait of our governing dynamical system (4.3) presents in graphical form in small region near the equlibria. It is drawn by using the 'quiver command' in MATLAB software. The phase portraits in Figures 4.3, 4.4, 4.5 and 4.6 show a typical solution curves and a direction field (with arrows). Now, consider the trajectory corresponding to the general solution $(\hat{S}(\hat{t}),\hat{I}(\hat{t}),\hat{R}(\hat{t}),\hat{X}(\hat{t}))$ of model (4.3). The PFEP $E_0=(1,0,0,0)$ is asymptotically stable in Figures 4.3 (a), 4.3 (b) and 4.4. That means, in these figures, the corresponding trajectories: $(\hat{S}(\hat{t}),\hat{I}(\hat{t}))$, $(\hat{I}(\hat{t}),\hat{X}(\hat{t}))$ and $(\hat{S}(\hat{t}),\hat{R}(\hat{t}))$ head into the equilibrium point $(1,0)$, $(0,0)$ and $(1,0)$ as $\hat{t}\to\infty$, respectively.

The CEP $E^*=(\hat{S}^*,\hat{I}^*,\hat{R}^*,\hat{X}^*)$ is asymptotically stable in Figures 4.5 (a), 4.5 (b) and 4.6. That is, in these figures, the corresponding trajectories:
$(\hat{S}(\hat{t}),\hat{I}(\hat{t}))$, $(\hat{I}(\hat{t}),\hat{X}(\hat{t}))$ and $(\hat{S}(\hat{t}),\hat{R}(\hat{t}))$ head into the equilibrium point $(\hat{S}^*,\hat{I}^*)$, $(\hat{I}^*,\hat{X}^*)$ and $(\hat{S}^*,\hat{R}^*)$ as $\hat{t}\to\infty$, respectively. Note that the phase portrait analysis agree with the stability analysis presented in the previous sections.

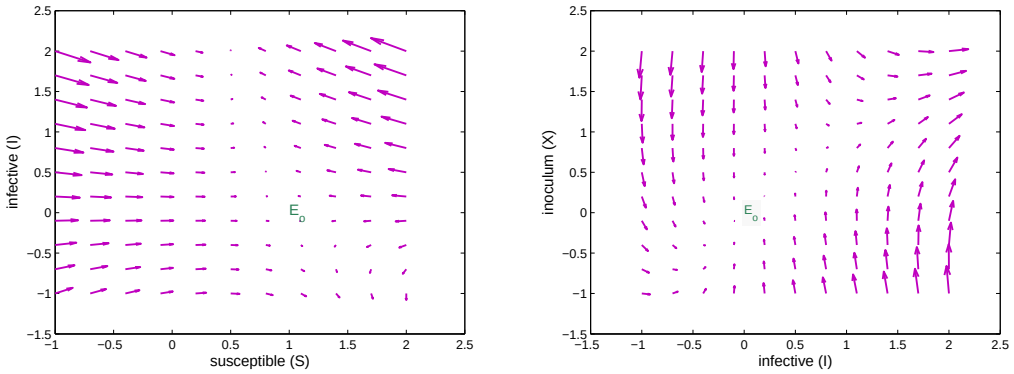

(a) Phase portrait for S vs I. (b) Phase portrait for I vs X.

Figure 4.3: Phase portrait analysis for (susceptible, infective) and (infective, inoculum) population when $R_0 < 1$. Parameter values are taken from numerical simulation section.

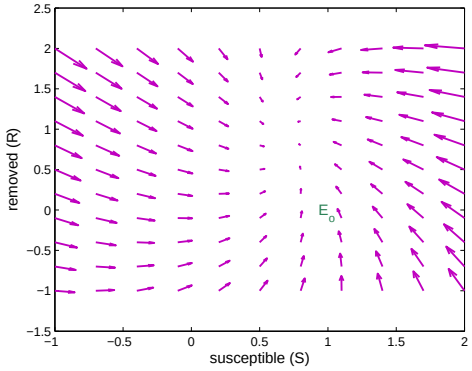

Phase portrait for S vs R.

Figure 4.4: Phase portrait analysis for (susceptible, removed) population when $R_0 < 1$.

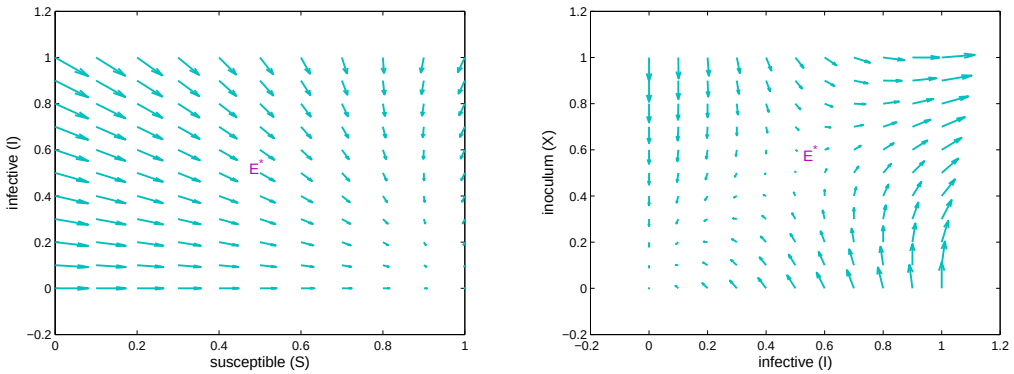

(a) Phase portraits for S vs I. (b) Phase portraits for I vs X.

Figure 4.5: Phase portrait analysis for (susceptible, infective), (infective, inoculum) population when $R_0 > 1$.

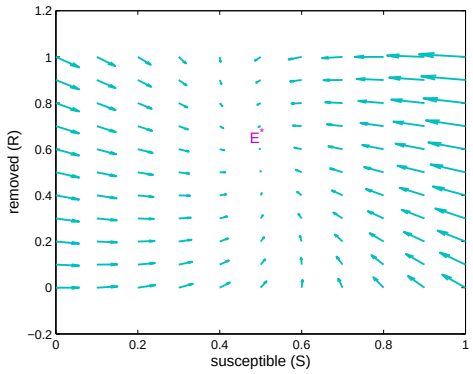

Phase portraits for S vs R.

Figure 4.6: Phase portrait analysis for (susceptible, removed) population when $R_0 > 1$.

4.3.12 Bifurcation Analysis

Bifurcation means a qualitative change due to parameter value change at non-hyperbolic equilibrium. To study the existence of the bifurcation of model (4.3) at $R_0 = 1$, we apply the center manifold theory as stated in (Castillo-Chavez and Song, 2004). For this, we have the following theorem.

Theorem 4.3.6. *If $R_0 < 1$, then model (4.3) exhibits forward bifurcation at $R_0 = 1$.*

Proof. To prove this theorem, first we consider change of variables as: $\hat{S} = y_1$, $\hat{I} = y_2$, $\hat{R} = y_3$, $\hat{X} = y_4$. Then the model equation can be rewritten compactly in the form $dy/d\hat{t} = (g_1, g_2, g_3, g_4)^T$:

$$\begin{cases} \dfrac{dy_1}{d\hat{t}} = 1 - y_1 - (\hat{\beta}_p y_4 + \hat{\beta}_s y_2) y_1, \\ \dfrac{dy_2}{d\hat{t}} = (\hat{\beta}_p y_4 + \hat{\beta}_s y_2) y_1 - (\hat{\mu} + \hat{h}) y_2, \\ \dfrac{dy_3}{d\hat{t}} = y_2 - \hat{h} y_3, \\ \dfrac{dy_4}{d\hat{t}} = y_2 - \hat{c} y_4. \end{cases} \tag{4.26}$$

We consider the primary transmission rate $\hat{\beta}_p$ as bifurcation parameter so that $R_0 = 1$ if

$$\hat{\beta}_p = \hat{\beta}_p^* = \hat{c}(\hat{\mu} + \hat{h} - \hat{\beta}_s). \tag{4.27}$$

The Jacobian matrix of Eq. (4.26) at pathogen free equilibrium E_0 is given by

$$J(E_0, \hat{\beta}_p^*) = \begin{bmatrix} -1 & -\hat{\beta}_s & 0 & -\hat{\beta}_p^* \\ 0 & \hat{\beta}_s - \hat{\mu} - \hat{h} & 0 & \hat{\beta}_p^* \\ 0 & 1 & -\hat{h} & 0 \\ 0 & 1 & 0 & -\hat{c} \end{bmatrix}.$$

The right eigenvector, $u = (u_1,\ u_2,\ u_3,\ u_4)^T$ are computed from $J(E_0, \hat{\beta}_p^*)u = 0$ as follows.

$$J(E_0,\hat{\beta}_p^*)u = \begin{cases} -u_1 - \hat{\beta}_s u_2 - \hat{\beta}_p^* u_4 = 0, \\ (\hat{\beta}_s - \hat{\mu} - \hat{h})u_2 + \hat{\beta}_p^* u_4 = 0, \\ u_2 - \hat{h}u_3 = 0, \\ u_2 - \hat{c}u_4 = 0. \end{cases} \tag{4.28}$$

Next, from Eq. (4.28), we get

$$u_1 = -(\hat{\mu} + \hat{h})u_2,\ u_3 = \frac{u_2}{\hat{h}},\ u_4 = \frac{u_2}{\hat{c}},$$

where $u_2 = u_2 > 0$. Also the left eigenvector, $v = (v_1,\ v_2,\ v_3,\ v_4)$ are computed from $vJ(E_0, \hat{\beta}_p^*) = 0$ as follows.

$$vJ(E_0,\hat{\beta}_p^*) = \begin{cases} -v_1 = 0, \\ -\hat{\beta}_s v_1 + (\hat{\beta}_s - \hat{\mu} - \hat{h})v_2 + v_3 + v_4 = 0, \\ -\hat{h}v_3 = 0, \\ -\hat{\beta}_p^* v_1 + \hat{\beta}_p^* v_2 - \hat{c}v_4 = 0. \end{cases} \tag{4.29}$$

Solving Eq. (4.29) and then we obtain

$$v_1 = v_3 = 0,\ v_2 = \frac{-1}{\hat{\beta}_s - \hat{\mu} - \hat{h}}v_4,$$

where $v_4 = v_4 > 0$. Based on Castillo-Chavez and Song (2004), the bifurcation coefficients: a and b are given by

$$\begin{aligned} a &= \sum_{i,j,k=1}^{4} v_k u_i u_j \frac{\partial^2 g_k}{\partial y_i \partial y_j}(E_0, \hat{\beta}_p^*), \\ b &= \sum_{i,k=1}^{4} v_k u_i \frac{\partial^2 g_k}{\partial y_i \partial \hat{\beta}_p^*}(E_0, \hat{\beta}_p^*). \end{aligned} \tag{4.30}$$

The nonzero second partial derivatives of g_1 and g_2 at E_0 are given as follows.

$$\begin{aligned} &\frac{\partial^2 g_1}{\partial y_1 \partial y_2} = \frac{\partial^2 g_1}{\partial y_2 \partial y_1} = -\hat{\beta}_s,\ \frac{\partial^2 g_1}{\partial y_1 \partial y_4} = \frac{\partial^2 g_1}{\partial y_4 \partial y_1} = -\hat{\beta}_p^*, \\ &\frac{\partial^2 g_2}{\partial y_1 \partial y_2} = \frac{\partial^2 g_2}{\partial y_2 \partial y_1} = \hat{\beta}_s,\quad \frac{\partial^2 g_2}{\partial y_1 \partial y_4} = \frac{\partial^2 g_2}{\partial y_4 \partial y_1} = \hat{\beta}_p^*, \\ &\frac{\partial^2 g_1}{\partial y_4 \partial \hat{\beta}_p^*} = \frac{\partial^2 g_1}{\partial \hat{\beta}_p^* \partial y_4} = -1,\ \frac{\partial^2 g_2}{\partial y_4 \partial \hat{\beta}_p^*} = \frac{\partial^2 g_2}{\partial \hat{\beta}_p^* \partial y_4} = 1. \end{aligned} \tag{4.31}$$

All the others second partial derivatives of $g_i,\ i = 1,...,4$ are zero. By using Eq. (4.30), we

get

$$\begin{aligned} a &= 2v_1u_1u_2\frac{\partial^2 g_1}{\partial y_1\partial y_2} + 2v_4u_1u_4\frac{\partial^2 g_1}{\partial y_1\partial y_4} + 2v_2u_1u_2\frac{\partial^2 g_2}{\partial y_1\partial y_2} + 2v_2u_1u_4\frac{\partial^2 g_2}{\partial y_1\partial y_4} \\ &= \frac{2(\hat{\mu}+\hat{h})v_4u_2^2}{\hat{\beta}_s-\hat{\mu}-\hat{h}}\left(\hat{\beta}_s+\frac{\hat{\beta}_p^*}{\hat{c}}\right) \\ &= -\frac{2(\hat{\mu}+\hat{h})^2v_4u_2^2}{\hat{\mu}+\hat{h}-\hat{\beta}_s} < 0, \end{aligned} \tag{4.32}$$

and

$$\begin{aligned} b &= 2v_1u_4\frac{\partial^2 g_1}{\partial y_4\partial\hat{\beta}_p^*} + 2v_2u_4\frac{\partial^2 g_2}{\partial y_4\partial\hat{\beta}_p^*} \\ &= \frac{2(-v_4)}{\hat{\beta}_s-\hat{\mu}-\hat{h}}\frac{u_2}{\hat{c}}, \\ &= \frac{2v_4u_2}{\hat{c}(\hat{\mu}+\hat{h}-\hat{\beta}_s)} > 0, \end{aligned} \tag{4.33}$$

where $\hat{\beta}_p/\hat{c} = \hat{\mu}+\hat{h}-\hat{\beta}_s > 0$ directly follows from Eq. (4.27). Since the coefficient a is negative and b is positive, then the model exhibits forward bifurcation at $R_0 = 1$ and there exists at least one stable coexistence equilibrium when $R_0 > 1$. □

4.4 The Extended Model into Optimal Control

In this section, we extend model (4.3) into an optimal control problem by including control variables. This helped us to choose appropriate control strategies that are used to eliminate pathogens from the plant population at the end of the control strategy. The two introduced control variables are quarantine (prevent the entrance and establishment of a plant pathogen in a country where it does not exist) and chemical (using chemical spray to kill the pathogens and their carriers). At time t, $u_1(t)$ and $u_2(t)$ respectively, denotes quarantine and chemical control. All these assumptions are based on Hall et al. (2004) who discussed that chemical control may reduce the infectious periods and Cook and Baker Cook et al. (1983) who discussed that cultural or biological control may accelerate the decay of inoculum pathogen. Thus, we assume that the proposed controls are appropriate for the pathogen elimination

from the system. Hence, the corresponding state system for the model (4.3) is given by

$$\begin{cases} \dfrac{d\hat{S}}{d\hat{t}} = 1-\hat{S}-(\hat{\beta}_p\hat{X}+(1-u_1)\hat{\beta}_s\hat{I})\hat{S}, \\ \dfrac{d\hat{I}}{d\hat{t}} = (\hat{\beta}_p\hat{X}+(1-u_1)\hat{\beta}_s\hat{I})\hat{S}-(\hat{\mu}+\hat{h})\hat{I}, \\ \dfrac{d\hat{R}}{d\hat{t}} = \hat{I}-\hat{h}\hat{R}, \\ \dfrac{d\hat{X}}{d\hat{t}} = \hat{I}-(1+u_2)\hat{c}\hat{X}, \end{cases} \tag{4.34}$$

with initial data: $\hat{S}(0)=\hat{S}_0$, $\hat{I}(0)=\hat{I}_0$, $\hat{R}(0)=\hat{R}_0$, $\hat{X}(0)=\hat{X}_0$.
The objective function J is given by

$$J(u) = \min_{u} \int_0^{\hat{t}_f} \left(d\hat{I} + \frac{1}{2}\sum_{i=1}^{2} b_i u_i^2 \right) d\hat{t}, \tag{4.35}$$

where $\hat{t}_f$ is the final time, the constants $d,\ b_1,\ b_2 > 0$, and $u=(u_1,u_2)$. The term $0.5b_1u_1^2$ and $0.5b_2u_2^2$ represent cost functions which are corresponding to the control u_1 and u_2, respectively. The performance specification involves the minimization of infected plants and the cost incurred due to control strategies. Our aim is to find the optimal controls u_1^* and u_2^* such that

$$J(u^*) = min\left\{J(u_1,\ u_2):\ u_i \in U\right\}, \tag{4.36}$$

where U is a measurable set:

$$U = \left\{u(\hat{t}) = (u_1(\hat{t}),\ u_2(\hat{t})) : 0 \le u_i(\hat{t}) \le 1,\ 0 \le \hat{t} \le \hat{t}_f,\ i = 1,2\right\}.$$

4.4.1 The Hamiltonian Function

Pontryagin's minimum principle (Pontryagin, 2018) helps to reduces problems (4.34)-(4.36) to a problem of minimizing the Hamiltonian H given by

$$\begin{aligned} H(\varphi,u,\lambda) = {} & d\hat{I} + \frac{b_1u_1^2}{2} + \frac{b_2u_2^2}{2} + \lambda_1(1-\hat{S}-(\hat{\beta}_p\hat{X}+(1-u_1)\hat{\beta}_s\hat{I})\hat{S}) \\ & + \lambda_2((\hat{\beta}_p\hat{X}+(1-u_1)\hat{\beta}_s\hat{I})\hat{S}-(\hat{\mu}+\hat{h})\hat{I}) + \lambda_3(\hat{I}-\hat{h}\hat{R}) + \lambda_4(\hat{I}-(1+u_2)\hat{c}\hat{X}), \end{aligned} \tag{4.37}$$

where $\varphi=(\hat{S},\hat{I},\hat{R},\hat{X})$. Based on Pang et al. (2015), if the control u^* and corresponding state φ^* are an optimal couple, necessarily there is a non-zero adjoint vector $\lambda=(\lambda_1,\lambda_2,\lambda_3,\lambda_4)$

so that

$$\begin{cases} \dfrac{d\varphi}{d\hat{t}} = \dfrac{\partial H(\varphi,u,\lambda)}{\partial \lambda}, \\ \dfrac{d\lambda}{d\hat{t}} = -\dfrac{\partial H(\varphi,u,\lambda)}{\partial \varphi}, \\ \dfrac{\partial H(\varphi,u,\lambda)}{\partial u} = 0. \end{cases} \tag{4.38}$$

From the boundedness of u_i^* on $[0,1]$ and the third equation of Eq. (4.38) (minimality condition), we have

$$\begin{cases} u_i^* = 0, & \dfrac{\partial H}{\partial u_i} > 0, \\ 0 < u_i^* < 1, & \dfrac{\partial H}{\partial u_i} = 0, \\ u_i^* = 1, & \dfrac{\partial H}{\partial u_i} < 0. \end{cases}$$

To obtain the adjoint variables $\lambda_i,\ i = 1,...,4$, we follow the classical result of (Pontryagin, 2018). So the next theorem can be established.

4.4.2 Characterization of Optimal Control Solutions

Theorem 4.4.1. *Let u^* be the solution to the optimal control problem, Eqs. (4.34)-(4.36) and φ^* be the corresponding optimal state. Then there exist adjoint variables $\lambda_i,\ i = 1,...,4$ that satisfy the adjoint system*

$$\begin{cases} \dfrac{d\lambda_1}{d\hat{t}} = \lambda_1(1+\hat{\beta}_p\hat{X}+(1-u_1)\hat{\beta}_s\hat{I}) - \lambda_2(\hat{\beta}_p\hat{X}+(1-u_1)\hat{\beta}_s\hat{I}), \\ \dfrac{d\lambda_2}{d\hat{t}} = -d+\lambda_1(1-u_1)\hat{\beta}_s\hat{S} - \lambda_2((1-u_1)\hat{\beta}_s\hat{S}-\hat{\mu}-\hat{h}) - \lambda_3 - \lambda_4, \\ \dfrac{d\lambda_3}{d\hat{t}} = \lambda_3\hat{h}, \\ \dfrac{d\lambda_4}{d\hat{t}} = (\lambda_1-\lambda_2)\hat{\beta}_p\hat{I} + \lambda_4(1+u_2)\hat{c}. \end{cases} \tag{4.39}$$

Together with transversality condition: $\lambda_i(t_f) = 0,\ i = 1,...,4$.
And also, we get optimal controls $u_1^*(\hat{t})$ and $u_2^*(\hat{t})$ which are characterized by

$$\begin{aligned} u_1^*(\hat{t}) &= min\left\{max\left\{0, \frac{\hat{\beta}_s\hat{S}\hat{I}(\lambda_2-\lambda_1)}{b_1}\right\}, 1\right\}, \\ u_2^*(\hat{t}) &= min\left\{max\left\{0, \frac{\hat{c}\hat{X}\lambda_4}{b_2}\right\}, 1\right\}. \end{aligned} \tag{4.40}$$

Proof. We find that the adjoint equations from the second equation of (4.38):

$$\begin{cases} \dfrac{d\lambda_1}{d\hat{t}} = -\dfrac{\partial H}{\partial \hat{S}} = \lambda_1(1+\hat{\beta}_p\hat{X}+(1-u_1)\hat{\beta}_s\hat{I}) - \lambda_2(\hat{\beta}_p\hat{X}+(1-u_1)\hat{\beta}_s\hat{I}), \\ \dfrac{d\lambda_2}{d\hat{t}} = -\dfrac{\partial H}{\partial \hat{I}} = -d+\lambda_1(1-u_1)\hat{\beta}_s\hat{S} - \lambda_2((1-u_1)\hat{\beta}_s\hat{S} - \hat{\mu} - \hat{h}) - \lambda_3 - \lambda_4, \\ \dfrac{d\lambda_3}{d\hat{t}} = -\dfrac{\partial H}{\partial \hat{R}} = \lambda_3\hat{h}, \\ \dfrac{d\lambda_4}{d\hat{t}} = -\dfrac{\partial H}{\partial \hat{X}} = (\lambda_1-\lambda_2)\hat{\beta}_p\hat{I} + \lambda_4(1+u_2)\hat{c}. \end{cases} \tag{4.41}$$

We assume that $\hat{S}(\hat{t}_f)$, $\hat{I}(\hat{t}_f)$, $\hat{R}(\hat{t}_f))$ and $\hat{X}(\hat{t}_f)$ are free, then we obtain the transversality condition: $\lambda_i(\hat{t}_f) = 0$.
We find that the optimal controls $u_1^*(\hat{t})$ and $u_2^*(\hat{t})$ from the third equation of (4.38) as follows.

$$\begin{aligned} \frac{\partial H}{\partial u_1} &= b_1u_1 + \hat{\beta}_s\hat{S}\hat{I}(\lambda_1-\lambda_2) = 0 \Rightarrow u_1^*(\hat{t}) = \frac{\hat{\beta}_s\hat{S}\hat{I}(\lambda_2-\lambda_1)}{b_1}, \\ \frac{\partial H}{\partial u_2} &= b_2u_2 - \hat{c}\hat{X}\lambda_4 = 0 \qquad\qquad \Rightarrow u_2^*(\hat{t}) = \frac{\hat{c}\hat{X}\lambda_4}{b_2}. \end{aligned}$$

Since $0 \le u_i^*(\hat{t}) \le 1$, then $u_i^*(\hat{t})$ can be rewritten in compact form as in Eq. (4.40). □

It is clear that the second derivative of Hamiltonian function H with respect to (u_1,u_2) at (u_1^*,u_2^*) (i.e., Hessian matrix) is positive definite. This shows that the optimal control pairs (u_1^*,u_2^*) is a minimizer.

4.5 Numerical Simulations

In this section, we illustrate the solutions of the dimensionless model (4.3) and corresponding state system (4.34) numerically with the impact of controls: quarantine control u_1 and chemical control u_2 on the dynamics of plant pathogen. Since the optimal system under investigation is a two point boundary value problem with separated boundary conditions at times $\hat{t}=0$ and $\hat{t}=\hat{t}_f$, we use the forward-backward iterative scheme discussed in (Lenhart and Workman, 2007).

To obtain the intended numerical solutions, we first fix the initial guess for the control variables, then solve the governing model (4.34) forward in time by using a fourth-order Runge-Kutta method. Next, using the current iteration solutions obtained for the state system and the transversality conditions, the adjoint systems (4.39) are also solved backward in time by applying the fourth-order Runge-Kutta algorithm. At each iteration time, the controls (4.40) are then updated using a convex combination of the previously computed results. The updated controls are, then utilized to repeat the iteration and compute the solutions of the state and adjoint system until a predefined convergence criterion is met.

For simulation purposes, parameter values and initial data are presented to support our previous analytical results. Accordingly, we assumed the parameter values as: $\hat{\beta}_p = 1$, $\hat{\beta}_s = 1$, $\hat{\mu} = 0.2$, $\hat{h} = 0.8$, $\hat{c} = 0.9$ and initial condition: $\hat{S}(0) = 0$, $\hat{I}(0) = 2$, $\hat{R}(0) = 4$, and $\hat{X}(0) = 1$. Further, the weight constants of the objective functional are assumed as: $d = 1000$, $b_1 = 3$, $b_2 = 3$, and the adjoint system with terminal condition: $\lambda_i(\hat{t}_f) = 0$, $i = 1,...,4$ and final implementation time $\hat{t}_f = 12$ months.

In the following subsections, we compare the impact of control strategies on the spread of disease under different scenarios. In the figures, we compare the cases with (blue curve) and without (red broken curve) controls in the presence of pathogens.

4.5.1 Control Strategy using Quarantine

In the first case, we consider quarantine $u_1 \neq 0$ as control without using chemical $u_2 = 0$. The aim of this case is to investigate the impact of quarantine alone on pathogen dynamics. The simulation results are displayed in Figure 4.7. As shown in Figure 4.7 (a) the susceptible plants are increasing when they are protected from pathogens. On the contrary, Figure 4.7 (b) illustrates the scenario in which the infected plants are declining. This is due to the separation of infected plants from susceptible ones. Hence, the applied strategy seems reasonable in reducing the impact of pathogens within the intervention period and thus can be considered an optimal candidate to minimize the spread of pathogens in the plant population.

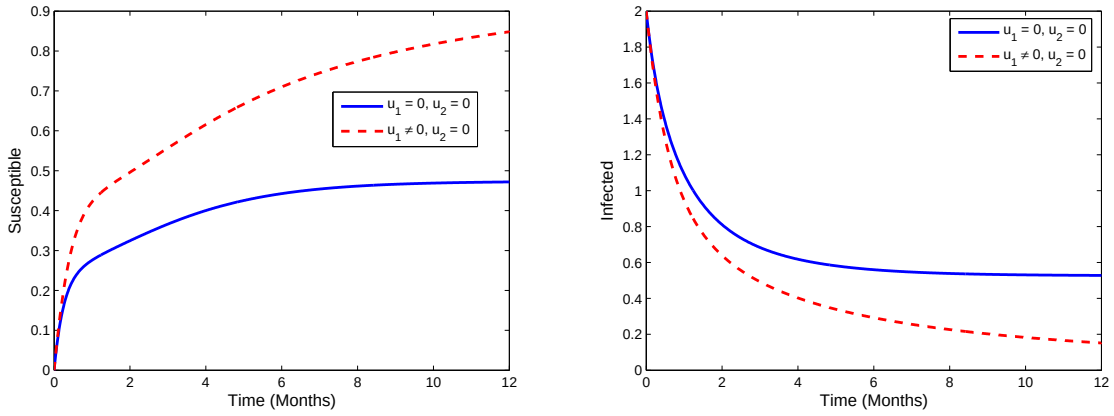

(a) Susceptible population with and without quarantine.

(b) Infected population with and without quarantine.

Figure 4.7: Simulation results comparing the impact of quarantine on susceptible and infected plant population

4.5.2 Control Strategy using Chemical

In the second simulation case, we used chemicals as a control strategy to investigate the behaviors of these state variables. That is, $u_1 = 0$ and $u_2 \neq 0$. This means spraying insecticide on the farm instead of quarantining the infected plant. The corresponding simulation result is illustrated in Figure 4.8. Despite its environmental issues, this approach is also effective in managing the impact of pathogens on plant populations as shown in Figure 4.8 (a) and 4.8 (b). The use of chemicals reduces the infected size while the susceptible raise in size.

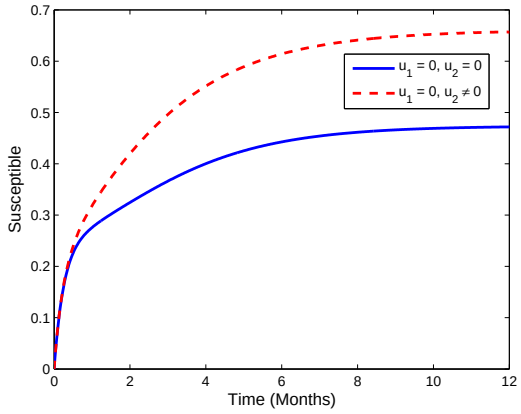

(a)Susceptible population with and without chemical.

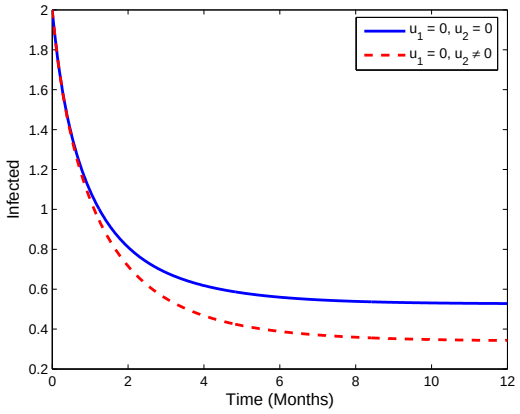

(b)Infected population with and without chemical.

Figure 4.8: Simulation results of susceptible and infected plant population in the case of using chemical as control strategy.

4.5.3 Control Strategy using Quarantine and Chemical

In this case, we discuss how quarantine and chemicals affect the pathogen spread in the plant population. Again, we assume the same initial data and parameter values as above. The corresponding simulation results are displayed in Figure 4.9. From this figure, one can easily see that the size of infected plants is highly reduced while the susceptible gain in size. Thus, the combined effect of both quarantine and chemicals strongly reduced the infected plant population compared to other cases. Furthermore, Figure 4.9 (c) displays that the number of inoculum pathogens approaches zero at the end of intervention time. Hence, the best choice is to apply both controls to effectively manage the impact of pathogens on the spread of plant pathogens.

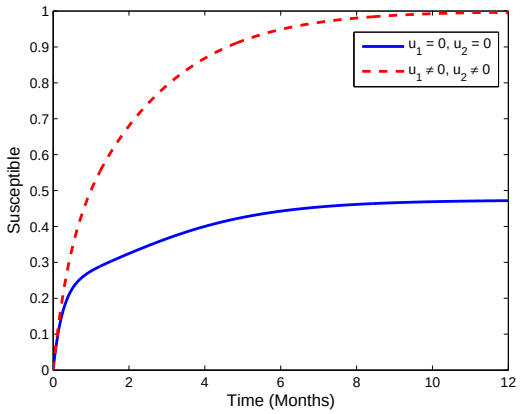

(a)Susceptible population with and without controls.

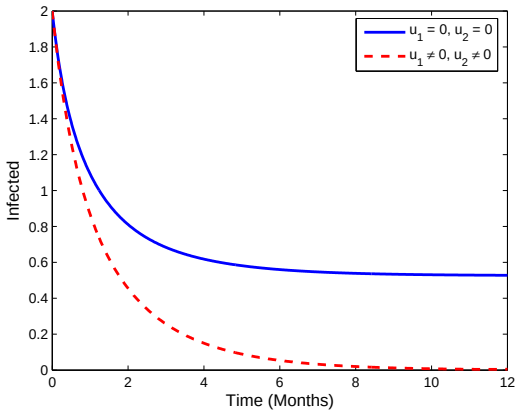

(b) Infected population with and without controls.

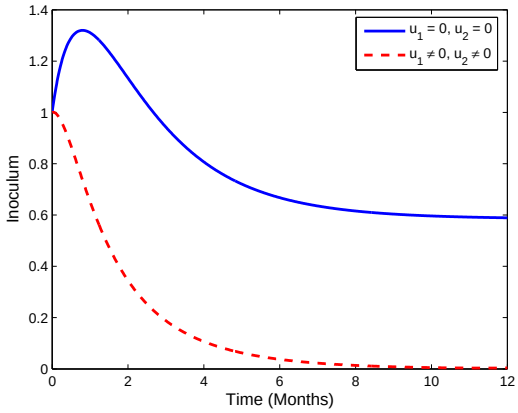

(c) Pathogen population with and without controls.

Figure 4.9: Simulation results of susceptible, infected plant and pathogen population in the case of using quarantine and chemical as controls strategy.

CHAPTER 5

MODELLING THE DYNAMICS OF COFFEE BERRY DISEASE WITH OPTIMAL CONTROL

5.1 Model Derivation

This study considers the coffee berry population and vector population with the interaction of fungal pathogen concentration. Coffee berry is sometimes affected by fungal pathogen (B). The CBD occurrence depended mostly on altitude ranges; higher sites were more frequently infected than lower sites due to more favorable climatic conditions for the reproduction of pathogen.

The coffee berry population is considered into two forms: the susceptible coffee berry (S_c) and infected coffee berry (I_c). Due to the limited size of a coffee plantation, we adopted a logistic growth function for the biomass density of coffee berries. The coffee berry population grows logistically (Abraha et al., 2021) with growth rate r and environmental carrying capacity K. Susceptible coffee berry moves to the infected class following contact with the infected vector at a per capita rate of β_2 and its mortality rate is θ. The infected coffee berry is induced to pathogen reserver at rate η and its death rate is γ due to the disease. The coffee berry once became infected, never recovers, and gives no or very low yield of coffee.

The vector population is divided into two form: the susceptible vector (S_v) and infected vector (I_v). Susceptible vectors can be infected in two ways: by direct interaction with the pathogen from the environment at rate β_1 and by interaction with an already infected coffee berry at rate β_3. The susceptible vector is recruited at rate λ. The susceptible and infected vector death rate is represented by δ. The fungal pathogens in the environment may be transported to the coffee plant via the infected vectors, once the coffee berry becomes infected, the fungal increases within the infected coffee and destroy it. This invariably adds to the fungal pathogens in the environment at rate η and the infected coffee berry fungal pathogen contribution to the environment is (ηI_c). The fungal pathogen's decay rate is m. The schematic diagram of CBD transmission is illustrated in Figure 5.1.

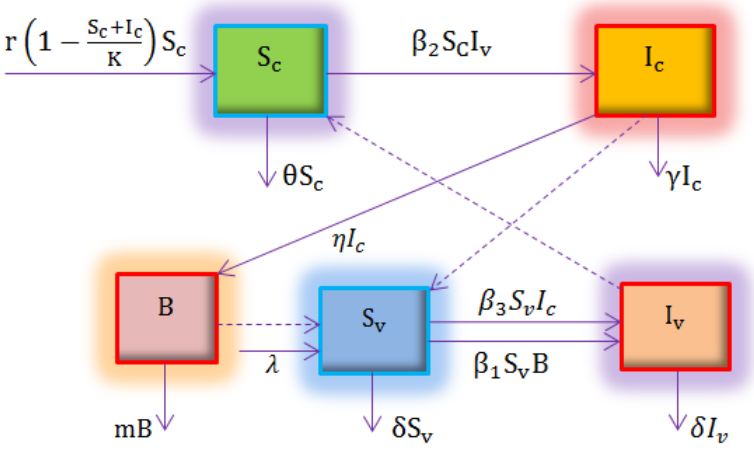

Figure 5.1: Schematic diagram of CBD dynamics

The governing mathematical model is described by the following nonlinear systems of differential equations:

$$\begin{aligned}
\frac{dS_c}{dt} &= rS_c\left(1-\frac{S_c+I_c}{K}\right)-\beta_2 S_c I_v-\theta S_c,\\
\frac{dI_c}{dt} &= \beta_2 S_c I_v-(\gamma+\eta)I_c,\\
\frac{dS_v}{dt} &= \lambda-(\beta_1 B+\beta_3 I_c)S_v-\delta S_v,\\
\frac{dI_v}{dt} &= (\beta_1 B+\beta_3 I_c)S_v-\delta I_v,\\
\frac{dB}{dt} &= \eta I_c-mB.
\end{aligned} \tag{5.1}$$

Together with initial condition:

$$S_c(0)=S_{c0}>0,\ I_c(0)=I_{c0}\geq 0,\ S_v(0)=S_{v0}>0,\ I_v(0)=I_{v0}\geq 0,\ B(0)=B_0\geq 0. \tag{5.2}$$

5.2 Model Analysis

In this section, we study the existence-uniqueness, positivity and boundedness of the solutions, invariant region, disease-free and endemic equilibrium point, basic reproduction number and its sensitivity index, bifurcation analysis, local and global stability of the system (5.1).

5.2.1 Positivity and Boundedness of Solutions

In this subsection, we need to prove that the solutions of system (5.1) are nonnegative for all $t \geq 0$. This will be stated as follows.

Theorem 5.2.1. *Every solution of system* (5.1) *with initial condition* (5.2) *will remain positive in* $\mathbb{R}^5_+$ *as* $t > 0$.

Proof. (See Fotso et al. (2019)). From the system (5.1), we obtain
$\left.\frac{dS_c}{dt}\right|_{[S_c=0]} \geq 0$, $\left.\frac{dI_c}{dt}\right|_{[I_c=0]} = \beta_2 S_c I_v \geq 0$, $\left.\frac{dS_v}{dt}\right|_{[S_v=0]} = \lambda > 0$, $\left.\frac{dI_v}{dt}\right|_{[I_v=0]} = (\beta_1 B + \beta_3 I_c) S_v \geq 0$,
$\left.\frac{dB}{dt}\right|_{[B=0]} = \eta I_c > 0$.

This implies that all the solutions with positive initial data remains nonnegative in $\mathbb{R}^5_+$ for all $t \geq 0$. This means, the region attracts all solutions of the governing system (5.1). □

Moreover, it is easy to verify that there exist an invariant region Ω_2 where a solution set for the system (5.1) is bounded.

Theorem 5.2.2. *Every solution of system* (5.1) *initiating in* $\mathbb{R}^5_+$ *is uniformly bounded in the region*

$$\Omega_2 = \Omega_c \times \Omega_v \times \Omega_p = \left\{ (S_c,\ I_C,\ S_v,\ I_v,\ B) \in \mathbb{R}^5_+ : N_c \leq \frac{M(1+r)}{h},\ N_v \leq \frac{\lambda}{\delta}, B \leq \frac{M(1+r)\eta}{mh} \right\},$$

where

$$\Omega_c = \left\{ (S_c,\ I_c) \in \mathbb{R}^2_+ : N_c \leq \frac{M(1+r)}{h} \right\},$$
$$\Omega_v = \left\{ (S_v,\ I_v) \in \mathbb{R}^2_+ : N_v \leq \frac{\lambda}{\delta} \right\},$$
$$\Omega_p = \left\{ B \in \mathbb{R}_+ : 0 \leq B \leq \frac{M(1+r)\eta}{mh} \right\},$$

with $M = max\{S_c(0),\ K\}$, $h = min\{1, \gamma + \eta\}$.

Proof. Let $N_c(t) = S_c(t) + I_c(t)$ be the total population of coffee berry. Then differentiating $N_c(t)$ with respect to time t and adding the first two equations of system (5.1), we get

$$\frac{dN_c}{dt} \leq rS_c - (\gamma + \eta) I_c = (1+r)S_c - S_c - (\gamma + \eta) I_c. \tag{5.3}$$

The last inequality in Eq. (5.3) can be rewritten as

$$\frac{dN_c}{dt} + hN_c \leq M(1+r). \tag{5.4}$$

Integrating Eq. (5.4) by separation of variables, we get

$$N_c(t) \leq \frac{M(1+r)}{h} + \left(N_c(0) - \frac{M(1+r)}{h} \right) e^{-ht}. \tag{5.5}$$

As $t \to \infty$ in Eq. (5.5), the population size $N_c(t) \to M(1+r)/h$. Thus, the feasible region of the system (5.1) for coffee population is given by

$$\Omega_c = \left\{ (S_c,\, I_c) \in \mathbb{R}^2_+ : N_c \leq \frac{M(1+r)}{h} \right\}.$$

We also consider the total population of vector as $N_v(t) = S_v(t) + I_v(t)$. Then the derivative of $N_v(t)$ with respect to t is given by

$$\frac{dN_v}{dt} = \lambda - \delta N_v. \tag{5.6}$$

By solving Eq. (5.6) and as $t \to \infty$, we get $N_v(t) \leq \lambda/\delta$. Thus, the feasible region of the system (5.1) for vector population is given by

$$\Omega_v = \left\{ (S_v,\, I_v) \in \mathbb{R}^2_+ : N_v \leq \frac{\lambda}{\delta} \right\}. \tag{5.7}$$

From the fifth equation of system (5.1) and by the comparison, we have

$$\begin{aligned} \frac{dB}{dt} = \eta I_c - mB &\leq \eta (S_c + I_c) - mB, \\ &\leq \frac{\hat{K}(1+r)\eta}{h} - mB. \end{aligned} \tag{5.8}$$

Solving the last inequality of Eq. (5.8) and $t \to \infty$ results $0 \leq B(t) \leq (M(1+r)\eta)/mh$. Consequently, the feasible region of the system (5.1) is given by

$$\Omega_2 = \left\{ (S_c,\, I_C,\, S_v,\, I_v,\, B) \in \mathbb{R}^5_+ : N_c \leq \frac{M(1+r)}{h},\, N_v \leq \frac{\lambda}{\delta}, 0 \leq B \leq \frac{M(1+r)\eta}{mh} \right\}$$

is positively invariant. □

Hence, the solutions of the model are bounded in Ω_2. Therefore, the model is suitable to conduct the study, and the analysis of the system dynamics can be considered in Ω_2.

5.2.2 Existence and Uniqueness of Solutions

In this section, we provide the following results which guarantee that the CBD model governed by system (5.1) is epidemiologically and mathematically well posed.

Theorem 5.2.3. *(Existence-uniqueness of solution). Let Θ be the domain:*

$$|t - t_0| \leq a, \|x - x_0\| \leq b, x = (x_1, x_2, ..., x_n), x_0 = (x_{10}, x_{20}, ..., x_{n0}) \tag{5.9}$$

and suppose that $f(t,x)$ satisfies the Lipschitz condition:

$$\|f(t,x_1)-f(t,x_2)\| \leq \kappa \|x_1-x_2\|, \tag{5.10}$$

where (t,x_1), $(t,x_2) \in \Theta$, and $\kappa > 0$. Then, there exist a constant $\nu > 0$ such that there exists a unique continuous vector solution $x(t)$ of the system (5.1) in the interval $|t-t_0| \leq \nu$. From Eq (5.10), f is satisfied by requirement that $\partial f_i/\partial x_j$, $i,j = 1,2,...,5$ be continuous and bounded in Θ.

If $f(t,x)$ has continuous partial derivative $\partial f_i/\partial x_j$ on a bounded closed convex domain $\mathbb{R}$, then it satisfies a Lipschitz condition in $\mathbb{R} \in (0,\infty)$. Our concern is in the domain:

$$1 \leq \varepsilon \leq \mathbb{R}. \tag{5.11}$$

Let Θ denote the region defined in Eq (5.9) such that Eqs (5.10) and (5.11) hold. Then, there exist a solution of system (5.1) which is bounded in Θ.

Proof. (See Ayoade et al. (020b)). We need to show $\partial f_i/\partial x_j$, $i,j = 1,2,...,5$ are continuous and bounded. Suppose that the right side of system (5.1) is re-written as:

$$\begin{aligned}
f_1 &= rS_c\left(1-\frac{S_c+I_c}{K}\right)-\beta_2 S_c I_v-\theta S_c,\\
f_2 &= \beta_2 S_c I_v-(\gamma+\eta)I_c,\\
f_3 &= \lambda-(\beta_1 B+\beta_3 I_c)S_v-\delta S_v,\\
f_4 &= (\beta_1 B+\beta_3 I_c)S_v-\delta I_v,\\
f_5 &= \eta I_c-mB.
\end{aligned} \tag{5.12}$$

From the first equation of (5.12),

$$\left|\frac{\partial f_1}{\partial S_c}\right| = \left|r-\left(\frac{2rS_c+rI_c}{K}+\beta_2 I_v+\theta\right)\right| \leq r+\frac{2rS_c+rI_c}{K}+\beta_2 I_v+\theta < \infty; \left|\frac{\partial f_1}{\partial I_c}\right| = \frac{rS_c}{K} < \infty;$$
$$\left|\frac{\partial f_1}{\partial S_v}\right| = 0 < \infty; \left|\frac{\partial f_1}{\partial I_v}\right| = |-\beta_2 S_c| = \beta_2 S_c < \infty; \left|\frac{\partial f_1}{\partial B}\right| = 0 < \infty.$$

Also, consider second equation of (5.12),

$$\left|\frac{\partial f_2}{\partial S_c}\right| = |-\beta_2 I_v| = \beta_2 I_v < \infty; \left|\frac{\partial f_2}{\partial I_c}\right| = |-(\gamma+\eta)| = \gamma+\eta < \infty; \left|\frac{\partial f_2}{\partial S_v}\right| = 0 < \infty; \left|\frac{\partial f_2}{\partial I_v}\right| =$$
$$|-\beta_2 S_c| = \beta_2 S_c < \infty; \left|\frac{\partial f_2}{\partial B}\right| = 0 < \infty.$$

From the third equation of (5.12),

$$\left|\frac{\partial f_3}{\partial S_c}\right| = 0 < \infty; \left|\frac{\partial f_3}{\partial I_c}\right| = |-\beta_3 S_v| = \beta_3 S_v < \infty; \left|\frac{\partial f_3}{\partial S_v}\right| = |-(\beta_1 B+\beta_3 I_c+\delta)| = \beta_1 B+\beta_3 I_c+$$

$$\delta < \infty; \left|\frac{\partial f_3}{\partial I_v}\right| = 0 < \infty; \left|\frac{\partial f_3}{\partial B}\right| = |-\beta_1 S_v| = \beta_1 S_v < \infty.$$

From the fourth equation of (5.12),

$$\left|\frac{\partial f_4}{\partial S_c}\right| = 0 < \infty; \left|\frac{\partial f_4}{\partial I_c}\right| = |-\beta_3 S_v| = \beta_3 S_v < \infty; \left|\frac{\partial f_4}{\partial S_v}\right| = |\beta_1 B + \beta_3 I_c| = \beta_1 B + \beta_3 I_c < \infty;$$
$$\left|\frac{\partial f_4}{\partial I_v}\right| = |-\delta| = \delta < \infty; \left|\frac{\partial f_4}{\partial B}\right| = |-\beta_1 S_v| = \beta_1 S_v < \infty.$$

And lastly, from the fifth equation of (5.12),

$$\left|\frac{\partial f_5}{\partial S_c}\right| = 0 < \infty; \left|\frac{\partial f_5}{\partial I_c}\right| = \eta < \infty; \left|\frac{\partial f_5}{\partial S_v}\right| = 0 < \infty; \left|\frac{\partial f_5}{\partial I_v}\right| = 0 < \infty; \left|\frac{\partial f_5}{\partial B}\right| = |-m| = m < \infty.$$

Since the functions in Eq. (5.12) are polynomial, then they are infinitely differentiable. Thus, for the detailed proof, we can follow the proof of classical Cauchy-Lypschitz theorem (Peyser, 1958). Therefore, all the partial derivatives exist and are finite, then there exists a solution for the model and hence, we can say that there exist a unique solution of system (5.1) in the domain Θ. □

5.2.3 Disease-Free Equilibrium Point (DFEP)

At DFE, there is no infections (i.e., $I_c = I_v = B = 0$) in the populations. To find DFE, we equate the right hand side of system (5.1) to zero and solving for the noninfected state variables we get $S_c = 0$ or $S_c = K - K\theta/r$, $S_v = \lambda/\delta$. Thus, the equilibrium points of the system (5.1) are $(0,\ 0,\ \lambda/\delta,\ 0,\ 0)$ and $(K((r-\theta)/r),\ 0,\ \lambda/\delta,\ 0,\ 0)$. Hence, DFE, ε_0 is given by

$$\varepsilon_0 = \left(\frac{K(r-\theta)}{r},\ 0,\ \frac{\lambda}{\delta},\ 0,\ 0\right). \tag{5.13}$$

Remark 5.2.1. *The disease-free equilibrium point ε_0 in Eq. (5.13) exists and is biologically feasible when $\mathscr{R}_0 < 1$ and $r > \theta$.*

5.2.4 Basic Reproduction Number

The expression of basic reproduction number $\mathscr{R}_0$ for the system (5.1) can be derived using the next generation matrix method (Van den Driessche and Watmough, 2002). The first step

to find $\mathscr{R}_0$ is rewriting the model equations starting with newly infective classes:

$$\begin{cases} \dfrac{dI_c}{dt} = \beta_2 S_c I_v - (\gamma+\eta) I_c, \\ \dfrac{dI_v}{dt} = (\beta_1 B + \beta_3 I_c) S_v - \delta I_v, \\ \dfrac{dB}{dt} = \eta I_c - mB. \end{cases} \tag{5.14}$$

The right hand side of system (5.14) is written as $f - g$, where

$$f = \begin{bmatrix} \beta_2 ScIv \\ (\beta_1 B + \beta_3 Ic) Sv \\ 0 \end{bmatrix}, \quad g = \begin{bmatrix} (\gamma+\eta) Ic \\ \delta Iv \\ -\eta Ic + mB \end{bmatrix}. \tag{5.15}$$

Then by linearization approach, the associated matrices of f and g at DFE ε_0 are given by

$$\mathbb{F} = \begin{bmatrix} 0 & k(1-\dfrac{\theta}{r})\beta_2 & 0 \\ \dfrac{\beta_3 \lambda}{\delta} & 0 & \dfrac{\beta_1 \lambda}{\delta} \\ 0 & 0 & 0 \end{bmatrix}, \quad \mathbb{G} = \begin{bmatrix} \gamma+\eta & 0 & 0 \\ 0 & \delta & 0 \\ -\eta & 0 & m \end{bmatrix}.$$

$\mathscr{R}_0 = \rho(\mathbb{F}\mathbb{G}^{-1})$ is the spectral radius of the product $\mathbb{F}\mathbb{G}^{-1}$. Thus, $\mathscr{R}_0$ is given by

$$\mathscr{R}_0 = \sqrt{\frac{K\beta_2\lambda\left[m\beta_3 + \beta_1\eta\right](r-\theta)}{rm\delta^2(\gamma+\eta)}}. \tag{5.16}$$

5.2.5 Local Stability of Disease-Free Equilibrium Point

In this section, we investigated the local stability of disease-free equilibrium point ε_0 based on the basic reproduction number $\mathscr{R}_0$.

Theorem 5.2.4. *If $\mathscr{R}_0 < 1$, then disease-free equilibrium ε_0 of the system (5.1) is locally asymptotically stable in Ω_2.*

Proof. The Jacobian matrix of the system (5.1) at disease-free equilibrium $\varepsilon_0 = (K(1-\theta/r),\ 0,\ \lambda/\delta,\ 0,\ 0)$ is given by

$$J(\varepsilon_0) = \begin{bmatrix} \theta - r & -(r-\theta) & 0 & -\dfrac{K(r-\theta)\beta_2}{r} & 0 \\ 0 & -\gamma-\eta & 0 & \dfrac{K(r-\theta)\beta_2}{r} & 0 \\ 0 & -\dfrac{\beta_3\lambda}{\delta} & -\delta & 0 & -\dfrac{\beta_1\lambda}{\delta} \\ 0 & \dfrac{\beta_3\lambda}{\delta} & 0 & -\delta & \dfrac{\beta_1\lambda}{\delta} \\ 0 & \eta & 0 & 0 & -m \end{bmatrix}. \tag{5.17}$$

From the Jacobian matrix (5.17), we obtained characteristic polynomial:

$$(\delta+\Lambda)(r-\theta+\Lambda)(\Lambda^3+A_2\Lambda^2+A_1\Lambda+A_0)=0. \tag{5.18}$$

From Eq. (5.18), we obtain that $\Lambda_1=-\delta<0,\ \Lambda_2=-(r-\theta)<0$ (see remark 5.2.1, $r>\theta$) and from the last characteristic equation,

$$\Lambda^3+A_2\Lambda^2+A_1\Lambda+A_0=0, \tag{5.19}$$

where

$$\begin{aligned}
A_2&=\gamma+\eta+m+\delta,\\
A_1&=m(\delta+\gamma+\eta)+\frac{\delta(\gamma+\eta)\eta\beta_1}{m\beta_3+\eta\beta_1}+\frac{\delta(\gamma+\eta)m\beta_3}{m\beta_3+\eta\beta_1}(1-\mathscr{R}_0^2),\\
A_0&=m\delta(\gamma+\eta)-\frac{K\beta_2\lambda(r-\theta)(m\beta_3+\eta\beta_1)}{r\delta}=\delta(\gamma+\eta)m(1-\mathscr{R}_0^2).
\end{aligned}$$

Using Routh-Hurwitz criteria (Martcheva, 2015), Eq. (5.19) has eigenvalues which are negative real part whenever $A_2>0,\ A_1>0, A_1A_2-A_0>0$ and $A_0(A_1A_2-A_0)>0$. But, $A_0>0$ if $R_0<1$. Therefore, ε_0 is locally asymptotically stable for $\mathscr{R}_0<1$. □

5.2.6 Global Stability of Disease-Free Equilibrium Point

Theorem 5.2.5. *If $\mathscr{R}_0<1$, then the disease-free equilibrium point $\varepsilon_0=(K(r-\theta)/r,\ 0,\ \lambda/\delta,\ 0,\ 0)$ of the system (5.1) is globally asymptotically stable in Ω_2.*

Proof. To proof this theorem, we first define the linear Lyapunov function:

$$U=\varepsilon_1 I_c+\varepsilon_2 I_v+\varepsilon_3 B,$$

where $\varepsilon_1,\varepsilon_2$ and ε_3 are positive constants to be computed.

Then differentiating U with respect to t, we obtain

$$\frac{dU}{dt}=[-\varepsilon_1(\gamma+\eta)+\varepsilon_2\beta_3 S_v^0+\varepsilon_3\eta]I_c+[\varepsilon_1\beta_2 S_c^0-\varepsilon_3\delta]I_v+[\varepsilon_2\beta_1 S_v^0-\varepsilon_3 m]B, \tag{5.20}$$

with $S_c^0=K(r-\theta)/r$ and $S_v^0=\lambda/\delta$. The $\varepsilon_1,\varepsilon_2,\varepsilon_3$ can be chosen such that

$$\begin{aligned}
-\varepsilon_1(\gamma+\eta)+\varepsilon_2\beta_3 S_v^0+\varepsilon_3\eta&=0,\\
\varepsilon_1\beta_2 S_c^0-\varepsilon_3\delta&=0,\\
\varepsilon_2\beta_1 S_v^0-\varepsilon_3 m&=0.
\end{aligned} \tag{5.21}$$

If we choose $\varepsilon_1=1$, then $\varepsilon_2=\beta_2K(r-\theta)/r\delta$ and $\varepsilon_3=\beta_1\beta_2K(r-\theta)\lambda/r\delta^2 m$. Substituting

$\varepsilon_1, \varepsilon_2$ and ε_3 into Eq. (5.21) leads to

$$\begin{aligned}\frac{dU}{dt} &= (-\varepsilon_1(\gamma+\eta)+\varepsilon_2\frac{\beta_3\lambda}{\delta}+\varepsilon_3\eta)I_c+\left(\frac{\beta_2K(r-\theta)}{r}-\frac{\beta_2K(r-\theta)}{r}\right)I_v\\ &+\left(\frac{\beta_1\beta_2K(r-\theta)\lambda}{r\delta^2}-\frac{m\beta_1\beta_2K(r-\theta)\lambda}{r\delta^2m}\right)B,\\ &= (\gamma+\eta)\left(R_0^2-1\right)I_c.\end{aligned}$$

Since $R_0 < 1$ and $R_0 \geq 0$ imply that $R_0^2 < 1$, we have $dU/dt \leq 0$.

Moreover, the largest compact invariant set in $\{(S_c,\, I_c,\, S_v,\, I_v,\, B) \in \Omega_2 : dU/dt = 0\}$ is the singleton $\{\varepsilon_0\}$. By La Salle (1976) principle, ε_0 is globally asymptotically stable in Ω_2. □

5.2.7 Endemic Equilibrium Point (EEP)

Endemic equilibrium point (E^*) exists when CBD persist in the populations. To obtain EEP, we set each equation in the system (5.1) equal to zero. That is,

$$\begin{aligned}rS_c^*\left(1-\frac{S_c^*+I_c^*}{K}\right)-\beta_2S_c^*I_v^*-\theta S_c^* &= 0,\\ \beta_2S_c^*I_v^*-(\gamma+\eta)I_c^* &= 0,\\ \lambda-(\beta_1B^*+\beta_3I_c^*)S_v^*-\delta S_v^* &= 0,\\ (\beta_1B^*+\beta_3I_c^*)S_v^*-\delta I_v^* &= 0,\\ \eta I_c^*-mB^* &= 0.\end{aligned} \tag{5.22}$$

From the first equation of Eq (5.22) we find $S_c^* = 0$ or $r(1-(S_c^*+I_c^*)/K)-\beta_2I_v^*-\theta = 0$.
Case i: $S_c^* = 0$, we obtain $I_c^* = \delta m/(\beta_1\eta+m\beta_3)$, $S_v^* = \lambda/2\delta$, $I_v^* = \lambda/2\delta$, $B^* = \eta\delta/(\beta_1\eta+m\beta_3)$. This endemic point is a point where the disease distroys all coffee berries.
Case ii: $r(1-(S_c^*+I_c^*)/K)-\beta_2I_v^*-\theta = 0$, then we get S_c^*, S_v^*, I_v^* and B^*:

$$\begin{aligned}S_c^* &= \frac{\delta(\gamma+\eta)(m+(\beta_1\eta+m\beta_3)I_c^*)}{\lambda\beta_2(\beta_1\eta+m\beta_3)}, & S_v^* &= \frac{\lambda m}{\delta(m+(\beta_1\eta+\beta_3m)I_c^*)},\\ I_v^* &= \frac{\lambda(\beta_1\eta+m\beta_3)I_c^*}{\delta(m+(\beta_1\eta+m\beta_3)I_c^*)}, & B^* &= \frac{\eta I_c^*}{m},\end{aligned} \tag{5.23}$$

where I_c^* is the positive root of

$$f(I_c^*) = A(I_c^*)^2+BI_c^*+C = 0, \tag{5.24}$$

with

$$A = \frac{r^3 m^2 \delta^5 (\delta(\gamma+\eta)+\beta_2\lambda)(\gamma+\eta)^2 R_0^4}{K^2\beta_2^2\lambda^2(r-\theta)^2} > 0,$$
$$B = \frac{r^2 m^2 \delta^3(\gamma+\eta)}{K\beta_2\lambda(r-\theta)}\left[\beta_2\lambda + 2\delta(\gamma+\eta) + \frac{\delta(\beta_2\lambda - r\delta)(\gamma+\eta)R_0^2}{r-\theta}\right] R_0^2,$$
$$C = r\delta^2 m^2(\gamma+\eta)\left[\frac{r-\theta-r\delta R_0^2}{r-\theta}\right].$$

The feasibility of the endemic equilibrium is determined by the next proposition.

Proposition 5.2.1. *(Feasibility of the endemic equilibrium point).*
Let $E^* = (S_c^*, I_c^*, S_v^*, I_v^*, B^*)$ *be as Eq* (5.23).
(i) If $B > 0$ *and* $C < 0$ *or* $B < 0$ *and* $C < 0$, *then there is a unique endemic equilibrium* E^*.
(ii) If $B < 0$ *or* $C > 0$, *then there exist two endemic equilibrium* E^* *of the system.*

Proof. The result follows Descartes' rule of signs to $f(I_c^*)$ given in Eq. (5.24). □

5.2.8 Local Stability of Endemic Equilibrium Point

Theorem 5.2.6. *If* $\mathscr{R}_0 > 1$, $B_i > 0, i = 1,2,...,5$, $B_1B_2 - B_3 > 0, B_1(B_2B_3+B_5) - B_3^2 - B_1^2B_4 > 0, (B_2B_3 - B_1(B_2^2 - 2B_4))B_5 - B_4^2(-B_1B_2B_3 + B_3^2 + B_1^2B_4) - B_5^2 > 0, B_5(-B_4(-B_1B_2B_3 + B_3^2 + B_1^2B_4) + (B_2B_3 - B_1(B_2^2 - 2B_4))B_5 - B_5^2) > 0$, *then the endemic equilibrium* E^* *of system* (5.1) *is locally asymptotically stable in* Ω_2.

Proof. The Jacobian matrix of system (5.1) at the endemic equilibrium E^* is given by

$$J(E^*) = \begin{bmatrix} \frac{r_- r(I_c^* + 2S_c^*)}{K} - \beta_2 I_v^* - \theta & -(r-\theta) & 0 & -\beta_2 S_c^* & 0 \\ \beta_2 I_v^* & -\gamma - \eta & 0 & \beta_2 S_c^* & 0 \\ 0 & -\beta_3 S_v^* & -\beta_1 B^* - \beta_3 I_c^* - \delta & 0 & -\beta_1 S_v^* \\ 0 & \beta_3 S_v^* & \beta_1 B^* + \beta_3 I_c^* & -\delta & \beta_1 S_v^* \\ 0 & \eta & 0 & 0 & -m \end{bmatrix} \tag{5.25}$$

The eigenvalues of matrix (5.25) are computed from the following equation.

$$\begin{vmatrix} \frac{r_- r(I_c^* + 2S_c^*)}{K} - \beta_2 I_v^* - \theta - \Lambda & -(r-\theta) & 0 & \beta_2 S_c^* & 0 \\ \beta_2 I_v^* & -\gamma - \eta - \Lambda & 0 & \beta_2 S_c^* & 0 \\ 0 & -\beta_3 S_v^* & -\beta_1 B^* - \beta_3 I_c^* - \delta - \Lambda & 0 & -\beta_1 S_v^* \\ 0 & \beta_3 S_v^* & \beta_1 B^* + \beta_3 I_c^* & -\delta - \Lambda & \beta_1 S_v^* \\ 0 & \eta & 0 & 0 & -m - \Lambda \end{vmatrix} = 0 \tag{5.26}$$

Let us consider the non-zero entities of matrix (5.26) as

$$b_{11} = -\theta - r(I_c^* + 2S_c^*)/K - \beta_2 I_v^* + r/K,\ b_{12} = -(r-\theta),\ b_{21} = \beta_2 I_v^*,\ b_{22} = -\gamma - \eta,$$
$$b_{32} = -\beta_3 S_v^*,\ b_{42} = \beta_3 S_v^*,\ b_{52} = \eta,\ b_{33} = -\beta_1 B^* - \beta_3 I_c^* - \delta,\ b_{43} = \beta_1 B^* + \beta_3 I_c^*,$$
$$b_{14} = -\beta_2 S_c^*,\ b_{24} = \beta_2 S_c^*,\ b_{44} = -\delta,\ b_{35} = -\beta_1 S_v^*,\ b_{45} = \beta_1 S_v^*,\ b_{55} = -m.$$

Then, the characteristic polynomial of Eq. (5.26) is given by

$$\Lambda^5 + B_1\Lambda^4 + B_2\Lambda^3 + B_3\Lambda^2 + B_4\Lambda + B_5 = 0, \tag{5.27}$$

where

$$\begin{aligned}
B_1 &= -(b_{11} + b_{22} + b_{33} + b_{44} + b_{55}),\\
B_2 &= b_{33}b_{44} + b_{22}(b_{33} + b_{44} + b_{55}) + (b_{33} + b_{44})b_{55} + b_{11}(b_{33} + b_{44} + b_{55}) + b_{24}b_{42}(b_{11} - b_{14})\\
&\quad - b_{11}((b_{44} + b_{55})b_{33} + b_{22} + b_{44}b_{55}),\\
B_3 &= b_{24}b_{33}b_{42} - b_{14}b_{21}b_{42} - b_{24}b_{32}(b_{43} - b_{24}b_{45}b_{52} - b_{22}b_{44}b_{55} - (b_{44} + b_{55})b_{22}b_{33})\\
&\quad + (b_{24}b_{42} - b_{44})b_{55} + b_{11}b_{24}b_{42} - (b_{44} + b_{55})b_{11}b_{33} - b_{11}b_{22} - b_{11}b_{44}b_{55},\\
B_4 &= b_{14}b_{21}(b_{33}b_{42} - b_{32}b_{43} - b_{45}b_{52}) + b_{24}(b_{33}b_{45} - b_{35}b_{43})b_{52}\\
&\quad + (b_{22}b_{33}b_{44} + b_{24}b_{32}b_{43} + b_{14}b_{21}b_{42})b_{55} + b_{11}b_{24}(b_{32}b_{43} + b_{45}b_{52} - b_{33}b_{42})\\
&\quad + b_{11}b_{33}b_{44}b_{55} + b_{11}b_{22}(b_{33} + b_{44}) - b_{11}b_{24}b_{42}b_{55},\\
B_5 &= b_{14}b_{21}((b_{33}b_{45} - b_{35}b_{43})b_{52} + (b_{32}b_{43} - b_{42})b_{55} + b_{11}b_{24}((b_{35}(b_{43} - b_{33}b_{45})b_{52}\\
&\quad + (b_{33}b_{42} - b_{32}b_{43})b_{55}) - b_{11}b_{22}b_{33}b_{44}.
\end{aligned}$$

Using the Routh Hurwitz criterion (Martcheva, 2015), the endemic equilibrium E^* is locally asymptotically stable for $R_0 > 1$ if $B_i > 0,\ i = 1, ..., 5,$

$$\begin{aligned}
B_1B_2 - B_3 &> 0,\\
B_1(B_2B_3 + B_5) - B_3^2 - B_1^2B_4 &> 0,\\
(B_2B_3 - B_1(B_2^2 - 2B_4))B_5 - B_4^2(-B_1B_2B_3 + B_3^2 + B_1^2B_4) - B_5^2 &> 0,\\
B_5(-B_4(-B_1B_2B_3 + B_3^2 + B_1^2B_4) + (B_2B_3 - B_1(B_2^2 - 2B_4))B_5 - B_5^2) &> 0.
\end{aligned}$$

Hence, all eigenvalues of Eq. (5.27) evaluated at the endemic equilibrium E^* have negative real parts whenever $\mathscr{R}_0 > 1$. □

5.2.9 Global Stability of Endemic Equilibrium Point

Theorem 5.2.7. *If $\mathscr{R}_0 > 1$, then the endemic equilibrium E^* of the model (5.1) is globally asymptotically stable in Ω_2.*

Proof. To establish the global stability of the endemic equilibrium E^*, we consider the fol-

lowing Lyapunov function:

$$V = \frac{[(S_c - S_c^*) + (I_c - I_c^*)]^2}{2} + \frac{[(S_v - S_v^*) + (I_v - I_v^*)]^2}{2} + \frac{(B - B^*)^2}{2}. \tag{5.28}$$

Then by taking the derivative of V with respect to t, we obtain

$$\begin{aligned} \frac{dV}{dt} &= [(S_c - S_c^*) + (I_c - I_c^*)] \frac{d}{dt}[S_c + I_c] + [(S_v - S_v^*) + (I_v - I_v^*)] \frac{d}{dt}[S_v + I_v] + (B - B^*)\frac{dB}{dt}, \\ &= [(S_c - S_c^*) + (I_c - I_c^*)] \frac{dN_c}{dt} + [(S_v - S_v^*) + (I_v - I_v^*)] \frac{dN_v}{dt} + (B - B^*)\frac{dB}{dt}. \end{aligned} \tag{5.29}$$

On the other hand, from Eqs. (5.4), (5.6) and (5.8), respectively, we have

$$\begin{aligned} \frac{dN_c}{dt} &= \frac{d}{dt}[S_c + I_c] \leq M(1+r) - hN_c, \\ \frac{dN_v}{dt} &= \frac{d}{dt}[S_v + I_v] = \lambda - \delta N_v, \\ \frac{dB}{dt} &\leq \frac{M(1+r)\eta}{h} - mB. \end{aligned} \tag{5.30}$$

Substituting expression for dN_c/dt, dN_v/dt and dB/dt from Eq. (5.30) into Eq. (5.29) leads to

$$\begin{aligned} \frac{dV}{dt} &= [(S_c - S_c^*) + (I_c - I_c^*)] \frac{dN_c}{dt} + [(S_v - S_v^*) + (I_v - I_v^*)] \frac{dN_v}{dt} + (B - B^*)\frac{dB}{dt}, \\ &\leq [(S_c - S_c^*) + (I_c - I_c^*)] [M(1+r) - hN_c] + [(S_v - S_v^*) + (I_v - I_v^*)] [\lambda - \delta N_v] \\ &+ (B - B^*) \left[\frac{M(1+r)\eta}{h} - mB\right], \\ &\leq \left[N_c - \frac{M(1+r)}{h}\right] [M(1+r) - hN_c] + \left[N_v - \frac{\lambda}{\delta}\right] [\lambda - \delta N_v] \\ &+ \left[B - \frac{M(1+r)\eta}{hm}\right] \left[\frac{M(1+r)\eta}{h} - mB\right]. \end{aligned} \tag{5.31}$$

By re-arranging and simplify the Eq. (5.31), we obtain

$$\frac{dV}{dt} \leq -\frac{1}{h}[M(1+r) - hN_h]^2 - \frac{1}{\delta}[\lambda - \delta N_v]^2 - \frac{1}{m}\left[\frac{M(1+r)\eta}{h} - mB\right]^2. \tag{5.32}$$

Thus $(dV/dt)(S_c,\, I_c,\, S_v,\, I_v,\, B) \leq 0$. Furthermore, $(dV/dt)(S_c,\, I_c,\, S_v,\, I_v,\, B) = 0$ if and only if $S_c = S_c^*,\ I_c = I_c^*,\ S_v = S_v^*,\ I_v = I_v^*,\ B = B^*$. Therefore, the largest compact invariant set in $\{(S_c,\, I_c,\, S_v,\, I_v,\, B) \in \Omega_2 : dV/dt = 0\}$ is the singleton $\{E^*\}$. By La Salle (1976) invariance principle, E^* is globally asymptotically stable in Ω_2. □

5.2.10 Bifurcation Analysis

To investigate the possibility of existence of the bifurcation analysis of the system (5.1) at $\mathscr{R}_0 = 1$, we use the center manifold theory as given in the previous chapter 4. So using this approach, the following theorem can be established.

Theorem 5.2.8. *If $\mathscr{R}_0 < 1$, then the system (5.1) exhibits forward bifurcation at $\mathscr{R}_0 = 1$.*

Proof. Using center manifold theory (Castillo-Chavez and Song, 2004), we carry out bifurcation analysis of system (5.1) at $\mathscr{R}_0 = 1$. Let us consider the change of variables $S_c = x_1$, $I_c = x_2$, $S_v = x_3$, $I_v = x_4$, $B = x_5$. Then the system (5.1) can be written in the form $\frac{dx}{dt} = (g_1, g_2, g_3, g_4, g_5)^T$ as:

$$\begin{cases} \frac{dx_1}{dt} = rx_1\left(1 - \frac{x_1 + x_2}{K}\right) - \beta_2 x_1 x_4 - \theta x_1, \\ \frac{dx_2}{dt} = \beta_2 x_1 x_4 - (\gamma + \eta)x_2, \\ \frac{dx_3}{dt} = \lambda - (\beta_1 x_5 + \beta_3 x_2)x_3 - \delta x_3, \\ \frac{dx_4}{dt} = (\beta_1 x_5 + \beta_3 x_2)x_3 - \delta x_4, \\ \frac{dx_5}{dt} = \eta x_2 - m x_5. \end{cases} \tag{5.33}$$

We consider the transmission rate β_2 as bifurcation parameter so that $\mathscr{R}_0 = 1$ if

$$\beta_2 = \beta_2^* = \frac{r(\gamma + \eta)\delta^2 m}{K\lambda(r - \theta)(m\beta_3 + \beta_1\eta)}. \tag{5.34}$$

The Jacobian matrix of Eq. (5.33) at disease-free equilibrium ε_0 is given by

$$J(\varepsilon_0) = \begin{bmatrix} \theta - r & -(r-\theta) & 0 & -K(\frac{r-\theta}{r})\beta_2^* & 0 \\ 0 & -\gamma - \eta & 0 & K(\frac{r-\theta}{r})\beta_2^* & 0 \\ 0 & -\frac{\beta_3\lambda}{\delta} & -\delta & 0 & -\frac{\beta_1\lambda}{\delta} \\ 0 & \frac{\beta_3\lambda}{\delta} & 0 & -\delta & \frac{\beta_1\lambda}{\delta} \\ 0 & \eta & 0 & 0 & -m \end{bmatrix}.$$

The right eigenvector, $u = (u_1,\ u_2,\ u_3,\ u_4,\ u_5)^T$ are computed from $J(\varepsilon_0)u = 0$ as follows.

$$J(\varepsilon_0)u = \begin{cases} (\theta - r)u_1 - K(\dfrac{r-\theta}{r})\beta_2^* u_4 = 0, \\ (-\gamma - \eta)u_2 + K(\dfrac{r-\theta}{r})\beta_2^* u_4 = 0, \\ -\dfrac{\beta_3\lambda}{\delta}u_2 - \delta u_3 - \dfrac{\beta_1\lambda}{\delta}u_5 = 0, \\ \dfrac{\beta_3\lambda}{\delta}u_2 - \delta u_4 + \dfrac{\beta_1\lambda}{\delta}u_5 = 0, \\ \eta u_2 - m u_5 = 0. \end{cases} \tag{5.35}$$

From Eq. (5.35), we get

$$u_1 = -\frac{K\beta_2^*}{r}\left(\frac{r-\theta}{\gamma+\eta}+1\right)u_4,\ \ u_2 = \frac{K(r-\theta)\beta_2^*}{r(\gamma+\eta)}u_4,\ \ u_3 = -u_4,\ \ u_5 = \frac{\eta K(r-\theta)\beta_2^*}{r(\gamma+\eta)m}u_4, \tag{5.36}$$

where $u_4 = u_4 > 0$. Also the left eigenvector, $z = (z_1,\ z_2,\ z_3,\ z_4,\ z_5)$ are computed from $zJ(\varepsilon_0) = 0$ so that

$$z_1 = z_3 = 0,\ z_2 = \frac{\delta r}{K(r-\theta)\beta_2^*}z_4,\ z_5 = \frac{\beta_1\lambda}{\delta m}z_4;\ \ z_4 = z_4 > 0.$$

Based on center manifold theorem (Castillo-Chavez and Song, 2004), we have to compute a and b such that

$$a = \sum_{i,j,k=1}^{5} z_k u_i u_j \frac{\partial^2 g_k}{\partial x_i \partial x_j}(\varepsilon_0);\ \ b = \sum_{i,k=1}^{5} z_k u_i \frac{\partial^2 g_k}{\partial x_i \partial \beta_2^*}(\varepsilon_0). \tag{5.37}$$

The nonzero second partial derivatives of $g_1,\ g_2,\ g_3$ and g_4 are given as follows:

$$\begin{aligned}
&\frac{\partial^2 g_1}{\partial x_1 \partial x_1} = \frac{\partial^2 g_1}{\partial x_1 \partial x_1} = -\frac{2r}{K},\ \frac{\partial^2 g_1}{\partial x_1 \partial x_2} = \frac{\partial^2 g_1}{\partial x_2 \partial x_1} = -\frac{r}{K}, \\
&\frac{\partial^2 g_1}{\partial x_1 \partial x_4} = \frac{\partial^2 g_1}{\partial x_4 \partial x_1} = -\beta_2^*,\ \frac{\partial^2 g_2}{\partial x_1 \partial x_2} = \frac{\partial^2 g_2}{\partial x_2 \partial x_1} = \beta_2^*, \\
&\frac{\partial^2 g_3}{\partial x_2 \partial x_3} = \frac{\partial^2 g_3}{\partial x_3 \partial x_2} = -\beta_3,\ \frac{\partial^2 g_3}{\partial x_3 \partial x_5} = \frac{\partial^2 g_3}{\partial x_5 \partial x_3} = -\beta_1, \\
&\frac{\partial^2 g_4}{\partial x_2 \partial x_3} = \frac{\partial^2 g_4}{\partial x_3 \partial x_2} = \beta_3,\ \ \frac{\partial^2 g_4}{\partial x_3 \partial x_5} = \frac{\partial^2 g_4}{\partial x_5 \partial x_3} = \beta_1, \\
&\frac{\partial^2 g_1}{\partial x_4 \partial \beta_2^*} = \frac{\partial^2 g_1}{\partial \beta_2^* \partial x_4} = -x_1^*,\ \ \frac{\partial^2 g_2}{\partial x_4 \partial \beta_2^*} = \frac{\partial^2 g_2}{\partial \beta_2^* \partial x_4} = x_1^*.
\end{aligned} \tag{5.38}$$

All the others second partial derivatives of $g_i,\ i = 1,...,5$ are zero. By using Eq. (5.37), we

get

$$\begin{aligned} a &= 2z_2u_1u_4\beta_2^* + 2z_4u_2u_3\beta_3 + 2z_4u_3u_5\beta_1 \\ &= -\left[\frac{2\delta^3 r(\gamma+\eta)m}{K\lambda(r-\theta)^2(m\beta_3+\beta_1\eta)}\left(\frac{r-\theta}{\gamma+\eta}+1\right)+\frac{2\delta\beta_3}{\gamma+\eta}+2\eta K(r-\theta)\delta^2\right]z_4u_4^2 < 0 \end{aligned} \tag{5.39}$$

and

$$\begin{aligned} b &= z_1u_4\frac{\partial^2 g_1}{\partial x_4\partial\beta_2^*}+z_2u_4\frac{\partial^2 g_2}{\partial x_4\partial\beta_2^*} \\ &= \frac{K(r-\theta)(m\beta_3+\beta_1\eta)}{r(\gamma+\eta)\delta m}z_4u_4 > 0. \end{aligned} \tag{5.40}$$

Since the coefficient a is negative and b is positive, then the system (5.1) exhibits forward bifurcation at $\mathscr{R}_0 = 1$ and there exists at least one stable endemic equilibrium when $\mathscr{R}_0 > 1$ (See Figure 5.2). □

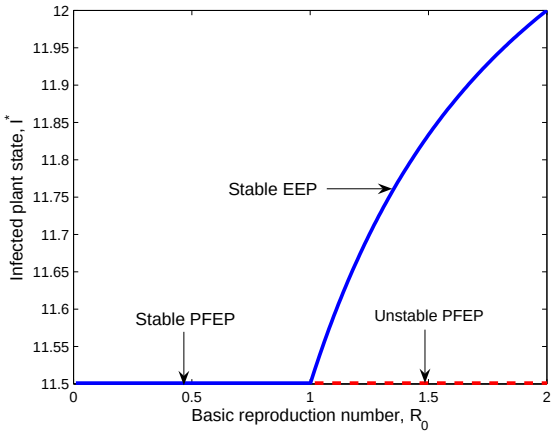

Figure 5.2: Forward bifurcation diagram. Parameter values are taken from Table 5.2 (except $\beta_2 = 0.5,\ \gamma = 0.99,\ \lambda = 0.02,\ d = 0.99$).

5.2.11 Sensitivity of Basic Reproduction Number ($\mathscr{R}_0$)

In this section, we compute the sensitivity indices of basic reproduction number $\mathscr{R}_0$ with respect to the main parameters (Chitnis et al., 2008). This help us to check and identify parameters which highly affect $\mathscr{R}_0$.

The sensitivity index of R_0 with respect to K is given by

$$\Delta_K^{\mathscr{R}_0} = \frac{\partial\mathscr{R}_0}{\partial K}\times\frac{K}{R_0} = 0.5.$$

In a similar way the others sensitivity index of $\mathscr{R}_0$ are computed and their sensitivity indeces: $\Delta_{\beta_1}^{\mathscr{R}_0}$, $\Delta_{\beta_2}^{\mathscr{R}_0}$, $\Delta_{\beta_3}^{\mathscr{R}_0}$, $\Delta_{\eta}^{\mathscr{R}_0}$, $\Delta_{r}^{\mathscr{R}_0}$, $\Delta_{\theta}^{\mathscr{R}_0}$, $\Delta_{\lambda}^{\mathscr{R}_0}$, $\Delta_{\delta}^{\mathscr{R}_0}$, $\Delta_{\gamma}^{\mathscr{R}_0}$ and $\Delta_{m}^{\mathscr{R}_0}$ are given in Table 5.1.

Table 5.1: Sensitivity indices of $\mathscr{R}_0$

Parameter	**Sensitivity indices of $\mathscr{R}_0$**
K	+0.5
β_1	+0.0616258
β_2	+0.5
β_3	+0.438374
η	-0.259803
r	+0.0454545
θ	-0.0454545
λ	+0.5
δ	-1
γ	-0.178571
m	-0.0616258

5.2.12 Interpretation of the Sensitivity Indices

The sensitivity indices of the basic reproduction number, $\mathscr{R}_0$, with respect to the main parameters were given in Table 5.1. The parameters: K, β_1, β_2, β_3, r and λ have positive sensitivity indices showing that the more impact on expanding the disease in the population if their values are increasing since $\mathscr{R}_0$ increases. And also the parameters: θ, η, δ, γ, and m have negative sensitivity indices show that less impact on expanding the disease in the population as their values increase. And also as their values increase, $\mathscr{R}_0$ decreases, which leads to minimizing the endemicity of the disease in the population. The bar diagram of the sensitivity indices of $\mathscr{R}_0$ in Table 5.1 is depicted in Figure 5.3. From Table 5.1 the parameters: K, β_2, and λ are the most in influential in expanding the disease.

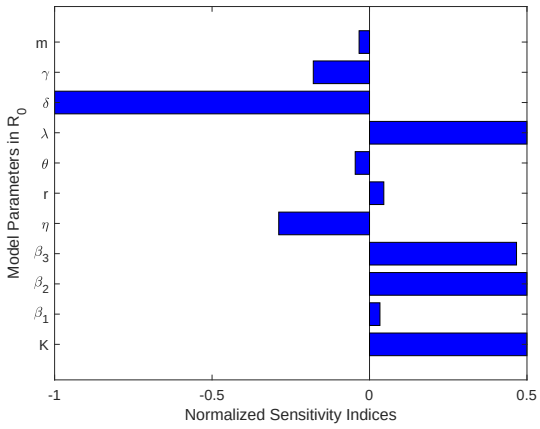

Figure 5.3: Normalized sensitivity indices of $\mathscr{R}_0$ with respect to parameters of the system (5.1). Parameter values are taken from Table 5.2.

Furthermore, in Figure 5.4, we have seen that the contour plot of basic reproduction number $\mathscr{R}_0$ with respect to the parameters K, β_2 and K, λ, respectively. It can be observed

from Figure 5.4 (a) that for decreasing value of K and β_2, $\mathscr{R}_0$ decreases. For increasing K and λ the basic reproduction number $\mathscr{R}_0$ increases, which has been shown in Figure 5.4 (b).

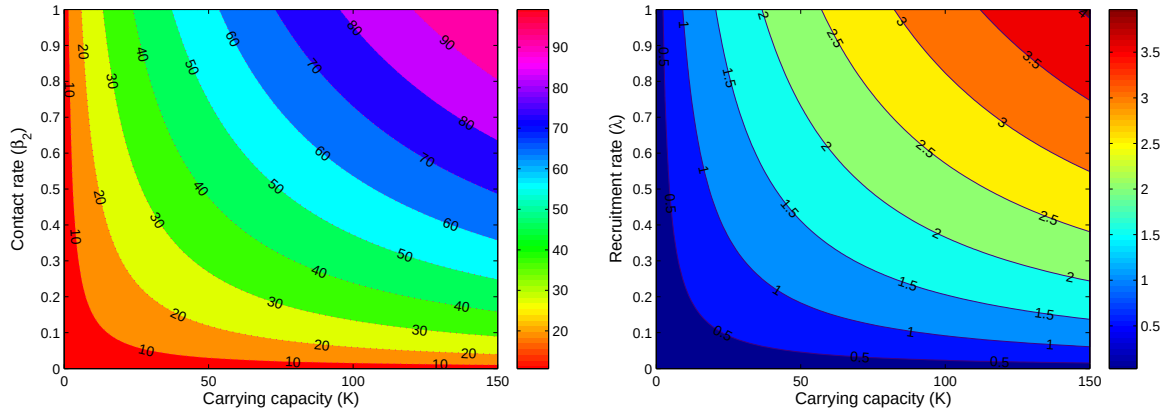

(a) (b)

Figure 5.4: Contour plots of $\mathscr{R}_0$ versus (a) (K, β_2)-plane and (b) (K, λ)-plane. Parameter values are taken from Table 5.2.

5.3 Simulation Results

In order to illustrate the analytical results, the numerical simulations of the system (5.1) were performed. Some parameter values were assumed and some of them were obtained from the literature. In addition to parameter values in Table 5.2 we used the initial data: $S_c(0) = 100$, $I_c(0) = 50$, $S_v(0) = 50$, $I_v(0) = 10$, $B(0) = 2$.

Table 5.2: Meaning of the parameters of model (5.1) with corresponding values.

Parameter	Description	Value	Source
β_1	Contact rate of vector with pathogen	0.000209818	Assumed
β_2	Contact rate of coffee berry with infected vector	0.000795455	Assumed
β_3	Contact rate of vector with infected coffee berry	0.000149091	Assumed
θ	Mortality rate of healthy coffee berry	0.01	(Fotso et al., 2018)
γ	Removal rate of infected coffee berry	0.005	Assumed
r	Growth rate of new coffee berries	0.12	(Campanha et al., 2007b)
K	Carrying capacity	150	Assumed
η	Induced rate of infected coffee berry	0.009	Assumed
λ	Recruitment rate of vector	0.488364	Assumed
m	Decay rate of pathogen	0.0900982	Assumed
δ	Death rate of vector	0.009	Assumed

Figures 5.5 (a) and 5.6 (a) depict the global asymptotic behavior of the infected coffee

and infected vector at the disease-free equilibrium ε_0 when $\mathscr{R}_0 < 1$ where the disease dies out regardless of large initial values of the infectious population. On the other hand, Figures 5.5 (b) and 5.6 (b) show the global asymptotic behavior of the infected coffee and infected vector at the endemic equilibrium E^* when $\mathscr{R}_0 > 1$ where the disease persists regardless of the initial sizes of the infectious population.

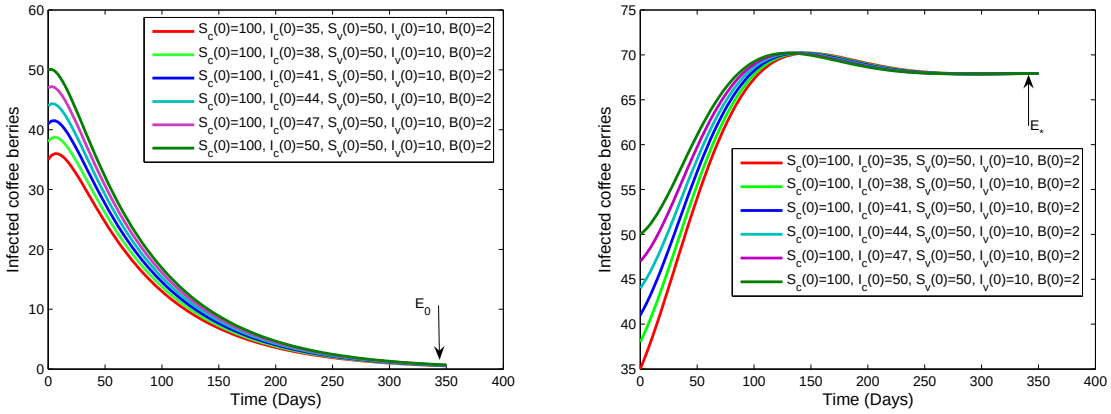

(a) (b)

Figure 5.5: Numerical simulation of the convergence of the infected coffee berries to the disease-free and endemic equilibrium points when (a) $\mathscr{R}_0 < 1$ and (b) $\mathscr{R}_0 > 1$, respectively.

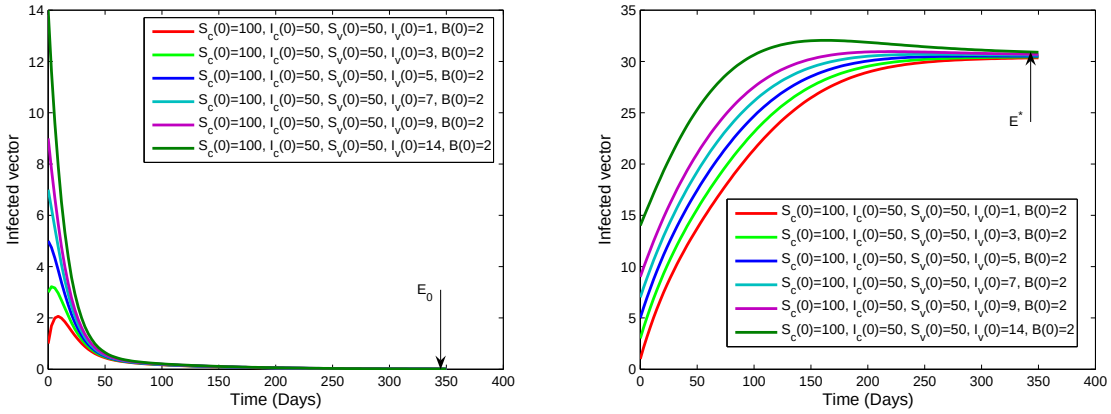

(a) (b)

Figure 5.6: Numerical simulation of the convergence of the infected vectors to the disease-free and endemic equilibrium points.

From the Figure 5.7 (a) susceptible coffee berries decrease while the infected coffee berries increase with $\mathscr{R}_0 > 1$ due to there are very favorable conditions for the breeding of pathogen and vector that transmit the disease. The susceptible vector population in Figure 5.7 (b) decreases while the infected vector population increases. The CBD pathogen population in Figure 5.8 increases to a maximum point and then proceeds decrease with a minimum

at unfavorable climate.

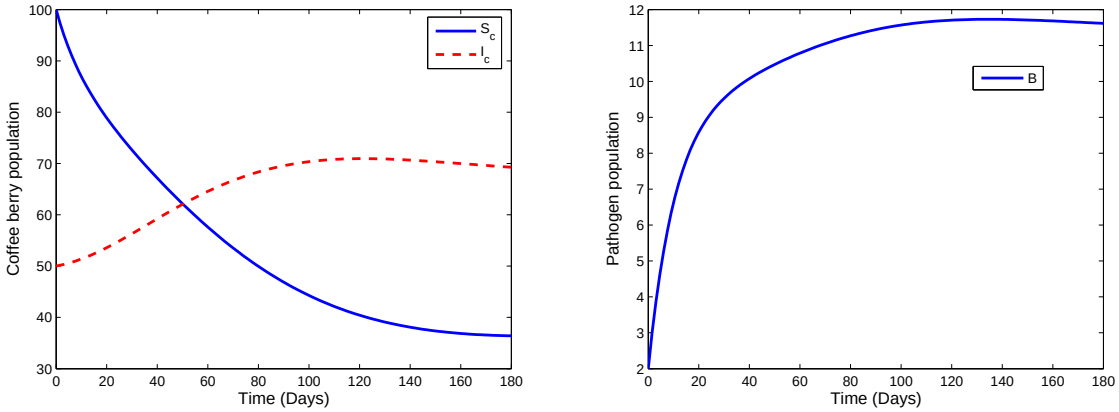

(a) (b)

Figure 5.7: Numerical simulation of coffee berries and vector population when $\mathscr{R}_0 = 2.83$

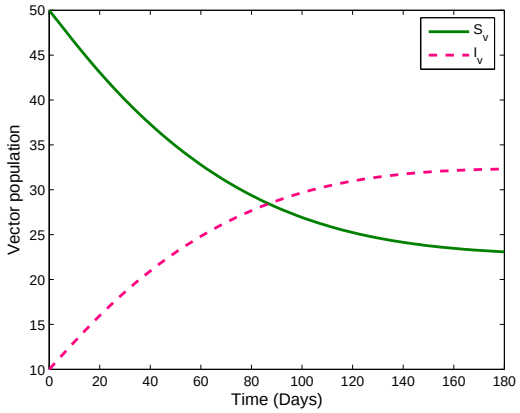

Figure 5.8: Numerical simulation of pathogen population when $\mathscr{R}_0 = 2.83$

In the Figures 5.9(a) and 5.9 (b), the effects of the modification factor for asymptomatic coefficient at different values: $K = 150$ and $\beta_2 = 0.000795455$ are displayed. The projection shows that the cumulative number of individuals becoming infected with coffee berries is high when K and β_2 become high and becoming decreasing with low values of K and β_2, which minimize also the values of basic reproduction number less one. As shown in Figures 5.10 (a) and 5.10 (b), when the rates: K and β_2 increase, the number of individuals becoming infected vector is high and decreasing the value of decreases the number of individuals becoming infected. As shown in Figures 5.10 (c) and 5.10 (d), when the rates: K and β_2 increase, the concentration of the pathogen becomes high and decreasing the value of decreases the pathogen.

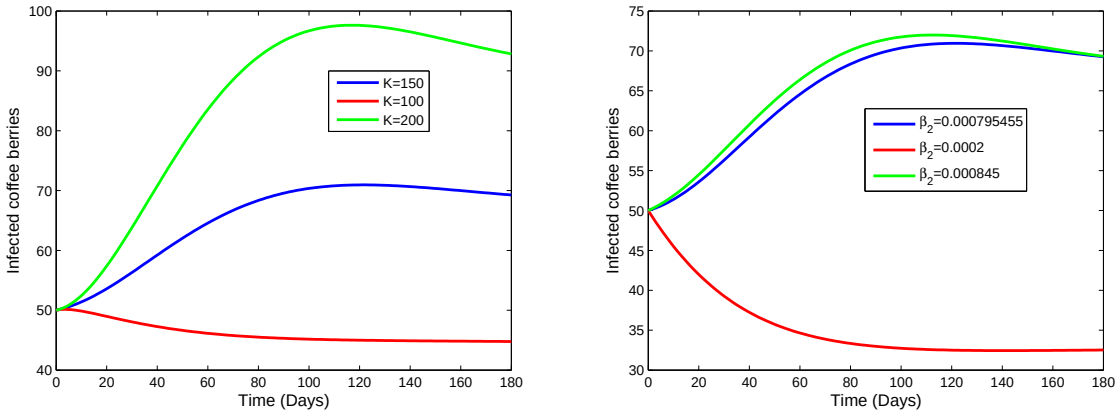

(a) (b)

Figure 5.9: Projections of infected coffee berries population with varying effect of parameters at values of $K = 100, K = 150, K = 200; \beta_2 = 0.0002, \beta_2 = 0.000795455, \beta_2 = 0.000845$.

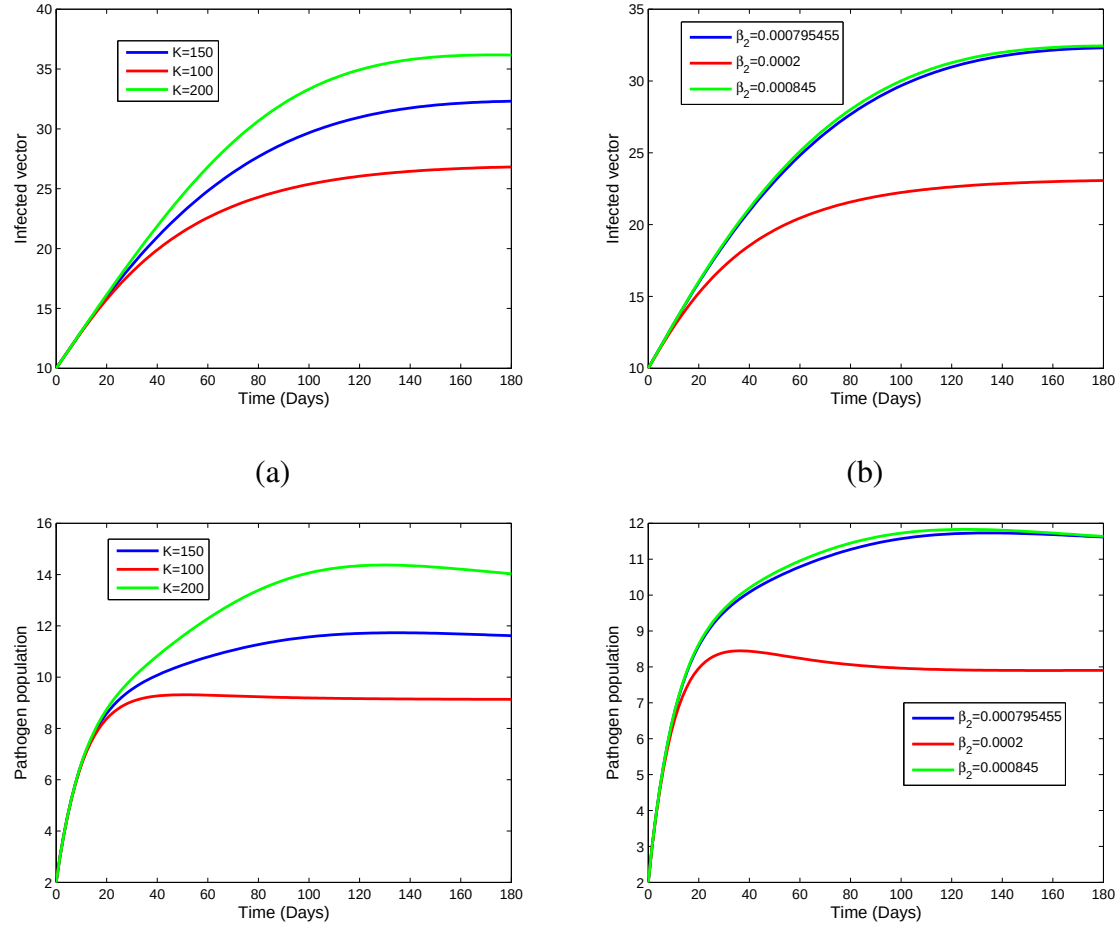

(a) (b)

(c) (d)

Figure 5.10: Projections of infected vector and pathogen population with varying effect of parameters at values of $K = 100, K = 150, K = 200; \beta_2 = 0.0002, \beta_2 = 0.000795455, \beta_2 = 0.000845$.

5.4 The Induced Model into an Optimal Control

In this section, an optimal control problem is proposed to minimize the losses due to infection and the corresponding cost of controls.

To ensure full protection of the coffee plants, three control interventions $u_i,\ i = 1,2,3$ are incorporated. The control variable u_1 denotes genetic resistance of the plant (coffee plant selection for disease-resistant varieties to decrease the infection rate), and the control variable u_2 represents chemical control of the vector (i.e., insecticide spray against insects), while the control variable u_3 represents cultural control (mainly based on cultural practice such as maintenance pruning, removal of mummified berries and mixed cropping with shade plants which create environmental conditions that limit CBD dynamics). Hence, the corresponding control induced state system for the model (5.1) is given by

$$\begin{aligned}
\frac{dS_c}{dt} &= rS_c\left(1-\frac{S_c+I_c}{K}\right)-(1-u_1)\beta_2 S_c I_v-\theta S_c,\\
\frac{dI_c}{dt} &= (1-u_1)\beta_2 S_c I_v-(\gamma+\eta)I_c,\\
\frac{dS_v}{dt} &= \lambda-(\beta_1 B+\beta_3 I_c)S_v-(1+u_2)\delta S_v,\\
\frac{dI_v}{dt} &= (\beta_1 B+\beta_3 I_c)S_v-(1+u_2)\delta I_v,\\
\frac{dB}{dt} &= \eta I_c-(1+u_3)mB,
\end{aligned} \tag{5.41}$$

with initial data:

$$S_c(0)=S_{c^0},\ I_c(0)=I_{c^0},\ S_v(0)=S_{v^0},\ I_v(0)=I_{v^0},\ B(0)=B_0. \tag{5.42}$$

Here, our target is to minimize the number of infectious coffee, infectious vector and the number of pathogen population at the least cost with respect to the controls $u_1(t),u_2(t)$ and $u_3(t)$. With this in mind, we define the cost functional for the minimization problem as

$$J=\min_{u}\int_0^{t_f}\left(a_1I_c(t)+a_2I_v(t)+a_3B(t)+\frac{1}{2}\sum_{i=1}^{3}b_iu_i^2(t)\right)dt, \tag{5.43}$$

subject to state system (5.41) with initial data (5.42) and $u=(u_1.u_2,u_3)$. The fixed constant t_f denotes the final intervention time while the coefficients a_1,a_2 and a_3 are positive constants to keep a balance in the size of $I_c(t),I_v(t)$ and $B(t)$, respectively. That means, a_1 is the cost associated with infected coffee I_c, a_2 is the cost associated with infected vector I_v while a_3 the cost corresponds to pathogen B. The term $0.5b_1u_1^2,\ 0.5b_2u_2^2$ and $0.5b_3u_3^2$ represent the costs for the use of genetic resistance variety, chemical control of vector and use of cultural practice, respectively.

In the system (5.41), the case $u_i = 0,\ i = 1,2,3$, implies no control measure is taken. On the other hand, $u_i = 1, i = 1,2,3$ implies a 100% success of intervention which is unrealistic. Thus, we assume that $0 \leq u(t) \leq u_{\max} < 1$ for our numerical implementation.

The current cost at time t can be obtained using the integrand $a_1 I_c + a_2 I_v + a_3 B + 1/2 \sum_{i=1}^{3} b_i u_i^2$. For the system (5.41), we need to compute the optimal control $u^*(t) = (u_1^*(t), u_2^*(t), u_3^*(t))$ such that

$$J(u^*) = \min(J(u) : u \in U), \tag{5.44}$$

where a measurable set U is defined by

$$U = \left\{(u_1(t), u_2(t), u_3(t)) : u_i \text{ are measurable } \& \ 0 \leq u_i(t) \leq (u_i)_{max} < 1, 0 \leq t \leq t_f,\ i = 1,2,3\right\}, \tag{5.45}$$

In the following, we briefly discuss the existence of optimal control and associated trajectories on the intervention time interval $[0, t_f]$ of the state system (5.41) and satisfying condition (5.43).

5.4.1 Existence of the Optimal Controls

The existence of the optimal controls can be showed by using an approach of (Pontryagin et al., 2018). Here, the boundedness of solutions to state system (5.41) in finite time interval is very crucial to determine the existence and uniqueness of optimal control to our model. Based on Eqs. (5.4), (5.6) and (5.8), we can find from the state system (5.41): $N_c \leq (1+r)\hat{K}/h$, $N_v \leq \lambda/(1+u_2)\delta$ and $B \leq (\hat{K}(1+r)\eta)/(1+u_3)mh$, where N_c, N_v and B, respectively, denotes the total population of coffee berry, vector and pathogen. This implies that the upper bound for N_c, N_v and B respectively dominates the state variables S_c, I_c; S_v, I_v and B. This result can be used to prove the existence of optimal controls. For detailed proof, see Coddington and Levinson (1955) [Theorem 4.1 and its corresponding Corollary 4.1 (Fleming and Lions, 2012)].

5.4.2 Characterization of the Optimal Controls

In this subsection, we briefly present the characterization of optimal control. Assume that $u^*(t) \in U$ is an optimal solution for problems (5.41)-(5.42) and (5.43) with fixed final time t_f. Then there exists a non-trivial absolutely continuous adjoint vector $\Lambda : [0, t_f] \to \mathbb{R}^5$, $\Lambda = (\lambda_1(t), \lambda_2(t), \lambda_3(t), \lambda_4(t), \lambda_5(t))$ that satisfy the following conditions.

(1) The Hamiltonian function associated to our problem is given by

$$\begin{aligned} H(Q,u,\Lambda,t) = {} & a_1 I_c + a_2 I_v + a_3 B + \frac{1}{2} b_1 u_1^2 + \frac{1}{2} b_2 u_2^2 + \frac{1}{2} b_3 u_3^2 \\ & + \lambda_1 \left(r S_c \left(1 - \frac{S_c + I_c}{K} \right) - (1-u_1)\beta_2 S_c I_v - \theta S_c \right) \\ & + \lambda_2 \left((1-u_1)\beta_2 S_c I_v - (\gamma+\eta) I_c \right) + \lambda_3 (\lambda - (\beta_1 B + \beta_3 I_c) S_v + (1+u_2)\delta S_v) \\ & + \lambda_4 ((\beta_1 B + \beta_3 I_c) S_v - (1+u_2)\delta I_v) + \lambda_5 \left(\eta I_c - (1+u_3) m B \right), \end{aligned} \tag{5.46}$$

where $Q = (S_c, I_c, S_v, I_v, B)$.

(2) The control system:

$$\frac{dS_c}{dt} = \frac{\partial H}{\partial \lambda_1}, \ \frac{dI_c}{dt} = \frac{\partial H}{\partial \lambda_2}, \ \frac{dS_v}{dt} = \frac{\partial H}{\partial \lambda_3}, \ \frac{dI_v}{dt} = \frac{\partial H}{\partial \lambda_4}, \ \frac{dB}{dt} = \frac{\partial H}{\partial \lambda_5}. \tag{5.47}$$

(3) The adjoint system:

$$\frac{d\lambda_1}{dt} = -\frac{\partial H}{\partial S_c}, \ \frac{d\lambda_2}{dt} = -\frac{\partial H}{\partial I_c}, \ \frac{d\lambda_3}{dt} = -\frac{\partial H}{\partial S_v}, \ \frac{d\lambda_4}{dt} = -\frac{\partial H}{\partial I_v}, \ \frac{d\lambda_5}{dt} = -\frac{\partial H}{\partial B}. \tag{5.48}$$

(4) The optimality condition:

$$\frac{\partial H}{\partial u_i} = 0, \ \ i = 1,2,3. \tag{5.49}$$

(5) Furthermore, the transversality condition:

$$\lambda_i(t_f) = 0, \ i = 1,...,5. \tag{5.50}$$

To obtain the adjoint variables λ_i, $i = 1,...,5$, we follow the classical result of (Pontryagin, 1987). The Pontryagin's Maximum Principle (PMP) stated in (Fleming and Rishel (2012), theorem 4.1) gives the required necessary optimality condition as given in the following theorem. Note that since we look for minimization, we use Pontryagin's Minimum Principle.

Theorem 5.4.1. *Let $u^* = (u_1^*, u_2^*, u_3^*)$ be the optimal control and $Q^* = (S_c^*, I_v^*, S_v^*, I_v^*, B^*)$ be the associated unique solutions of the optimal control problem (5.41)-(5.42) and (5.43)-(5.45) with fixed final time t_f. Then there exists adjoint variables λ_i, $i = 1,...,5$ which satisfies the*

following adjoint system:

$$\begin{aligned}
\frac{d\lambda_1}{dt} &= -\lambda_1\left(r-\frac{2rS_c}{K}-\frac{rI_c}{K}-\theta\right)+(\lambda_1-\lambda_2)(1-u_1)\beta_2 I_v,\\
\frac{d\lambda_2}{dt} &= -a_1+\frac{\lambda_1 rS_c}{K}+\lambda_2(\gamma+\eta)+(\lambda_3-\lambda_4)\beta_3 S_v-\lambda_5\eta,\\
\frac{d\lambda_3}{dt} &= \lambda_3(1+u_2)\delta+(\lambda_3-\lambda_4)(\beta_1 B+\beta_3 I_c),\\
\frac{d\lambda_4}{dt} &= -a_2+(\lambda_1-\lambda_2)(1-u_1)\beta_2 S_c+\lambda_4(1+u_2)\delta,\\
\frac{d\lambda_5}{dt} &= -a_3+(\lambda_3-\lambda_4)\beta_1 S_v+\lambda_5(1+u_3)m.
\end{aligned} \tag{5.51}$$

Together with transversality condition: $\lambda_i(t_f)=0,\ i=1,...,5.$
And also, we get optimal controls $u_1^*(t),\ u_2^*(t)$ *and* $u_3^*(t)$ *which are characterized by*

$$\begin{aligned}
u_1^*(t) &= min\left\{max\left\{0,\frac{\beta_2 S_c^* I_v^*(-\lambda_1+\lambda_2)}{b_1}\right\},0.95\right\},\\
u_2^*(t) &= min\left\{max\left\{0,\frac{\delta(\lambda_3 S_v^*+\lambda_4 I_v^*)}{b_2}\right\},0.95\right\},\\
u_3^*(t) &= min\left\{max\left\{0,\frac{\lambda_5 mB^*}{b_3}\right\},0.95\right\}.
\end{aligned} \tag{5.52}$$

Proof. The adjoint equations are computed by differentiating the Hamiltonian (5.46) with respect to the corresponding state variables: $S_c,\ I_c,\ S_v,\ I_v,\ B$ as Eq. (5.48). We assume that the final state $S_c(t_f),\ I_c(t_f),\ S_v(t_f),\ I_v(t_f)$ and $B(t_f)$ are free, then we obtain the transversality condition: $\lambda_i(t_f)=0,\ i=1,...,5.$

The optimal controls: $u_1^*(t),\ u_2^*(t)$ and $u_3^*(t)$ are computed from optimality condition (5.49) as follows.

(i) $\dfrac{\partial H}{\partial u_1}=b_1u_1+\beta_2 S_c I_v(\lambda_1-\lambda_2)=0$, at $u_1(t)=u_1^*(t)$

$$u_1^*(t)=\frac{\beta_2 S_c^* I_v^*(-\lambda_1+\lambda_2)}{b_1}.$$

(ii) $\dfrac{\partial H}{\partial u_2}=b_2u_2-\delta(\lambda_3 S_v+\lambda_4 I_v)=0$, at $u_2(t)=u_2^*(t)$

$$u_2^*(t)=\frac{\delta(\lambda_3 S_v^*+\lambda_4 I_v^*)}{b_2}.$$

(iii) $\dfrac{\partial H}{\partial u_3}=b_3u_3-\lambda_5 mB=0$, at $u_3(t)=u_3^*(t)$

$$u_3^*(t)=\frac{\lambda_5 mB^*}{b_3}.$$

Since $0\le u_i^*(t)\le (u_i)_{max}<1,\ i=1,2,3,$ we can rewrite the optimal controls: $u_1^*(t)$, $u_2^*(t)$, $u_3^*(t)$ as Eq. (5.52). □

5.5 Numerical Simulations for Optimal Control

In this section, we illustrate numerically the solutions of the CBD model (4.3) and corresponding state system (5.41) with the impact of controls: genetic control u_1, chemical control u_2 and cultural control u_3.

To obtain the intended numerical solutions, we first fix the initial guess for the control functions, then solve the state system (5.41) forward in time by using a fourth-order Runge-Kutta method. Next, using the current iteration solutions obtained for the state system and the transversality conditions, the adjoint systems (5.51) are also solved backward in time by applying the fourth-order Runge-Kutta algorithm. At each iteration time, the controls (5.52) are then updated using a convex combination of the previously computed results. The updated controls are, then utilized to repeat the iteration and compute the solutions of state and adjoint systems until a predefined convergence criterion is met (Lenhart and Workman, 2007).

For illustrative purposes, parameters values and initial data are presented to support our previous analytical results. Accordingly, some of parameter values were assumed while the remaining were obtained from literature. In addition to parameter values in Table 5.2, we assumed the initial dat: $S_c(0) = 100,\ I_c(0) = 15,\ S_v(0) = 10,\ I_v(0) = 2,\ B(0) = 10$. The weight constants of the objective functional are selected, for illustrative purposes, as $b_1 = 20,\ b_2 = 250,\ b_3 = 20,\ a_1 = 100,\ a_2 = 100$ and $a_3 = 10000$. Since the disease infects green berries between 4 - 14 after flowing, and more prevalent between 8 - 20 weeks (Bedimo et al., 2007), we simulate the system over a period $t_f = 120$ days.

We implement the simulations of optimal control strategy using the three scenarios of controls. We graphically present the simulation results of the governing system (5.41) with no contact rates (green curve), with controls (red broken curve) and without controls (blue curve).

5.5.1 Strategy A: Genetic Resistance and Chemical Controls

In the first case, we consider genetic control $u_1 \neq 0$ and chemical control $u_2 \neq 0$ without using cultural control $u_3 = 0$. The simulation results are displayed in Figures 5.11 (b), 5.12 (c) and 5.12 (d) depict that the number infected coffee, infected vector and pathogen population decrease due to the implementation of genetic resistance variety and chemical as control strategies. The yield increases with the controls due to effective use of the controls: u_1 and u_2, it remains above its value in the vector-free case (Figure 5.11 (a)).

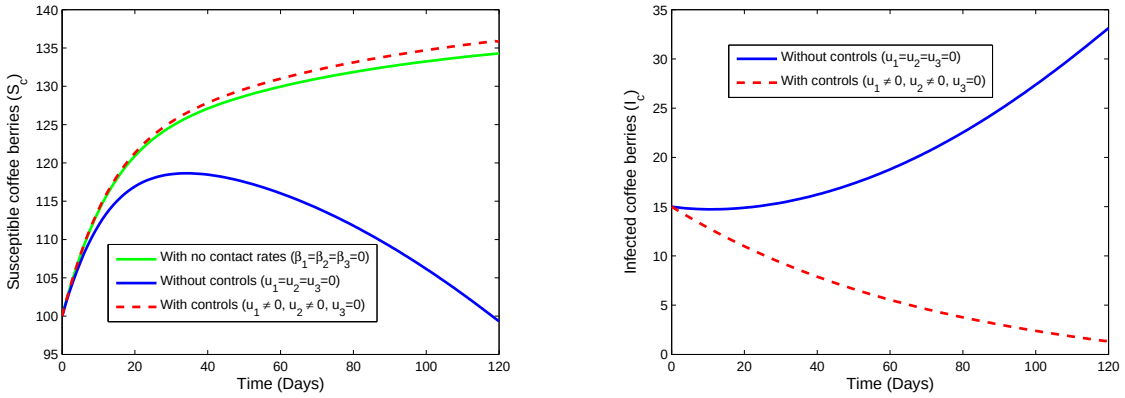

(a) (b)

Figure 5.11: Simulation results when both genetic resistance and chemical are implemented as controls on coffee population.

.

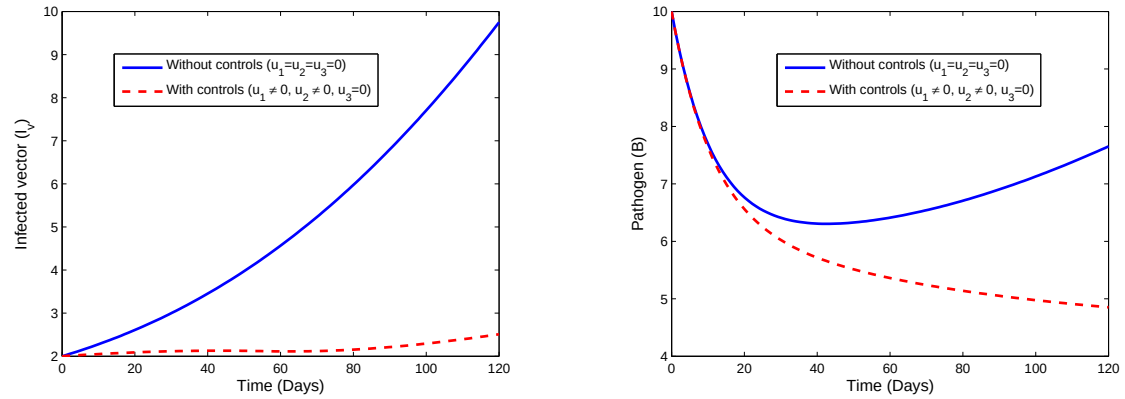

(a) (b)

Figure 5.12: Simulation results when both genetic resistance and chemical are implemented as controls to minimize the impact of infected vector and pathogen population.

5.5.2 Strategy B: Chemical and Cultural Controls

In the second case, we applied chemicals and culture as control strategies to minimize the objective function without genetic control. Due to these control strategies, the number of infected coffee, infected vector, and the pathogen is significantly reduced as shown in Figure 5.13 (b), Figures 5.14 (c) and 5.14 (d), while an increasing number was observed for the situation when there were no controls. Thus, in the absence of sufficient genetic resistant variety one can use cultural approaches as an alternative control mechanism in combination with chemical control to limit the economic impact of the disease. The coffee production increases with the controls but, due to the limited effectiveness of the controls: u_2 and u_3, it remains below its value in the vector-free case (Figure 5.13 (a)).

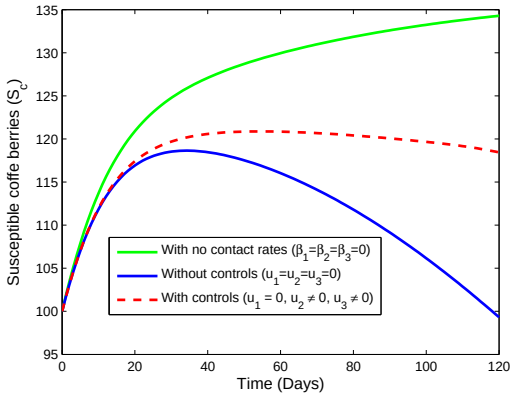

(a)

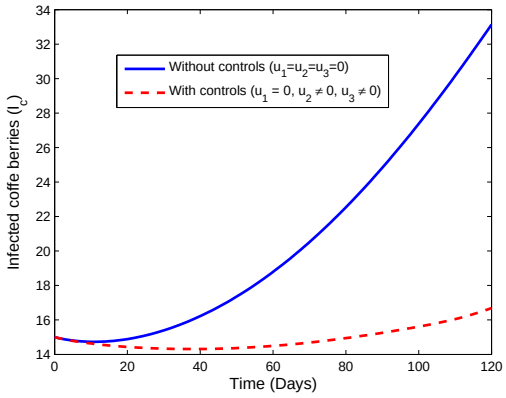

(b)

Figure 5.13: Simulation results when chemical and cultural practice are implemented as controls on coffee population.

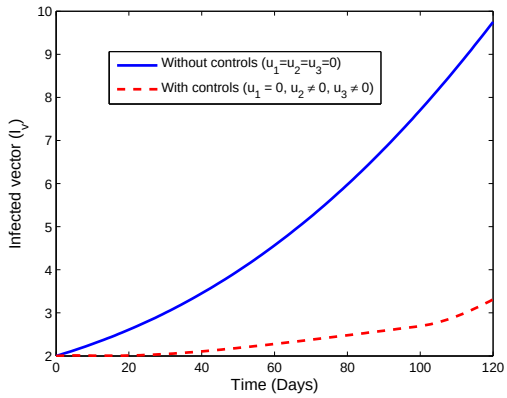

(a)

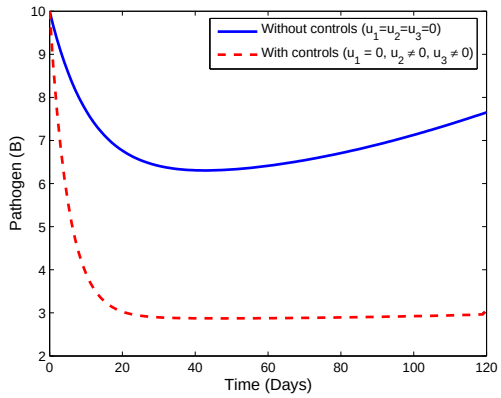

(b)

Figure 5.14: Simulation results when chemical and cultural practice are implemented as controls to minimize the impact of infected vector and pathogen population.

5.5.3 Strategy C: Genetic Resistance, Chemical and Cultural Controls

Lastly, we studied the combined effect of the three control strategies. As one can easily observe from Figure 5.15 (b), Figures 5.16 (c) and 5.16 (d), the combined control strategies produces similar results with the cases discussed above. In particular, Figure 5.16 (d) depicts that the concentration of pathogens is significantly reduced due to the implementation of all controls. The yield increases with the controls due to effective use of the controls, it remains above its value in the vector-free case (Figures 5.15 (a)). Hence, one can use any combination of these control strategies to combat the impact of coffee berry disease.

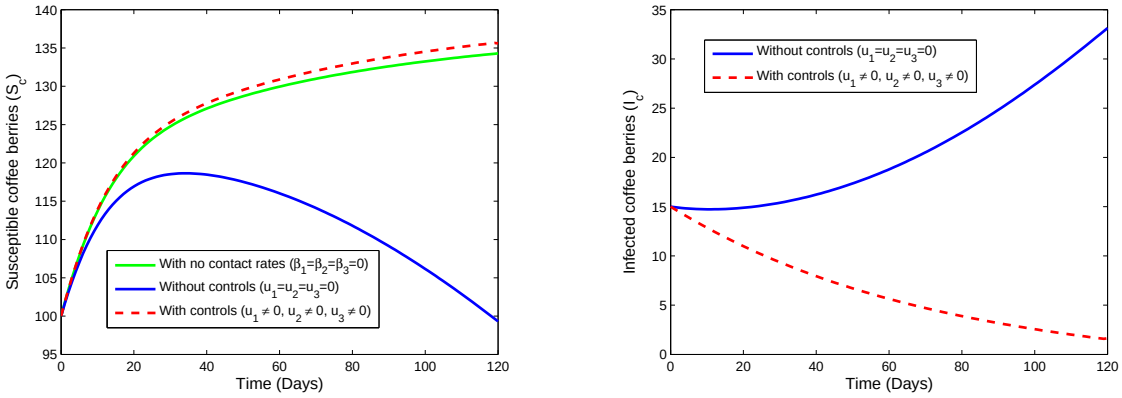

(a) (b)

Figure 5.15: Simulation results when genetic resistance, chemical and cultural practice are implemented as controls on coffee population.

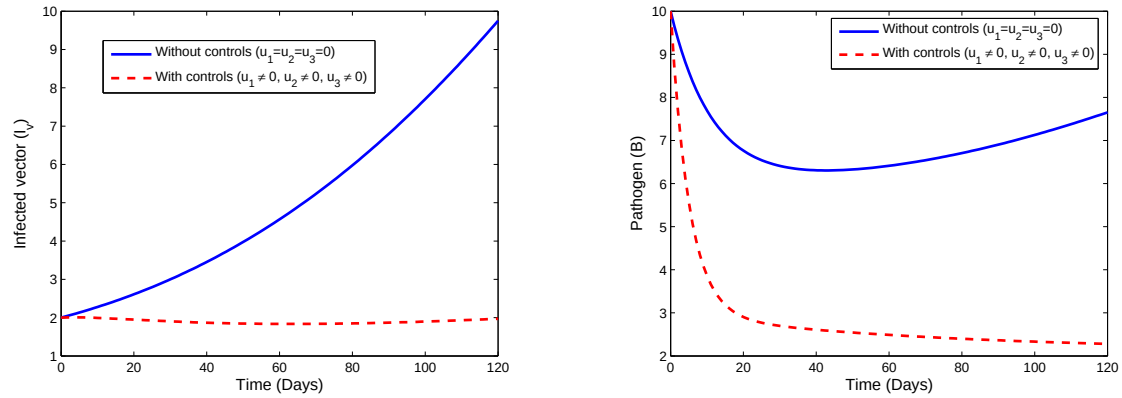

(a) (b)

Figure 5.16: Simulation results when genetic resistance, chemical and cultural practice are implemented as controls to minimize the impact of infected vector and pathogen population.

The bar diagram (i.e., bar graph is a diagram consists a sequence of vertical or horizontal rectangles) of the total susceptible coffee berries, infected coffee berries, infected vector and pathogen population over a period $t_f = 120$ days in Figures 5.11- 5.16 are summarized in Figure 5.17 (a-d).

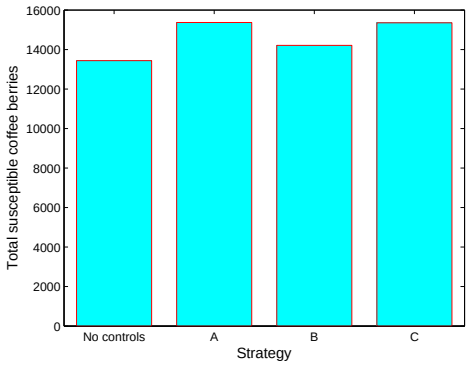

(a)

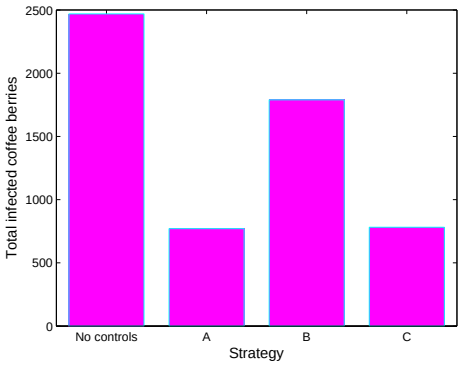

(b)

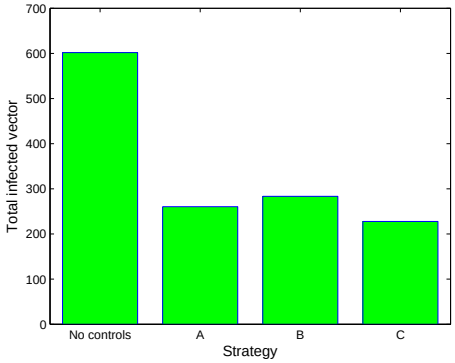

(a)

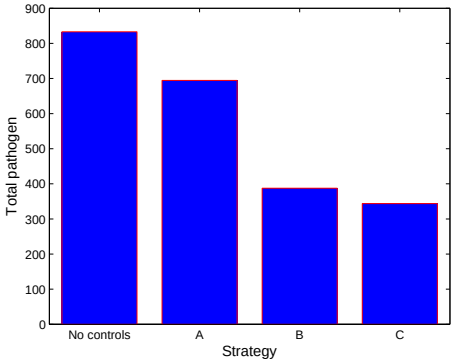

(b)

Figure 5.17: The comparison of the total susceptible coffee berries, infected coffee berries, infected vector and pathogen population result between no controls and control strategies.

The corresponding control profiles for the control strategies A, B and C are depicted in Figure 5.18 (a-c). Figure 5.18 (a) shows that the control profiles u_1 and u_2 are implemented for the whole period. Although the control u_2 is kept 95% for the first 55 days, but still it declines afterwards to zero. From the control profiles u_2 and u_3 are shown in Figure 5.18 (b), control u_2 is a maximum level (95%) for 98 days and decline afterwards to zero. From the control profiles u_1, u_2 and u_3 in Figure 5.18 (c), the controls u_1 and u_3 are at a maximum level (95%) for 118 days and decreased to zero. But the control u_2 is increased to maximum level for 30 days and then decreased to zero.

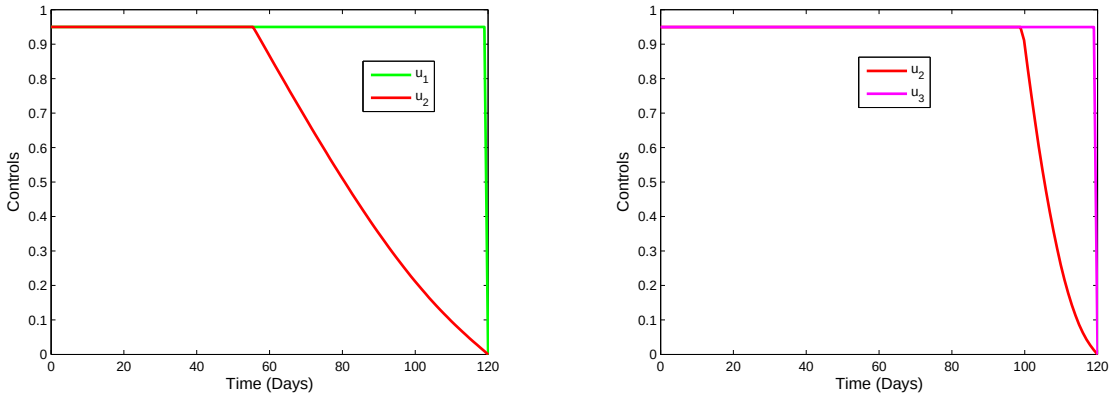

(a) (b)

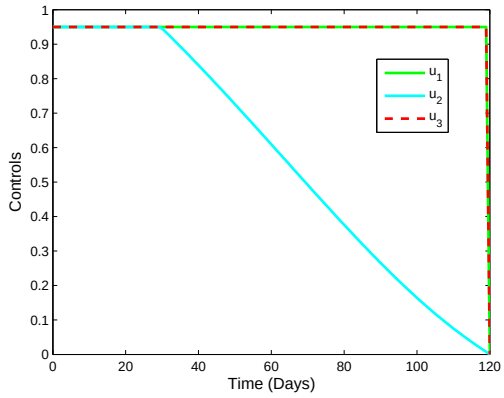

(c)

Figure 5.18: Control profiles corresponding to strategies A, B and C.

5.6 Cost-Effectiveness Analysis

In this section, we study cost-effectiveness for three different control strategies. To achieve this, we followed the method used in (Kinene et al., 2015; Alemneh et al., 2020). It relies on calculating the incremental cost-effectiveness ratio (ICER) and given by

$$\text{ICER} = \frac{\text{Difference of costs between two strategies}}{\text{Difference of the total number of their infection saverted}}.$$

Total number of infected averted is computed for each strategy by subtracting total infected with control from without any control implementation throughout the simulation. It is estimated for each strategy by subtracting total infected with control from without control. That is, the ICER strategy A, B and C is given as

$$\text{Total number of infections averted} = \int_0^{120} I_c(t)dt - \int_0^{120} I_{cc}^*(t)dt, \tag{5.53}$$

where I_c is an infections coffee berry without controls, I^*_{cc} is an infections coffee berry with controls. Each control strategy is compared with the next less effective options. The total control cost is given by

$$C(u) = \min_u \int_0^{120} \left(\frac{1}{2} b_1 u_1^2 + \frac{1}{2} b_2 u_2^2 + \frac{1}{2} b_3 u_3^2 \right) dt \tag{5.54}$$

The functions $0.5b_1u_1^2$, $0.5b_2u_2^2$ and $0.5b_3u_3^2$ represent the cost weights associated with each control measure. The numerical output for the three control strategies are rated incrementally in the form of infection coffee averted as shown in Table 5.3.

Table 5.3: Total infections coffee berries averted and control costs.

Strategy	Infections coffee averted	Control costs ($)	ICER
B	679.6471	1.2837	0.00189
C	1687.6478	8.7564	0.00741
A	1698.7086	9.4316	0.061044

We calculate the ICER for strategies B and C which are given in Table 5.3 and then compare their results as follows.

$$ICER(B) = \frac{1.2837}{679.6471} = 0.00189,$$
$$ICER(C) = \frac{8.7564 - 1.2837}{1687.6478 - 679.6471} = 0.00741.$$

The comparison between ICER of strategy B and strategy C shows a cost saving of 0.00189 for strategy B over strategy C. This shows that strategy B is cheaper than strategy C. Hence, strategy C is removed from subsequent ICER computations, as shown in Table 5.4 and we continue to compare strategy B over strategy A as follows.

$$ICER(B) = \frac{1.2837}{679.6471} = 0.00189,$$
$$ICER(A) = \frac{9.4316 - 1.2837}{1698.7086 - 679.6471} = 0.00799.$$

Table 5.4: Total infections coffee berries averted and control costs.

Strategy	Infections coffee averted	Control costs ($)	ICER
B	679.6471	1.2837	0.00189
A	1698.7086	9.4316	0.00799

Comparing strategy B and strategy A, we observe that ICER (A) is greater than ICER (B), showing that strategy A is more expensive than strategy B. Thus, we conclude that strategy B

is the most cost-effective compared to other strategies. Furthermore, the bar diagram of the total infections coffee berries averted, control costs, and ICER in Table 5.3 are represented in Figure 5.19.

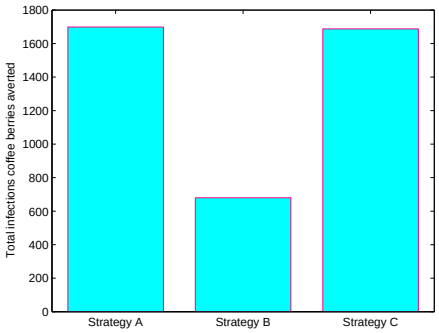

(a)

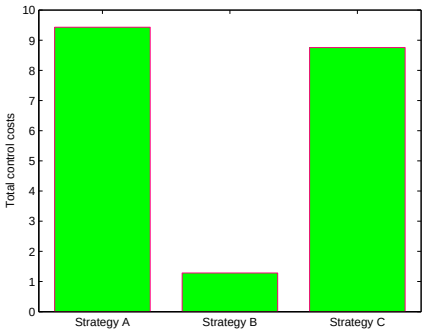

(b)

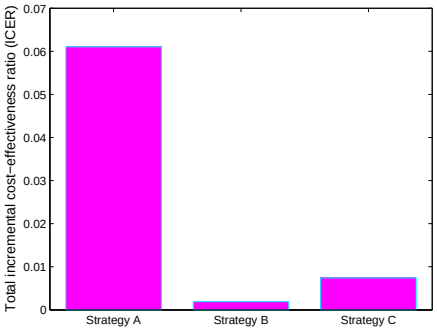

(c)

Figure 5.19: The comparison of the total infections coffee berries averted, control costs and ICER result among control strategies A, B and C.

CHAPTER 6

MODELLING THE DYNAMICS OF COFFEE BERRY DISEASE WITH OPTIMAL CONTROL IN THE PRESENCE OF TEMPERATURE VARIABILITY

In this chapter, we study the dynamics of CBD by taking into account temperature variability. We considered all the assumption given under Section 5.1.

6.1 Model Derivation

The proposed mathematical model contains two populations: the coffee population and the insect vector population with the interaction of CBD pathogen $B(t)$ and temperature variability $T(t)$. The parameters such as $\beta_1, \beta_2, \beta_3, \lambda, \delta, \pi$ and m are temperature dependent. The system can be summarized in the flow diagram shown in Figure 6.1.

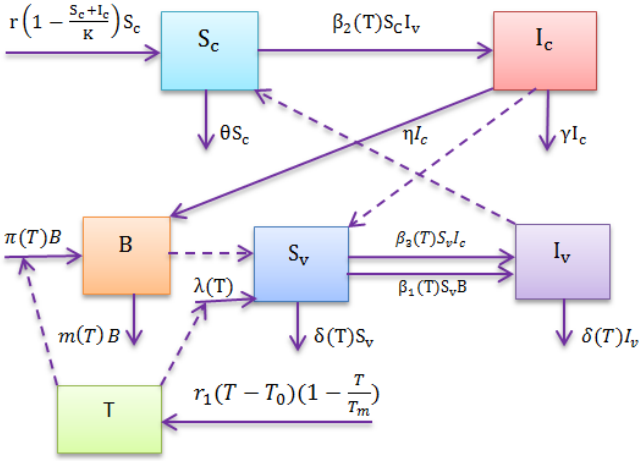

Figure 6.1: Schematic diagram for the transmission dynamics of CBD

Remark 6.1.1. *Note that the rates β_{11}, β_{21}, β_{31}, λ_{41}, δ_{51} π_{61} and m_{71} are given when there is no variation in temperature, while β_{12}, β_{22}, β_{32}, λ_{42}, δ_{52}, π_{62} and m_{72} are incremental rates due temperature variations.*

Hence, the governing mathematical model is described by the following nonlinear systems

of differential equations:

$$\begin{cases} \dfrac{dS_c}{dt} = rS_c\left(1-\dfrac{S_c+I_c}{K}\right) - \beta_2(T)S_cI_v - \theta S_c, \\ \dfrac{dI_c}{dt} = \beta_2(T)S_cI_v - (\gamma+\eta)I_c, \\ \dfrac{dS_v}{dt} = \lambda(T) - (\beta_1(T)B+\beta_3(T)I_c)S_v - \delta(T)S_v, \\ \dfrac{dI_v}{dt} = (\beta_1(T)B+\beta_3(T)I_c)S_v - \delta(T)I_v, \\ \dfrac{dB}{dt} = \eta I_c - (m(T)-\pi(T))B, \\ \dfrac{dT}{dt} = r_1(T-T_0)\left(1-\dfrac{T}{T_m}\right), \end{cases} \tag{6.1}$$

where

$$\beta_1(T) = \beta_{11} + \beta_{12}(\frac{T-T_0}{T_m}), \beta_2(T) = \beta_{21} + \beta_{22}(\frac{T-T_0}{T_m}), \beta_3(T) = \beta_{31} + \beta_{32}(\frac{T-T_0}{T_m}),$$
$$\lambda(T) = \lambda_{41} + \lambda_{42}(\frac{T-T_0}{T_m}), \delta(T) = \delta_{51} + \delta_{52}(\frac{T-T_0}{T_m}), \pi(T) = \pi_{61} + \pi_{62}(\frac{T-T_0}{T_m}),$$
$$m(T) = m_{71} + m_{72}(\frac{T-T_0}{T_m}),$$

with initial data: $S_c(0) = S_{0c} > 0$, $I_c(0) = I_{0c} \geq 0$, $S_v(0) = S_{0v} > 0$, $I_v(0) = I_{0v} \geq 0$, $B(0) = B_0 \geq 0$ and $T(0) = T_0 > 0$. We assume that there is a temperature range, $T_0 \leq T \leq T_m$, where insect vectors may survive and CBD pathogen less or more spread.

6.2 Model Analysis

In this section, we study the invariant region, the positivity of the solutions, disease-free and endemic equilibrium, basic reproduction number, bifurcation, and sensitivity analysis, and local and global stability of equilibria.

6.2.1 Invariant Region

We found the invariant region Ω_3, in which the model system (6.1) solution set is bounded. To do this, let us consider total population $Y(t) = S_c(t) + I_c(t) + S_v(t) + I_v(t) + B(t)$. Then taking derivative both sides of $Y(t)$ with respect to time t and adding the first five equations from system (6.1), we get

$$\begin{aligned} \frac{dY}{dt} &= rS_c\left(1-\frac{S_c+I_c}{K}\right) - \theta S_c + \lambda(\bar{T}) - \gamma I_c - \delta(\bar{T})S_v - \delta(\bar{T})I_v + (\pi(\bar{T}) - m(\bar{T}))B, \\ &\leq \lambda(\bar{T}) + rS_c - \gamma I_c - \delta(\bar{T})S_v - \delta(\bar{T})I_v + (\pi(\bar{T}) - m(\bar{T}))B, \\ &\leq \lambda(\bar{T}) + (1+r)S_c - S_c - \gamma I_c - \delta(\bar{T})S_v - \delta(\bar{T})I_v - (m(\bar{T}) - \pi(\bar{T}))B, \end{aligned} \tag{6.2}$$

where $\bar{T} \in [T_0, T_m]$. Then Eq. (6.2) can be rewritten as

$$\frac{dY}{dt} + hY \leq \lambda(\bar{T}) + \hat{K}(1+r), \tag{6.3}$$

where $\hat{K} = max\{S_c(0),\ K\}$, $h = min\{1, \gamma,\ \delta(\bar{T}),\ m(\bar{T}) - \pi(\bar{T})\}$ and $m(\bar{T}) - \pi(\bar{T}) > 0$. By solving Eq. (6.3) we get

$$Y \leq \frac{1}{h}\left(\lambda(\bar{T}) + \hat{K}(1+r)\right) + Ce^{-ht}, \tag{6.4}$$

where C is constant. Assume that the initial condition $Y(0) = Y_0$ in Eq. (6.4) holds, and re-arranging equation, we obtain

$$Y(t) \leq \frac{1}{h}\left(\lambda(\bar{T}) + \hat{K}(1+r)\right) + (Y_0 - \frac{1}{h}\left(\lambda(\bar{T}) + \hat{K}(1+r)\right))e^{-ht}. \tag{6.5}$$

As $t \to \infty$ in Eq. (6.5), the population size $Y(t) \to \left(\lambda(\bar{T}) + \hat{K}(1+r)\right)/h$. Thus, the invariant region of the system (6.1) is given by

$$\Omega_3 = \left\{(S_c,\ I_c,\ S_v,\ I_v,\ B) \in \Re^5_+ : 0 \leq S_c + I_c + S_v + I_v + B \leq \frac{1}{h}\left(\lambda(\bar{T}) + \hat{K}(1+r)\right)\right\}. \tag{6.6}$$

is positive invariant and therefore, all the solution set of system (6.1) is bounded in Ω_3.

6.2.2 Positivity of the Solutions

For the model (6.1) to be epidemiologically meaningful and well posed, we need to prove that all the solutions with positive initial data are non-negative for all $t \geq 0$. This will be stated as follows.

Theorem 6.2.1. *Assume that the initial conditions in the model (6.1) holds. Then the solutions $S_c(t)$, $I_c(t)$, $S_v(t)$, $I_v(t)$, $B(t)$, and $T(t)$ of system (6.1) are positive $\forall t \geq 0$.*

Proof. From the first equation of system (6.1), we obtain the expression

$$\frac{dS_c}{dt} = rS_c\left(1 - \frac{S_c + I_c}{K}\right) - \beta_2(T)S_cI_v - \theta S_c \leq rS_c(1 - \frac{S_c}{K}). \tag{6.7}$$

Then, by solving the last inequality of Eq. (6.7) and applying initial condition, we obtained

$$S_c(t) \leq \frac{KS_c(0)}{(K - S_c(0))e^{-rt} + S_c(0)}. \tag{6.8}$$

As $t \to \infty$ in equation (6.8), we get

$$0 \leq S_c(t) \leq K.$$

In a similar way, we show that the positivity of state variables: I_c, S_v, I_v, B and T. This shows that all solutions of system (6.1) are non-negative for all $t \geq 0$. Hence, the proposed model (6.1) is both epidemiological meaningful and mathematically well posed in the domain Ω. □

6.2.3 Disease Free Equilibrium Point (DFEP)

To find DFEP, we equated the left hand side of model system (6.1) to zero and solving for the non-infected state variables, we get $S_c = 0$ or $S_c = K - K\theta/r$, $S_v = \lambda(T)/\delta(T)$, $T = T_0$ or $T = T_m$. Then, the DFE of the model system (6.1) at $T = T_0$ and $T = T_m$ respectively are $\bar{E}_1$ and $\bar{E}_2$ where

$$\bar{E}_1 = \left(\frac{K(r-\theta)}{r},\ 0,\ \frac{\lambda(T_0)}{\delta(T_0)},\ 0,\ 0\right), \quad \bar{E}_2 = \left(\frac{K(r-\theta)}{r},\ 0,\ \frac{\lambda(T_m)}{\delta(T_m)},\ 0,\ 0\right). \tag{6.9}$$

6.2.4 The Basic Reproduction Number

The basic reproduction number $\bar{R}_0$ can be derived using the approach of the next-generation matrix method from (Van den Driessche and Watmough, 2002). The model system (6.1) is rewritten beginning with newly infective groups:

$$\begin{cases} \dfrac{dI_c}{dt} = \beta_2(T)S_cI_v - (\gamma+\eta)I_c, \\ \dfrac{dI_v}{dt} = (\beta_1(T)B + \beta_3(T)I_c)S_v - \delta(T)I_v, \\ \dfrac{dB}{dt} = \eta I_c - (m(T) - \pi(T))B. \end{cases} \tag{6.10}$$

The right hand side of system (6.10) is written as $f - g$, where

$$f = \begin{bmatrix} \beta_2(T)ScIv \\ (\beta_1(T)B + \beta_3(T)Ic)Sv \\ 0 \end{bmatrix}, \quad g = \begin{bmatrix} (\gamma+\eta)Ic \\ \delta(T)Iv \\ -\eta Ic + (m(T) - \pi(T))B \end{bmatrix}. \tag{6.11}$$

Then, by linearization approach, the associated matrices of f and g at the DFE gives F and G respectively, where

$$F = \begin{bmatrix} 0 & \dfrac{K(r-\theta)\beta_2(T^*)}{r} & 0 \\ \dfrac{\beta_3(T^*)\lambda(T^*)}{\delta(T^*)} & 0 & \dfrac{\beta_1(T^*)\lambda(T^*)}{\delta(T^*)} \\ 0 & 0 & 0 \end{bmatrix},$$

$$G = \begin{bmatrix} \gamma+\eta & 0 & 0 \\ 0 & \delta(T^*) & 0 \\ -\eta & 0 & m(T^*)-\pi(T^*) \end{bmatrix},$$

with $T^* = T_0$ or $T^* = T_m$. Then G^{-1} is computed and given as:

$$G^{-1} = \begin{bmatrix} \frac{1}{\gamma+\eta} & 0 & 0 \\ 0 & \frac{1}{\delta(T^*)} & 0 \\ \frac{\eta}{(m(T^*)-\pi(T^*)(\gamma+\eta)} & 0 & \frac{1}{m(T^*)-\pi(T^*)} \end{bmatrix}.$$

So we have

$$FG^{-1} = \begin{bmatrix} 0 & \frac{K(r-\theta)\beta_2(T^*)}{r\delta(T^*)} & 0 \\ \frac{K\beta_2(T^*)\lambda(T^*)\left[(m(T^*)-\pi(T^*))\beta_3(T^*)+\beta_1(T^*)\eta\right](r-\theta)}{r(m(T^*)-\pi(T^*))\delta^2(T^*)(\gamma+\eta)} & 0 & \bar{x} \\ 0 & 0 & 0 \end{bmatrix}.$$

where $\bar{x} = \dfrac{\beta_1(T^*)\lambda(T^*)}{\delta(T^*)(m(T^*)-\pi(T^*))}$. Since $\bar{R}_0 = \rho(FG^{-1})$ is the spectral radius of FG^{-1} and it follows that for model (6.1), the R_1 at $\bar{E}_1$ and R_2 at $\bar{E}_2$ are given respectively, by the Eq. (6.12):

$$\begin{aligned} R_1 &= \sqrt{\frac{K\beta_{21}\lambda_{41}\left[(m_{71}-\pi_{61})\beta_{31}+\beta_{11}\eta\right](r-\theta)}{r(m_{71}-\pi_{61})\delta_{51}^2(\gamma+\eta)}}, \\ R_2 &= \sqrt{\frac{K\beta_2(T_m)\lambda(T_m)\left[(m(T_m)-\pi(T_m))\beta_3(T_m)+\beta_1(T_m)\eta\right](r-\theta)}{r(m(T_m)-\pi(T_m))\delta^2(T_m)(\gamma+\eta)}}. \end{aligned} \tag{6.12}$$

In Eq. (6.12), R_1 become real number whenever both $r-\theta \geq 0$ and $m_{71}-\pi_{61} \geq 0$ and also, R_2 come real number whenever $r-\theta \geq 0$ and $m(T_m)-\pi(T_m) \geq 0$. Hence, the basic reproduction number R_2 at maximum temperature T_m can be expressed interms of the basic reproduction number R_1 which is at minimum temperature T_0 as:

$$R_2 = \sqrt{\frac{R_1^2 + \frac{K(r-\theta)}{r(\gamma+\eta)\delta_{51}^2}\left(\beta_{21}\lambda_{41}\frac{m_{72}-\pi_{62}}{m_{71}-\pi_{61}}(\beta_{31}d+\beta_{32}d^2)+\beta_{21}\lambda_{41}\beta_{32}d+n+W\right)}{1+2\delta_{52}d+\left(\frac{\delta_{52}}{\delta_{51}}\right)^2 d^2+\frac{m_{72}-\pi_{62}}{m_{71}-\pi_{61}}\left(d+2\frac{\delta_{52}}{\delta_{51}}d^2+\left(\frac{\delta_{52}}{\delta_{51}}\right)^2 d^3\right)}} \tag{6.13}$$

where

$$W = \left((\beta_{21}\lambda_{42}+\beta_{22}\lambda_{41})d+\beta_{22}\lambda_{42}d^2\right)\left(\beta_{31}+\beta_{31}\frac{m_{72}-\pi_{62}}{m_{61}-\pi_{61}}d+\beta_{32}d+\beta_{32}\frac{m_{72}-\pi_{62}}{m_{61}-\pi_{61}}d^2\right)$$
$$+\left((\beta_{21}\lambda_{42}+\beta_{22}\lambda_{41})d+\beta_{22}\lambda_{42}d^2\right)\left(\frac{\beta_{11}+\beta_{12}d}{m_{61}-\pi_{61}}\eta\right),\ n=\frac{\beta_{21}\lambda_{41}\beta_{12}\eta d}{m_{71}-\pi_{61}},\ d=\frac{T_m-T_0}{T_m}.$$

6.2.5 Local Stability of Disease Free Equilibrium Point

Theorem 6.2.2. *If $R_1 < R_2 < 1$, then disease-free equilibrium $\bar{E}_1$ or $\bar{E}_2$ of the model (6.1) is locally asymptotically stable in Ω_3.*

Proof. The Jacobian matrix of the system (6.1) at $\bar{E}_1$ or $\bar{E}_2$ is given by

$$J(E_*)=\begin{bmatrix} \theta-r & -(r-\theta) & 0 & -\frac{K(r-\theta)\beta_2(T^*)}{r} & 0 \\ 0 & -\gamma-\eta & 0 & \frac{K(r-\theta)\beta_2(T^*)}{r} & 0 \\ 0 & -\frac{\beta_3(T^*)\lambda(T^*)}{\delta(T^*)} & -\delta(T^*) & 0 & -\frac{\beta_1(T^*)\lambda(T^*)}{\delta(T^*)} \\ 0 & \frac{\beta_3(T^*)\lambda(T^*)}{\delta(T^*)} & 0 & -\delta(T^*) & \frac{\beta_1(T^*)\lambda(T^*)}{\delta(T^*)} \\ 0 & \eta & 0 & 0 & \pi(T^*)-m(T^*) \end{bmatrix} \tag{6.14}$$

where $E_* = \bar{E}_1$ or $E_* = \bar{E}_2, T^* = T_0$ or $T^* = T_m$.
The characteristic polynomial of Eq. (6.14) is given by

$$(\delta(T^*)+\Lambda)(r-\theta+\Lambda)(\Lambda^3+A_2\Lambda^2+A_1\Lambda+A_0)=0. \tag{6.15}$$

From Eq. (6.15), we obtain that $\Lambda_1 = -\delta(T^*) < 0,\ \Lambda_2 = -(r-\theta) < 0$ (see Remark 5.2.1, $r > \theta$), and from the last characteristic equation, we have

$$\Lambda^3+A_2\Lambda^2+A_1\Lambda+A_0=0, \tag{6.16}$$

where

$$A_2 = \gamma+\eta+m(T^*)-\pi(T^*)+\delta(T^*),$$
$$A_1 = (\gamma+\eta)(m(T^*)-\pi(T^*)+\delta(T^*))+\delta(T^*)(m(T^*)-\pi(T^*))-\frac{K\beta_2\beta_3(T^*)\lambda(T^*)(r-\theta)}{r\delta(T^*)},$$
$$A_0 = \delta(T^*)(\gamma+\eta)(m(T^*)-\pi(T^*))-\frac{K\beta_3(T^*)\lambda(T^*)(r-\theta)(\beta_3(T^*)m(T^*)-\beta_3(T^*)\pi(T^*))}{r\delta(T^*)}$$
$$-\frac{\beta_1(T^*)\eta}{r\delta(T^*)}.$$

Using Routh-Hurwitz criteria, equation (6.16) has negative eigenvalues whenever $A_i > 0, A_1A_2 - A_0 > 0$ and $A_0(A_1A_2-A_0) > 0$. But, from the third inequality A_0 can be rearranged at $T^* = T_m$

as

$$A_0 = \delta(T_m)(\gamma+\eta)(m(T_m)-\pi(T_m))(1-R_2^2). \tag{6.17}$$

From Eq. (6.17) A_0 to be positive if $R_2 < 1$. Since $R_1 < R_2$, therefore, the DFEP $\bar{E}_1$ or $\bar{E}_2$ is locally asymptotically stable for $R_1 < R_2 < 1$ in Ω_3. □

6.2.6 Global Stability of Disease Free Equilibrium Point

Theorem 6.2.3. *If $R_1 < R_2 < 1$, then the disease-free equilibrium $\bar{E}_1$ or $\bar{E}_2$ of the model (6.1) is globally asymptotically stable in Ω_3.*

Proof. To proof this theorem, we first developed the following Lyapunov function:

$$\bar{U} = I_c + I_v + B. \tag{6.18}$$

Then, differentiating the above Lyapunov function U with respect to time t, we get

$$\begin{aligned}
\frac{d\bar{U}}{dt} &= \frac{dI_c}{dt} + \frac{dI_v}{dt} + \frac{dB}{dt} \\
&= \beta_2(T^*)S_cI_v - \gamma I_c + (\beta_1(T^*)B + \beta_3(T^*)I_c)S_v - \delta(T^*)I_v - (m(T^*)-\pi(T^*))B \\
&= (Q-V)\begin{bmatrix} I_c \\ I_v \\ B \end{bmatrix} - \begin{bmatrix} 0 & 0 & 0 \\ 0 & \dfrac{\beta_2(T^*)K\theta}{r} & 0 \\ 0 & 0 & 0 \end{bmatrix}\begin{bmatrix} I_c \\ I_v \\ B \end{bmatrix},
\end{aligned} \tag{6.19}$$

where the matrices Q and V are given by

$$Q = \begin{bmatrix} \dfrac{\beta_3(T^*)\lambda(T^*)}{\delta(T^*)} & 0 & 0 \\ 0 & \beta_2(T^*)K & 0 \\ 0 & 0 & \dfrac{\beta_1(T^*)\lambda(T^*)}{\delta(T^*)} \end{bmatrix}, \quad V = \begin{bmatrix} \gamma & 0 & 0 \\ 0 & \delta(T^*) & 0 \\ 0 & 0 & m(T^*)-\pi(T^*) \end{bmatrix}.$$

Since $\beta_2(T^*)K\theta/r > 0$, then Eq. (6.19) can be written as

$$\frac{d\bar{U}}{dt} \leq (Q-V)\begin{bmatrix} I_c \\ I_v \\ B \end{bmatrix}. \tag{6.20}$$

The eigenvalues of matrix $(Q-V)$ all have negative real parts if $\beta_3(T^*)\lambda(T^*)/\delta(T^*) < \gamma$, $\beta_2(T^*)K < \delta(T^*)$ and $\beta_1(T^*)\lambda(T^*)/\delta(T^*) < m(T^*)-\pi(T^*)$. It follows by the comparison approach from (Diekmann et al., 1990) that $(I_c(t),\ I_v(t),\ B(t)) \to (0,\ 0,\ 0)$. Substituting $I_c = I_v = B = 0$ at DFE, we obtain $S_c(t) \to K(r-\theta)/r$ and $S_v(t) \to \lambda(T^*)/\delta(T^*)$ as $t \to \infty$. Thus, $(S_c(t),\ I_c(t),\ S_v(t),\ I_v(t),\ B(t)) \to (K(r-\theta)/r,\ 0,\ \lambda(T^*)/\delta(T^*),\ 0,\ 0)$ as $t \to \infty$ for

$R_1 < R_2 < 1$. Hence, the DFEP $\bar{E}_1$ or $\bar{E}_2$ is globally asymptotically stable for $R_1 < R_2 < 1$ in Ω_3. □

6.2.7 Endemic Equilibrium Point (EEP)

An endemic equilibrium point is denoted by $\bar{E}^* = (S_c^*,\ I_c^*,\ S_v^*,\ I_v^*,\ B^*,\ T^*)$, and is computed as follows

$$\begin{aligned} rS_c^*\left(1-\frac{S_c^*+I_c^*}{K}\right)-\beta_2(T)S_c^*I_v^*-\theta S_c^* &= 0,\\ \beta_2(T)S_c^*I_v^*-(\gamma+\eta)I_c^* &= 0,\\ \lambda(T)-(\beta_1(T)B^*+\beta_3(T)I_c^*)S_v^*-\delta(T)S_v^* &= 0,\\ (\beta_1(T)B^*+\beta_3(T)I_c^*)S_v^*-\delta(T)I_v^* &= 0,\\ \eta I_c^*-(m(T)-\pi(T))B^* &= 0,\\ r_1(T^*-T_0)\left(1-\frac{T^*}{T_m}\right) &= 0. \end{aligned} \tag{6.21}$$

By solving Eq. (6.21), we get $S_c^*,\ S_v^*,\ I_v^*$ and B^* interms of I_c^* at $T^* = T_0$:

$$\begin{aligned} S_c^* &= \frac{\delta_{51}(\gamma+\eta)[(\beta_{31}(m_{71}-\pi_{61})+\beta_{11}\eta)I_c^*+\delta_{51}(m_{71}-\pi_{61})]}{\beta_{21}\lambda_{41}(\beta_{31}(m_{71}-\pi_{61})+\beta_{11}\eta)I_c^*},\\ S_v^* &= \frac{\lambda_{41}(m_{71}-\pi_{61})}{(\beta_{31}(m_{71}-\pi_{61})+\beta_{11}\eta)I_c^*+\delta_{51}(m_{71}-\pi_{61})},\\ I_v^* &= \frac{\lambda_{41}(\beta_{31}(m_{71}-\pi_{61})+\beta_{11}\eta)I_c^*}{\delta_{51}(\beta_{31}(m_{71}-\pi_{61})+\beta_{11}\eta)I_c^*+\delta_{51}^2(m_{71}-\pi_{61})},\\ B^* &= \frac{\eta}{m_{71}-\pi_{61}}I_c^*. \end{aligned} \tag{6.22}$$

Since all parameters are positive, $m_{71} > \pi_{61}$. Let us find the expressions for I_c^* that satisfy Eq. (6.22) and $S_c^* > 0$. From Eq. (6.22) substituting S_c^* and I_v^* into the first equation of (6.21), we obtain I_c^* that satisfies the following equation.

$$f_1(I_c^*) = A_1(I_c^*)^3 + B_1(I_c^*)^2 + C_1I_c^* + D_1 = 0, \tag{6.23}$$

where

$$\begin{aligned} A_1 &= \frac{r^3\delta_{51}^5(m_{71}-\pi_{61})^2(\gamma+\eta)^2R_{01}^4}{K^2\beta_{21}\lambda_{41}(r-\theta)^2},\\ B_1 &= \frac{r^3(\gamma+\eta)^3\delta_{51}^5(m_{71}-\pi_{61})^2R_{01}^4}{\beta_{21}^2\lambda_{41}^2K^2(r-\theta)^2}+\frac{r^2(m_{71}-\pi_{61})^2\delta_{51}^4(\gamma+\eta)R_{01}^2}{K(r-\theta)}\\ &\quad+\frac{r^2(m_{71}-\pi_{61})^2\delta_{51}^4(\gamma+\eta)^2(1+\delta_{51}(\theta-r))R_{01}^4}{K\beta_{21}\lambda_{41}(r-\theta)^2}. \end{aligned}$$

$$C_1 = \delta_{51}^2(\beta_{31}(m_{71}-\pi_{61})+\beta_{11}\eta)(m_{71}-\pi_{61})(r\delta_{51}+1+K\theta\beta_{21}\lambda_{41}),$$
$$D_1 = \delta_{51}^3(m_{71}-\pi_{61}) - rK\delta_{51}^2\beta_{21}\lambda_{41}(\beta_{31}(m_{71}-\pi_{61})+\beta_{11}\eta)(m_{71}-\pi_{61}).$$

Similarly, by computing the EEP at $T^* = T_m$, we get

$$\begin{aligned}
S_c^* &= \frac{\delta(T_m)(\gamma+\eta)[(\beta_3(T_m)(m(T_m)-\pi(T_m))+\beta_1(T_m)\eta)I_c^* + \delta(T_m)(m(T_m)-\pi(T_m))]}{\beta_2(T_m)\lambda(T_m)(\beta_3(T_m)(m(T_m)-\pi(T_m))+\beta_1(T_m)\eta)I_c^*},\\
S_v^* &= \frac{\lambda(T_m)(m(T_m)-\pi(T_m))}{(\beta_3(T_m)(m(T_m)-\pi(T_m))+\beta_1(T_m)\eta)I_c^* + \delta(T_m)(m(T_m)-\pi(T_m))},\\
I_v^* &= \frac{\lambda(T_m)(\beta_3(T_m)(m(T_m)-\pi(T_m))+\beta_1(T_m)\eta)I_c^*}{\delta(T_m)(\beta_3(T_m)(m(T_m)-\pi(T_m))+\beta_1(T_m)\eta)I_c^* + \delta^2(T_m)(m(T_m)-\pi(T_m))},\\
B^* &= \frac{\eta}{m(T_m)-\pi(T_m)}I_c^*.
\end{aligned} \tag{6.24}$$

From Eq. (6.24) substituting S_c^* and I_v^* into the first equation of (6.21), we get I_c^* such that

$$f_2(I_c^*) = A_2(I_c^*)^3 + B_2(I_c^*)^2 + C_2I_c^* + D_2 = 0, \tag{6.25}$$

where

$$\begin{aligned}
A_2 &= \frac{r^3\delta^5(T_m)(m(T_m)-\pi(T_m))^2(\gamma+\eta)^2R_{02}^4}{K^2\beta_2(T_m)\lambda(T_m)(r-\theta)^2},\\
B_2 &= \frac{r^3(\gamma+\eta)^3\delta^5(T_m)(m(T_m)-\pi(T_m))^2R_{02}^4}{\beta_2^2(T_m)\lambda^2(T_m)K^2(r-\theta)^2} + \frac{r^2(m(T_m)-\pi(T_m))^2\delta^4(T_m)(\gamma+\eta)R_{02}^2}{K(r-\theta)}\\
&\quad + \frac{r^2(m(T_m)-\pi(T_m))^2\delta^4(T_m)(\gamma+\eta)^2(1+\delta(T_m)(\theta-r))R_{02}^4}{K\beta_2(T_m)\lambda(T_m)(r-\theta)^2},\\
C_2 &= \delta^2(T_m)(\beta_3(T_m)(m(T_m)-\pi(T_m))+\beta_1(T_m)\eta)(m(T_m)-\pi(T_m))(r\delta(T_m)+1)\\
&\quad + \delta^2(T_m)(\beta_3(T_m)(m(T_m)-\pi(T_m))+\beta_1(T_m)\eta)(m(T_m)-\pi(T_m))K\theta\beta_2(T_m)\lambda(T_m),\\
D_2 &= \delta^3(T_m)(m(T_m)-\pi(T_m)) - rK\delta^2(T_m)\beta_2(T_m)\lambda(T_m)(\beta_3(T_m)(m(T_m)-\pi(T_m))\\
&\quad + \beta_1(T_m)\eta)(m(T_m)-\pi(T_m)).
\end{aligned}$$

6.2.8 Local Stability of Endemic Equilibrium Point

Theorem 6.2.4. *If $R_2 > R_1 > 1$, $B_i > 0, i = 1,\ldots,5, B_1B_2 - B_3 > 0, -B_3^2 - B_1^2B_4 + B_1(B_2B_3 + B_5) > 0, -B_4^2(-B_1B_2B_3 + B_3^2 + B_1^2B_4) + (B_2B_3 - B_1(B_2^2 - 2B_4))B_5 - B_5^2 > 0, B_5(-B_4(-B_1B_2B_3 + B_3^2 + B_1^2B_4) + (B_2B_3 - B_1(B_2^2 - 2B_4))B_5 - B_5^2) > 0$, then endemic equilibrium $\bar{E}^*$ of model (6.1) is locally asymptotically stable in Ω_3.*

Proof. The Jacobian matrix of system (6.1) at the endemic equilibrium $\bar{E}^*$ is given by

$$J(\bar{E}^*) = \begin{bmatrix} M_{11} & -(r-\theta) & 0 & -\beta_2(T^*)S_c^* & 0 \\ \beta_2(T^*)I_v^* & -\gamma-\eta & 0 & \beta_2(T^*)S_c^* & 0 \\ 0 & -\beta_3(T^*)S_v^* & M_{33} & 0 & -\beta_1(T^*)S_v^* \\ 0 & \beta_3(T^*)S_v^* & \beta_1(T^*)B^* + \beta_3(T^*)I_c^* & -\delta(T^*) & \beta_1(T^*)S_v^* \\ 0 & \eta & 0 & 0 & \pi(T^*) - m(T^*) \end{bmatrix} \tag{6.26}$$

where $M_{11} = r - \dfrac{rI_c^*}{K} - \dfrac{2rS_c^*}{K} - \beta_2(T^*)I_v^* - \theta$, $M_{33} = -\beta_1(T^*)B^* - \beta_3(T^*)I_c^* - \delta(T^*)$, $T^* = T_0$ or $T^* = T_m$.

The eigenvalues of matrix (6.26) are computed from the following equation:

$$\begin{vmatrix} b_{11}-\Lambda & b_{12} & 0 & b_{14} & 0 \\ b_{21} & b_{22}-\Lambda & 0 & b_{24} & 0 \\ 0 & b_{32} & b_{33}-\Lambda & 0 & b_{35} \\ 0 & b_{42} & b_{43} & b_{44}-\Lambda & b_{45} \\ 0 & b_{52} & 0 & 0 & b_{55}-\Lambda \end{vmatrix} = 0 \tag{6.27}$$

where $b_{11} = -\theta - rI_c^*/K - 2rS_c^*/K - \beta_2(T^*)I_v^* + r$, $b_{12} = -(r-\theta)$, $b_{21} = \beta_2(T^*)I_v^*$, $b_{22} = -\gamma-\eta$, $b_{32} = -\beta_3(T^*)S_v^*$, $b_{42} = \beta_3(T^*)S_v^*$, $b_{52} = \eta$, $b_{33} = -\beta_1(T^*)B^* - \beta_3(T^*)I_c^* - \delta(T^*)$, $b_{43} = \beta_1(T^*)B^* + \beta_3(T^*)I_c^*$, $b_{14} = -\beta_2(T^*)S_c^*$, $b_{24} = \beta_2(T^*)S_c^*$, $b_{44} = -\delta(T^*)$, $b_{35} = -\beta_1(T^*)S_v^*$, $b_{45} = \beta_1(T^*)S_v^*$, $b_{55} = -(m(T^*) - \pi(T^*))$.

Then, the characteristic polynomial of Eq. (6.27) is given by

$$\Lambda^5 + B_1\Lambda^4 + B_2\Lambda^3 + B_3\Lambda^2 + B_4\Lambda + B_5 = 0, \tag{6.28}$$

where

$$
\begin{aligned}
B_1 &= -(b_{11}+b_{22}+b_{33}+b_{44}+b_{55}),\\
B_2 &= b_{33}b_{44}+b_{22}(b_{33}+b_{44}+b_{55})+(b_{33}+b_{44})b_{55}+b_{11}(b_{33}+b_{44}+b_{55})\\
&\quad +b_{24}b_{42}(b_{11}-b_{14})-b_{11}((b_{44}+b_{55})b_{33}+b_{22}+b_{44}b_{55}),\\
B_3 &= b_{24}b_{33}b_{42}-b_{14}b_{21}b_{42}-b_{24}b_{32}(b_{43}-b_{24}b_{45}b_{52}-b_{22}b_{44}b_{55}-(b_{44}+b_{55})b_{22}b_{33}\\
&\quad +(b_{24}b_{42}-b_{44})b_{55}+b_{11}b_{24}b_{42}-(b_{44}+b_{55})b_{11}b_{33}-b_{11}b_{22}-b_{11}b_{44}b_{55},\\
B_4 &= b_{14}b_{21}(b_{33}b_{42}-b_{32}b_{43}-b_{45}b_{52})+b_{24}(b_{33}b_{45}-b_{35}b_{43})b_{52}+(b_{22}b_{33}b_{44}+b_{24}b_{32}b_{43}\\
&\quad +b_{14}b_{21}b_{42})b_{55}+b_{11}b_{24}(b_{32}b_{43}+b_{45}b_{52}-b_{33}b_{42})+b_{11}b_{33}b_{44}b_{55}+b_{11}b_{22}(b_{33}+b_{44})\\
&\quad -b_{11}b_{24}b_{42}b_{55},\\
B_5 &= b_{14}b_{21}((b_{33}b_{45}-b_{35}b_{43})b_{52}+(b_{32}b_{43}-b_{42})b_{55}+b_{11}b_{24}((b_{35}(b_{43}-b_{33}b_{45})b_{52}\\
&\quad +(b_{33}b_{42}-b_{32}b_{43})b_{55})-b_{11}b_{22}b_{33}b_{44}.
\end{aligned}
$$

Using the Routh-Hurwitz criterion from (Martcheva, 2015) for $R_2 > R_1 > 1$, the endemic equilibrium point $\bar{E}^*$ is locally asymptotically stable if $B_i > 0, i = 1,...,5$ and

$$
\begin{aligned}
&B_1B_2 - B_3 > 0,\ -B_3^2 - B_1^2B_4 + B_1(B_2B_3 + B_5) > 0,\\
&-B_4{}^2(-B_1B_2B_3 + B_3^2 + B_1^2B_4) + (B_2B_3 - B_1(B_2^2 - 2B_4))B_5 - B_5^2 > 0,\\
&B_5(-B_4(-B_1B_2B_3 + B_3^2 + B_1^2B_4) + (B_2B_3 - B_1(B_2^2 - 2B_4))B_5 - B_5^2) > 0.
\end{aligned}
$$

Hence, according to the Routh-Hurwitz criterion, $\bar{E}^*$ is local asymptotically stable for $R_2 > R_1 > 1$ in Ω_3. □

6.2.9 Global Stability of Endemic Equilibrium Point

Theorem 6.2.5. *If $R_2 > R_1 > 1$, then the endemic equilibrium $\bar{E}^*$ of the model (6.1) is globally asymptotically stable in Ω_3.*

Proof. To establish the global stability of E^*, we consider the following Lyapunov function:

$$
\bar{V} = \frac{[(S_c - S_c^*) + (I_c - I_c^*) + (S_v - S_v^*) + (I_v - I_v^*) + (B - B^*)]^2}{2}, \tag{6.29}
$$

Then by taking the derivative of $\bar{V}$ with respect to t, we obtain

$$
\begin{aligned}
\frac{d\bar{V}}{dt} &= [(S_c - S_c^*) + (I_c - I_c^*) + (S_v - S_v^*) + (I_v - I_v^*) + (B - B^*)]\frac{d}{dt}[S_c + I_c + S_v + I_v + B],\\
&= [(S_c - S_c^*) + (I_c - I_c^*) + (S_v - S_v^*) + (I_v - I_v^*) + (B - B^*)]\frac{dY}{dt}.
\end{aligned} \tag{6.30}
$$

On the other hand, from Eq. (6.3), we have

$$\frac{dY}{dt} \leq \lambda(\bar{T}) + \hat{K}(1+r) - hY. \tag{6.31}$$

Substituting expression for dY/dt from equation (6.31) to equation (6.30) leads to

$$\begin{aligned}
\frac{dV}{dt} &= [(S_c - S_c^*) + (I_c - I_c^*) + (S_v - S_v^*) + (I_v - I_v^*) + (B - B^*)]\frac{dY}{dt} \\
&\leq [(S_c - S_c^*) + (I_c - I_c^*) + (S_v - S_v^*) + (I_v - I_v^*) + (B - B^*)][\lambda(\bar{T}) + \hat{K}(1+r) - hY] \\
&\leq \left[Y - \frac{\lambda(\bar{T}) + \hat{K}(1+r)}{h}\right][\lambda(\bar{T}) + \hat{K}(1+r) - hY].
\end{aligned} \tag{6.32}$$

By re-arranging and simplify the Eq. (6.32), we obtain

$$\frac{d\bar{V}}{dt} \leq -\frac{1}{h}\left(\lambda(\bar{T}) + \hat{K}(1+r) - hY\right)^2. \tag{6.33}$$

Therefore, $(d\bar{V}/dt)(S_c,\ I_c,\ S_v,\ I_v,\ B) \leq 0$ and $(d\bar{V}/dt)(S_c,\ I_c,\ S_v,\ I_v,\ B) = 0$ if and only if $S_c = S_c^*,\ I_c = I_c^*,\ S_v = S_v^*,\ I_v = I_v^*,\ B = B^*$. Thus, the largest compact invariant set in $\{(S_c,\ I_c,\ S_v,\ I_v,\ B) \in \Omega_3 : d\bar{V}/dt = 0\}$ is the singleton $\{\bar{E}^*\}$. Hence, from (La Salle, 1976) invariant principle, E^* is globally asymptotically stable in Ω_3. □

6.2.10 Bifurcation Analysis

From centre manifold theory approach given in the previous chapter, the following theorems can be stated.

Theorem 6.2.6. *If $R_1 < 1$, then the model (6.1) shows forward bifurcation at $R_1 = 1$.*

Proof. As in the previous chapter we perform bifurcation analysis of system (6.1) at $R_1 = 1$ using (Castillo-Chavez and Song, 2004). Let us consider change of variables: $S_c = x_1,\ I_c = x_2,\ S_v = x_3,\ I_v = x_4,\ B = x_5$. Moreover, using the vector notation: $X = (x_1, x_2, x_3, x_4, x_5)^T$. Then, at $T = T_0$ model (6.1) can be rewritten in the form $dX/dt = (g_1,\ g_2,\ g_3,\ g_4,\ g_5)^T$ as:

$$\begin{cases}
\dfrac{dx_1}{dt} = rx_1\left(1 - \dfrac{x_1 + x_2}{K}\right) - \beta_{21}x_1x_4 - \theta x_1, \\
\dfrac{dx_2}{dt} = \beta_{21}x_1x_4 - (\gamma + \eta)x_2, \\
\dfrac{dx_3}{dt} = \lambda_{41} - (\beta_{11}x_5 + \beta_{31}x_2)x_3 - \delta_{51}x_3, \\
\dfrac{dx_4}{dt} = (\beta_{11}x_5 + \beta_{31}x_2)x_3 - \delta_{51}x_4, \\
\dfrac{dx_5}{dt} = \eta x_2 - (m_{71} - \pi_{61})x_5.
\end{cases} \tag{6.34}$$

We consider the transmission rate β_{21} as bifurcation parameter so that $R_1 = 1$ if

$$\beta_{21} = \beta_{21}^* = \frac{r(\gamma+\eta)\delta_{51}^2(m_{71}-\pi_{61})}{K\lambda_{41}(r-\theta)\left((m_{71}-\pi_{61})\right)\beta_{31}+\beta_{11}\eta)}. \tag{6.35}$$

The Jacobian matrix of Eq. (6.34) at disease-free equilibrium E_1 is given by

$$J(E_1) = \begin{bmatrix} \theta - r & -(r-\theta) & 0 & -\dfrac{K(r-\theta)\beta_{21}^*}{r} & 0 \\ 0 & -\gamma-\eta & 0 & \dfrac{K(r-\theta)\beta_{21}^*}{r} & 0 \\ 0 & -\dfrac{\lambda_{41}}{\delta_{51}} & -\delta_{51} & 0 & -\dfrac{\beta_{11}\lambda_{41}}{\delta_{51}} \\ 0 & \dfrac{\beta_{31}\lambda_{41}}{\delta_{51}} & 0 & -\delta_{51} & \dfrac{\beta_{11}\lambda_{41}}{\delta_{51}} \\ 0 & \eta & 0 & 0 & \pi_{61}-m_{71} \end{bmatrix}. \tag{6.36}$$

The right eigenvector, $u = (u_1,\ u_2,\ u_3,\ u_4,\ u_5)^T$ is computed from $J(E_1)u = 0$ so that

$$u_1 = -\frac{K\beta_{21}^*}{r}\left(\frac{r-\theta}{\gamma+\eta}+1\right)u_4, u_2 = \frac{K(r-\theta)\beta_{21}^*}{r(\gamma+\eta)}u_4,\ u_3 = -u_4, u_5 = \frac{\eta K(r-\theta)\beta_{21}^*}{r(\gamma+\eta)(m_{71}-\pi_{61})}u_4, \tag{6.37}$$

where $u_4 = u_4 > 0$. Also the left eigenvector, $z = (z_1,\ z_2,\ z_3,\ z_4,\ z_5)$ is computed from $zJ(E_1) = 0$ results

$$z_1 = z_3 = 0,\ z_2 = \frac{\delta_{51}r}{K(r-\theta)\beta_{21}^*}z_4,\ z_5 = \frac{\beta_{11}\lambda_{41}}{\delta_{51}(m_{71}-\pi_{61})}z_4;\ \ z_4 = z_4 > 0. \tag{6.38}$$

Based on Castillo-Chavez and Song (2004), the coefficients a and b are given by

$$a = \sum_{i,j,k=1}^{5} z_k u_i u_j \frac{\partial^2 g_k}{\partial x_i \partial x_j}(E_1), \quad b = \sum_{i,k=1}^{5} z_k u_i \frac{\partial^2 g_k}{\partial x_i \partial \beta_{21}^*}(E_1). \tag{6.39}$$

The nonzero second partial derivatives of $g_1,\ g_2,\ g_3$ and g_4 are given as:

$$\begin{aligned}
&\frac{\partial^2 g_1}{\partial x_1 \partial x_1} = \frac{\partial^2 g_1}{\partial x_1 \partial x_1} = -\frac{2r}{K}, \quad \frac{\partial^2 g_1}{\partial x_1 \partial x_2} = \frac{\partial^2 g_1}{\partial x_2 \partial x_1} = -\frac{r}{K}, \quad \frac{\partial^2 g_1}{\partial x_1 \partial x_4} = \frac{\partial^2 g_1}{\partial x_4 \partial x_1} = -\beta_{21}^*, \\
&\frac{\partial^2 g_2}{\partial x_1 \partial x_2} = \frac{\partial^2 g_2}{\partial x_2 \partial x_1} = \beta_{21}^*, \quad \frac{\partial^2 g_3}{\partial x_2 \partial x_3} = \frac{\partial^2 g_3}{\partial x_3 \partial x_2} = -\beta_{31}, \quad \frac{\partial^2 g_3}{\partial x_3 \partial x_5} = \frac{\partial^2 g_3}{\partial x_5 \partial x_3} = -\beta_{11}, \\
&\frac{\partial^2 g_4}{\partial x_2 \partial x_3} = \frac{\partial^2 g_4}{\partial x_3 \partial x_2} = \beta_{31}, \quad \frac{\partial^2 g_4}{\partial x_3 \partial x_5} = \frac{\partial^2 g_4}{\partial x_5 \partial x_3} = \beta_{11}, \quad \frac{\partial^2 g_1}{\partial x_4 \partial \beta_{21}^*} = \frac{\partial^2 g_1}{\partial \beta_{21}^* \partial x_4} = -x_1^*, \\
&\frac{\partial^2 g_2}{\partial x_4 \partial \beta_{21}^*} = \frac{\partial^2 g_2}{\partial \beta_{21}^* \partial x_4} = x_1^*.
\end{aligned} \tag{6.40}$$

All the others second partial derivatives of $g_i,\ i=1,...,5$ are zero. By using Eq. (6.39), we get

$$a=-\left[\frac{2\delta_{51}^3 r(\gamma+\eta)(m_{71}-\pi_{61})}{K\lambda_{41}(r-\theta)^2((m_{71}-\pi_{61})\beta_{31}+\beta_{11}\eta)}\left(\frac{r-\theta}{\gamma+\eta}+1\right)+\frac{2\delta_{51}\beta_{31}}{\gamma+\eta}+2\eta K(r-\theta)\delta_{51}^2\right]z_4u_4^2$$
$$b=\frac{K(r-\theta)((m_{71}-\pi_{61})\beta_{31}+\beta_{11}\eta)}{r(\gamma+\eta)\delta_{51}(m_{71}-\pi_{61})}z_4u_4. \tag{6.41}$$

Since the coefficient a is negative and b is positive at T_0, then the system (6.1) exhibits forward bifurcation at $R_1=1$ and there exists at least one stable endemic equilibrium when $R_1>1$. □

Theorem 6.2.7. *If $R_2<1$, then the model (6.1) shows backward bifurcation at $R_2=1$.*

Proof. Let $S_c=y_1,\ I_c=y_2,\ S_v=y_3,\ I_v=y_4,\ B=y_5$ and $Y=(y_1,y_2,y_3,y_4,y_5)^T$. Then, at $T=T_m$ the model (6.1) can be written in the form $dY/dt=(f_1,\ f_2,\ f_3,\ f_4,\ f_5)^T$ as:

$$\begin{cases}\dfrac{dy_1}{dt}=ry_1\left(1-\dfrac{y_1+y_2}{K}\right)-\beta_2(T_m)y_1y_4-\theta y_1,\\ \dfrac{dy_2}{dt}=\beta_2(T_m)y_1y_4-(\gamma+\eta)y_2,\\ \dfrac{dy_3}{dt}=\lambda(T_m)-(\beta_1(T_m)y_5+\beta_3(T_m)y_2)y_3-\delta(T_m)y_3,\\ \dfrac{dy_4}{dt}=(\beta_1(T_m)y_5+\beta_3(T_m)y_2)y_3-\delta(T_m)y_4,\\ \dfrac{dy_5}{dt}=\eta y_2+(\pi(T_m)-m(T_m))y_5.\end{cases} \tag{6.42}$$

We considered $\beta_2(T_m)$ as bifurcation parameter. Then solving for $\beta_2(T_m)=\beta_2^*(T_m)$ from $R_2=1$ gives

$$\beta_2(T_m)=\beta_2^*(T_m)=\frac{r(\gamma+\eta)\delta^2(T_m)(m(T_m)-\pi(T_m))}{K\lambda(T_m)(r-\theta)\left((m(T_m)-\pi(T_m))\beta_3(T_m)+\beta_1(T_m)\eta\right)}. \tag{6.43}$$

As in the previous theorem, the right eigenvector, $v=(v_1,\ v_2,\ v_3,\ v_4,\ v_5)^T$ is computed as:

$$v_1=-\frac{K\beta_2^*(T_m)}{r}\left(\frac{r-\theta}{\gamma+\eta}+1\right)v_4,\quad v_2=\frac{K(r-\theta)\beta_2^*(T_m)}{r(\gamma+\eta)}v_4,\quad v_3=-v_4,$$
$$v_5=\frac{\eta K(r-\theta)\beta_2^*(T_m)}{r(\gamma+\eta)(m(T_m)-\pi(T_m))}v_4$$

where $v_4=v_4>0$. Likewise, the left eigenvector, $w=(w_1,\ w_2,\ w_3,\ w_4,\ w_5)$ becomes:

$$w_1=w_3=0,\ w_2=\frac{\delta(T_m)r}{K(r-\theta)\beta_2^*(T_m)}w_4,\ w_5=\frac{\beta_1(T_m)\lambda(T_m)}{\delta(T_m)(m(T_m)-\pi(T_m))}w_4;\ \ w_4=w_4>0. \tag{6.44}$$

The associated bifurcation coefficients c and d are given by

$$\begin{aligned} c &= 2w_2v_1v_4\beta_2^*(T_m) + 2w_4v_2v_3\beta_3(T_m) + 2w_4v_3v_5\beta_1(T_m) \\ d &= \frac{K(r-\theta)((m(T_m)-\pi(T_m))\beta_3(T_m)+\beta_1(T_m)\eta)}{r(\gamma+\eta)\delta(T_m)(m(T_m)-\pi(T_m))}w_4v_4 > 0. \end{aligned} \tag{6.45}$$

Clearly, d is always positive at maximum temperature T_m. If c is positive at T_m, then the model (6.1) exhibits backward bifurcation at $R_2 = 1$ and thus, there exists a stable endemic equilibrium when $R_2 < 1$. □

Note that in the case of forward bifurcation: having $R_1 < 1$ is the necessary condition for the disease elimination. In the case of backward bifurcation: having $R_2 < 1$ is not the necessary condition for the disease elimination. Hence, the disease can't be eliminated even if $R_2 < 1$ since the disease persists in the population.

6.2.11 Sensitivity of Basic Reproduction Numbers: R_1 and R_2

In this section, we study the sensitivity analysis of R_1 and R_2 for various model parameters. This help us to check and identify parameters which highly affect R_1 and R_2 on the eradication or spread of CBD. To perform sensitivity analysis, we used similar method outlined in (Chitnis et al., 2008).

The normalized forward sensitivity index of R_1 with respect to K is computed as:

$$\Delta_K^{R_1} = \frac{\partial R_1}{\partial K} \times \frac{K}{R_1} = \frac{\beta_{21}\lambda_{41}\left[(m_{71}-\pi_{61})\beta_{31}+\beta_{11}\eta\right](r-\theta)K}{2r(m_{71}-\pi_{61})\delta_{51}^2(\gamma+\eta)R_1^2} = 0.5.$$

In a similar way, the others sensitivity index of R_1 are computed and the corresponding sensitivity indeces are given in Table 6.1. From this table, the parameters: K, β_{11}, β_{21}, β_{31}, r, λ_{41} and π_{61} have positive sensitivity indices show that the more impact on expanding the disease in the population if their values are increasing since R_1 increases. Besides, the parameters θ, η, δ_{51}, γ and m_{71} have negative sensitivity indices show that the less impact as their values increase since R_1 decreases.

Table 6.1: Sensitivity indices of R_1 at $T = T_0$

Parameter	**Sensitivity indices of R_1**	**Parameter**	**Sensitivity indices of R_1**
K	0.5	θ	-0.00505051
β_{11}	0.0494505	λ_{41}	0.5
β_{21}	0.5	δ_{51}	-1
β_{31}	0.450549	γ	-0.178571
η	-0.271978	π_{61}	0.010855
r	0.00505051	m_{71}	-0.0603055

Table 6.2: Sensitivity indices of R_2 at $T = T_m$

Parameter	**Sensitivity indices of R_2**	**Parameter**	**Sensitivity indices of R_2**
K	0.5	λ_{41}	0.5
β_{11}	0.00259965	λ_{42}	0.5
β_{12}	0.00727399	δ_{51}	-1
β_{21}	0.5	δ_{52}	-1
β_{22}	0.5	γ	-0.178571
β_{31}	0.4974	π_{61}	0.0000271741
β_{32}	0.492726	π_{62}	0.000161928
η	-0.314155	m_{71}	-0.00262683
r	0.00505051	m_{72}	-0.00743592
θ	-0.00505051		

In the same way, the sensitivity index of R_{02} are also computed and the corresponding sensitivity indeces are given in Table 6.2. From this table, the parameters: K, β_{11}, β_{12}, β_{21}, β_{22}, β_{31}, β_{32}, r, λ_{41}, λ_{42}, π_{61} and π_{62} have positive sensitivity indices show that the more impact on expanding the disease in the population if their values are increasing since R_{02} increases. However, the parameters η, θ, δ_{51}, δ_{52}, γ, m_{71} and m_{72} have negative sensitivity indices show less impact.

6.3 Extension of the Model into Optimal Control

In this section, we extend the proposed model (6.1) into the optimal control problem by including three control variables: u_1, u_2, u_3. This helped us to identify the best control strategies that were used to eradicate the disease from coffee plants in the specified time.

The corresponding state system for the model (6.1) is given by

$$\begin{cases} \dfrac{dS_c}{dt} = rS_c\left(1-\dfrac{S_c+I_c}{K}\right) - (1-u_1)\beta_2(T)S_cI_v - \theta S_c, \\ \dfrac{dI_c}{dt} = (1-u_1)\beta_2(T)S_cI_v - (\gamma+\eta)I_c, \\ \dfrac{dS_v}{dt} = \lambda(T) - (\beta_1(T)B+\beta_3(T)I_c)S_v - (1+u_2)\delta(T)S_v, \\ \dfrac{dI_v}{dt} = (\beta_1(T)B+\beta_3(T)I_c)S_v - (1+u_2)\delta(T)I_v, \\ \dfrac{dB}{dt} = \eta I_c + [\pi(T) - (1+u_3)m(T)]B, \\ \dfrac{dT}{dt} = r_1(T-T_0)(1-\dfrac{T}{T_m}), \end{cases} \tag{6.46}$$

with initial data: $S_c(0) = S_{0c}$, $I_c(0) = I_{0c}$, $S_v(0) = S_{0v}$, $I_v(0) = I_{0v}$, $B(0) = B_0$, $T(0) = T_0$.

To investigate the optimal levels of controls the following set U must be bounded.

$$U = \{(u_1(t), u_2(t), u_3(t)) : \ 0 \leq u_i(t) \leq 1, 0 \leq t \leq t_f, \ i = 1,2,3\},$$

where t_f is the final time. The form of objective function J is taken from (Takaidza et al., 2017) and given by

$$J = \min_{u} \int_0^{t_f} \left(a_1 I_c + a_2 I_v + \frac{1}{2} \sum_{i=1}^{3} b_i u_i^2 \right) dt, \tag{6.47}$$

where $a_1, \ a_2, \ b_i > 0, \ i = 1,2,3$ and $u = (u_1, u_2, u_3)$. The term $0.5 b_i u_i^2$ represent cost functions which are corresponding to each control u_i, for $i = 1,2,3$, respectively. The performance specification involves minimizing number of infected coffee plants and vectors, as well as the cost of applying control strategies. So, we want to obtain the control (u_1^*, u_2^*, u_3^*):

$$J(u^*) = \min \{J(u_1, u_2, u_3) : u_i \in U\}.$$

We used Pontryagin's minimum principle from (Pontryagin et al., 2018) to obtain a Hamiltonian function H defined as:

$$H = a_1 I_c + a_2 I_v + \frac{1}{2} \sum_{i=1}^{3} b_i u_i^2 + \lambda_1 \frac{dS_c}{dt} + \lambda_2 \frac{dI_c}{dt} + \lambda_3 \frac{dS_v}{dt} + \lambda_4 \frac{dI_v}{dt} + \lambda_5 \frac{dB}{dt} + \lambda_6 \frac{dT}{dt}. \tag{6.48}$$

6.3.1 Characterization of Optimal Control Solutions

To obtain the adjoint variables $\lambda_i, \ i = 1, ..., 6$, we follow the classical result of (Pontryagin et al., 2018). So the following theorem can be established.

Theorem 6.3.1. *For an optimal control set $\{u_1, u_2, u_3\}$ that minimize J over U, there exist adjoint variables $\lambda_i, \ i = 1, ..., 6$ such that*

$$\begin{cases}
\frac{d\lambda_1}{dt} = -\lambda_1 \left(r - \frac{2rS_c}{K} - \frac{rI_c}{K} - (1-u_1)\beta_2(T)I_v - \theta \right) - \lambda_2(1-u_1)\beta_2(T)I_v, \\
\frac{d\lambda_2}{dt} = -a_1 + \lambda_1 \frac{rS_c}{K} + \lambda_2(\gamma + \eta) + \lambda_3 \beta_3(T)S_v - \lambda_4 \beta_3(T)S_v - \lambda_5 \eta, \\
\frac{d\lambda_3}{dt} = \lambda_3(\beta_1(T)B + \beta_3(T)I_c + (1+u_2)\delta(T)) - \lambda_4(\beta_1(T)B + \beta_3(T)I_c), \\
\frac{d\lambda_4}{dt} = -a_2 + \lambda_1(1-u_1)\beta_2(T)S_c - \lambda_2(1-u_1)\beta_2(T)S_c + \lambda_4(1+u_2)\delta(T), \\
\frac{d\lambda_5}{dt} = \lambda_3 \beta_1(T)S_v - \lambda_4 \beta_1(T)S_v - \lambda_5(\pi(T) - (1+u_3)m(T)), \\
\frac{d\lambda_6}{dt} = -\frac{1}{T_m}[(\lambda_1 + \lambda_2)(1-u_1)\beta_{22}S_c I_v + \lambda_3 (\lambda_{42} - \beta_{12}BS_v - \beta_{32}I_c S_v - (1+u_2)\delta_{52}S_v) \\
\qquad + \lambda_4 (\beta_{12}BS_v + \beta_{32}I_c S_v - (1+u_2)\delta_{52}I_V) + \lambda_5 B (\pi_{62} - (1+u_3)m_{72})] \\
\qquad - \frac{1}{T_m}\lambda_6 r_1 (T_m - 2T - T_0).
\end{cases} \tag{6.49}$$

Together with transversality condition: $\lambda_i(t_f) = 0, \ i = 1, ..., 6.$

And also, we get optimal controls $u_1^*(t)$, $u_2^*(t)$ and $u_3^*(t)$ which are characterized by

$$\begin{aligned} u_1^*(t) &= \min\left\{\max\left\{0, \frac{\beta_2(T)S_cI_v(-\lambda_1+\lambda_2)}{b_1}\right\}, 1\right\}, \\ u_2^*(t) &= \min\left\{\max\left\{0, \frac{\delta(T)(\lambda_3 S_v+\lambda_4 I_v)}{b_2}\right\}, 1\right\}, \\ u_3^*(t) &= \min\left\{\max\left\{0, \frac{\lambda_5 m(T)B}{b_3}\right\}, 1\right\}. \end{aligned} \tag{6.50}$$

Proof. The adjoint equation is found by differentiating the Hamiltonian function with respect to the corresponding state variables. That is,

$$\frac{d\lambda_1}{dt} = -\frac{dH}{dS_c}, \frac{d\lambda_2}{dt} = -\frac{dH}{dI_c}, \frac{d\lambda_3}{dt} = -\frac{dH}{dS_v}, \frac{d\lambda_4}{dt} = -\frac{dH}{dI_v}, \frac{d\lambda_5}{dt} = -\frac{dH}{dB}, \frac{d\lambda_6}{dt} = -\frac{dH}{dT}.$$

We assume that $S_c(t_f)$, $I_c(t_f)$, $S_v(t_f)$, $I_v(t_f)$, $B(t_f)$ and $T(t_f)$ are free, then we obtain the transversality condition: $\lambda_i(t_f) = 0$. We find that optimal controls: $u_1^*(t)$, $u_2^*(t)$ and $u_3^*(t)$ from optimality condition, $\partial H/\partial u_i = 0$:

$$u_1^*(t) = \frac{\beta_2(T)S_cI_v(-\lambda_1+\lambda_2)}{b_1}, \quad u_2^*(t) = \frac{\delta(T)(\lambda_3 S_v+\lambda_4 I_v)}{b_2}, \quad u_3^*(t) = \frac{\lambda_5 m(T)B}{b_3}.$$

Since $0 \le u_i^*(t) \le 1$, we can rewrite the optimal controls as Eq. (6.50) □

In order to confirm that the optimal control is really a minimizer we need to check the Hessian matrix of the Hamiltonian H. Now the Hessian matrix for H with respect the control u is given by

$$\frac{\partial^2 H}{\partial u^2} = \begin{bmatrix} b_1 & 0 & 0 \\ 0 & b_2 & 0 \\ 0 & 0 & b_3 \end{bmatrix}.$$

This matrix is found to be a positive definite matrix as a consequence of the positive weights b_1, b_2 and b_3. This results in the convexity of the corresponding Hamiltonian function H and consequently the optimal control (u_1^*, u_2^*, u_3^*) is a minimizer.

6.4 Numerical Simulations

In this section, we implemented numerical simulations of the proposed model (6.1) and corresponding state system (6.46) with impact of controls: genetic u_1, chemical u_2 and cultural control u_3 on coffee plants and vector population. We used an iterative scheme to find numerical solutions for the optimality system. The state system starts to be solved with an estimate for the controls over the implemented time using the Runge-Kutta method of fourth-order.

Based on the realistic qualitative results obtained from the model analysis, we assumed the parameter values: $K = 150$, $r = 0.5$, $r_1 = 0.16$, $\eta = 0.009$, $\theta = 0.005$, $\gamma = 0.005$, $\beta_{11} = 0.0001$, $\beta_{12} = 0.0005$, $\beta_{21} = 0.0002$, $\beta_{22} = 0.008$, $\beta_{31} = 0.0002$, $\beta_{32} = 0.0001$, $\lambda_{41} = 0.08$,

$\lambda_{42} = 0.1,\ \delta_{51} = 0.01,\ \delta_{52} = 0.008, \pi_{61} = 0.009,\ \pi_{62} = 0.02,\ m_{71} = 0.05,\ m_{72} = 0.03, T_0 = 15\ ^\circ c,\ \ T_m = 30\ ^\circ c$ and with initial data: $S_c(0) = 100,\ I_c(0) = 50,\ S_v(0) = 50,\ I_v(0) = 10,\ B(0) = 10,\ T(0) = 15.01\ ^\circ c$. Additionally, we assumed the weight constants: $a_1 = 20,\ a_2 = 30,\ b_1 = 3,\ b_2 = 800$ and $b_3 = 1000$.

We examine and compare numerical simulations of the following four control strategies with two or more controls. To eradicate the disease, we address either prevention or treatment of coffee plants and vector infection.

6.4.1 Control Strategy I: Genetic and Chemical

The simulation results from Figures 6.2 and 6.3 show that the number of susceptible coffee increases, infected coffee and vector goes dawn at the end of the implemented period. This control strategy applied is well effective to eradicate the disease from the coffee population at minimum temperature T_0. The corresponding control profile is depicted in Figure 6.4. The control u_1 is at its peak for 178 days, while u_2 is increased to a certain maximum level and then gradually declines to zero at the time, t=180 days.

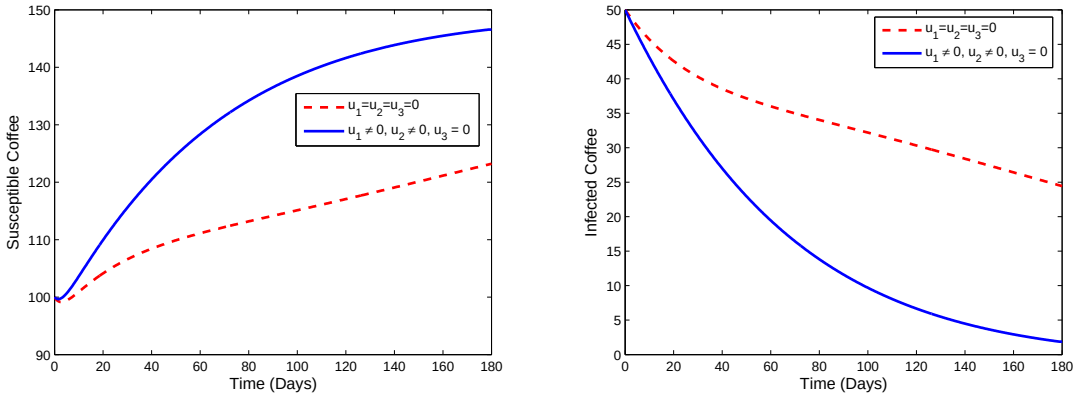

(a) (b)

Figure 6.2: Impact of genetic and chemical control on coffee berry population at $T = T_0$.

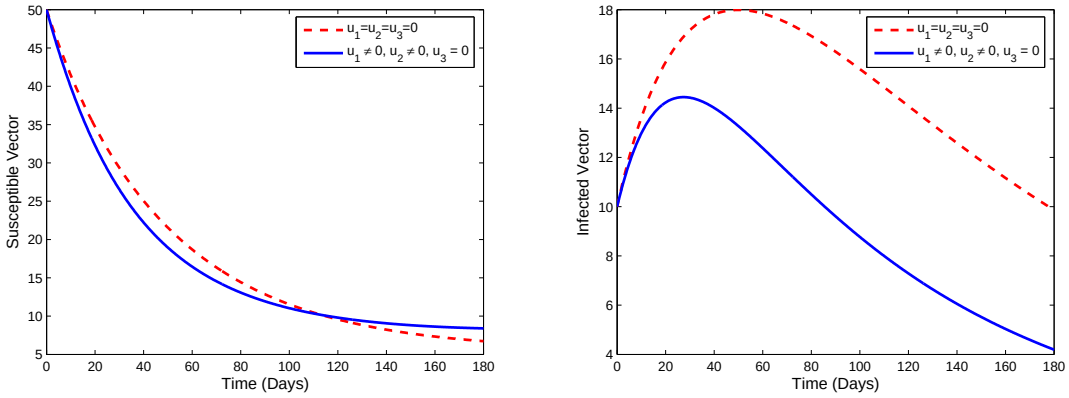

(a) (b)

Figure 6.3: Impact of genetic and chemical control on vector population at $T = T_0$.

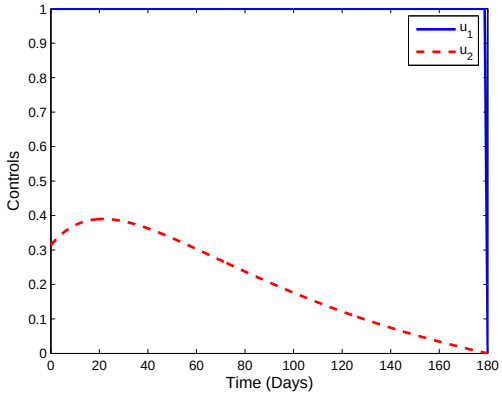

Figure 6.4: Control profiles for the effect of the controls u_1 and u_2 on the dynamics of the co-infection optimal control model (6.46) at $T = T_0$.

At maximum temperature T_m, Figures 6.5 (a), 6.5 (b), 6.6 (a) and 6.6 (b) show that the total number of susceptible coffee increases, infected coffee and insect vectors decrease. Hence, the control strategy at T_0 is more effective than the strategy at T_m. The applied controls profile is presented in Figure 6.7. Clearly, the control u_1 is at its peak for 180 days, while u_2 is increased to certain maximum level and then gradually declining to zero at final time.

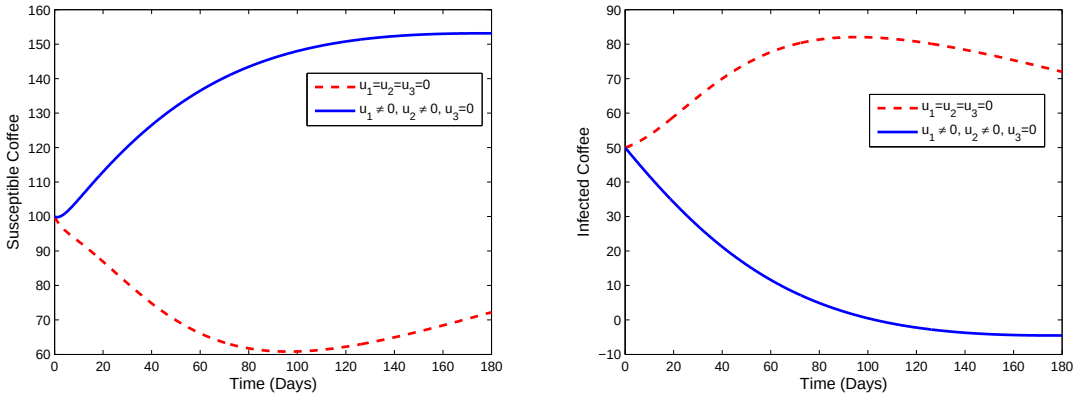

(a) (b)

Figure 6.5: Impact of genetic and chemical control on coffee berry population at $T = T_m$.

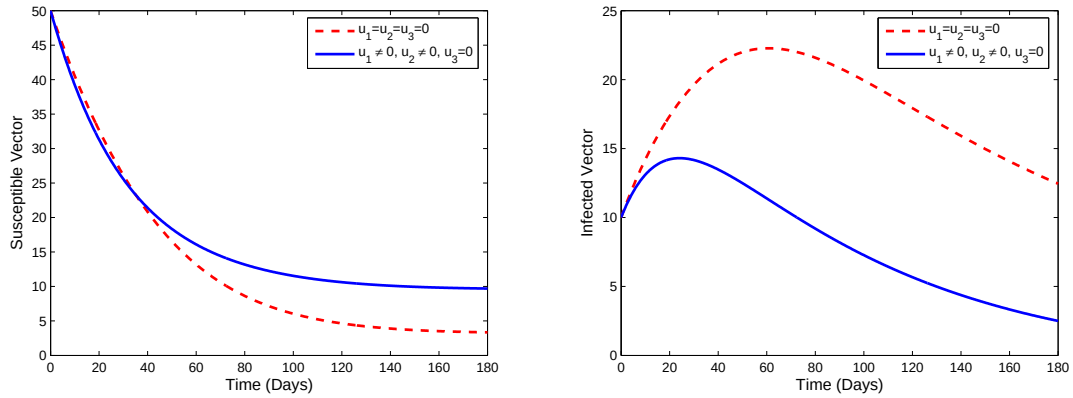

(a) (b)

Figure 6.6: Impact of genetic and chemical control on vector population at $T = T_m$.

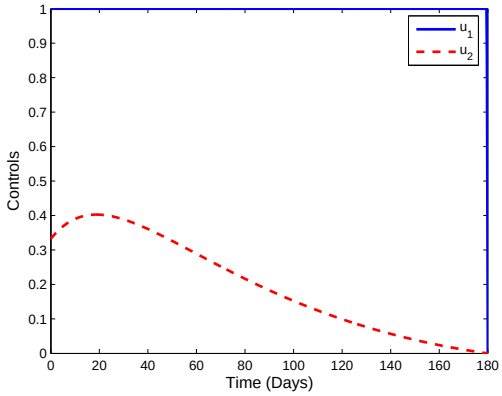

Figure 6.7: Control profiles for the effect of the controls u_1 and u_2 on the dynamics of the co-infection optimal control model (6.46) at $T = T_m$.

6.4.2 Control Strategy II: Genetic and Cultural

The simulation results are illustrated in Figures 6.8 (a), 6.8 (b), 6.9 (a) and 6.9 (b) when genetic and cultural control are applied to the system. At $T = T_0$, these figures clearly reveal that the number of susceptible coffee increases, while infected coffee and insect vectors go down at the end of simulation time.

Figures 6.10 (a), 6.10 (b), 6.10 (c) and 6.10 (d) show that the number of susceptible coffee increases, while infected coffee and insect vectors decrease. The result shows that this strategy is more effective at T_m. The corresponding control profile is depicted in Figure 6.11.

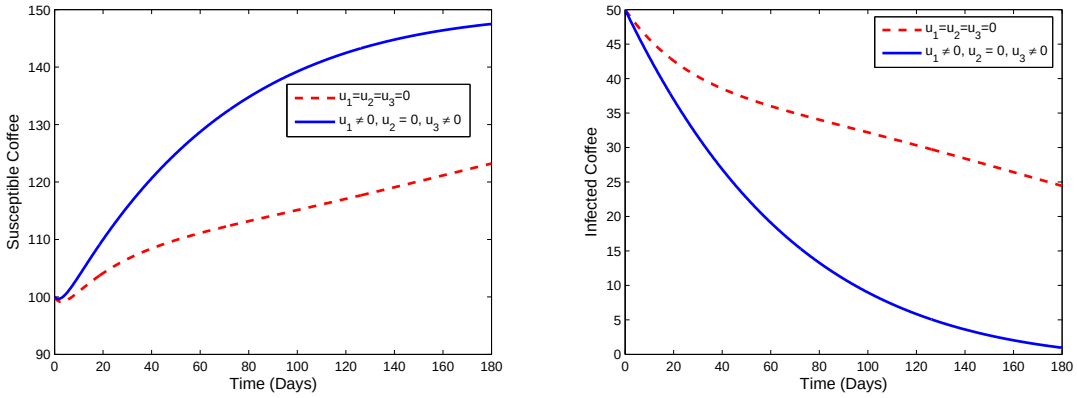

(a) (b)

Figure 6.8: Impact of genetic and cultural control on coffee berry population at $T = T_0$

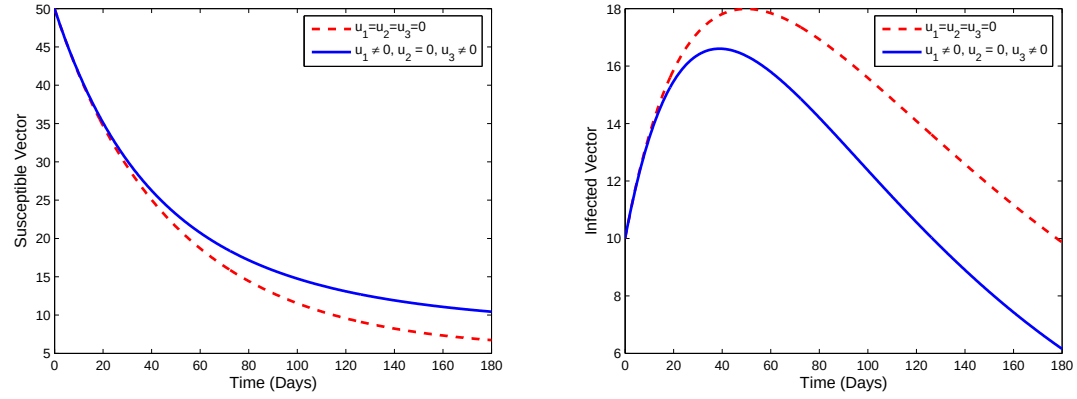

(a) (b)

Figure 6.9: Impact of genetic and cultural control on insect vector population at $T = T_0$

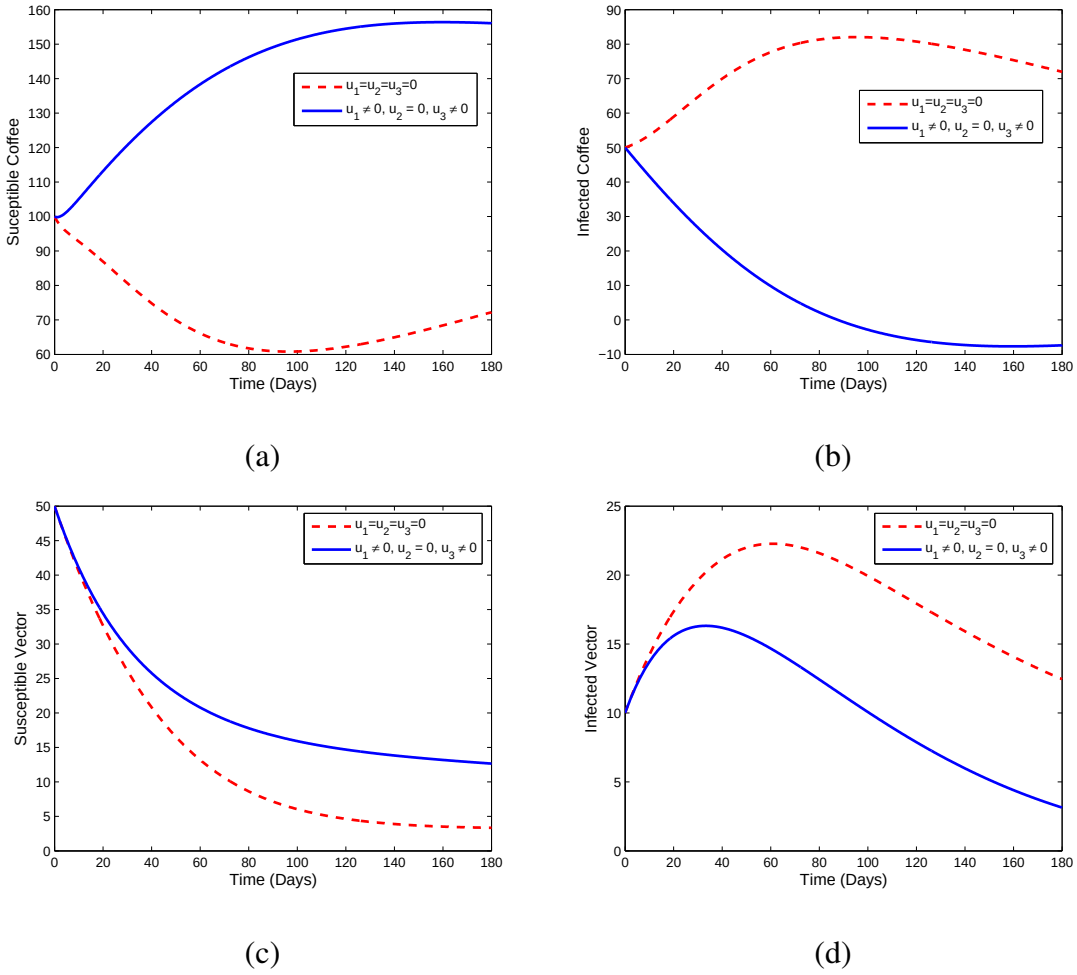

Figure 6.10: Impact of genetic and cultural control on coffee berry and insect vector population at $T = T_m$

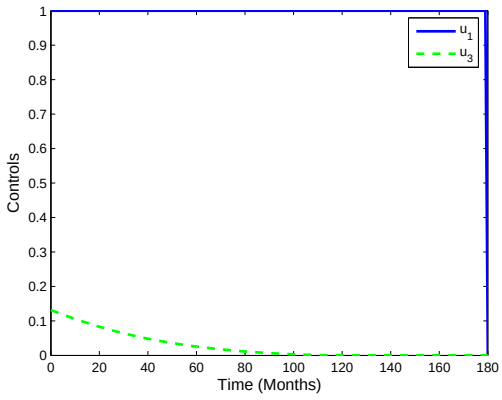

Figure 6.11: Control profiles for the effect of the controls: u_1 and u_3 on the dynamics of the co-infection optimal control model (6.46) at $T = T_m$.

6.4.3 Control Strategy III: Chemical and Cultural

We observe that from Figure 6.12 (a) and 6.12 (b) the infected coffee decreases because of removing the infected plants and the infected vector decreases by increasing insecticides to the system at T_0. The control profile for this control strategy is presented in Figure 6.13.

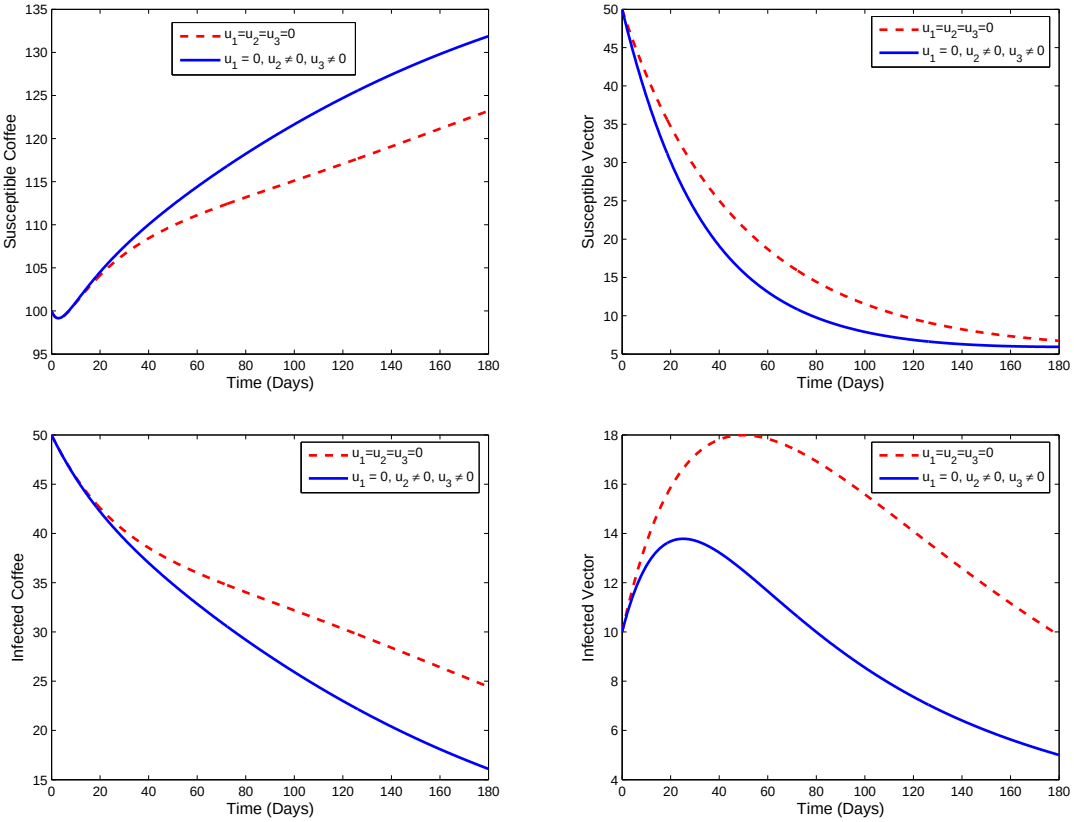

(a) (b)

Figure 6.12: Impact of chemical and cultural control on coffee berry and insect vector population at $T = T_0$

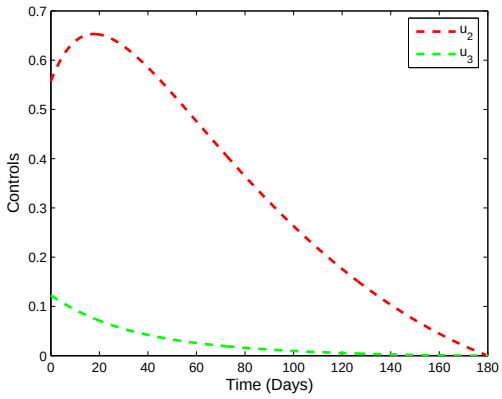

Figure 6.13: Control profiles for the effect of the controls: u_2 and u_3 on the dynamics of the co-infection optimal control model (6.46) at $T = T_0$.

Figures 6.14 (a) and 6.14 (b) show that the susceptible coffee increases, while infected coffee and vectors goes dawn at T_m. We conclude that this control strategy is the more effective at T_0 than at T_m.

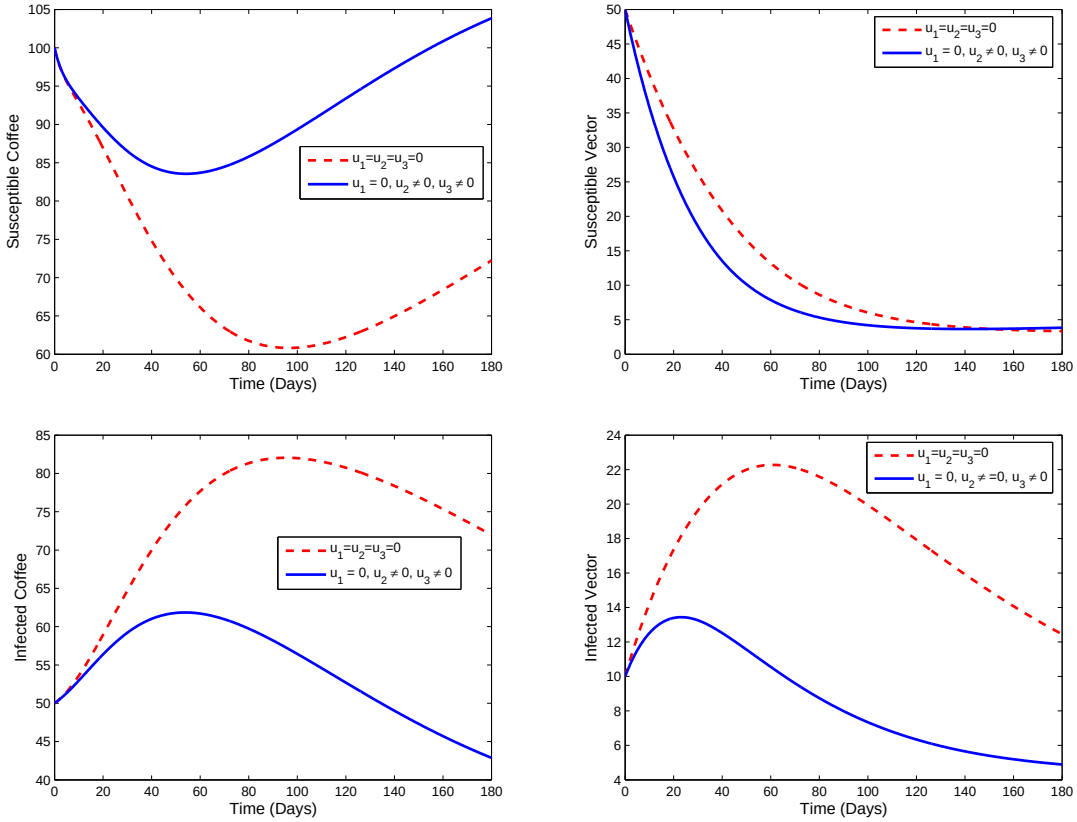

(a) (b)

Figure 6.14: Impact of chemical and cultural control on coffee berry and insect vector population at $T = T_m$

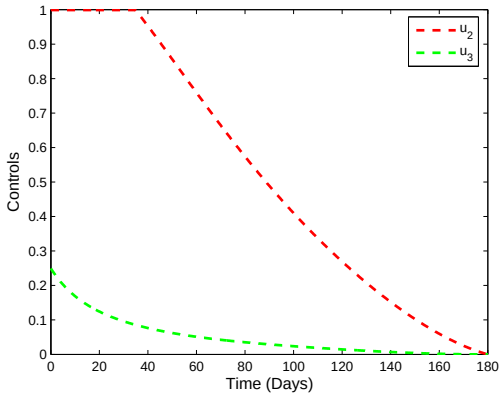

Figure 6.15: Control profiles for the effect of the controls: u_2 and u_3 on the dynamics of the co-infection optimal control model (6.46) at $T = T_m$.

6.4.4 Control Strategy IV: Genetic, Chemical and Cultural

In this strategy, we implemented all the three controls: genetic, chemical and cultural in the system. Figures 6.16 (a) and 6.16 (b) show that the number of susceptible coffee increases, infected coffee and vector goes dawn at T_0.

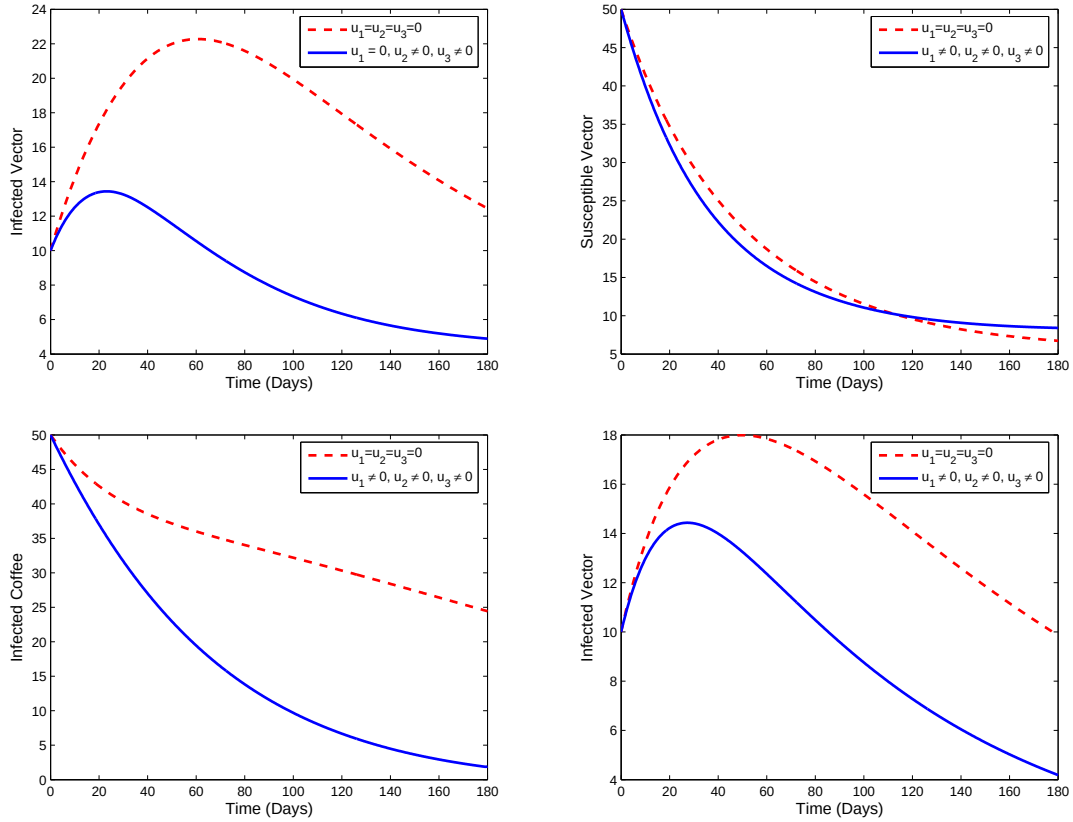

(a) (b)

Figure 6.16: Impact of genetic, chemical and cultural control on coffee berry and insect vector population at $T = T_0$

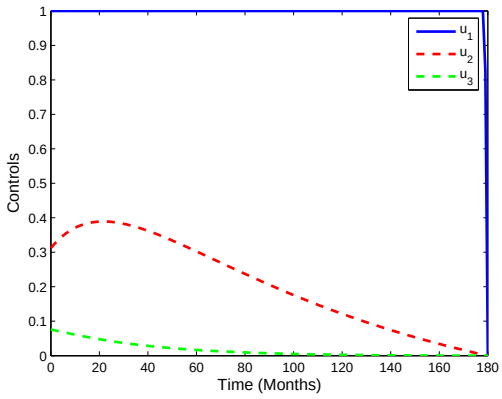

Figure 6.17: Control profiles for the effect of the controls: u_1, u_2 and u_3 on the dynamics of the co-infection optimal control model (4.1) at $T = T_0$.

And also, Figures 6.18 (a) and 6.18 (b) show that the number of susceptible coffee increases, where as infected coffee and insect vectors decrease at T_m.

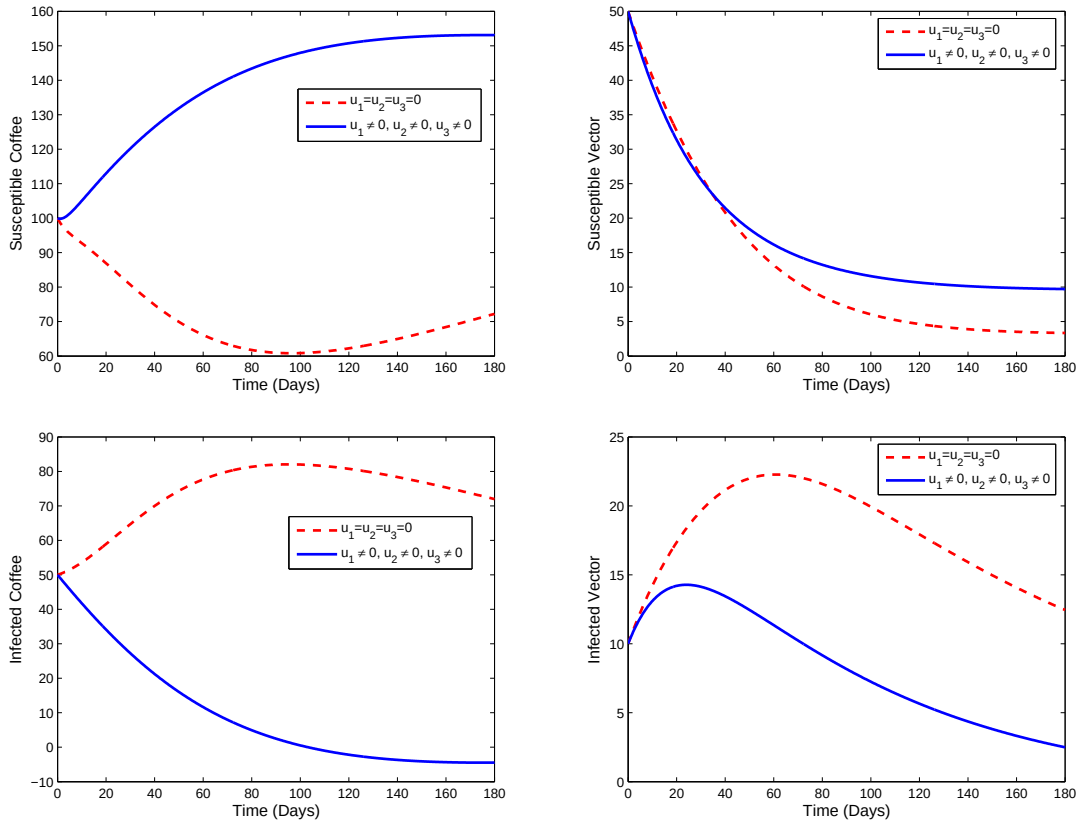

(a) (b)

Figure 6.18: Impact of genetic, chemical and cultural control on coffee berry and insect vector population at $T = T_m$

Furthermore, Figures 6.19 (a) and 6.19 (b) show that number of CBD pathogen population decrease at the end of implementation of strategy. Hence, applying this control strategy at temperatures T_0 and T_m is effective to decrease CBD pathogen from the coffee population in a specified period of time.

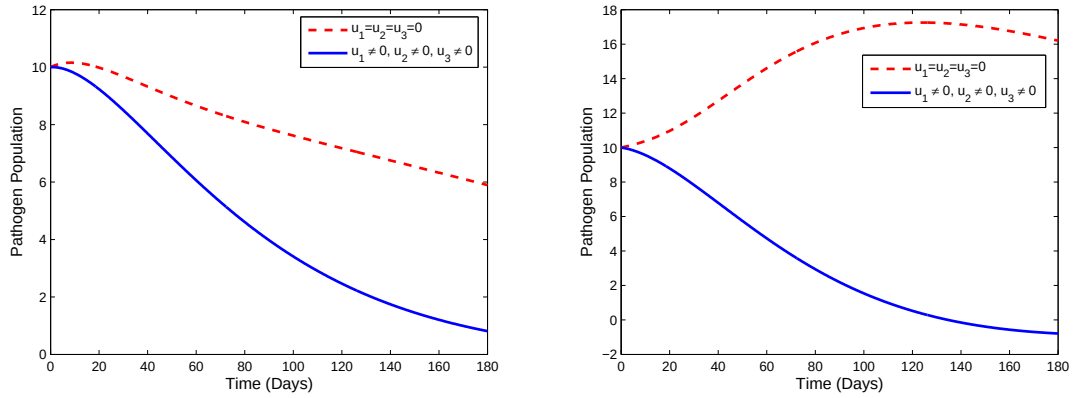

(a) (b)

Figure 6.19: Impact of genetic, chemical and cultural control on pathogen population at (a) $T = T_0$ and at (b) $T = T_m$.

6.5 Cost-Effective Analysis

In this section, we study the cost-effectiveness of strategies with two or more controls. It helps us to identify the most cost-effective control strategy. We apply two approaches to implement the cost-effectiveness analysis. They are: average cost-effectiveness ratio (ACER) (Asamoah et al., 2021) and incremental cost-effectiveness ratio (ICER) (Tilahun et al., 2017). The average cost-effectiveness ratio (ACER) is given by

$$\text{ACER} = \frac{\text{Total control cost of a particular intervention strategy}}{\text{Total number of infections averted by the intervention strategy}}.$$

The total costs of a particular intervention strategy is given by

$$C(u) := \min_{u} \int_0^{180} \left(\frac{1}{2} \sum_{i=1}^{3} b_i u_i^2 \right) dt. \tag{6.51}$$

The functions $0.5b_1u_1^2$, $0.5b_2u_2^2$ and $0.5b_3u_3^2$ represent the cost weights associated with each control measure u_i, $i = 1,2,3$, respectively. Considering strategies i and j as two competing control intervention, then ICER is stated as

$$\text{ICER} = \frac{\text{Difference in cost in strategy i and j}}{\text{Difference in infected averted in strategy i and j}}.$$

The total number of infected averted is computed for each strategy by subtracting the total infected with control from without any control implementation throughout the simulation. Each control strategy is compared with the next less effective options as applied in (Lenhart and Workman, 2007). The numerical output for the control strategies is ranked in increasing order of effectiveness in form of infection averted as shown in Table 6.3.

Table 6.3: First computation of the total number of infections averted, total costs, ACER and ICER of strategies.

Strategy	Total infections averted	Total Costs ($)	ACER	ICER
Strategy III	879.8920	463.5900	0.5269	0.5267
Strategy IV	3179.9090	666.5317	0.2096	0.0882
Strategy I	3180.3530	526.4174	0.1655	-315.5727
Strategy II	3277.3560	488.0466	0.1489	-0.3956

We calculated the ICER for strategies which are given in Table 6.3 and then compared their results as follows.

$$ICER(III) = \frac{463.5900}{879.8920} = 0.5267,$$

$$ICER(IV) = \frac{666.5317 - 463.5900}{3179.9090 - 879.8920} = 0.0882.$$

The comparison between ICER of strategy III and strategy IV shows a cost saving of 0.0882 for strategy IV over strategy III. This shows that strategy IV is cheaper than strategy III. Hence, strategy III is removed from subsequent ICER computations, as shown in Table 6.4 and we continue to compare strategy IV over strategy I as follows.

$$ICER(IV) = \frac{666.5317}{3179.9090} = 0.2096,$$

$$ICER(I) = \frac{526.4174 - 666.5317}{3180.3530 - 3179.9090} = -315.5727.$$

Table 6.4: Second computation of the total number of infections averted, total costs, ACER and ICER of strategies.

Strategy	Total infections averted	Total Costs ($)	ACER	ICER
Strategy IV	3179.9090	666.5317	0.2096	0.2096
Strategy I	3180.3530	526.4174	0.1655	-315.5727
Strategy II	3277.3560	488.0466	0.1489	-0.3956

Comparing strategy IV and strategy I, we observe that ICER (IV) is greater than ICER (I), showing that strategy IV is more expensive than strategy I. Therefore, strategy IV is removed from the list of next alternative strategies and we re-calculate ICER for the remaining

competing strategy I and strategy II, as shown in Table 6.5.

$$ICER(I) = \frac{526.4174}{3180.3530} = 0.1655,$$

$$ICER(II) = \frac{488.0466 - 526.4174}{3277.3560 - 3180.3530} = -0.3956.$$

Table 6.5: Third computation of the total number of infections averted, total costs, ACER and ICER of strategies.

Strategy	Total infections averted	Total Costs ($)	ACER	ICER
Strategy I	3180.3530	526.4174	0.1655	0.1655
Strategy II	3277.3560	488.0466	0.1489	-0.3956

Comparing strategy I and strategy II shows that strategy II is cheaper than strategy I by saving 0.3956. Strategy II has the least ICER among the above ICER. We conclude that strategy II is the most effective and cost-saving strategy compared to other strategies to control the disease.

Remark 6.5.1. *The negative sign in the above ICER indicates that the control strategies consume the least resources to implement.*

CHAPTER 7

OPTIMAL CONTROL ANALYSIS OF COFFEE BERRY DISEASE IN THE PRESENCE OF TEMPERATURE AND RAINFALL VARIABILITY

In this chapter, we proposed a nonlinear deterministic mathematical model governed by systems of ordinary differential equations at the presence of temperature and rainfall variability, expecting that the analysis of the proposed model might benefit coffee growers in the management of CBD. The fundamental assumptions are as given in 5.1.

7.1 Model Derivation

This model considers the coffee berry population and vector population with the interaction of fungal pathogen concentration, temperature, and rainfall variability.

As reported in Nicholls et al. (1996), a global mean temperature of $0.61^{\circ}C$ increment has been recorded since the beginning of the twentieth century and predicted to rise to $2^{\circ}C$ - $6^{\circ}C$ by 2100. Thus, global warming causes changes in the precipitation pattern. Hence, in view of the global scenario, the model for global temperature variation (T) and rainfall change (R) follow a logistic model equation with a growth rate of r_2 and a precipitation growth rate of M, respectively. Further, the temperature and rainfall variations are assumed to be adapted to the seasonal change scenario. The coffee berry, once infected, never recovers and gives no or very low yield of coffee.

The parameters: β_1, β_2, β_3, λ and m on temperature and precipitation distribution dependent since they appear to be the key climatic parameters that favour pathogens and vectors (i.e. insects, etc.) which invariably boost the development of CBD epidemics. Hence, pathogens and vectors are less active at low temperature and rainfall variation (T_0, R_0), and most active at high temperature and rainfall variation (T_m, R_m) (Bale et al., 2002; Ahmed et al., 2016). The schematic diagram for the dynamics of CBD is illustrated in Fig. 7.1.

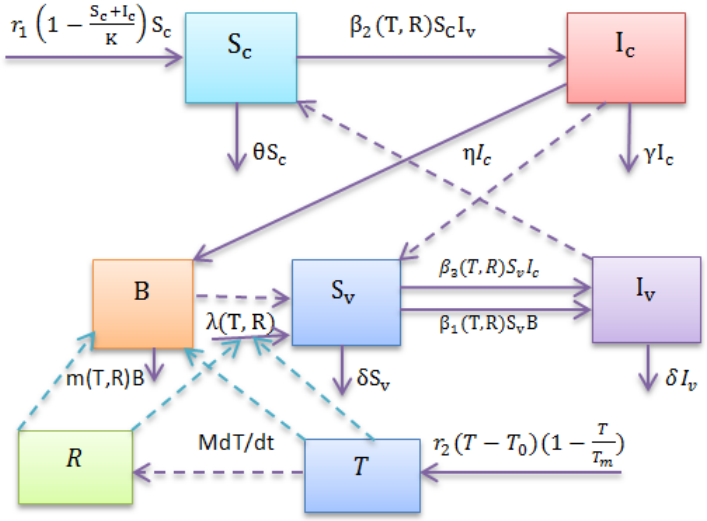

Figure 7.1: Schematic diagram of CBD dynamics

The mathematical model is formulated and presented in Eq. (7.1) from the schematic diagram:

$$\begin{aligned}
\frac{dS_c}{dt} &= r_1 S_c\left(1-\frac{S_c+I_c}{K}\right)-\beta_2(T,R)S_cI_v-\theta S_c,\\
\frac{dI_c}{dt} &= \beta_2(T,R)S_cI_v-(\gamma+\eta)I_c,\\
\frac{dS_v}{dt} &= \lambda(T,R)-(\beta_1(T,R)B+\beta_3(T,R)I_c)S_v-\delta S_v,\\
\frac{dI_v}{dt} &= (\beta_1(T,R)B+\beta_3(T,R)I_c)S_v-\delta I_v,\\
\frac{dB}{dt} &= \eta I_c-m(T,R)B,\\
\frac{dT}{dt} &= r_2(t)(T-T_0)\left(1-\frac{T}{T_m}\right),\\
\frac{dR}{dt} &= Mr_2(t)(T-T_0)\left(1-\frac{T}{T_m}\right),
\end{aligned} \tag{7.1}$$

where,
$\beta_1(T,R)=\beta_{01}+\beta_{m1}D$, $\beta_2(T,R)=\beta_{02}+\beta_{m2}D$, $\beta_3(T,R)=\beta_{03}+\beta_{m3}D$, $\lambda(T,R)=\lambda_0+\lambda_mD$, $m(T,R)=m_0+m_mD$; $D=\frac{(1+M)(T-T_0)}{T_m}$; $r2(t)=r_0+\bar{h}cos(2\pi t)$ with $r_0=0.5,\bar{h}=0.36$.
The corresponding initial data:

$$\begin{aligned}
&S_c(0)=S_{c^0}>0,\ I_c(0)=I_{c^0}\geq 0,\ S_v(0)=S_{v^0}>0,\ I_v(0)=I_{v^0}\geq 0,\ B(0)=B_0\geq 0,\\
&\quad T(0)=T_{0^0}\geq 0,\ R(0)=R_0\geq 0.
\end{aligned} \tag{7.2}$$

Remark 7.1.1. *The rates: β_{01}, β_{02}, β_{03}, λ_0 and m_0 are assume to be given constant in the absence of temperature and rainfall variation while β_{m1}, β_{m2}, β_{m3}, λ_m and m_m are incremental rates due temperature and rainfall variation.*

Remark 7.1.2. *The expression $R(t)=M(T(t)-T_0)+\varepsilon$, implies that rainfall changes as an incremental function of temperature. Moreover, M is the temperature dependent rate of precipitation and*

ε *is the amount of precipitation at* $T = T_0$. *Hence* $\varepsilon = R_0$ *and* $R_m = M(T_m - T_0) + R_0$ *at* $T = T_m$.

Table 7.1: Parameters descriptions and values to be used later in Section 7.3.

Parameter	Description	Estimated value	Source
β_{01}	Contact rate of vector with pathogen	0.0001	Assumed
β_{02}	Contact rate of coffee berry with infected vector	0.00001	Assumed
β_{03}	Contact rate of vector with infected coffee berry	0.0002	Assumed
β_{m1}	Incremental contact rate of vector with pathogen	0.005	Assumed
β_{m2}	Incremental contact rate of coffee berry with infected vector	0.008	Assumed
β_{m3}	Incremental contact rate of vector with infected coffee berry	0.0001	Assumed
θ	Mortality rate of healthy coffee berry	0.01	(Fotso et al., 2018)
γ	Removal rate of infected coffee berry	0.005	Assumed
r_1	Growth rate of new coffee berry	0.12	(Campanha et al., 2007a)
M	Precipitation (rainfall) growth rate	0.08	(Ho and Michalak, 2020)
K	Carrying capacity	150	Assumed
η	Induced rate of infected coffee berry	0.009	Assumed
λ_0	Recruitment rate of vector	0.4	Assumed
m_0	Decay rate of pathogen	0.09	Assumed
δ	Death rate of vector	0.009	Assumed
λ_m	Incremental breeding rate of vector	0.9	Assumed
m_m	Incremental decay rate of pathogen	0.001	Assumed
T_0	Minimum temperature of pathogen	20 $^\circ C$	(Jirata and Asefa, 2000)
T_m	Maximum temperature of pathogen	22 $^\circ C$	(Jirata and Asefa, 2000)
R_0	Minimum rainfall	10 mm	(Waller, 1972)
R_m	Maximum rainfall	700 mm	(Belachew et al., 2015)

7.2 Model Analysis

In this section, we study the invariant region, the positivity of the solutions, disease-free equilibrium, basic reproduction number, endemic equilibrium, bifurcation analysis, local and global stability of the model (7.1).

7.2.1 Invariant Region

We obtained the invariant region Ω_4, in which the model (7.1) solution set is bounded. Let $N_1(t) = S_c(t) + I_c(t)$ be the total population of coffee berry. Then differentiating $N_1(t)$ with

respect to time t and adding the first two equations of model (7.1), we get

$$\frac{dN_1}{dt} \leq rS_c - (\gamma+\eta)I_c = (1+r_1)S_c - S_c - (\gamma+\eta)I_c. \tag{7.3}$$

The last inequality in Eq. (7.3) can be rewritten as

$$\frac{dN_1}{dt} + hN_1 \leq \hat{K}(1+r_1), \tag{7.4}$$

where $\hat{K}$ and h are given in Chapter 5. Integrating Eq. (7.4) by separation of variables, we get

$$N_1(t) \leq \frac{\hat{K}(1+r_1)}{h} + \left(N_1(0) - \frac{\hat{K}(1+r_1)}{h}\right) e^{-ht}. \tag{7.5}$$

As $t \to \infty$ in Eq. (7.5), the population size $N_1(t) \to \hat{K}(1+r_1)/h$. Thus, the feasible region of the model (7.1) for coffee population is given by

$$\Omega_{c1} = \left\{ (S_c,\, I_c) \in \mathbb{R}^2_+ : N_1 \leq \frac{\hat{K}(1+r_1)}{h} \right\}.$$

We also consider the total population of vector as $N_2(t) = S_v(t) + I_v(t)$. Then the derivative of $N_2(t)$ with respect to t is given by

$$\frac{dN_2}{dt} = \lambda(\hat{T},\hat{R}) - \delta N_2, \tag{7.6}$$

where $\hat{T} \in [T_0, T_m]$, $\hat{R} \in [R_0, R_m]$. By solving Eq. (7.6) and as $t \to \infty$, we get $N_2(t) \leq \lambda(\hat{T},\hat{R})/\delta$. Thus, the feasible region of the model (7.1) for vector population is given by

$$\Omega_{v2} = \left\{ (S_v,\, I_v) \in \mathbb{R}^2_+ : N_2 \leq \frac{\lambda(\hat{T},\hat{R})}{\delta} \right\}. \tag{7.7}$$

From the fifth equation of model (7.1) and by the comparison, we have

$$\begin{aligned} \frac{dB}{dt} = \eta I_c - mB &\leq \eta(S_c + I_c) - m(\hat{T},\hat{R})B, \\ &\leq \frac{\hat{K}(1+r_1)\eta}{h} - m(\hat{T},\hat{R})B. \end{aligned} \tag{7.8}$$

Solving the last inequality of Eq. (7.8) and $t \to \infty$ results $B(t) \leq [\hat{K}(1+r_1)\eta]/m(\hat{T},\hat{R})h$. Consequently, the feasible region of the model (7.1) is given by

$$\Omega_4 = \left\{ (S_c,\, I_c,\, S_v,\, I_v,\, B) \in \mathbb{R}^5_+ : N_1 \leq \frac{\hat{K}(1+r_1)}{h},\, N_2 \leq \frac{\lambda(\hat{T},\hat{R})}{\delta}, B \leq \frac{\hat{K}(1+r_1)\eta}{m(\hat{T},\hat{R})h} \right\}$$

is positively invariant. Therefore, the model is considered to be epidemiologically meaningful inside Ω_4.

7.2.2 Positivity of the Solutions

In this subsection, we need to prove that the solutions of model (7.1) are nonnegative for all $t \geq 0$. This will be stated as follows.

Theorem 7.2.1. *Every solution of model* (7.1) *with initial condition* (7.2) *will remain positive in* $\mathbb{R}^7_+$ *as* $t > 0$.

Proof. (See Fotso et al. (2019)). From the model (7.1), we obtain

$$\left.\frac{dS_c}{dt}\right|_{[S_c=0]} > 0, \left.\frac{dI_c}{dt}\right|_{[I_c=0]} = \beta_2(T,R)S_cI_v \geq 0, \left.\frac{dS_v}{dt}\right|_{[S_v=0]} = \lambda(T,R) > 0,$$
$$\left.\frac{dI_v}{dt}\right|_{[I_v=0]} = [\beta_1(T,R)B + \beta_3(T,R)I_c]S_v \geq 0, \left.\frac{dB}{dt}\right|_{[B=0]} = \eta I_c > 0, \left.\frac{dT}{dt}\right|_{[T=T_0]} \geq 0,$$
$$\left.\frac{dR}{dt}\right|_{[R=R_0]} \geq 0.$$

This implies that all the solutions with positive initial data remains nonnegative in $\mathbb{R}^7_+$ for all $t \geq 0$. This means, the region attracts all solutions of the governing model (7.1). □

7.2.3 Disease Free Equilibrium Point (EEP)

Here, in order to find the disease-free equilibrium point, we equate the right hand side of (7.1) to zero with $I_c = I_v = B = 0$. This is due to the absence of infection in the coffee berry and vector population. Then solving the system one can easily obtain that $S_c = 0$ or $S_c = K - K\theta/r_1$, $S_v = \lambda(T,R)/\delta$, $T = T_0$ or $T = T_m$, $R = R_0$ or $R = R_m$. The DFEP of the model (7.1) at $(T_0,\ R_0)$ and $(T_m,\ R_m)$ respectively denoted as:

$$\begin{aligned} E_1 &= \left(\frac{K(r_1-\theta)}{r_1},\ 0,\ \frac{\lambda(T_0,R_0)}{\delta},\ 0,\ 0\right), \\ E_2 &= \left(\frac{K(r_1-\theta)}{r_1},\ 0,\ \frac{\lambda(T_m,R_m)}{\delta},\ 0,\ 0\right). \end{aligned} \tag{7.9}$$

Remark 7.2.1. *The disease-free equilibrium points:* E_1 *and* E_2 *in Eq.* (7.9) *are biologically feasible when* $r_1 > \theta$.

7.2.4 The Basic Reproduction Number

The expression of basic reproduction number $\tilde{\mathfrak{R}}_0$ for the model (7.1) can be derived using the next generation matrix method (Van den Driessche and Watmough, 2002). The first step

to find $\tilde{\Re}_0$ is rewriting the model equations starting with newly infective classes:

$$\begin{cases} \dfrac{dI_c}{dt} = \beta_2(T,R)S_cI_v - (\gamma+\eta)I_c, \\ \dfrac{dI_v}{dt} = (\beta_1(T,R)B + \beta_3(T,R)I_c)S_v - \delta I_v, \\ \dfrac{dB}{dt} = \eta I_c - m(T,R)B. \end{cases} \tag{7.10}$$

The right hand side of system (7.10) is written as $\tilde{f} - \tilde{g}$, where

$$\tilde{f} = \begin{bmatrix} \beta_2(T,R)ScIv \\ (\beta_1(T,R)B + \beta_3(T,R)Ic)Sv \\ 0 \end{bmatrix}, \quad \tilde{g} = \begin{bmatrix} (\gamma+\eta)Ic \\ \delta Iv \\ -\eta Ic + m(T,R)B \end{bmatrix}. \tag{7.11}$$

Then by linearization approach, the associated matrices of $\tilde{f}$ and $\tilde{g}$ at the DFE are given by

$$\mathscr{F} = \begin{bmatrix} 0 & k(1-\dfrac{\theta}{r_1})\beta_2(T^*,R^*) & 0 \\ \dfrac{\beta_3(T^*,R^*)\lambda(T^*,R^*)}{\delta} & 0 & \dfrac{\beta_1(T^*,R^*)\lambda(T^*,R^*)}{\delta} \\ 0 & 0 & 0 \end{bmatrix},$$

$$\mathscr{V} = \begin{bmatrix} \gamma+\eta & 0 & 0 \\ 0 & \delta & 0 \\ -\eta & 0 & m(T^*,R^*) \end{bmatrix},$$

where $(T^*,R^*) = (T_0,R_0)$ or $(T^*,R^*) = (T_m,R_m)$.
$\tilde{\Re}_0 = \rho(\mathscr{F}\mathscr{V}^{-1})$ is the spectral radius of the product $\mathscr{F}\mathscr{V}^{-1}$. Thus, R_{01} and R_{02} at DFE points E_1 and E_2 are given as the following, respectively.

$$\begin{aligned} R_{01} &= \sqrt{\frac{K\beta_{02}\lambda_0\left[m_0\beta_{03}+\beta_{01}\eta\right](r_1-\theta)}{r_1 m_0\delta^2(\gamma+\eta)}}, \\ R_{02} &= \sqrt{\frac{K\beta_2(T_m,R_m)\lambda(T_m,R_m)\left[m(T_m,R_m)\beta_3(T_m,R_m)+\beta_1(T_m,R_m)\eta\right](r_1-\theta)}{r_1 m(T_m,R_m)\delta^2(\gamma+\eta)}} \end{aligned} \tag{7.12}$$

Hence, R_{02} can be written interms of R_{01} as:

$$R_{02} = \sqrt{\frac{m_0(\lambda_0+W_2)R_{01}^2}{\lambda_0(m_0+m_mD)D} + \frac{K(r-\theta)(\beta_{02}\lambda_0+W_2)W_1}{r\delta^2(\gamma+\eta)(m_0+m_mD)}}, \tag{7.13}$$

where $W_1 = (m_m\beta_{m3}+m_m\beta_{03}+\beta_{m1}\eta)D + m_m\beta_{m3}D^2$, $W_2 = (\beta_{02}\lambda_m+\beta_{m2}\lambda_0)D + \beta_{m2}\lambda_m D^2$, $D = (1+M)(T_m-T_0)/T_m$.

7.2.5 Local Stability of Disease Free Equilibrium Point

In this section, we shall investigate the local stability of disease-free equilibrium point(s) based on the basic reproduction numbers R_{01} and R_{02}.

Theorem 7.2.2. *If $R_{01} < R_{02} < 1$, then disease-free equilibrium E_1 or E_2 of the model (7.1) is locally asymptotically stable in Ω_4.*

Proof. The Jacobian matrix of the model (7.1) at disease-free equilibrium E_1 or $E_2 = (K(1-\theta/r_1),\ 0,\ \lambda(T^*,R^*)/\delta,\ 0,\ 0)$ is given by

$$J = \begin{bmatrix} \theta - r_1 & -(r_1-\theta) & 0 & K(\frac{r_1-\theta}{r_1})\beta_2(T^*,R^*) & 0 \\ 0 & -\gamma-\eta & 0 & K(\frac{r_1-\theta}{r_1})\beta_2(T^*,R^*) & 0 \\ 0 & -\beta_3(T^*,R^*)\dfrac{\lambda(T^*,R^*)}{\delta} & -\delta & 0 & -\beta_1(T^*,R^*)\dfrac{\lambda(T^*,R^*)}{\delta} \\ 0 & \beta_3(T^*,R^*)\dfrac{\lambda(T^*,R^*)}{\delta} & 0 & -\delta & -\beta_1(T^*,R^*)\dfrac{\lambda(T^*,R^*)}{\delta} \\ 0 & \eta & 0 & 0 & -m(T^*,R^*) \end{bmatrix} \tag{7.14}$$

where $(T^*,R^*) = (T_0,T_0)$ or $(T^*,R^*) = (T_m,R_m)$. From the Jacobian matrix (7.14), we obtained characteristic polynomial:

$$(\delta+\Lambda)(r_1-\theta+\Lambda)(\Lambda^3+\tilde{A}_2\Lambda^2+\tilde{A}_1\Lambda+\tilde{A}_0) = 0. \tag{7.15}$$

From Eq. (7.15), we obtain that $\Lambda_1 = -\delta < 0$, $\Lambda_2 = -(r_1-\theta) < 0$, and from the last characteristic polynomial,

$$\Lambda^3+\tilde{A}_2\Lambda^2+\tilde{A}_1\Lambda+\tilde{A}_0 = 0, \tag{7.16}$$

where

$$\begin{aligned}
\tilde{A}_2 &= \gamma+\eta+m(T_m,R_m)+\delta, \\
\tilde{A}_1 &= m(T_m,R_m)(\delta+\gamma+\eta) + \frac{\delta(\gamma+\eta)\eta\beta_1(T_m,R_m)}{m(T_m,R_m)\beta_3(T_m,R_m)+\eta\beta_1(T_m,R_m)} \\
&\quad + \frac{\delta(\gamma+\eta)m(T_m,R_m)\beta_3(T_m,R_m)}{m\beta_3(T_m,R_m)+\eta\beta_1(T_m,R_m)}(1-R_{02}^2), \\
\tilde{A}_0 &= \delta(\gamma+\eta)m(T_m,R_m) - \frac{K\beta_3(T_m,R_m)\lambda(T_m,R_m)(r_1-\theta)(\beta_3(T_m,R_m)m(T_m,R_m)+\beta_1(T_m,R_m)\eta)}{r_1\delta}, \\
&= \delta(\gamma+\eta)m(T_m,R_m)(1-R_{02}^2).
\end{aligned}$$

Using Routh-Hurwitz criteria from (Martcheva, 2015), Eq. (7.16) has eigenvalues which are negative real part if $\tilde{A}_2 > 0$, $\tilde{A}_1\tilde{A}_2 - \tilde{A}_0 > 0$ and $\tilde{A}_0(\tilde{A}_1\tilde{A}_2-\tilde{A}_0) > 0$. However, $\tilde{A}_0$ is positive if $R_{02} < 1$. Since $R_{01} < R_{02}$, then DFEP E_1 or E_2 is locally asymptotically stable for $R_{01} < R_{02} < 1$. □

7.2.6 Global Stability of Disease Free Equilibrium Point

Theorem 7.2.3. *If $R_{01} < R_{02} < 1$ and $\tilde{P} \leq \tilde{Q}$, then the disease-free equilibrium E_1 or E_2 of the model (7.1) is globally asymptotically stable in Ω_4.*

Proof. To proof this theorem, we first define the following Lyapunov function $\tilde{U}$ at $(T^*, R^*) = (T_0, R_0)$ or $(T^*, R^*) = (T_m, R_m)$:

$$\tilde{U} = \frac{1}{2}(S_c - S_c^0)^2 + I_c + \frac{1}{2}(S_v - S_v^0)^2 + I_v + B. \tag{7.17}$$

Then differentiating $\tilde{U}$ with respect to t, we obtain

$$\frac{d\tilde{U}}{dt} = (S_c - S_c^0)\frac{dS_c}{dt} + \frac{dI_c}{dt} + (S_v - S_v^0)\frac{dS_v}{dt} + \frac{dI_v}{dt} + \frac{dB}{dt}, \tag{7.18}$$

Substituting expression for dS_c/dt, dI_c/dt, dS_v/dt, dI_v/dt and dB/dt from model (7.1) into Eq. (7.18) leads to

$$\begin{aligned} \frac{d\tilde{U}}{dt} = &-r_1\left(S_c - \frac{K(r_1-\theta)}{r_1}\right)^2\left(\frac{S_c+I_c}{K} + \beta_2(T^*,R^*)I_v + \theta\right) \\ &- \left(S_v - \frac{\lambda(T^*,R^*)}{\delta}\right)^2(\beta_1 B(T^*,R^*) + \beta_3(T^*,R^*)I_c + \delta) + \tilde{P} - \tilde{Q}, \end{aligned} \tag{7.19}$$

where

$$\begin{aligned} \tilde{P} &= r_1 S_c^2 + \lambda S_v + \frac{K^2(r_1-\theta)^2}{r_1^2}\left(\frac{S_c+I_c}{K} + \beta_2(T^*,R^*)I_v + \theta\right) + \frac{\lambda^2}{\delta^2}(\beta_1 B + \beta_3 I_c + \delta) \\ &\quad + \beta_2 S_c I_v + (\beta_1 B + \beta_3 I_c)S_v + \eta I_c, \\ \tilde{Q} &= K(r_1-\theta)S_c + \frac{K(r_1-\theta)S_c}{r_1}\left(\frac{S_c+I_c}{K} + \beta_2(T^*,R^*)I_v + \theta\right) + \frac{\lambda^2(T^*,R^*)}{\delta} \\ &\quad + \frac{\lambda(T^*,R^*)S_v}{\delta}(\beta_1(T^*,R^*)B + \beta_3(T^*,R^*)I_c + \delta) + (\gamma+\eta)I_c + \delta I_v + m(T^*,R^*)B. \end{aligned}$$

From Eq. (7.19), we have $d\tilde{U}/dt \leq 0$ if and only if $S_c = S_c^0$, $S_v = S_v^0$, $I_c = I_c^0 = I_v = I_v^0 = B = B^0 = 0$ and $\tilde{P} \leq \tilde{Q}$.

Therefore, the largest compact invariant set in $\{(S_c, I_c, S_v, I_v, B) \in \Omega_4 : d\tilde{U}/dt = 0\}$ is the singleton $\{E_{01}\}$ or $\{E_{02}\}$. By La Salle (1976) invariant, it then implies that E_{01} or E_{02} is globally asymptotically stable in Ω_4. □

7.2.7 Endemic Equilibrium Point (EEP)

The endemic equilibrium point exists whenever CBD persists in the coffee berry population. For simplicity, denote the EEP by E^*. To obtain EEP, we set the right side of model (7.1)

equal to zero. That is,

$$\begin{aligned}
r_1 S_c^* \left(1 - \frac{S_c^* + I_c^*}{K}\right) - \beta_2(T,R) S_c^* I_v^* - \theta S_c^* &= 0,\\
\beta_2(T,R) S_c^* I_v^* - (\gamma+\eta) I_c^* &= 0,\\
\lambda(T,R) - (\beta_1(T,R)B^* + \beta_3(T,R) I_c^*) S_v^* - \delta S_v^* &= 0,\\
(\beta_1(T,R)B^* + \beta_3(T,R) I_c^*) S_v^* - \delta I_v^* &= 0,\\
\eta I_c^* - m(T,R) B^* &= 0,\\
r_2(t)(T^* - T_0)\left(\frac{T_m - T^*}{T_m}\right) &= 0,\\
r_2(t)(R^* - R_0)\left(1 + \frac{R_0 - R^*}{M T_m} - \frac{T_0}{T_m}\right) &= 0.
\end{aligned} \tag{7.20}$$

By solving Eq. (7.20), we get S_c^*, S_v^*, I_v^* and B^* interms of I_c^* at $(T^*, R^*) = (T_0, R_0)$:

$$\begin{aligned}
S_c^* &= \frac{\delta(\gamma+\eta)(m_0\delta + (\beta_{01}\eta + m_0\beta_{03}) I_c^*) I_c^*}{\lambda_0 \beta_{02}(\beta_{01}\eta + m_0\beta_{03}) I_c^*},\\
S_v^* &= \frac{\lambda_0 m_0}{m_0\delta + (\beta_{01}\eta + \beta_{03} m_0) I_c^*},\\
I_v^* &= \frac{\lambda_0(\beta_{01}\eta + m_0\beta_{03}) I_c^*}{\delta(m_0\delta + (\beta_{01}\eta + m_0\beta_{03}) I_c^*)},\\
B^* &= \frac{\eta I_c^*}{m_0}.
\end{aligned} \tag{7.21}$$

Replacing the expression for S_c^* and I_v^* into the first equation in (7.20) one can obtain the expression of I_c^* as

$$f_0(I_c^*) = A_1 (I_c^*)^3 + B_1 (I_c^*)^2 + C_1 I_c^* + D_1 = 0, \tag{7.22}$$

where

$$\begin{aligned}
A_1 &= \frac{r_1^3 m_0^2 \delta^4 (\gamma+\eta)^2}{\lambda_0 K^2 \beta_{02}(r_1 - \theta)^2}\left(1 + \frac{\delta(\gamma+\eta)}{\lambda_0\beta_{02}}\right) R_{01}^4,\\
B_1 &= [r_1^3 m_0 \delta^2(\gamma+\eta)\left(\frac{m_0\delta(\lambda_0\beta_{02} + \delta(\gamma+\eta))}{\lambda_0 K \beta_{02}(r_1-\theta)}\right) + r_1^3 m_0\delta^2(\gamma+\eta)\\
&\quad \frac{r_1(\gamma+\eta) m_0\delta^2}{\lambda_0 K\beta_{02}(r_1-\theta)} - r_1^3 m_0\delta^2(\gamma+\eta)\left(\frac{m_0\delta^2(\gamma+\eta)}{\lambda_0 K\beta_{02}(r_1-\theta)}\right) R_{01}^2] R_{01}^2,\\
C_1 &= r_1 m_0^2(\gamma+\eta)\delta^3 - r_1 m_0^2 \delta^3(\gamma+\eta) R_{01}^2,\\
D_1 &= -\frac{\beta_{01} m_0^2 r_1 \delta^3(\gamma+\eta)}{\beta_{01}\eta + m_0\beta_{03}} R_{01}^2.
\end{aligned}$$

Similarly, by computing the EEP at $(T^*,R^*)=(T_m,R_m)$, we get

$$\begin{aligned}
S_c^* &= \frac{\delta(\gamma+\eta)(m\delta+(\beta_1\eta+m\beta_3)I_c^*)I_c^*}{\lambda\beta_2(\beta_1\eta+m\beta_3)I_c^*},\\
S_v^* &= \frac{\lambda m}{m\delta+(\beta_1\eta+\beta_3 m)I_c^*},\\
I_v^* &= \frac{\lambda(\beta_1\eta+m\beta_3)I_c^*}{\delta(m\delta+(\beta_1\eta+m\beta_3 I_c^*))}\\
B^* &= \frac{\eta I_c^*}{m}.
\end{aligned} \tag{7.23}$$

Substituting the expression of S_c^* and I_v^* into Eq. (7.20) and simplifying we get an expression for I_c^* which satisfy:

$$f_m(I_c^*) = A_2(I_c^*)^3 + B_2(I_c^*)^2 + C_2 I_c^* + D_2 = 0, \tag{7.24}$$

where

$$\begin{aligned}
A_2 &= \frac{r_1^3 m^2\delta^4(\gamma+\eta)^2}{\lambda K^2\beta_2(r_1-\theta)^2}\left(1+\frac{\delta(\gamma+\eta)}{\lambda\beta_2}\right)R_{02}^4,\\
B_2 &= r_1^3 m\delta^2(\gamma+\eta)\left(\frac{m\delta(\lambda\beta_2+\delta(\gamma+\eta))}{\lambda K\beta_2(r_1-\theta)}\right)R_{02}^2 + r_1^3 m\delta^2(\gamma+\eta)\\
&\quad\left(\frac{r_1(\gamma+\eta)m\delta^2}{\lambda K\beta_2(r_1-\theta)}\right)R_{02}^2 - r_1^3 m\delta^2(\gamma+\eta)\left(\frac{m\delta^2(\gamma+\eta)}{\lambda K\beta_2(r_1-\theta)}\right)R_{02}^4,\\
C_2 &= r_1 m^2(\gamma+\eta)\delta^3 - r_1 m^2\delta^2(\gamma+\eta)R_{02}^2,\\
D_2 &= -\frac{\beta_1 m^2 r_1\delta^3(\gamma+\eta)}{\beta_1\eta+m\beta_3}R_{02}^2,
\end{aligned} \tag{7.25}$$

where, $\beta_1,\ \beta_2,\ \beta_3,\ \lambda$ and m in Eqs. (7.23) and (7.25) are considered at (T_m,R_m).

7.2.8 Local Stability of Endemic Equilibrium Point

Theorem 7.2.4. *If* $R_{02}>R_{01}>1$, $B_i>0, i=1,...,5, B_1B_2-B_3>0$, $-B_3^2-B_1^2B_4+B_1(B_2B_3+B_5)>0$, $-B_4^2(-B_1B_2B_3+B_3^2+B_1^2B_4)+(B_2B_3-B_1(B_2^2-2B_4))B_5-B_5^2>0$, $B_5(-B_4(-B_1B_2B_3+B_3^2+B_1^2B_4)+(B_2B_3-B_1(B_2^2-2B_4))B_5-B_5^2)>0$, *then the endemic equilibrium* E^* *of model* (7.1) *is locally asymptotically stable in* Ω_4.

Proof. The Jacobian matrix of model (7.1) at the endemic equilibrium E^* is given by

$$J(E^*) = \begin{bmatrix}
M_{11} & -(r_1-\theta) & 0 & \beta_2 S_c^* & 0\\
\beta_2 I_v^* & -\gamma-\eta & 0 & \beta_2 S_c^* & 0\\
0 & -\beta_3 S_v^* & M_{33} & 0 & -\beta_1 S_v^*\\
0 & \beta_3 S_v^* & \beta_1 B^*+\beta_3 I_c^* & -\delta & \beta_1 S_v^*\\
0 & \eta & 0 & 0 & -m
\end{bmatrix} \tag{7.26}$$

where $M_{11} = r_1 - r_1(I_c^* + 2S_c^*)/K - \beta_2(T^*,R^*)I_v^* - \theta$, $M_{33} = -\beta_1(T^*,R^*)B^* - \beta_3(T^*,R^*)I_c^* - \delta$, $(T^*,R^*) = (T_0,R_0)$ or $(T^*,R^*) = (T_m,R_m)$.
The eigenvalues of matrix (7.26) are computed from the following equation.

$$\begin{vmatrix} b_{11}-\Lambda & b_{12} & 0 & b_{14} & 0 \\ b_{21} & b_{22}-\Lambda & 0 & b_{24} & 0 \\ 0 & b_{32} & b_{33}-\Lambda & 0 & b_{35} \\ 0 & b_{42} & b_{43} & b_{44}-\Lambda & b_{45} \\ 0 & b_{52} & 0 & 0 & b_{55}-\Lambda \end{vmatrix} = 0 \tag{7.27}$$

where
$b_{11} = -\theta - r_1(I_c^* + 2S_c^*)/K - \beta_2(T^*,R^*)I_v^* + r_1/K$, $b_{12} = -(r_1 - \theta)$, $b_{21} = \beta_2(T^*,R^*)I_v^*$, $b_{22} = -\gamma - \eta$, $b_{32} = -\beta_3(T^*,R^*)S_v^*$, $b_{42} = \beta_3(T^*,R^*)S_v^*$, $b_{52} = \eta$, $b_{33} = -\beta_1(T^*,R^*)B^* - \beta_3(T^*,R^*)I_c^* - \delta$, $b_{43} = \beta_1(T^*,R^*)B^* + \beta_3(T^*,R^*)I_c^*$, $b_{14} = \beta_2(T^*,R^*)S_c^*$, $b_{24} = \beta_2(T^*,R^*)S_c^*$, $b_{44} = -\delta$, $b_{35} = -\beta_1(T^*,R^*)S_v^*$, $b_{45} = \beta_1(T^*,R^*)S_v^*$, $b_{55} = -m(T^*,R^*)$. Then the characteristic polynomial of Eq. (7.27) is given by

$$\Lambda^5 + B_1\Lambda^4 + B_2\Lambda^3 + B_3\Lambda^2 + B_4\Lambda + B_5 = 0, \tag{7.28}$$

where

$$\begin{aligned}
B_1 &= -(b_{11} + b_{22} + b_{33} + b_{44} + b_{55}),\\
B_2 &= b_{33}b_{44} + b_{22}(b_{33} + b_{44} + b_{55}) + (b_{33} + b_{44})b_{55} + b_{11}(b_{33} + b_{44} + b_{55})\\
&\quad + b_{24}b_{42}(b_{11} - b_{14}) - b_{11}((b_{44} + b_{55})b_{33} + b_{22} + b_{44}b_{55}),\\
B_3 &= b_{24}b_{33}b_{42} - b_{14}b_{21}b_{42} - b_{24}b_{32}(b_{43} - b_{24}b_{45}b_{52} - b_{22}b_{44}b_{55}\\
&\quad - (b_{44} + b_{55})b_{22}b_{33} + (b_{24}b_{42} - b_{44})b_{55} + b_{11}b_{24}b_{42}\\
&\quad - (b_{44} + b_{55})b_{11}b_{33} - b_{11}b_{22} - b_{11}b_{44}b_{55},\\
B_4 &= b_{14}b_{21}(b_{33}b_{42} - b_{32}b_{43} - b_{45}b_{52}) + b_{24}(b_{33}b_{45} - b_{35}b_{43})b_{52} + (b_{22}b_{33}b_{44}\\
&\quad + b_{24}b_{32}b_{43} + b_{14}b_{21}b_{42})b_{55} + b_{11}b_{24}(b_{32}b_{43} + b_{45}b_{52} - b_{33}b_{42})\\
&\quad + b_{11}b_{33}b_{44}b_{55} + b_{11}b_{22}(b_{33} + b_{44}) - b_{11}b_{24}b_{42}b_{55},\\
B_5 &= b_{14}b_{21}((b_{33}b_{45} - b_{35}b_{43})b_{52} + (b_{32}b_{43} - b_{42})b_{55}\\
&\quad + b_{11}b_{24}((b_{35}(b_{43} - b_{33}b_{45})b_{52} + (b_{33}b_{42} - b_{32}b_{43})b_{55}) - b_{11}b_{22}b_{33}b_{44}.
\end{aligned}$$

Using the Routh Hurwitz criterion, the endemic equilibrium E^* will be locally asymptotically stable for $R_{02} > R_{01} > 1$ if $B_i > 0, i = 1,...,5$,

$B_1 > 0$, $B_1B_2 - B_3 > 0$, $-B_3^2 - B_1^2B_4 + B_1(B_2B_3 + B_5) > 0$, $-B_4^2(-B_1B_2B_3 + B_3^2 + B_1^2B_4) + (B_2B_3 - B_1(B_2^2 - 2B_4))B_5 - B_5^2 > 0$, $B_5(-B_4(-B_1B_2B_3 + B_3^2 + B_1^2B_4) + (B_2B_3 - B_1(B_2^2 - 2B_4))B_5 - B_5^2) > 0$.

Thus, all eigenvalues of Eq. (7.28) evaluated at the endemic equilibrium E^* have negative real parts whenever $R_{02} > R_{01} > 1$. Therefore, the endemic equilibrium E^* is locally asymptotically stable for $R_{02} > R_{01} > 1$ □

7.2.9 Global Stability of Endemic Equilibrium Point

Theorem 7.2.5. *If $R_{02} > R_{01} > 1$, then the endemic equilibrium E^* of the model (7.1) is globally asymptotically stable in Ω_4.*

Proof. To establish the global stability of the endemic equilibrium E^*, we consider the following Lyapunov function $\tilde{V}$ at $(T^*, R^*) = (T_0, R_0)$ or $(T^*, R^*) = (T_m, R_m)$:

$$\tilde{V} = \frac{[(S_c - S_c^*) + (I_c - I_c^*)]^2}{2} + \frac{[(S_v - S_v^*) + (I_v - I_v^*)]^2}{2} + \frac{(B - B^*)^2}{2}. \tag{7.29}$$

Then by taking the derivative of $\tilde{V}$ with respect to t, we obtain

$$\begin{aligned} \frac{d\tilde{V}}{dt} &= [(S_c - S_c^*) + (I_c - I_c^*)] \frac{d}{dt}[S_c + I_c] + [(S_v - S_v^*) + (I_v - I_v^*)] \frac{d}{dt}[S_v + I_v] + (B - B^*)\frac{dB}{dt}, \\ &= [(S_c - S_c^*) + (I_c - I_c^*)] \frac{dN_c}{dt} + [(S_v - S_v^*) + (I_v - I_v^*)] \frac{dN_v}{dt} + (B - B^*)\frac{dB}{dt}. \end{aligned} \tag{7.30}$$

On the other hand, from Eqs. (7.4), (7.6) and (7.8), respectively, we have

$$\begin{aligned} \frac{dN_c}{dt} &= \frac{d}{dt}[S_c + I_c] \leq \hat{K}(1 + r_1) - hN_c, \\ \frac{dN_v}{dt} &= \frac{d}{dt}[S_v + I_v] = \lambda(T^*, R^*) - \delta N_v, \\ \frac{dB}{dt} &\leq \frac{\hat{K}(1 + r_1)\eta}{h} - m(T^*, R^*)B. \end{aligned} \tag{7.31}$$

Substituting expression for dN_c/dt, dN_v/dt and dB/dt from Eq. (7.31) into Eq. (7.30) leads to

$$\begin{aligned} \frac{d\tilde{V}}{dt} &= [(S_c - S_c^*) + (I_c - I_c^*)] \frac{dN_c}{dt} + [(S_v - S_v^*) + (I_v - I_v^*)] \frac{dN_v}{dt} + (B - B^*)\frac{dB}{dt}, \\ &\leq [(S_c - S_c^*) + (I_c - I_c^*)] \left[\hat{K}(1 + r_1) - hN_c\right] + [(S_v - S_v^*) + (I_v - I_v^*)] [\lambda - \delta N_v] \\ &+ (B - B^*) \left[\frac{\hat{K}(1 + r_1)\eta}{h} - mB\right], \\ &\leq \left[N_c - \frac{\hat{K}(1 + r_1)}{h}\right] \left[\hat{K}(1 + r_1) - hN_c\right] + \left[N_v - \frac{\lambda}{\delta}\right] [\lambda - \delta N_v] \\ &+ \left[B - \frac{\hat{K}(1 + r_1)\eta}{hm}\right] \left[\frac{\hat{K}(1 + r_1)\eta}{h} - mB\right]. \end{aligned} \tag{7.32}$$

By re-arranging and simplify the Eq. (7.32), we obtain

$$\frac{d\tilde{V}}{dt} \leq -\frac{1}{h}\left[\hat{K}(1+r_1) - hN_c\right]^2 - \frac{1}{\delta}\left[\lambda - \delta N_v\right]^2 - \frac{1}{m}\left[\frac{\hat{K}(1+r_1)\eta}{h} - mB\right]^2, \tag{7.33}$$

where the parameters: λ and m in Eq. (7.33) are considered at (T^*, R^*).

Thus $(d\tilde{V}/dt)(S_c,\ I_c,\ S_v,\ I_v,\ B) \leq 0$. Furthermore, $(d\tilde{V}/dt)(S_c,\ I_c,\ S_v,\ I_v,\ B) = 0$ if and only if $S_c = S_c^*,\ I_c = I_c^*,\ S_v = S_v^*,\ I_v = I_v^*,\ B = B^*$.

Therefore, the largest compact invariant set in $\left\{(S_c,\ I_c,\ S_v,\ I_v,\ B) \in \Omega_4 : d\tilde{V}/dt = 0\right\}$ is the singleton $\{E^*\}$. By La Salle (1976) invariance principle, E^* is globally asymptotically stable in Ω_4. □

7.2.10 Bifurcation Analysis

Theorem 7.2.6. *If $R_{01} < 1$, then the system (7.1) exhibits forward bifurcation at $R_{01} = 1$.*

Proof. Introducing $S_c = \tilde{x}_1,\ I_c = \tilde{x}_2,\ S_v = \tilde{x}_3,\ I_v = \tilde{x}_4,\ B = \tilde{x}_5$, the model (7.1) at (T_0, R_0) can be written as $d\tilde{x}/dt = (\tilde{g}_1,\ \tilde{g}_2,\ \tilde{g}_3,\ \tilde{g}_4,\ \tilde{g}_5)^T$, where

$$\begin{cases} \dfrac{d\tilde{x}_1}{dt} = r_1\tilde{x}_1\left(1 - \dfrac{\tilde{x}_1 + \tilde{x}_2}{K}\right) - \beta_{02}\tilde{x}_1\tilde{x}_4 - \theta\tilde{x}_1, \\ \dfrac{d\tilde{x}_2}{dt} = \beta_{02}\tilde{x}_1\tilde{x}_4 - (\gamma+\eta)\tilde{x}_2, \\ \dfrac{d\tilde{x}_3}{dt} = \lambda_0 - \beta_{01}\tilde{x}_3\tilde{x}_5 - \beta_{03}\tilde{x}_2\tilde{x}_3 - \delta\tilde{x}_3, \\ \dfrac{d\tilde{x}_4}{dt} = \beta_{01}\tilde{x}_3\tilde{x}_5 + \beta_{03}\tilde{x}_2\tilde{x}_3 - \delta\tilde{x}_4, \\ \dfrac{d\tilde{x}_5}{dt} = \eta\tilde{x}_2 - m_0\tilde{x}_5. \end{cases} \tag{7.34}$$

Let us consider β_{02} at (T_0, R_0) as bifurcation parameter so that $R_{01} = 1$ if

$$\beta_{02} = \beta_{02}^* = \frac{r_1(\gamma+\eta)\delta^2 m_0}{K\lambda_0(r_1-\theta)(m_0\beta_{03} + \beta_{01}\eta)}. \tag{7.35}$$

The Jacobian matrix of Eq. (7.34) at disease-free equilibrium E_1 is given by

$$J(E_1) = \begin{bmatrix} \theta - r_1 & -(r_1-\theta) & 0 & -\dfrac{K(r_1-\theta)\beta_{02}^*}{r_1} & 0 \\ 0 & -\gamma-\eta & 0 & \dfrac{K(r_1-\theta)\beta_{02}^*}{r_1} & 0 \\ 0 & -\dfrac{\beta_{03}\lambda_0}{\delta} & -\delta & 0 & -\dfrac{\beta_{01}\lambda_0}{\delta} \\ 0 & \dfrac{\beta_{03}\lambda_0}{\delta} & 0 & -\delta & \dfrac{\beta_{01}\lambda_0}{\delta} \\ 0 & \eta & 0 & 0 & -m_0 \end{bmatrix}.$$

The right eigenvector, $\tilde{u} = (\tilde{u}_1,\ \tilde{u}_2,\ \tilde{u}_3,\ \tilde{u}_4,\ \tilde{u}_5)^T$ are computed from $J(E_1)\tilde{u} = 0$ as follows.

$$J(E_1) = \begin{cases} (\theta - r_1)\tilde{u}_1 - (r_1 - \theta)\tilde{u}_2 - \dfrac{K(r_1-\theta)\beta_{02}^*}{r_1}\tilde{u}_4 = 0, \\ (-\gamma - \eta)\tilde{u}_2 + \dfrac{K(r_1-\theta)\beta_{02}^*}{r_1}\tilde{u}_4 = 0, \\ -\dfrac{\beta_{03}\lambda_0}{\delta}\tilde{u}_2 - \delta\tilde{u}_3 - \dfrac{\beta_{01}\lambda_0}{\delta}\tilde{u}_5 = 0, \\ \dfrac{\beta_{03}\lambda_0}{\delta}\tilde{u}_2 - \delta\tilde{u}_4 + \dfrac{\beta_{01}\lambda_0}{\delta}\tilde{u}_5 = 0, \\ \eta\tilde{u}_2 - m_0\tilde{u}_5 = 0. \end{cases} \tag{7.36}$$

From Eq. (7.36), we get

$$\begin{aligned} \tilde{u}_1 &= -\frac{K\beta_{02}^*}{r_1}\left(\frac{r_1-\theta}{\gamma+\eta} + 1\right)\tilde{u}_4, \\ \tilde{u}_2 &= \frac{K(r_1-\theta)\beta_{02}^*}{r_1(\gamma+\eta)}\tilde{u}_4, \\ \tilde{u}_3 &= -\tilde{u}_4, \\ \tilde{u}_5 &= \frac{\eta K(r_1-\theta)\beta_{02}^*}{r_1(\gamma+\eta)m_0}\tilde{u}_4, \end{aligned} \tag{7.37}$$

where $\tilde{u}_4 = \tilde{u}_4 > 0$. Also the left eigenvector, $\tilde{z} = (\tilde{z}_1,\ \tilde{z}_2,\ \tilde{z}_3,\ \tilde{z}_4,\ \tilde{z}_5)$ are computed from $J(E_1) = 0$ so that

$$\tilde{z}_1 = \tilde{z}_3 = 0,\ \tilde{z}_2 = \frac{\delta r_1}{K(r_1-\theta)\beta_{02}^*}\tilde{z}_4,\ \tilde{z}_5 = \frac{\beta_{01}\lambda_0}{\delta m_0}\tilde{z}_4;\quad \tilde{z}_4 = \tilde{z}_4 > 0.$$

Based on center manifold theorem from (Castillo-Chavez and Song, 2004), we have to compute $\tilde{a}$ and $\tilde{b}$ such that

$$\tilde{a} = \sum_{i,j,k=1}^{5} z_k u_i u_j \frac{\partial^2 g_k}{\partial x_i \partial x_j}(E_1),\ \ \tilde{b} = \sum_{i,k=1}^{5} z_k u_i \frac{\partial^2 g_k}{\partial x_i \partial \beta_{02}^*}(E_1). \tag{7.38}$$

The nonzero second partial derivatives of $\tilde{g}_1,\ \tilde{g}_2, \tilde{g}_3$ and $\tilde{g}_4$ are given as follows:

$$\begin{aligned} &\frac{\partial^2\tilde{g}_1}{\partial\tilde{x}_1\partial\tilde{x}_1} = \frac{\partial^2\tilde{g}_1}{\partial\tilde{x}_1\partial\tilde{x}_1} = -\frac{2r_1}{K},\ \frac{\partial^2\tilde{g}_1}{\partial\tilde{x}_1\partial\tilde{x}_2} = \frac{\partial^2\tilde{g}_1}{\partial\tilde{x}_2\partial\tilde{x}_1} = -\frac{r_1}{K}, \\ &\frac{\partial^2\tilde{g}_1}{\partial\tilde{x}_1\partial\tilde{x}_4} = \frac{\partial^2\tilde{g}_1}{\partial\tilde{x}_4\partial\tilde{x}_1} = -\beta_{02}^*,\ \frac{\partial^2\tilde{g}_2}{\partial\tilde{x}_1\partial\tilde{x}_2} = \frac{\partial^2\tilde{g}_2}{\partial\tilde{x}_2\partial\tilde{x}_1} = \beta_{02}^*, \\ &\frac{\partial^2\tilde{g}_3}{\partial\tilde{x}_2\partial\tilde{x}_3} = \frac{\partial^2\tilde{g}_3}{\partial\tilde{x}_3\partial\tilde{x}_2} = -\beta_{03},\ \frac{\partial^2\tilde{g}_3}{\partial\tilde{x}_3\partial\tilde{x}_5} = \frac{\partial^2\tilde{g}_3}{\partial\tilde{x}_5\partial\tilde{x}_3} = -\beta_{01}, \\ &\frac{\partial^2\tilde{g}_4}{\partial\tilde{x}_2\partial\tilde{x}_3} = \frac{\partial^2\tilde{g}_4}{\partial\tilde{x}_3\partial\tilde{x}_2} = \beta_{03},\quad \frac{\partial^2\tilde{g}_4}{\partial\tilde{x}_3\partial\tilde{x}_5} = \frac{\partial^2\tilde{g}_4}{\partial\tilde{x}_5\partial\tilde{x}_3} = \beta_{01}, \\ &\frac{\partial^2\tilde{g}_1}{\partial\tilde{x}_4\partial\beta_{02}^*} = \frac{\partial^2\tilde{g}_1}{\partial\beta_{02}^*\partial\tilde{x}_4} = -\tilde{x}_1^*,\ \frac{\partial^2\tilde{g}_2}{\partial\tilde{x}_4\partial\beta_{02}^*} = \frac{\partial^2\tilde{g}_2}{\partial\beta_{02}^*\partial\tilde{x}_4} = \tilde{x}_1^*. \end{aligned} \tag{7.39}$$

All the others second partial derivatives of $\tilde{g}_i,\ i=1,...,5$ are zero. By using Eq. (7.38), we get

$$\begin{aligned}\tilde{a} &= 2\tilde{z}_2\tilde{u}_1\tilde{u}_4\beta_{02}^* + 2\tilde{z}_4\tilde{u}_2\tilde{u}_3\beta_{03} + 2\tilde{z}_4\tilde{u}_3\tilde{u}_5\beta_{01} \\ &= -\left[\frac{2\delta^3 r_1(\gamma+\eta)m_0}{K\lambda_0(r_1-\theta)^2(m_0\beta_{03}+\beta_{01}\eta)}\left(\frac{r_1-\theta}{\gamma+\eta}+1\right)+\frac{2\delta\beta_{03}}{\gamma+\eta}+2\eta K(r_1-\theta)\delta^2\right]\tilde{z}_4\tilde{u}_4^2 < 0\end{aligned} \tag{7.40}$$

and

$$\begin{aligned}\tilde{b} &= \tilde{z}_1\tilde{u}_4\frac{\partial^2\tilde{g}_1}{\partial\tilde{x}_4\partial\beta_{02}^*}+\tilde{z}_2\tilde{u}_4\frac{\partial^2\tilde{g}_2}{\partial\tilde{x}_4\partial\beta_{02}^*} \\ &= \frac{\delta}{\beta_{02}^*}\tilde{z}_4\tilde{u}_4 \\ &= \frac{K(r_1-\theta)(m_0\beta_{03}+\beta_{01}\eta)}{r_1(\gamma+\eta)\delta m_0}\tilde{z}_4\tilde{u}_4 > 0.\end{aligned} \tag{7.41}$$

Since the coefficient $\tilde{a}$ is negative and $\tilde{b}$ is positive at (T_0,R_0), then the system (7.1) exhibits forward bifurcation at $R_{01}=1$ and there exists at least one stable endemic equilibrium when $R_{01}>1$ (See Figure 7.2). □

Theorem 7.2.7. *If $R_{02}<1$, then the model (7.1) exhibits backward bifurcation at $R_{02}=1$.*

Proof. We consider the change of variables: $S_c=y_1,\ I_c=y_2,\ S_v=y_3,\ I_v=y_4,\ B=y_5$. Then, at (T_m,R_m) the model (7.1) can be written in the form $dy/dt=(f_1,\ f_2,\ f_3,\ f_4,\ f_5)^T$:

$$\begin{cases}\dfrac{dy_1}{dt} = r_1y_1\left(1-\dfrac{y_1+y_2}{K}\right)-\beta_2(T_m,R_m)y_1y_4-\theta y_1, \\ \dfrac{dy_2}{dt} = \beta_2(T_m,R_m)y_1y_4-(\gamma+\eta)y_2, \\ \dfrac{dy_3}{dt} = \lambda(T_m,R_m)-[\beta_1(T_m,R_m)y_5+\beta_3(T_m,R_m)y_2]y_3-\delta y_3, \\ \dfrac{dy_4}{dt} = [\beta_1(T_m,R_m)y_5+\beta_3(T_m,R_m)y_2]y_3-\delta y_4, \\ \dfrac{dy_5}{dt} = \eta y_2-m(T_m,R_m)x_5.\end{cases} \tag{7.42}$$

Let us consider β_3 at (T_m,R_m) as bifurcation parameter so that $R_{02}=1$ if

$$\beta_3(T_m,R_m)=\beta_3^*(T_m,R_m)=\frac{r_1(\gamma+\eta)\delta^2m-\beta_2K\lambda(r_1-\theta)\beta_1\eta}{\beta_2K\lambda(r_1-\theta)m},$$

where $\beta_1,\ \beta_2,\ \lambda$ and m are considered at (T_m,R_m). The right eigenvector, $v=(v_1,\ v_2,\ v_3,\ v_4,\ v_5)^T$

are computed from $J(E_2)v = 0$ (where $J(E_2)$ is Jacobian matrix of Eq. (7.42) at E_2) so that

$$v_1 = \frac{K\beta_2(T_m,R_m)(\theta - r_1 - \gamma - \eta)}{r_1(\gamma+\eta)}v_4,\ v_2 = \frac{K(r_1-\theta)\beta_2(T_m,R_m)}{r_1(\gamma+\eta)}v_4,\ v_3 = -v_4,$$
$$v_5 = \frac{\eta K(r_1-\theta)\beta_2(T_m,R_m)}{r_1(\gamma+\eta)m(T_m,R_m)}v_4;\ \ v_4 = v_4 > 0.$$

The left eigenvector, $w = (w_1,\ w_2,\ w_3,\ w_4,\ w_5)$ are computed from $wJ(E_2) = 0$:
$w_1 = w_3 = 0,\ w_2 = \frac{\delta r_1}{K(r_1-\theta)\beta_2(T_m,R_m)}w_4,\ w_5 = -\frac{\beta_1(T_m,R_m)\lambda(T_m,R_m)}{\delta m(T_m,R_m)}w_4;\ \ w_4 = w_4 > 0.$
The signs of the bifurcation coefficients c and d are given as

$$c = \sum_{i,j,k=1}^{5} w_k v_i v_j \frac{\partial^2 f_k}{\partial y_i \partial y_j}(E_2), \qquad d = \sum_{i,k=1}^{5} w_k v_i \frac{\partial^2 f_k}{\partial y_i \partial \beta_3^*(T_m,R_m)}(E_2) \tag{7.43}$$

The nonzero partial derivatives of $f_1,\ f_2,\ f_3$ and $f_4$are given as follows:

$$\begin{aligned}
\frac{\partial^2 f_1}{\partial y_1 \partial y_1} &= \frac{\partial^2 f_1}{\partial y_1 \partial y_1} = -\frac{2r_1}{K},\ \frac{\partial^2 f_1}{\partial y_1 \partial y_2} = \frac{\partial^2 f_1}{\partial y_2 \partial y_1} = -\frac{r_1}{K},\\
\frac{\partial^2 f_1}{\partial y_1 \partial y_4} &= \frac{\partial^2 f_1}{\partial y_4 \partial y_1} = -\beta_2(T_m,R_m),\ \frac{\partial^2 f_2}{\partial y_1 \partial y_2} = \frac{\partial^2 f_2}{\partial y_2 \partial y_1} = \beta_2(T_m,R_m),\\
\frac{\partial^2 f_3}{\partial y_2 \partial y_3} &= \frac{\partial^2 f_3}{\partial y_3 \partial y_2} = -\beta_3^*(T_m,R_m),\ \frac{\partial^2 f_3}{\partial y_3 \partial y_5} = \frac{\partial^2 f_3}{\partial y_5 \partial y_3} = -\beta_1(T_m,R_m),\\
\frac{\partial^2 f_4}{\partial y_2 \partial y_3} &= \frac{\partial^2 f_4}{\partial y_3 \partial y_2} = \beta_3^*(T_m,R_m),\ \frac{\partial^2 f_4}{\partial y_3 \partial y_5} = \frac{\partial^2 f_4}{\partial y_5 \partial y_3} = \beta_1(T_m,R_m),\\
\frac{\partial^2 f_3}{\partial y_2 \partial \beta_3^*(T_m,R_m)} &= \frac{\partial^2 f_3}{\partial \beta_3^*(T_m,R_m)\partial y_2} = -y_3^*,\ \frac{\partial^2 f_4}{\partial y_2 \partial \beta_3^*(T_m,R_m)} = \frac{\partial^2 f_4}{\partial \beta_3^*(T_m,R_m)\partial y_2} = y_3^*.
\end{aligned} \tag{7.44}$$

The others derivatives of $f_i,\ i = 1,...,5$ are zero. From Eq. (7.43) it follows that

$$\begin{aligned}
c = \frac{2}{r_1(\gamma+\eta)m(T_m,R_m)}&\left(\frac{r_1+\gamma+\eta-\theta}{\theta-r_1} + \beta_2(T_m,R_m)K\lambda(T_m,R_m)(r_1-\theta)\beta_1(T_m,R_m)\eta\right)w_4v_4^2\\
+\frac{2\eta K m(T_m,R_m)\beta_1(T_m,R_m)\beta_2(T_m,R_m)(\theta-r_1) - 2r_1(\gamma+\eta)\delta^2 m(T_m,R_m)}{\gamma+\eta)m(T_m,R_m)}&w_4v_4^2
\end{aligned} \tag{7.45}$$

and

$$d = \frac{\lambda(T_m,R_m)K(r_1-\theta)\beta_2(T_m,R_m)}{\delta r_1(\gamma+\eta)}w_4v_4 > 0. \tag{7.46}$$

Note that d is always positive at (T_m,R_m). If c is positive at (T_m,R_m), then the model (7.1) exhibits backward bifurcation at $R_{02} = 1$ (See Figure 7.2). □

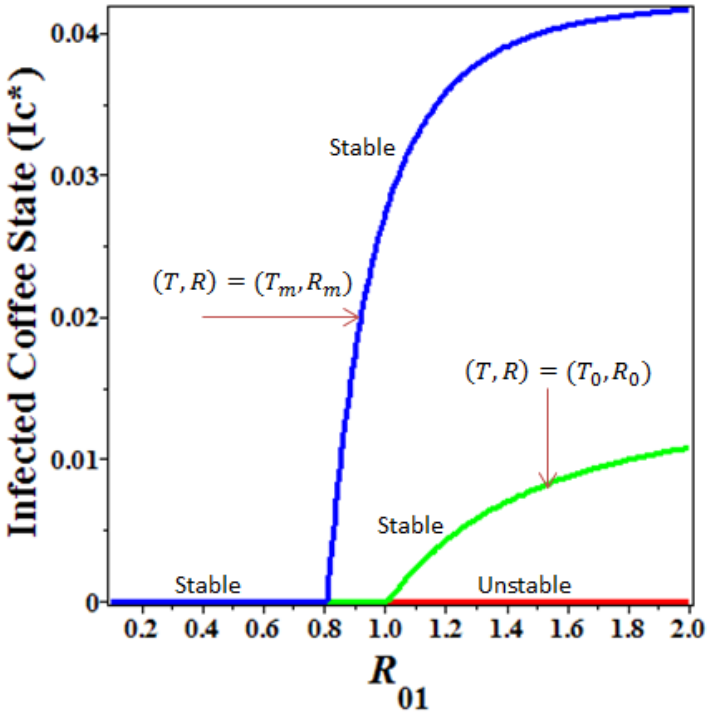

Figure 7.2: Forward and backward bifurcation diagram at $(T,R) = (T_0,R_0)$ and $(T,R) = (T_m,R_m)$, respectively.

7.2.11 Sensitivity of Basic Reproduction Numbers: R_{01} and R_{02}

In this section, we study the sensitivity analysis of the basic reproduction numbers for various model parameters. This helps us to check and identify parameters which highly affect the R_{01} and R_{02}. For example, sensitivity index of R_{01} with respect to K is given by

$$\Delta_K^{R_{01}} = \frac{\partial R_{01}}{\partial K} \times \frac{K}{R_{01}} = 0.5.$$

Like way the others sensitivity index of R_{01} are computed and their sensitivity indeces: $\Delta_{\beta_{01}}^{R_{01}}$, $\Delta_{\beta_{02}}^{R_{01}}$, $\Delta_{\beta_{03}}^{R_{01}}$, $\Delta_{\eta}^{R_{01}}$, $\Delta_{r_1}^{R_{01}}$, $\Delta_{\theta}^{R_{01}}$, $\Delta_{\lambda_0}^{R_{01}}$, $\Delta_{\delta}^{R_{01}}$, $\Delta_{\gamma}^{R_{01}}$ and $\Delta_{m_0}^{R_{01}}$ are given in Table 7.2.

Table 7.2: Sensitivity indices of R_{01} at (T_0, R_0)

Parameter	**Sensitivity indices of R_{01}**
K	+0.5
β_{01}	+0.0238095
β_{02}	+0.5
β_{03}	+0.47619
η	-0.297619
r_1	+0.0454545
θ	-0.0454545
λ_0	+0.5
δ	-1
γ	-0.178571
m_0	-0.0238095

Also, the sensitivity index of R_{02} computed and their sensitivity indeces are given in the Table 7.3.

Table 7.3: Sensitivity indices of R_{02} at (T_m, R_m)

Parameter	**Sensitivity indices of R_{02}**	**Parameter**	**Sensitivity indices of R_{02}**
K	+0.5	λ_0	+0.409531
β_{01}	+0.0222266	λ_m	+0.0904691
β_{m1}	+0.0109112	r_1	+0.0454545
β_{02}	+0.00628571	θ	-0.0454545
β_{m2}	+0.493714	δ	-1
β_{03}	+0.445016	γ	-0.178571
β_{m3}	+0.0218462	m_0	-0.0331017
η	-0.288291	m_m	-0.0000361109

7.2.12 Interpretation of the Sensitivity Indices

The sensitivity indices of the basic reproduction number, R_{01}, with respect to the main parameters were given in Table 7.1. The parameters K, β_{01}, β_{02}, β_{03}, r_1 and λ_0 have positive sensitivity indices show that the more impact on expanding the disease in the population if their values are increasing since R_{01} increases. Also, the parameters θ, η, δ, γ and m_0 have negative sensitivity indices show that less impact on expanding the disease in the population as their values increase. And also as their values increase, R_{01} decreases, which leads to minimizing the endemicity of the disease in the population. The bar diagram of the sensitivity indices of R_{01} in Table 7.2 is depicted in Figure 7.3 (a).

In a similar way, the sensitivity indices of the basic reproduction number, R_{02}, with respect to the main parameters were given in Table 7.3. Those parameters that have positive sensitivity indices show that they have more impact on expanding the disease in the population if their

values are increasing since R_{02} increases. Also, those parameters in which their indices are negative have less impact on expanding the disease in the population as their values increase. The bar diagram of the sensitivity indices of R_{02} in Table 7.3 is depicted in Figure 7.3 (b).

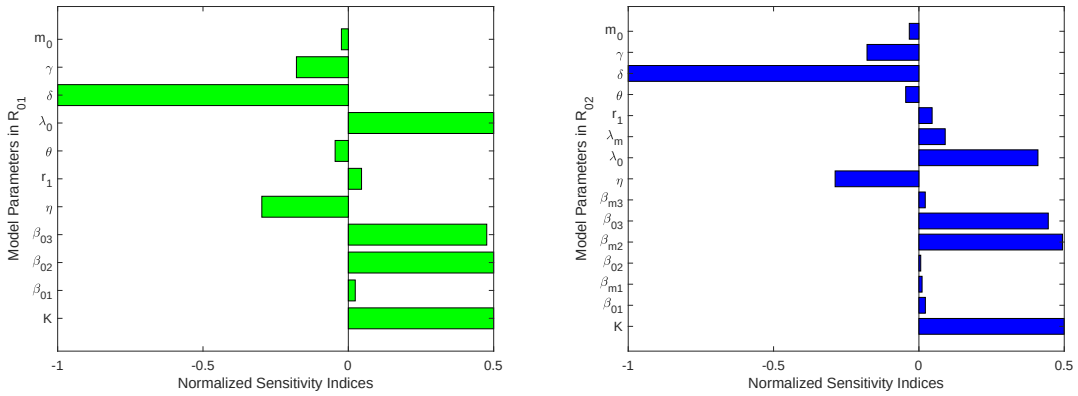

(a) (b)

Figure 7.3: Normalized sensitivity indices of R_{01} and R_{02} with respect to parameters of the model (7.1), respectively. Parameter values are taken from Table 7.1.

7.3 Numerical Results

In order to illustrate the analytical results of the study, we performed numerical simulations of the model (7.1). In addition to the parameter values in Table 7.1 we assumed the initial condition: $S_c(0) = 100$, $I_c(0) = 50$, $S_v(0) = 50$, $I_v(0) = 10$, $B(0) = 2$, $T(0) = 20.1$, $R(0) = 10.1$.

The susceptible coffee berries in Figure 7.4 (a) increase at (T_0, R_0) since they are not affected by CBD due low breeding of vectors that transmit the disease. Therefore, we expect at $(T,R) = (T_0, R_0)$, $R_{01} < 1$, the model reveals that the infected coffee berries will decrease. Both susceptible and infected vector populations in the Figure 7.4 (c) decrease since (T_0, R_0) is an unfavorable temperature and rainfall for vector breeding and CBD transmission. The CBD pathogen population in the environment increases as depicted in Figure 7.4 (b) to a certain maximum point and then proceeds to decrease to zero at (T_0, R_0). This shows the fact that fungi in the environment less affect the coffee berries at (T_0, R_0).

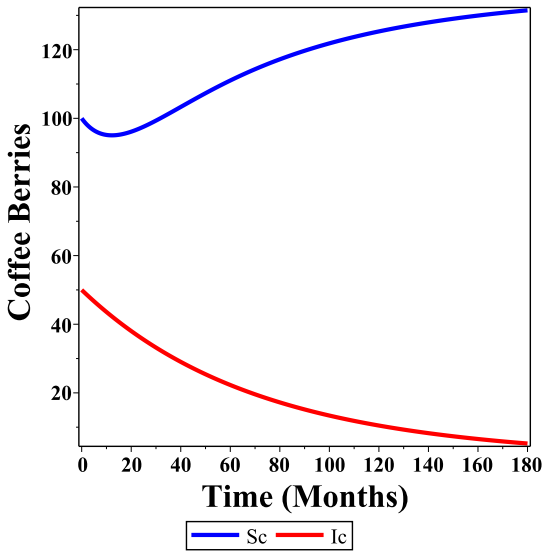

(a)

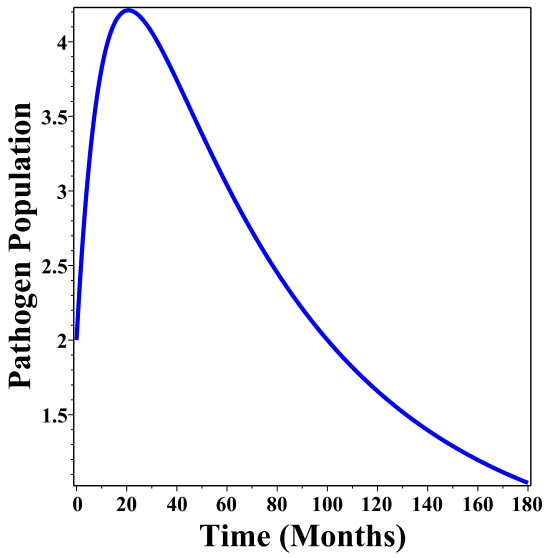

(b)

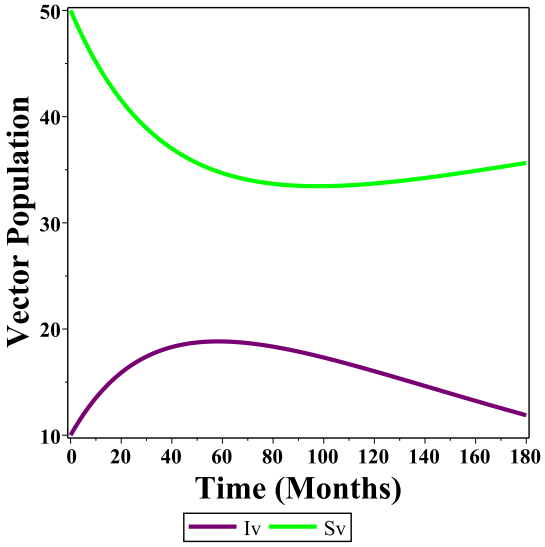

(c)

Figure 7.4: Simulation results of coffee berry, vector and pathogen population at $(T,R) = (T_0,R_0)$ when $R_{01} = 0.319142$.

Figure 7.5 (a) illustrates that the susceptible coffee berries decrease while the infected coffee berries increase by $R_{02} > 1$. This is due to the fact that maximum temperature and rainfall (T_m,R_m) are favorable for the reproduction of vectors. The susceptible vector population decreases while the infected vector population increases, as shown in Figure 7.5 (c). The reason is that at (T_m,R_m) vectors breed more and the transmission of CBD rises, resulting in more infection in coffee berries. The concentration of pathogens in the environment increases and then declines, as shown in Figure 7.5 (b) at (T_m,R_m).

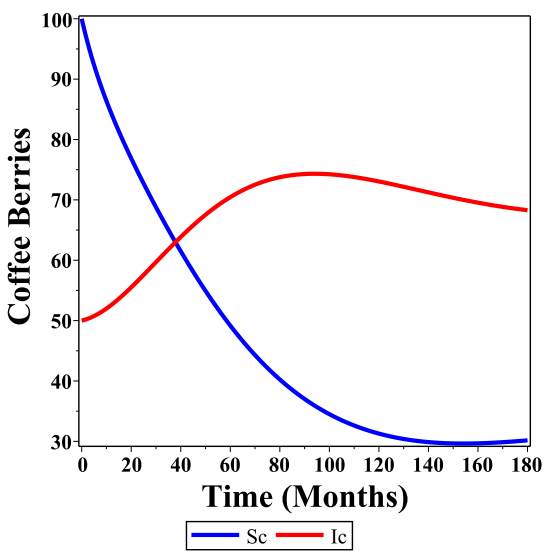

(a)

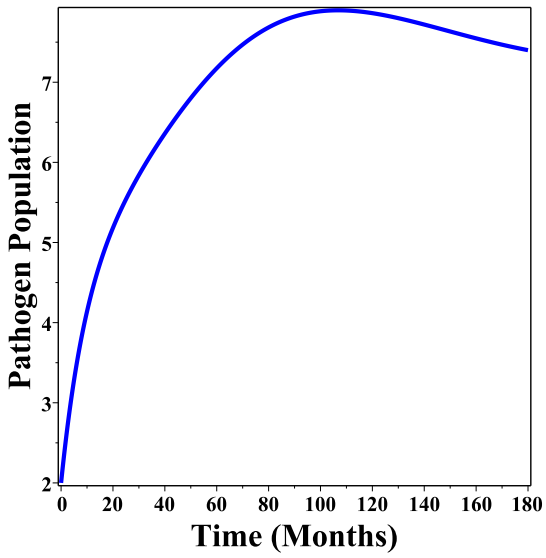

(b)

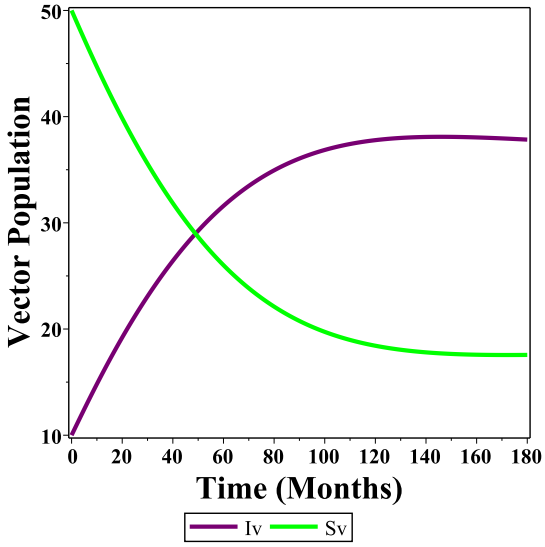

(c)

Figure 7.5: Simulation results of coffee berry, vector and pathogen population at $(T,R) = (T_m,R_m)$ when $R_{02} = 3.25339$.

In Figure 7.6 (a) as the intensity of rainfall increases due to temperature variation, the susceptible coffee berries decrease. However, in Figures 7.6 (b) and 7.6 (c) as the magnitude of rainfall rises, the infected coffee berry and pathogen population increase.

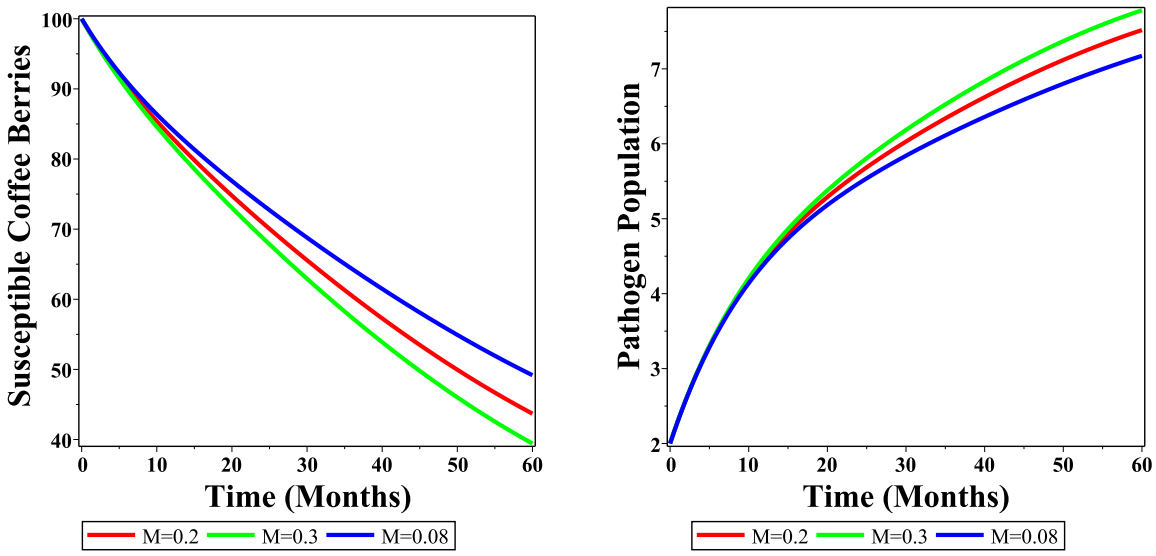

(a)

(b)

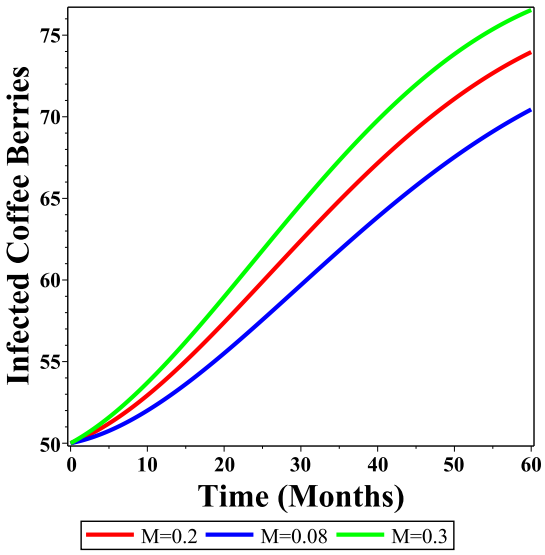

(c)

Figure 7.6: Simulation results of (a) susceptible coffee, (b) pathogen, (c) infected coffee at different growth precipitation rates: $M = 0.3,\ 0.2,\ 0.08$ with temperature $T = T_0/2$ and $T = T_m/2$.

In Figures 7.7 (a) and 7.7 (c) as seasonal temperature and rainfall vary, the susceptible coffee and vector populations decrease while the infected coffee and vector populations increase, respectively. However, in Figure 7.7 (b) under seasonal temperature and rainfall variation, more pathogen concentration results in more infection in the coffee farm.

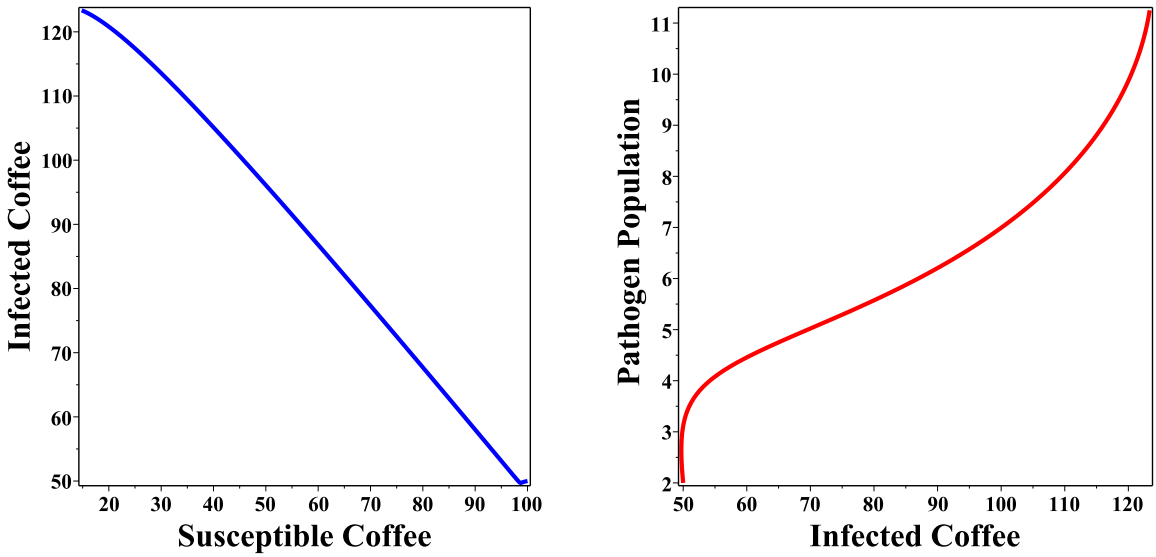

(a)

(b)

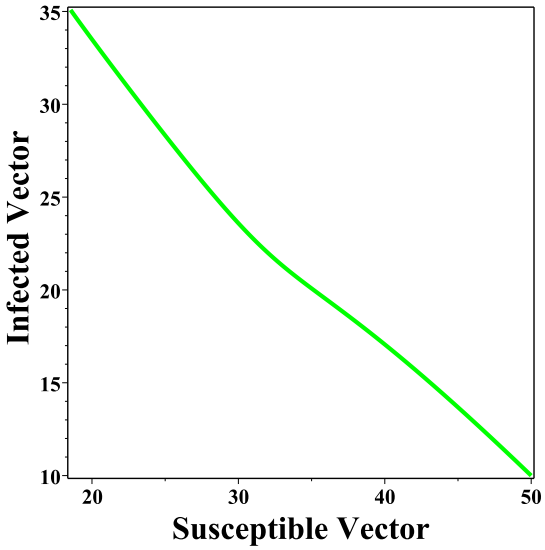

(c)

Figure 7.7: Phase portrait of (S_c, I_c), (I_c, B) and (S_v, I_v)-plane under seasonal temperature and rainfall change when $0.319142 \leq \Re_0 \leq 3.25339$.

Figure 7.8 depicts that the more vectors and pathogens are produced at the favorable temperature and rainfall from (T_0, R_0) to (T_m, R_m), which indirectly increases the rate of infected vectors and then infected coffee plants.

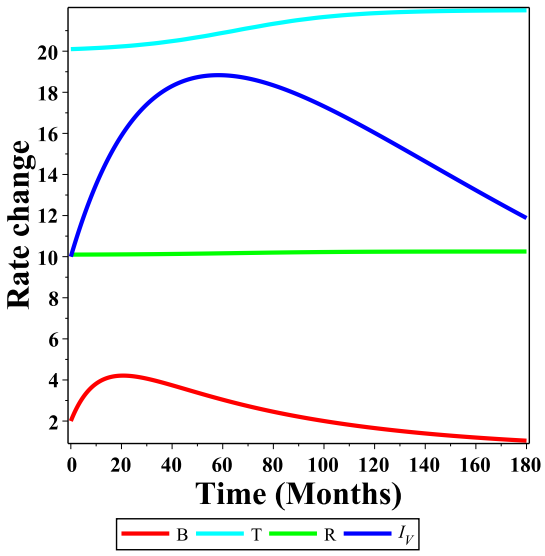

(a) $(T,R) = (T_0,R_0)$

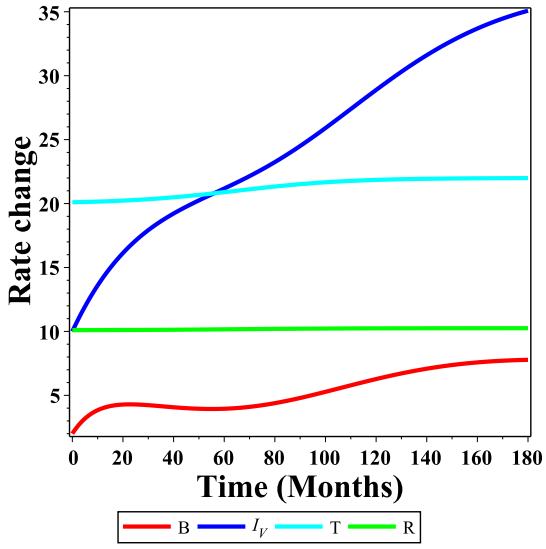

(b) $(T_0,R_0) \leq (T,R) \leq (T_m,R_m)$

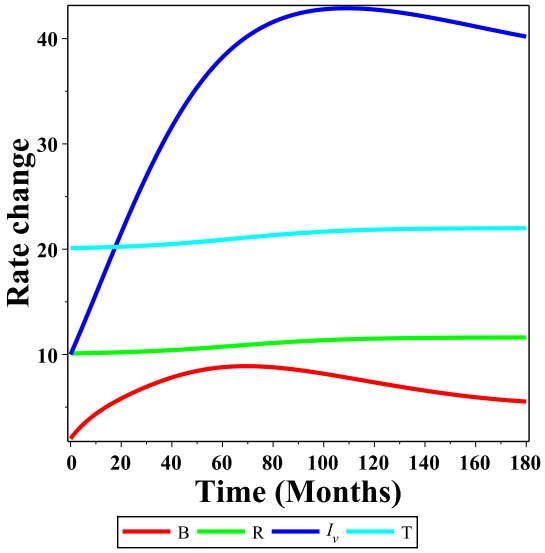

(c) $(T,R) = (T_m,R_m)$

Figure 7.8: The behavior of $I_v(t)$ and $B(t)$ corresponding to temperature and rainfall variation.

The global temperature and rainfall variation that we demonstrated graphically in Figures 7.9 (a) and 7.9 (b) grow logistically to a certain maximum point and then becomes constant. This property shows that more vectors and pathogens are produced at the favorable temperature of T_m and rainfall of R_m which indirectly increases the rate of infected vectors and finally infected coffee berries. The seasonal temperature and rainfall variation in the environment in Figures 7.10 (a) and 7.10 (b) grow up and down with gradual oscillation.

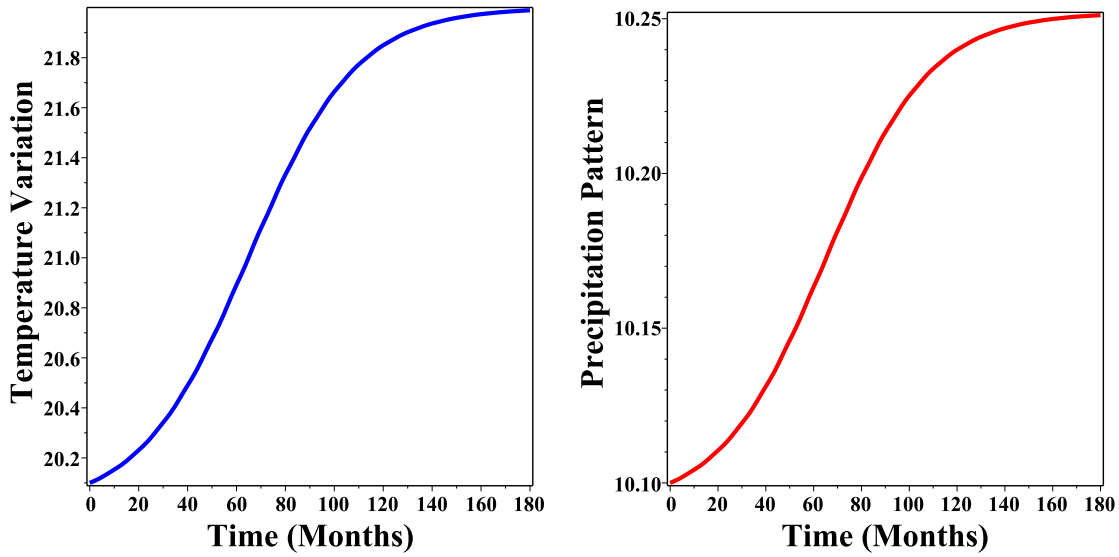

(a) (b)

Figure 7.9: Simulation results of temperature rainfall scenario for global variation.

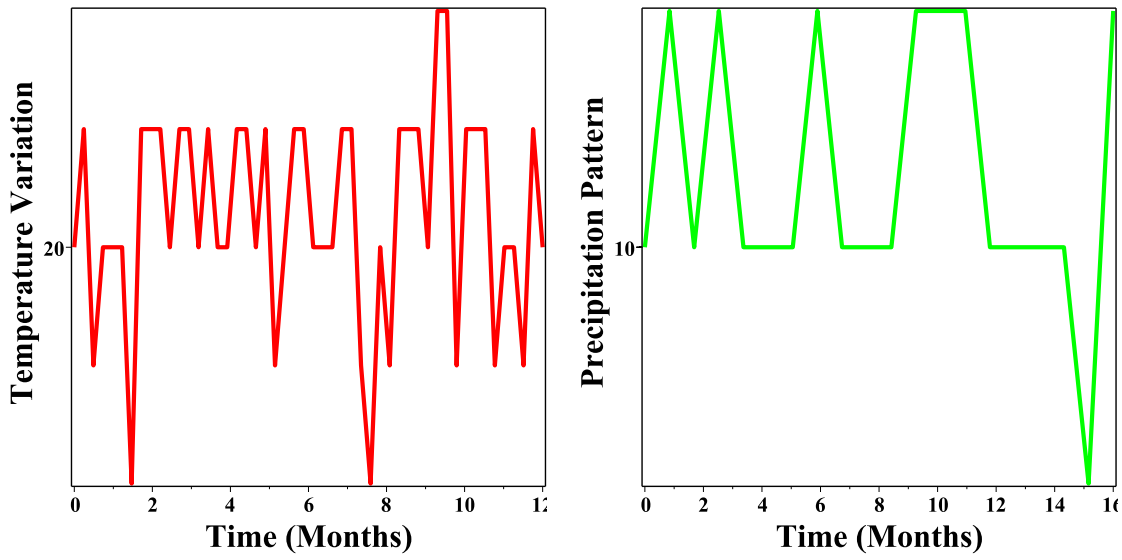

(a) (b)

Figure 7.10: Simulation results of temperature and rainfall scenario for seasonal variation

As temperature rate increasing, the rainfall changes is also increasing (Figure 7.11). That is, the growth rate of precipitation is the temperature-dependent.

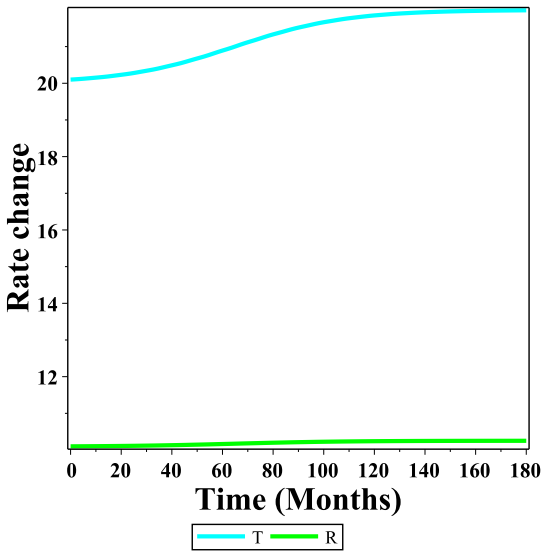

Figure 7.11: The plot of relationship between temperature and rainfall variation when $(T_0, R_0) \leq (T, R) \leq (T_m, R_m)$.

7.4 Extension of Proposed Model into Optimal Control

In this section, we extended the proposed model (7.1) into an optimal control problem, expecting that the analysis of the model might benefit coffee growers in the control of CBD with minimum costs. Hence, coffee berries in a coffee farm are fully protected by using three control interventions $u_i,\ i = 1,2,3$. Control variable u_1 affects the infection rate due to genetic resistance of the plant, the control variable u_2 represents chemical control of the vector, while the control variable u_3 represents cultural practices.

Susceptible coffee berry moves to the infected class following contacts with infected vector at rate $(1-u_1)\beta_2(T,R)$, where $\beta_2(T,R)$ is secondary transmission rate. The natural death rate of both susceptible and infected vectors is represented by δ and thus removed at rate $(1+u_2)\delta$. Besides, we assumed that the pathogen is removed at rate $(1+u_3)m(T,R)$, where $m(T,R)$ decay rate of pathogen. All these assumptions are based on (Hall et al., 2004; Cook et al., 1983).

Based on the above assumptions and discription, the corresponding state system of model

(7.1) is given by

$$\begin{aligned}
\frac{dS_c}{dt} &= r_1 S_c\left(1-\frac{S_c+I_c}{K}\right)-(1-u_1)\beta_2(T,R)S_cI_v-\theta S_c,\\
\frac{dI_c}{dt} &= (1-u_1)\beta_2(T,R)S_cI_v-(\gamma+\eta)I_c,\\
\frac{dS_v}{dt} &= \lambda(T,R)-(\beta_1(T,R)P+\beta_3(T,R)I_c)S_v-(1+u_2)\delta S_v,\\
\frac{dI_v}{dt} &= (\beta_1(T,R)P+\beta_3(T,R)I_c)S_v-(1+u_2)\delta I_v,\\
\frac{dB}{dt} &= \eta I_c-(1+u_3)m(T,R)B,\\
\frac{dT}{dt} &= r_2(T-T_0)\left(1-\frac{T}{T_m}\right),\\
\frac{dR}{dt} &= Mr_2(T-T_0)\left(1-\frac{T}{T_m}\right),
\end{aligned} \tag{7.47}$$

with initial data:

$$S_c(0)=S_{c0},\ I_c(0)=I_{c0},\ S_v(0)=S_{v0},\ I_v(0)=I_{v0},\ B(0)=B_0,\ T(0)=T_0, R(0)=R_0 \tag{7.48}$$

Here, we need to find the optimal u_i^* of the controls $u_i,\ i=1,2,3$, the associated state trajectories: $S_c^*, I_c^*, S_v^*, I_v^*, B^*, T^*$ and R^* which are solutions of the state system (7.47) in the time interval $[0,t_f]$ with initial condition (7.48) and minimize the cost functional (7.49).

Our main objective is to minimize the spread of infection and cost incurred during intervention. With this in mind, we define the cost functional for the minimization problem as:

$$J=\min_u \int_0^{t_f}\left(\bar{a}_1 I_c+\bar{a}_2 I_v+\bar{a}_3 B+\frac{1}{2}\sum_{i=1}^{3}\bar{b}_i u_i^2\right)dt, \tag{7.49}$$

where t_f is the final time, $\bar{a}_1 I_c$, $\bar{a}_2 I_v$ and $\bar{a}_3 B$ are the cost associated with infected coffee plant, infected vector and pathogen while $\bar{b}_1$, $\bar{b}_2$ and $\bar{b}_3$ are relative cost weight for each individual control measure.

The current cost at time t can be obtained using the integrand $\bar{a}_1 I_c+\bar{a}_2 I_v+\bar{a}_3 B+1/2\sum_{i=1}^{3}\bar{b}_i u_i^2$. As cost functional (7.49) shows, we aimed to minimize the number of infected coffee, infected vector, pathogen and costs. That is we need to get an optimal triple (u_1^*,u_2^*,u_3^*) such that

$$J(u^*)=\min(J(u_1,u_2,u_3):u_i\in U),$$

where $U=\left\{(u_1,u_2,u_3):\ 0\le u_i\le (u_i)_{max}<1 \text{ for } 0\le t\le t_f\right\}$ is measurable set.

7.4.1 Existence of the Optimal Controls

Here, the existence of the optimal controls can be indicated and proved by using a method of (Coddington and Levinson, 1955; Fleming and Lions, 2012). The boundedness of solutions to state system (7.47) in finite time interval $[0,t_f]$ is very important to determine the existence and uniqueness of optimal control to our model (7.47). Based on Eqs. (7.4), (7.6) and (7.8), we can find from the state system (7.1): $N_1 \leq (1+r)\hat{K}/h$, $N_2 \leq \lambda(\hat{T},\hat{R})/(1+u_2)\delta$ and $B \leq (\hat{K}(1+r)\eta)/(1+u_3)m(\hat{T},\hat{R})h$, where N_1, N_2 and B, respectively, denotes the total population of coffee berry, vector and pathogen. This implies that the upper bound for the total coffee berry population N_1, vector population N_2 and pathogen population B.

7.4.2 Characterization of the Optimal Controls

In this subsection, we briefly present the characterization of optimal control. Assume that $u_i^*(t) \in U$ is an optimal solution for problems (7.47)-(7.49) with fixed t_f. Then there exists adjoint vector $\lambda : [0,t_f] \to \mathbb{R}^7, \lambda = (\lambda_1(t),\lambda_2(t),\lambda_3(t),\lambda_4(t),\lambda_5(t),\lambda_6(t),\lambda_7(t))$ that satisfy the following conditions.

(1) The Hamiltonian function associated to our problem is given by

$$
\begin{aligned}
H &= \bar{a}_1 I_c + \bar{a}_2 I_v + \bar{a}_3 B + \frac{1}{2}\bar{b}_1 u_1^2 + \frac{1}{2}\bar{b}_2 u_2^2 + \frac{1}{2}\bar{b}_3 u_3^2 \\
&+ \lambda_1 \left(r_1 S_c \left(1 - \frac{S_c + I_c}{K}\right) - (1-u_1)\left(\beta_{02} + \beta_{m2}(1+M)\left(\frac{T-T_0}{T_m}\right)\right) S_c I_v - \theta S_c \right) \\
&+ \lambda_2 \left((1-u_1)\left(\beta_{02} + \beta_{m2}(1+M)\left(\frac{T-T_0}{T_m}\right)\right) S_c I_v - (\gamma+\eta) I_c \right) \\
&+ \lambda_3 \left(\lambda_0 + \lambda_m (1+M)\left(\frac{T-T_0}{T_m}\right) - \left(\beta_{01} + \beta_{m1}(1+M)\left(\frac{T-T_0}{T_m}\right)\right) B S_v \right) \\
&- \lambda_3 \left(\left(\beta_{03} + \beta_{m3}(1+M)\left(\frac{T-T_0}{T_m}\right)\right) I_c S_v + (1+u_2)\delta S_v \right) \\
&+ \lambda_4 \left(\left(\beta_{01} + \beta_{m1}(1+M)\left(\frac{T-T_0}{T_m}\right)\right) B S_v + \left(\beta_{03} + \beta_{m3}(1+M)\left(\frac{T-T_0}{T_m}\right)\right) I_c S_v \right) \\
&- \lambda_4 (1+u_2)\delta I_v + \lambda_5 \left(\eta I_c - (1+u_3) m_0 B\right) - \lambda_5 (1+u_3) m_m (1+M)\left(\frac{T-T_0}{T_m}\right) B \\
&+ \lambda_6 r_2 (T-T_0)\left(\frac{T_m - T}{T_m}\right) + \lambda_7 r_2 (R-R_0)\left(\frac{M(T_m - T_0) + R_0 - R}{M T_m}\right),
\end{aligned}
\tag{7.50}
$$

where $H = H(S_c, I_c, S_v, I_v, B, T, R, u_1, u_2, u_3, \lambda)$.

(2) The control system:

$$\frac{dS_c}{dt} = \frac{\partial H}{\partial \lambda_1}, \ \frac{dI_c}{dt} = \frac{\partial H}{\partial \lambda_2}, \ \frac{dS_v}{dt} = \frac{\partial H}{\partial \lambda_3}, \ \frac{dI_v}{dt} = \frac{\partial H}{\partial \lambda_4}, \ \frac{dB}{dt} = \frac{\partial H}{\partial \lambda_5}, \ \frac{dT}{dt} = \frac{\partial H}{\partial \lambda_6}, \ \frac{dR}{dt} = \frac{\partial H}{\partial \lambda_7}. \tag{7.51}$$

(3) The adjoint system:

$$\frac{d\lambda_1}{dt} = -\frac{\partial H}{\partial S_c}, \ \frac{d\lambda_2}{dt} = -\frac{\partial H}{\partial I_c}, \ \frac{d\lambda_3}{dt} = -\frac{\partial H}{\partial S_v}, \ \frac{d\lambda_4}{dt} = -\frac{\partial H}{\partial I_v}, \ \frac{d\lambda_5}{dt} = -\frac{\partial H}{\partial B}, \ \frac{d\lambda_6}{dt} = -\frac{\partial H}{\partial T}, \ \frac{d\lambda_7}{dt} = -\frac{\partial H}{\partial R}. \tag{7.52}$$

(4) The optimality condition:

$$\frac{\partial H}{\partial u_i} = 0, \ \ i = 1,2,3. \tag{7.53}$$

(5) Furthermore, the transversality condition:

$$\lambda_i(t_f) = 0, \ i = 1,...,7. \tag{7.54}$$

Theorem 7.4.1. *Let u_i^* be the optimal controls and $(S_c^*, I_v^*, S_v^*, I_v^*, B^*, T^*, R^*)$ be the associated unique solutions of the optimal control problem (7.47)-(7.49) with fixed final time t_f over U. Then there exists adjoint variables λ_i, $i = 1,...,7$ at (T_0, R_0) and (T_m, R_m) which*

satisfies the following adjoint system:

$$
\begin{aligned}
\frac{d\lambda_1}{dt} &= -\lambda_1\left(r_1 - \frac{2r_1S_c}{K} - \frac{r_1I_c}{K} - \theta\right) + (\lambda_1-\lambda_2)(1-u_1)\left(\beta_{02} + \beta_{m2}(1+M)\left(\frac{T-T_0}{T_m}\right)\right)I_v,\\
\frac{d\lambda_2}{dt} &= -\bar{a}_1 + \lambda_1\frac{r_1S_c}{K} + \lambda_2(\gamma+\eta) + (\lambda_3-\lambda_4)\left(\beta_{03} + \beta_{m3}(1+M)\left(\frac{T-T_0}{T_m}\right)\right)S_v - \lambda_5\eta,\\
\frac{d\lambda_3}{dt} &= \lambda_3(1+u_2)\delta + (\lambda_3-\lambda_4)\left(\left(\beta_{01} + \beta_{m1}(1+M)\left(\frac{T-T_0}{T_m}\right)\right)B\right)\\
&\quad + (\lambda_3-\lambda_4)\left(\beta_{03} + \beta_{m3}(1+M)\left(\frac{T-T_0}{T_m}\right)\right)I_c,\\
\frac{d\lambda_4}{dt} &= -\bar{a}_2 + (\lambda_1-\lambda_2)(1-u_1)\left(\beta_{02} + \beta_{m2}(1+M)\left(\frac{T-T_0}{T_m}\right)\right)S_c + \lambda_4(1+u_2)\delta,\\
\frac{d\lambda_5}{dt} &= -\bar{a}_3 + (\lambda_3-\lambda_4)\left(\beta_{01} + \beta_{m1}(1+M)\left(\frac{T-T_0}{T_m}\right)\right)S_v + \lambda_5(1+u_3)m_0\\
&\quad + \lambda_5(1+u_3)m_m(1+M)\left(\frac{T-T_0}{T_m}\right),\\
\frac{d\lambda_6}{dt} &= (\lambda_1-\lambda_2)(1-u_1)\frac{\beta_{m2}(1+M)S_cI_v}{T_m} - \frac{\lambda_3\lambda_m(1+M)}{T_m} + (\lambda_3-\lambda_4)\frac{(\beta_{m1}B+\beta_{m3}I_c)(1+M)S_v}{T_m}\\
&\quad - \frac{\lambda_5(\pi_m - (1+u_3)m_mP)(1+M)}{T_m} - \frac{\lambda_6r_2(T_m+T_0-2T)}{T_m},\\
\frac{d\lambda_7}{dt} &= -\lambda_7r_2\left(\frac{M(T_m-T_0)+2R_0-2R}{MT_m}\right).
\end{aligned}
\tag{7.55}
$$

Together with transversality condition: $\lambda_i(t_f) = 0,\ i = 1,...,7.$
And also, we get optimal controls $u_1^*(t),\ u_2^*(t)$ *and* $u_3^*(t)$ *which are characterized by*

$$
\begin{aligned}
u_1^*(t) &= min\left\{max\left\{0, \frac{S_cI_v(-\lambda_1+\lambda_2)}{\bar{b}_1}\left(\beta_{02} + \frac{\beta_{m2}(1+M)(T-T_0)}{T_m}\right)\right\}, 0.95\right\},\\
u_2^*(t) &= min\left\{max\left\{0, \frac{\delta(\lambda_3S_v+\lambda_4I_v)}{\bar{b}_2}\right\}, 0.95\right\},\\
u_3^*(t) &= min\left\{max\left\{0, \frac{\lambda_5B}{\bar{b}_3}\left(m_0 + \frac{m_m(1+M)(T-T_0)}{T_m}\right)\right\}, 0.95\right\}.
\end{aligned}
\tag{7.56}
$$

Proof. The adjoint variables are computed by differentiating the Hamiltonian (7.50) with respect to the corresponding state variables: $S_c,\ I_c,\ S_v,\ I_v,\ B,\ T,\ R$ as Eq. (7.52). We assume that the final state $S_c(t_f),\ I_c(t_f),\ S_v(t_f),\ I_v(t_f),\ B(t_f),\ T(t_f)$ and $R(t_f)$ are free, then we obtain the transversality condition: $\lambda_i(t_f) = 0,\ i = 1,...,7.$

The optimal controls: $u_1^*(t),\ u_2^*(t)$ and $u_3^*(t)$ are computed from optimality condition (7.53) as follows.

(i) $\dfrac{\partial H}{\partial u_1} = \bar{b}_1u_1 + S_cI_v(\lambda_1-\lambda_2)\left(\beta_{02} + \dfrac{\beta_{m2}(1+M)(T-T_0)}{T_m}\right) = 0$, at $u_1(t) = u_1^*(t)$

$$u_1^*(t) = \frac{S_c I_v(-\lambda_1+\lambda_2)}{\bar{b}_1}\left(\beta_{02} + \frac{\beta_{m2}(1+M)(T-T_0)}{T_m}\right).$$

(ii) $\dfrac{\partial H}{\partial u_2} = \bar{b}_2 u_2 - \delta(\lambda_3 S_v + \lambda_4 I_v) = 0$, at $u_2(t) = u_2^*(t)$

$$u_2^*(t) = \frac{\delta(\lambda_3 S_v + \lambda_4 I_v)}{\bar{b}_2}.$$

(iii) $\dfrac{\partial H}{\partial u_3} = \bar{b}_3 u_3 - \lambda_5 B\left(m_0 + \dfrac{m_m(1+M)(T-T_0)}{T_m}\right) = 0$, at $u_3(t) = u_3^*(t)$

$$u_3^*(t) = \frac{\lambda_5 B}{\bar{b}_3}\left(m_0 + \frac{m_m(1+M)(T-T_0)}{T_m}\right).$$

From the boundedness on $u_1^*(t)$, $u_2^*(t)$, $u_3^*(t)$ and minimality condition (7.53), we have:

$$u_1^*(t) = \begin{cases} 0, & if \quad \dfrac{\partial H}{\partial u_1} > 0, \\ \dfrac{S_c I_v(\lambda_2-\lambda_1)\beta_2(T,R)}{\bar{b}_1}, & if \quad \dfrac{\partial H}{\partial u_1} = 0, \\ (u_1)_{max}, & if \quad \dfrac{\partial H}{\partial u_1} < 0. \end{cases}$$

$$u_2^*(t) = \begin{cases} 0, & if \quad \dfrac{\partial H}{\partial u_2} > 0, \\ \dfrac{\delta(\lambda_3 S_v + \lambda_4 I_v)}{\bar{b}_2}, & if \quad \dfrac{\partial H}{\partial u_2} = 0, \\ (u_2)_{max}, & if \quad \dfrac{\partial H}{\partial u_2} < 0. \end{cases}$$

$$u_3^*(t) = \begin{cases} 0, & if \quad \dfrac{\partial H}{\partial u_3} > 0, \\ \dfrac{\lambda_5 B m(T,R)}{\bar{b}_3}, & if \quad \dfrac{\partial H}{\partial u_3} = 0, \\ (u_3)_{max}, & if \quad \dfrac{\partial H}{\partial u_3} < 0. \end{cases}$$

Since $0 \le u_i^*(t) \le (u_i)_{max} < 1,\ i = 1,2,3$, we can rewrite the optimal controls: $u_1^*(t)$, $u_2^*(t)$, $u_3^*(t)$ as Eq. (7.56).

Moreover, we check whether the optimal controls $u_i = u_i^*$ is a minimum by the condition $\partial^2 H/\partial u_i^2 > 0$. The second derivative of the Hamiltonian (7.50) with respect to control u_i at $u_i = u_i^*$ is given by

$$\left.\frac{\partial^2 H}{\partial u_i^2}\right|_{u_i = u_i^*} = \begin{bmatrix} \bar{b}_1 & 0 & 0 \\ 0 & \bar{b}_2 & 0 \\ 0 & 0 & \bar{b}_3 \end{bmatrix}.$$

Since this Hessian matrix is positive definite, the optimal control $(u_1^*,\ u_2^*, u_3^*)$ is a minimizer. □

7.5 Numerical Simulations

In this section, the numerical simulations of the impacts of optimal control strategies on susceptible coffee berries, infected coffee berries, infected vectorss and pathogen populations are illustrated and discussed.

For the numerical simulations, the parameter values are obtained from Table 7.1, except β_{02} =0.0002, β_{m1} =10^{-5}, β_{m2} =0.001, β_{m3} =10^{-8}, θ =0.12, r_2 =0.007, K =200, λ_0 =0.8, δ =0.008, λ_m=10^{-6}, m_m=10^{-7} which are assumed. In addition to these parameter values we assumed the initial condition: $S_c(0) = 100$, $I_c(0) = 15$, $S_v(0) = 10$, $I_v(0) = 2$, $B(0) = 10$, $T(0) = 20.1$, $R(0) = 10.1$.

In the next subsections 7.5.1, 7.5.2 and 7.5.3, we implement the simulations of the three strategies with a single control at temperature and rainfall variability.

7.5.1 Strategy I: Genetic Control

In the first case, we consider genetic control $u_1 \neq 0$ without using chemical control $u_2 = 0$ and cultural control $u_3 = 0$ in the system. Figure 7.12 depicts that the number of infected coffee, infected vector and pathogen decrease due to the implementation of strategy with genetic control alone.

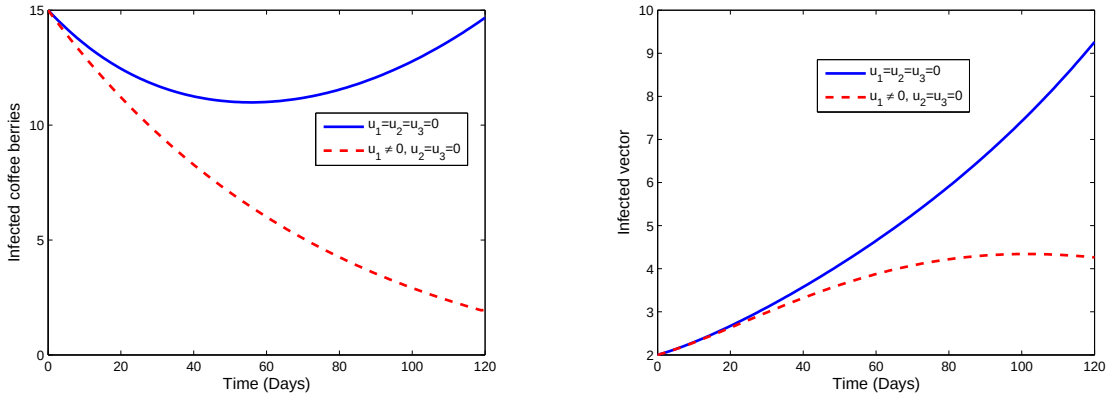

(a) (b)

Figure 7.12: Simulation results when genetic is implemented as control to minimize the impact of infected coffee and infected vector population.

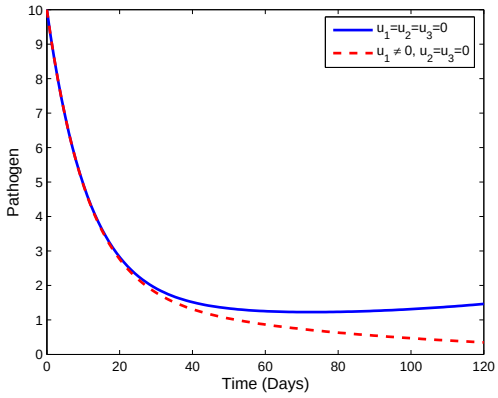

Figure 7.13: Simulation results when genetic is implemented as control to minimize the impact of pathogen population.

7.5.2 Strategy II: Chemical Control

Under this strategy, we apply chemical control $u_2 \neq 0$ without using genetic control $u_1 = 0$ and cultural control $u_3 = 0$ in the system. Figures 7.14 and 7.15 show that due to the implementation of strategy with chemical control alone there was a significant decrease in the number of infected coffee, infected vector and pathogen.

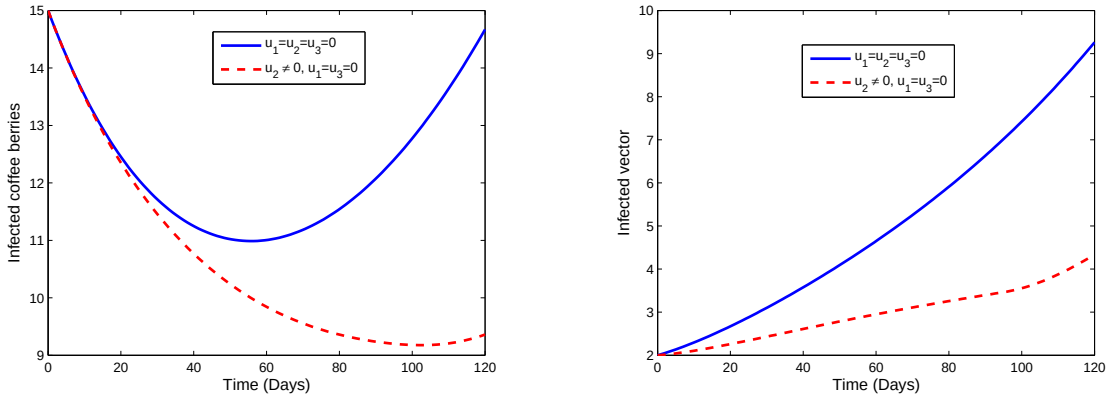

(a) (b)

Figure 7.14: Simulation results when chemical is implemented as control to minimize the impact of infected coffee and infected vector population.

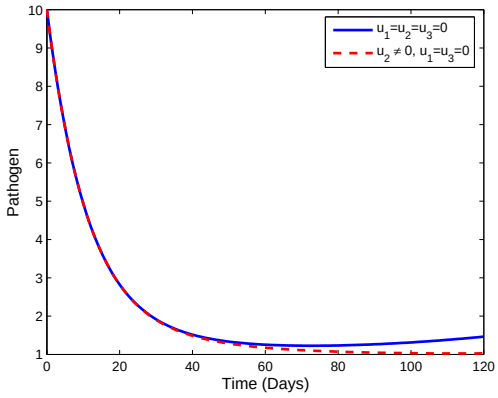

Figure 7.15: Simulation results when chemical is implemented as control to minimize the impact of pathogen population.

7.5.3 Strategy III: Cultural Control

In this case, we consider cultural control $u_3 \neq 0$ without using genetic control $u_1 = 0$ and chemical control $u_2 = 0$ in the system. As one can easily observe from Figures 7.16 and 7.17, the implementation of strategy with cultural control produces similar results with the cases discussed above.

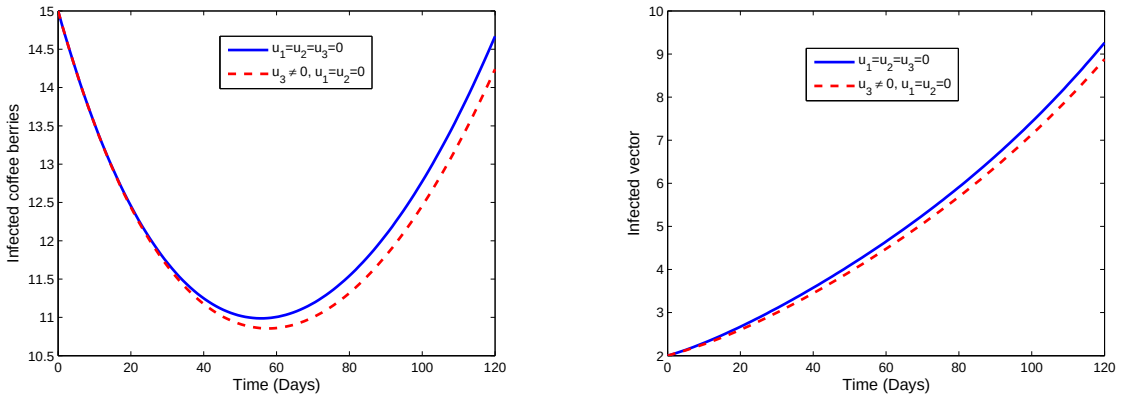

(a) (b)

Figure 7.16: Simulation results when cultural is implemented as control to minimize the impact of infected coffee and infected vector population.

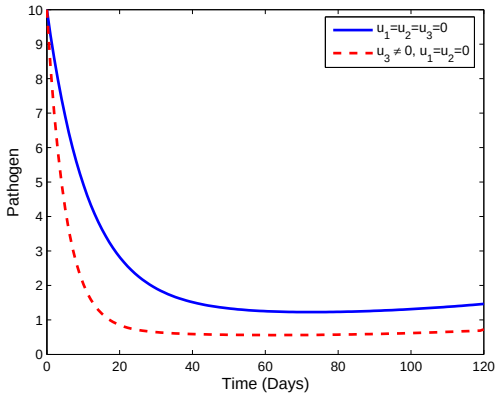

Figure 7.17: Simulation results when cultural is implemented as control to minimize the impact of pathogen population.

In the previous cases, the strategies implemented with a single control decrease the burden of the disease but they cannot eliminate the disease from the coffee berry population. So in the next subsections, we consider four control strategies with two or more controls. We graphically present the simulation results of the governing system (7.47) with controls (red broken curve) and without controls (blue curve).

7.5.4 Strategy IV: Genetic and Chemical Controls

In this case, we consider genetic control $u_1 \neq 0$ and chemical control $u_2 \neq 0$ without using cultural control $u_3 = 0$. This case aims to investigate the impact of genetic and chemical controls alone on coffee berry disease dynamics. The simulation results are displayed in Figure 7.18 depicts that the number of infected coffee, infected vector, and pathogen population decreased due to the implementation of genetic resistance variety and chemicals as control strategies.

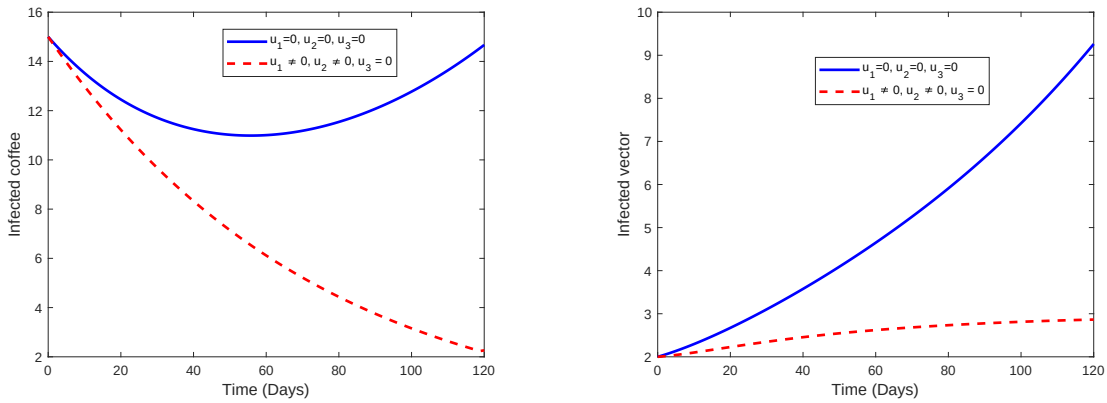

(a)

(b)

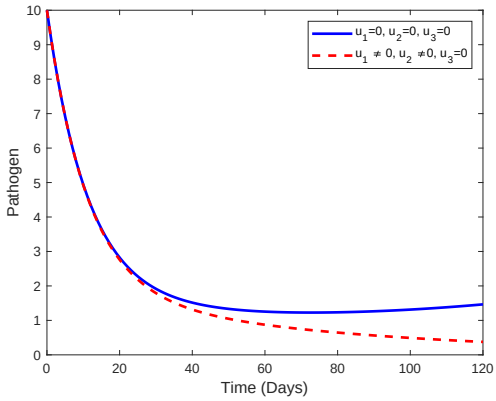

(c)

Figure 7.18: Simulation results when both genetic and chemical are implemented as controls to minimize the impact of infected coffee, infected vector and pathogen population.

7.5.5 Strategy V: Chemical and Cultural Controls

Here, we applied chemical and cultural control strategies to minimize the objective function without genetic control. Due to the control strategies, the number of infected coffee, infected vector, and the pathogen is significantly reduced as shown in Figure 7.19, while an increasing number was observed for the situation when there were no controls. Thus, in the absence of sufficient genetic resistance variety, one can use cultural approaches as an alternative control mechanism in combination with chemical control to limit the economic impact of the disease.

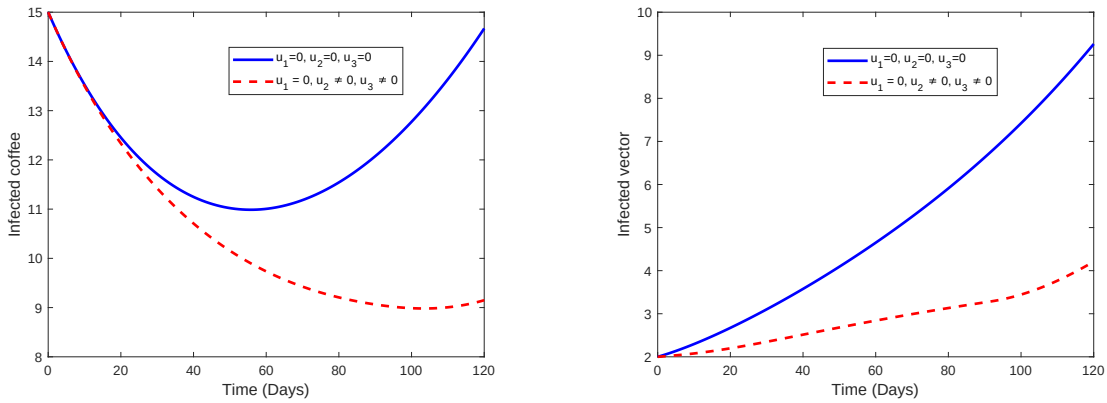

(a)

(b)

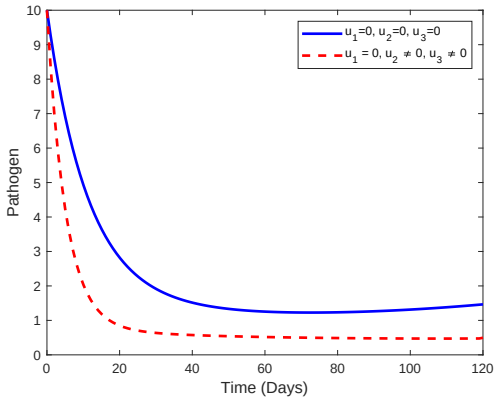

(c)

Figure 7.19: The plot shows the effect of chemical and cultural controls on infected coffee, vector and pathogen population.

7.5.6 Strategy VI: Genetic and Cultural Controls

In this case, we applied genetic and cultural control strategies to minimize the objective function without chemical control. In Figure 7.20, it is observed that there is a significant drop in the number of infected coffee, infected vector, and pathogen population when the controls are applied to the system. The result in this strategy is the best one when we compare it with the result of the strategy discussed above.

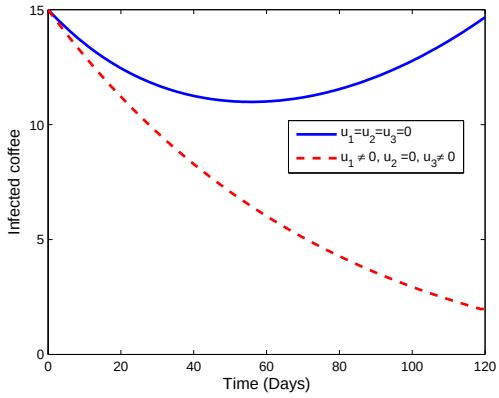

(a)

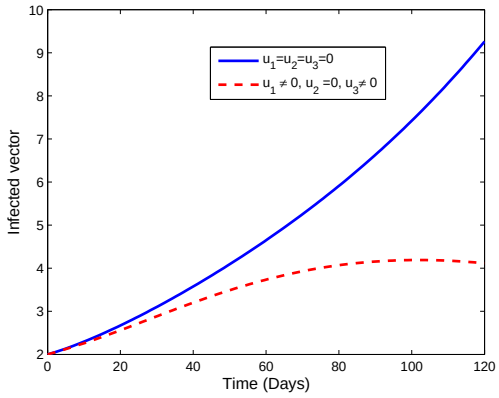

(b)

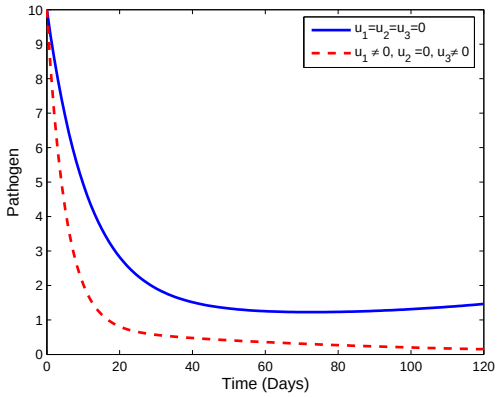

(c)

Figure 7.20: The plot shows the effect of genetic and cultural controls on infected coffee, vector and pathogen population.

7.5.7 Strategy VII: Genetic, Chemical and Cultural Controls

Lastly, we consider genetic control $u_1 \neq 0$, chemical control $u_2 \neq 0$ and cultural control $u_3 \neq 0$ in the system. The simulation results are displayed in Figure 7.21 depicts that the number of infected coffee, infected vector, and pathogen population decreased. In particular, Figure 7.21 (c) depicts that the concentration of pathogens is significantly reduced due to the implementation of the strategy with all controls. We conclude that this strategy is the best effect to compact the disease.

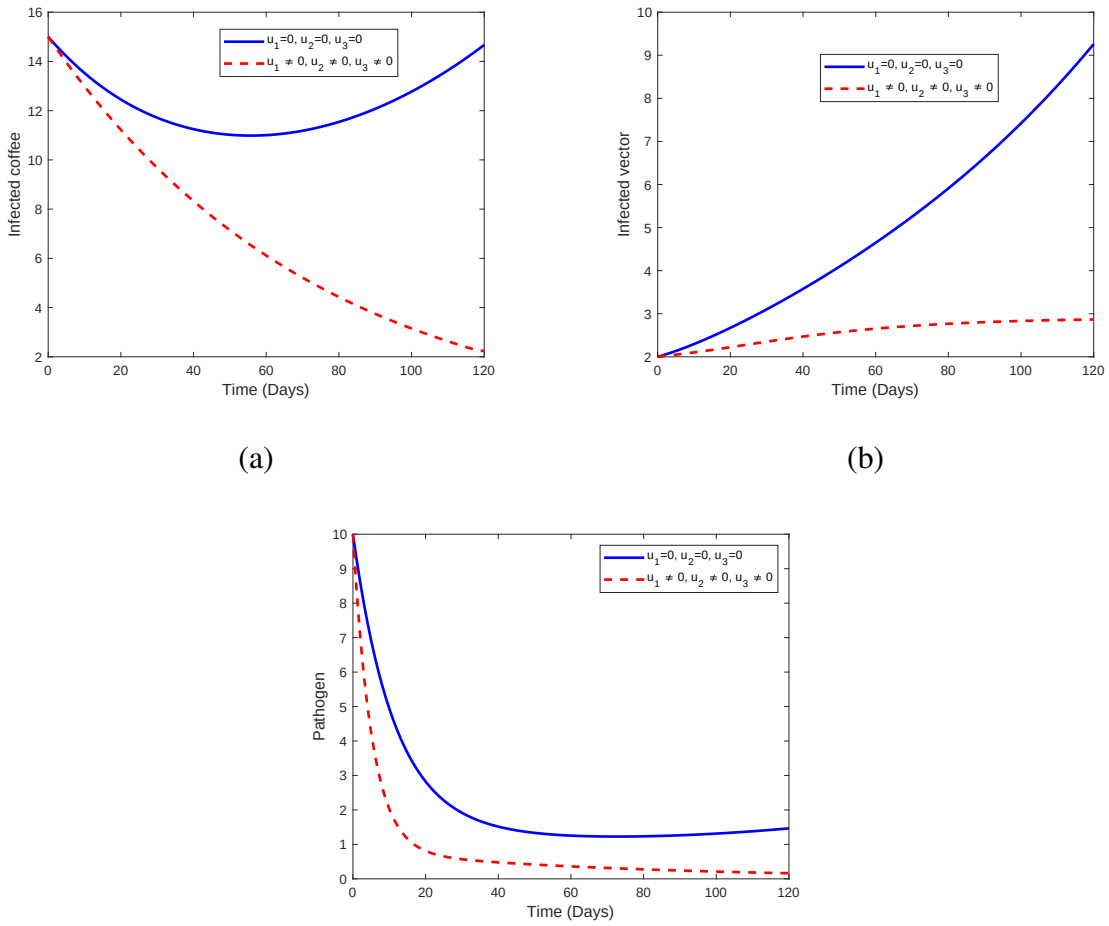

Figure 7.21: Simulation results when genetic, chemical and cultural practice are implemented as controls to minimize the impact of infected coffee, infected vector and pathogen population.

Figure 7.22 (a) shows that the control profiles u_1 and u_2 are implemented for the whole period. However, the control u_2 is increased to at a maximum level for 20 days and decline afterwards to zero. From the control profiles u_2 and u_3 are shown in Figure 7.22 (b), control u_2 is a maximum level (95%) for 90 days and decline afterwards to zero. From the control profiles u_1, u_2 and u_3 in Figure 7.22 (d), the controls u_1 and u_3 are at a maximum level (95%) for 118 days and declines afterwards to zero (Figure 7.22 (c)). But the control u_2 is increased to maximum level for 20 days and then decreased to zero.

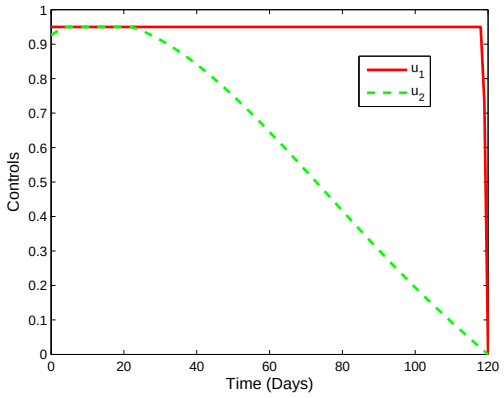

(a) Control profiles u_1 and u_2 when $u_3 = 0$

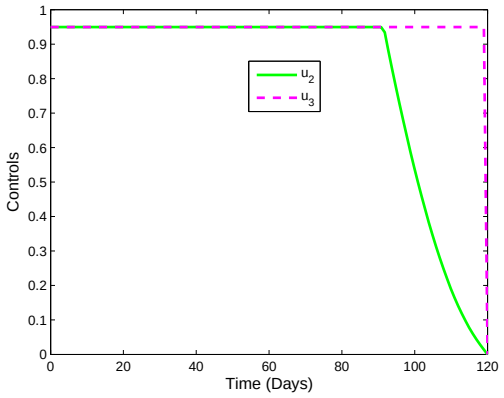

(b) Control profiles u_2 and u_3 when $u_1 = 0$

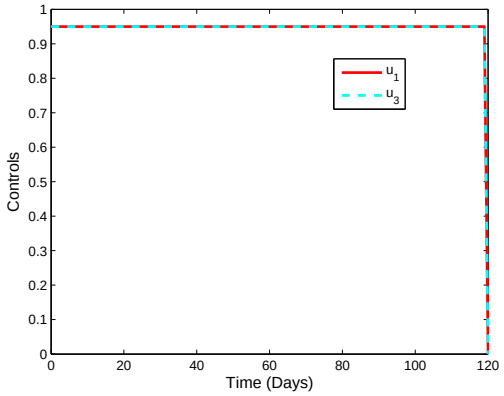

(c) Control profiles u_1 and u_3; $u_2 = 0$

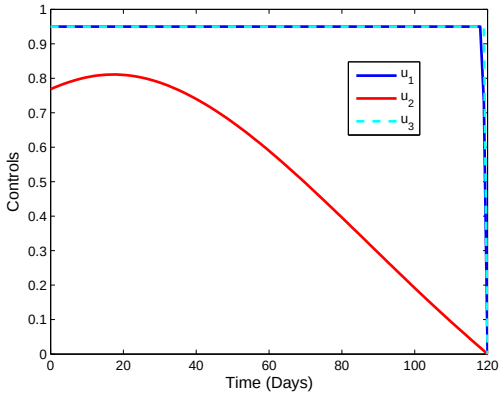

(d) Control profiles u_1, u_2, and u_3

Figure 7.22: Control profiles for strategies with two or more controls.

To determine the most efficient strategy from the above strategies with two or more controls, we consider a cost-effective analysis in the next section.

7.6 Cost-Effectiveness Analysis

In this section, cost-effectiveness analysis is done in a similar way to Chapter 6. The numerical output for the four control strategies is rated incrementally in the form of infection coffee averted as shown in Table 7.4.

Table 7.4: Total infections coffee berries averted and control costs.

Strategy	Description	Infections coffee averted	Control costs	ICER
V	Chemical and cultural	214.1629	1.2217	0.0057
IV	Genetic and chemical	637.4735	7.8365	0.0156
VII	Genetic, chemical and cultural	637.7388	7.3286	-1.9144
VI	Genetic and cultural	650.5882	2.1659	-0.40179

We calculate the ICER for strategies V and IV which are given in Table 7.4 and then compare their results as follows.

$$ICER(V) = \frac{1.2217}{214.1629} = 0.0057,$$
$$ICER(IV) = \frac{7.8365 - 1.2217}{637.4735 - 214.1629} = 0.0156,$$
$$ICER(VI) = \frac{2.1659 - 7.3286}{650.5882 - 637.7388} = -0.40179,$$
$$ICER(VII) = \frac{7.3286 - 7.8365}{637.7388 - 637.4735} = -1.9144.$$

The comparison among ICER of strategies V, IV, VI, and VII shows a cost saving of 1.9144 for strategy VII over strategies V, IV, and VI. This shows that strategy VII is the cheapest. Consequently, strategies V, IV, and VI have to be excluded from the set of alternatives since they consume more resources. Thus, we conclude that strategy VII is the most cost-effective compared to other strategies. The bar diagram of the total infections coffee berries averted and control costs and pie-charts of ICER in Table 7.4 are represented in Figure 7.23.

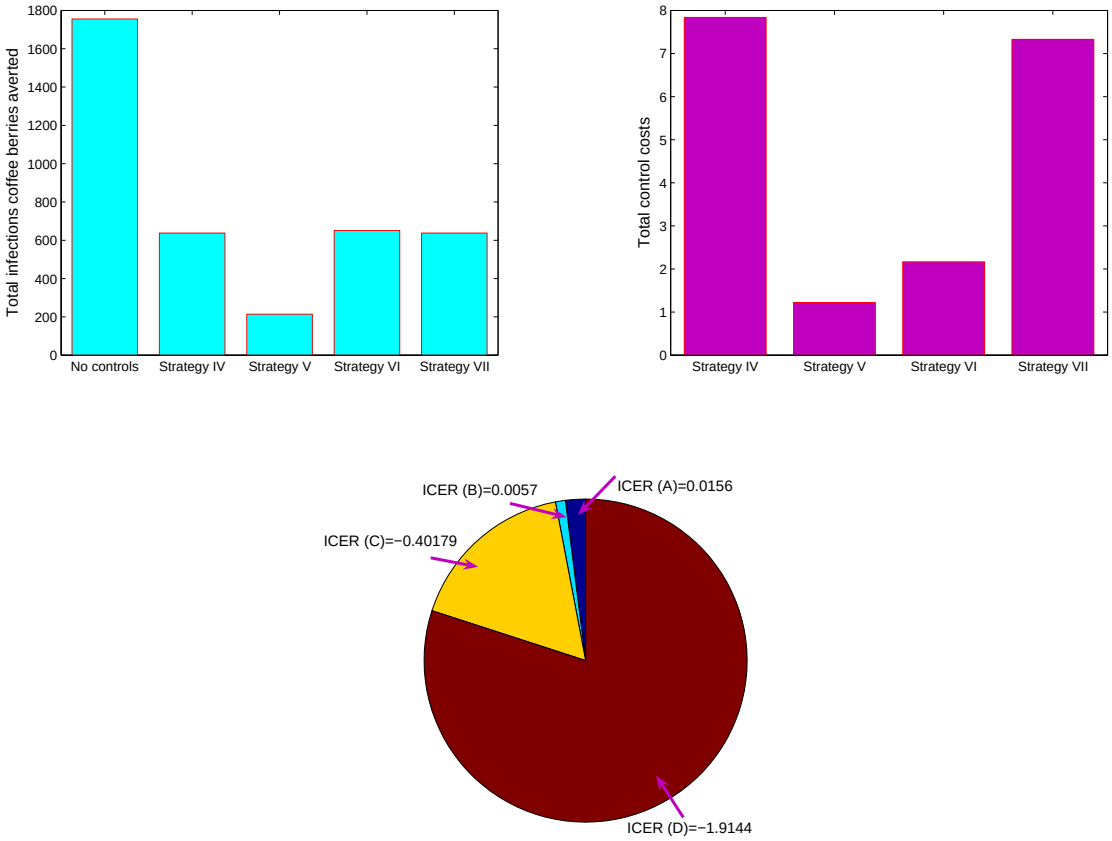

Figure 7.23: The comparison of the total infections coffee berries averted, control costs and ICER result among control strategies IV, V, VI and VII.

CHAPTER 8

SUMMARY, CONCLUSIONS AND RECOMMENDATIONS

In this chapter, we present the summary and conclusions of the study. We also give recommendations for further studies.

8.1 Summary

In this dissertation, we have investigated the dynamics of a mathematical model of coffee berry disease and its controls on the coffee farm. In chapter 1, some information on coffee berry disease, a statement of the problem, the object of the study, the significance of the study, and the structure of the dissertation were described. In chapter 2 review of related literature on mathematical modelling of coffee, berry disease transmission was discussed. In chapter 3 we have explained the methodology of the dissertation.

In chapter 4, we have formulated and analyzed a nonlinear deterministic mathematical model with optimal control analysis of plant pathogen. We first obtained the feasible region where the model is epidemiologically and mathematically well-posed. Then, we analyzed the qualitative behavior of the model by obtaining the positivity, PFEP, and CEP. The R_0 is computed using the next-generation matrix method. The analytical result shows that the PFEP is locally as well as globally asymptotically stable if $R_0 < 1$. From an epidemiological point of view, the pathogens can be reduced from the plant population if R_0 is less than unity. However, when R_0 is greater than unity, the pathogens persist in the plant population. The demonstrated phase portrait analysis also corresponds with the stability analysis. The local sensitivity analysis is studied based on the normalized sensitivity index while the global sensitivity analysis is performed by the means of LHS and PRCC combination. Moreover, we have shown that the model exhibits forward bifurcation using the central manifold theory. Furthermore, we extended the proposed model into an optimal control problem by incorporating two control measures: quarantine and chemical controls. The characterization of optimal control solutions is established using PMP. The obtained numerical results clearly demonstrated that the comprehensive impacts of the two control strategies outperform in reducing the impact of pathogens with optimum implementation cost.

Similarly, in chapter 5, we formulated and analyzed a non-linear deterministic mathematical modeling of CBD infestation in a coffee farm. The existence, uniqueness, positivity, and

boundedness of the solutions are demonstrated. We obtained the feasible region, DFEP, EEP, and $\mathscr{R}_0$ of the model. The stability of the equilibria is analyzed. Sensitivity and bifurcation analysis of the model was investigated. More vectors and CBD pathogen are produced in the favorable climate which indirectly increases the rate of infected vectors and finally infected coffee berries. Thus, the frequency and severity of climate extremes are increasing and making adaptation an absolute imperative necessary through using current information on climate variability to develop long-term plans for managing CBD. According to our mathematical model, we have an EEP and the CBD remains endemic provided that the $\mathscr{R}_0$ is greater than one. Thus, we developed a mathematical model with optimal control analysis for CBD transmission in a coffee farm. This will be done using chemical, cultural, and biological control strategies. We then showed the existence of the optimal control and its characterization using the PMP. Finally, we performed numerical simulations to investigate the impact of control strategies in combating CBD. Furthermore, we studied the cost-effectiveness of our control strategies to determine the best approach in order to minimize the burden of the disease. The ICER reveals that a combination of chemical and cultural strategies is the most cost-effective compared to other strategies.

Furthermore, chapter 6 presents the analysis of nonlinear mathematical model of CBD considering temperature variability. First, we obtained the feasible region where the model is epidemiologically and mathematically well-posed. Then, we computed equilibria, R_1 and R_2 of the model. The proposed model is then qualitatively analyzed for the stability (local and global) of their associated equilibria. The analysis of sensitivity and bifurcation is investigated. The results of the model revealed that R_1 and R_2 are not less than unity. Thus, we extended the proposed model to the optimal control problem in the present temperature variability by incorporating three controls: genetic u_1, chemical u_2, and cultural u_3. The Hamiltonian function, adjoint variables, characterization of controls, and optimality system are investigated. The necessary optimality condition for CBD is derived and analyzed by using PMP. Whenever the control is applied in the system, numerical simulations show that susceptible coffee increases while infected coffee and insect vectors decrease at T_0 and T_m. However, the effectiveness of the control strategy decreases as temperature increases from T_0 to T_m. The results of this study showed that the optimal control is sufficient to eradicate CBD from coffee plants at the end of the implementation period. In particular, the strategy of implementing the selection of coffee plants breeding for CBD resistant varieties and cultural control is found to be the most effective with minimum costs.

Finally, in chapter 7, we formulated and analyzed a nonlinear mathematical model of CBD considering temperature and rainfall variability. We obtained the feasible region, DFEP, EEP, R_{01} and R_{02}. The model was then qualitatively analyzed for the existence and stability of their associated equilibria. Sensitivity and bifurcation analysis of the model was

investigated. More vectors and CBD pathogen are produced at the favorable temperature and rainfall which indirectly increase the rate of infected vectors and finally infected coffee plants. Sensitivity analysis of the model suggested the need to apply effective control intervention parameters β_2, δ, and m in order to control the disease from the coffee plants. This could be done using chemical, cultural, and biological control strategies respectively. Therefore, we were trying to determine an optimal control test for CBD in the presence of temperature and precipitation variability. The existence and uniqueness of optimal control are proved. Also, the characterization of optimal trajectories is analytically derived. Finally, we performed numerical simulations to investigate the impact of control strategies in reducing the disease. Furthermore, we studied the cost-effectiveness of our control strategies to determine the best approach in order to minimize the burden of the disease. Thus, we conclude that a combination of chemical, resistance variety, and cultural practices is very helpful to eradicate the disease in a specified period of time.

8.2 Conclusions

- In our study, deterministic model for the transmission dynamics of plant pathogen and CBD was formulated.
- Model analysis demonstrates that its solution is positive and bounded.
- Basic reproduction number was computed and the stability of equilibria points was investigated.
- Using center mainfold theory, bifurcation analysis of the model was proved.
- We extend the proposed model in to optimal control using the control varabiales.
- Characterization of optimal control solutions was derived using PMP.
- From cost-effectiveness of control strategies the best approach in order to minimize the disease burden was determined.
- From simulation results of the firsr model, a combination of quarantine and chemical control was very helpful to reduce the impact of disease with minimum costs.
- From simulation results of the last model, a combination of genetic resistance, chemical, and cultural practices was very helpful to reduce the impact of disease with minimum costs.

8.3 Recommendations

We recommend that our study would be useful for the choice of policymakers in national agricultural authorities to implement the best effective control strategies for the disease control with minimum costs. Additionally, it is possible to recommend that

- Since temperature and rainfall variation play a significant role on the transmission dynamics of CBD, the coffee farmers should aware on the climatic variation through using current information on temperature and rainfall variability to develop long term plans to manage CBD.
- Coffee farmers should give awareness about CBD in order to reduce the contact rate between healthy coffee berries and infected vectors.
- From incremental cost effectiveness ratio (ICER) results, genetic resistance, chemical and cultural practices should be used to control the disease.

8.4 Future Work

Several interesting mathematical questions are still open for further study. Therefore, we suggest that researchers to think of the following points for future research:

- The model proposed in this dissertation is deterministic. Due to the probability of seasonal variation, it can be extended into stochastic model approach and then comparing their results with the results of deterministic models so as to determine the best approach to control CBD.
- The model proposed in this dissertation can be also extended into time-delay model considering the incubation period.
- Moreover, our model can be extended into real data.

Research Fund Acknowledgment

This research work is funded by Adama Science and Technology University under the grant number: ASTU/SP-R/001/19, Adama, Ethiopia.

REFERENCES

Abdulkhair, W. M. and Alghuthaymi, M. A. (2016). Plant pathogens. *Plant Growth*, 49.

Abraha, T., Al Basir, F., Obsu, L. L., and Torres, D. F. (2021). Pest control using farming awareness: Impact of time delays and optimal use of biopesticides. *Chaos, Solitons & Fractals*, 146:110869.

Agnew, P., Koella, J. C., and Michalakis, Y. (2000). Host life history responses to parasitism. *Microbes and Infection*, 2(8):891–896.

Agrios, G. N. (2010). *Introduction to plant pathology*. Elsevier.

Ahmed, A. G., Murungi, L. K., and Babin, R. (2016). Developmental biology and demographic parameters of antestia bug antestiopsis thunbergii (hemiptera: Pentatomidae), on coffea arabica (rubiaceae) at different constant temperatures. *International Journal of Tropical Insect Science*, 36(3):119–127.

Alemneh, H. T., Makinde, O. D., and Theuri, D. M. (2019). Mathematical modelling of msv pathogen interaction with pest invasion on maize plant. *Global Journal of Pure and Applied Mathematics*, 15(1):55–79.

Alemneh, H. T., Makinde, O. D., and Theuri, D. M. (2020). Optimal control model and cost effectiveness analysis of maize streak virus pathogen interaction with pest invasion in maize plant. *Egyptian Journal of Basic and Applied Sciences*, 7(1):180–193.

Alexander, H. M., Mauck, K. E., Whitfield, A. E., Garrett, K. A., and Malmstrom, C. M. (2014). Plant-virus interactions and the agro-ecological interface. *European Journal of Plant Pathology*, 138(3):529–547.

Allen, L. J. (2007). An introduction to mathematical biology. *Upper Saddle River, New Jersey*.

Alwora, G. O. and Gichuru, E. K. (2014). Advances in the management of coffee berry disease and coffee leaf rust in kenya. *Journal of Renewable Agriculture*, 2(1):5–10.

Anggriani, N., Mardiyah, M., Istifadah, N., and Supriatna, A. (2018). Optimal control issues in plant disease with host demographic factor and botanical fungicides. In *IOP conference series: Materials science and engineering*, volume 332, page 012036. IOP Publishing.

Asamoah, J. K. K., Okyere, E., Abidemi, A., Moore, S. E., Sun, G.-Q., Jin, Z., Acheampong, E., and Gordon, J. F. (2021). Optimal control and comprehensive cost-effectiveness analysis for covid-19. *arXiv preprint arXiv:2107.09595*.

Asamoah, J. K. K., Owusu, M. A., Jin, Z., Oduro, F., Abidemi, A., and Gyasi, E. O. (2020). Global stability and cost-effectiveness analysis of covid-19 considering the impact of the environment: using data from ghana. *Chaos, Solitons & Fractals*, 140:110103.

Ayoade, A., Folaranmi, R., and Latunde, T. (2020b). Mathematical analysis of the implication of the proposed rise in the retirement age on the unemployment situation in nigeria. *Athens J. of Sciences*, 7.

Balardin, R., Madalosso, M., Debortoli, M., and Lenz, G. (2010). Factors affecting fungicide efficacy in the tropics. *InTech*, pages 23–38.

Bale, J. S., Masters, G. J., Hodkinson, I. D., Awmack, C., Bezemer, T. M., Brown, V. K., Butterfield, J., Buse, A., Coulson, J. C., Farrar, J., et al. (2002). Herbivory in global climate change research: direct effects of rising temperature on insect herbivores. *Global change biology*, 8(1):1–16.

Bedimo, J. A. M., Bieysse, D., Njiayouom, I., Deumeni, J. P., Cilas, C., and Nottéghem, J. L. (2007). Effect of cultural practices on the development of arabica coffee berry disease, caused by colletotrichum kahawae. *European Journal of Plant Pathology*, 119(4):391–400.

Belachew, K., Teferi, D., and Livelihood, E. (2015). Climatic variables and impact of coffee berry diseases (colletotrichum kahawae) in ethiopian coffee production. *Journal of Biology, Agriculture and Healthcare*, 5(2015):55–64.

Bellachew, B. (2001). *Arabic a coffee breeding for yield and resistance to coffee berry (Colletotrichum kahawae sp. nov.)*. PhD thesis, University of London.

Boltyanskiy, V., Gamkrelidze, R. V., and Pontryagin, L. S. (1961). Theory of optimal processes. Technical report, joint publications research service Arlington VA.

Boyce, W. E., DiPrima, R. C., and Meade, D. B. (2017). *Elementary differential equations*. John Wiley & Sons.

Campanha, M. M., Santos, R. H. S., Freitas, G. B. d., Martinez, H. E. P., Jaramillo-Botero, C., and Garcia, S. L. (2007a). Análise comparativa das características da serrapilheira e do solo em cafezais (coffea arabica l.) cultivados em sistema agroflorestal e em monocultura, na zona da mata mg. *Revista Árvore*, 31:805–812.

Campanha, M. M., Santos, R. H. S., Freitas, G. B. d., Martinez, H. E. P., Jaramillo-Botero, C., and Garcia, S. L. (2007b). Comparative analysis of litter and soil characteristics under coffee (coffea arabica l.) crop in agroforestry and monoculture systems. *Revista Árvore*, 31(5):805–812.

Castillo-Chavez, C. and Song, B. (2004). Dynamical models of tuberculosis and their applications. *Mathematical Biosciences & Engineering*, 1(2):361.

Chitnis, N., Cushing, J. M., and Hyman, J. (2006). Bifurcation analysis of a mathematical model for malaria transmission. *SIAM Journal on Applied Mathematics*, 67(1):24–45.

Chitnis, N., Hyman, J. M., and Cushing, J. M. (2008). Determining important parameters in the spread of malaria through the sensitivity analysis of a mathematical model. *Bulletin of mathematical biology*, 70(5):1272.

Coddington, E. A. and Levinson, N. (1955). *Theory of ordinary differential equations*. Tata McGraw-Hill Education.

Contreras-Medina, L., Torres-Pacheco, I., Guevara-González, R., Romero-Troncoso, R., Terol-Villalobos, I., and Osornio-Rios, R. (2009). Mathematical modeling tendencies in plant pathology. *African Journal of Biotechnology*, 8(25).

Cook, R. J., Baker, K. F., et al. (1983). *The nature and practice of biological control of plant pathogens.* American Phytopathological Society.

Cunniffe, N. J. and Gilligan, C. A. (2010). Invasion, persistence and control in epidemic models for plant pathogens: the effect of host demography. *Journal of the Royal Society Interface*, 7(44):439–451.

Da Costal, A. L. P., Neto, O. A. R., and Silva-Júnior, A. C. S. (2019). Conditioners of the infectious diseases dynamics. *Estação Científica (UNIFAP)*, 8(3):09–23.

Danneberger, T., Vargas Jr, J., and Jones, A. (1984). A model for weather-based forecasting of anthracnose on annual bluegrass. *Phytopathology*, 74(4):448–451.

Derso, E., Adugna, G., and Gebrezgi, T. (2000). Control of coffee berry disease (cbd) by fungicides in ethiopia.

Dickson, L. E. (1922). *First course in the theory of equations*. J. Wiley & sons, Incorporated.

Diekmann, O., Heesterbeek, J. A. P., and Metz, J. A. (1990). On the definition and the computation of the basic reproduction ratio r 0 in models for infectious diseases in heterogeneous populations. *Journal of mathematical biology*, 28(4):365–382.

Djuikem, C., Grognard, F., Wafo, R. T., Touzeau, S., and Bowong, S. (2021). Modelling coffee leaf rust dynamics to control its spread. *Mathematical Modelling of Natural Phenomena*.

Doehlemann, G., Ökmen, B., Zhu, W., and Sharon, A. (2017). Plant pathogenic fungi. *Microbiology spectrum*, 5(1):5–1.

Ejeta, M. (1986). A review of coffee diseases and their control in ethiopia. In *Proceedings of the First Ethiopian Crop Protection Symposium, Addis Ababa (Ethiopia), 4-7 Feb 1985*. IAR.

Fisher, M. C., Gurr, S. J., Cuomo, C. A., Blehert, D. S., Jin, H., Stukenbrock, E. H., Stajich, J. E., Kahmann, R., Boone, C., Denning, D. W., et al. (2020). Threats posed by the fungal kingdom to humans, wildlife, and agriculture. *MBio*, 11(3):e00449–20.

Fleming, W. and Lions, P.-L. (2012). *Stochastic differential systems, stochastic control theory and applications: proceedings of a workshop, held at IMA, June 9-19, 1986*, volume 10. Springer Science & Business Media.

Fleming, W. H. and Rishel, R. W. (2012). *Deterministic and stochastic optimal control*, volume 1. Springer Science & Business Media.

Fotsa, D., Houpa, E., Bekolle, D., Thron, C., and Ndoumbe, M. (2013). Mathematical modelling and optimal control of anthracnose. *arXiv preprint arXiv:1307.1754*.

Fotso, Y. F., Grognard, F., Touzeau, S., Tsanou, B., and Bowong, S. (2019). Optimal control on a simple model of coffee berry borer infestation. In *BIOMATH 2019-International Conference on Mathematical Methods and Models in Biosciences*.

Fotso, Y. F., Grognard, F., Tsanou, B., and Touzeau, S. (2018). Modelling and control of coffee berry borer infestation. In *CARIâĂŹ2018-14. Colloque Africain sur la Recherche en Informatique et en Mathématiques Appliquées*.

Gaitan, A. L., Cristancho, M. A., Caicedo, B. C., Rivillas, C. A., and Gómez, G. C. (2015). *Compendium of coffee diseases and pests*. APS Press, The American Phytopathological Society.

Garedew, W., Lemessa, F., and Pinard, F. (2017). Assessment of berry drop due to coffee berry disease and non-cbd factors in arabica coffee under farmers fields of southwestern ethiopia. *Crop Protection*, 98:276–282.

Gergerich, R. C. and Dolja, V. V. (2006). Introduction to plant viruses, the invisible foe. *The plant health instructor*, 478.

Gilbert, G. S. (2002). Evolutionary ecology of plant diseases in natural ecosystems. *Annual review of phytopathology*, 40(1):13–43.

Gilligan, C. (1990). Mathematical modeling and analysis of soilborne pathogens. In *Epidemics of plant diseases*, pages 96–142. Springer.

Grahovac, M., Inđić, D., Vuković, S., Hrustć, J., Gvozdenac, S., Mihajlović, M., Tanović, B., et al. (2012). Morphological and ecological features as differentiation criteria for colletotrichum species. *Zemdirbyste Agriculture*, 99(21):89–196.

Griffiths, E., Gibbs, J., and Waller, J. (1971). Control of coffee berry disease. *Annals of Applied Biology*, 67(1):45–74.

Hall, R. J., Gubbins, S., and Gilligan, C. A. (2004). Invasion of drug and pesticide resistance is determined by a trade-off between treatment efficacy and relative fitness. *Bulletin of Mathematical Biology*, 66(4):825–840.

Heffernan, J. M., Smith, R. J., and Wahl, L. M. (2005). Perspectives on the basic reproductive ratio. *Journal of the Royal Society Interface*, 2(4):281–293.

Ho, J. C. and Michalak, A. M. (2020). Exploring temperature and precipitation impacts on harmful algal blooms across continental us lakes. *Limnology and Oceanography*, 65(5):992–1009.

Honěk, A., Kocourek, F., et al. (1990). Temperature and development time in insects: a general relationship between thermal constants. *Zoologische Jahrbücher, Abteilung für Systematik, Ökologie und Geographie der Tiere*, 117(4):401–439.

Hordofa, Z. W. (2019). Assessment of coffee berry disease, characterization of colletotrichum kahawae isolates and evaluation of resistance in coffea arabica collections from gidame, western ethiopia.

Horub, K. E., Julius, T., et al. (2017). A mathematical model for the vector transmission and control of banana xanthomonas wilt. *Journal of Mathematics Research*, 9(4):101–113.

Hugo, A., Kitengeso, R., et al. (2019). Optimal control and cost effectiveness analysis of tomato yellow leaf curl virus disease epidemic model.

Hussain, F. and Usman, F. (2019). Fungal biotic stresses in plants and its control strategy. *Abiotic and biotic stress in plants*.

Huynh, B.-L., Matthews, W. C., Ehlers, J. D., Lucas, M. R., Santos, J. R., Ndeve, A., Close, T. J., and Roberts, P. A. (2016). A major qtl corresponding to the rk locus for resistance to root-knot nematodes in cowpea (vigna unguiculata l. walp.). *Theoretical and Applied Genetics*, 129(1):87–95.

Jackson, M. and Chen-Charpentier, B. M. (2018). A model of biological control of plant virus propagation with delays. *Journal of Computational and Applied Mathematics*, 330:855–865.

Jeffrey, J. (2017). Bonga: Ethiopia's epicenter of arabica coffee – and so much more images:www.cnn.com/travel/article/ethiopia-coffee-origins-bonga/index.html.

Jeger, M., Holt, J., Van Den Bosch, F., and Madden, L. (2004). Epidemiology of insect-transmitted plant viruses: modelling disease dynamics and control interventions. *Physiological Entomology*, 29(3):291–304.

Jirata, M. and Asefa, S. (2000). The status of coffee berry disease in oromia.

Kennedy, B. W., Alcorn, S., et al. (1980). Estimates of us crop losses to procaryote plant pathogens. *Plant Disease*, 64(7):674–676.

Kermack, W. O. and McKendrick's, A. G. (1932). Contributions to the mathematical theory of epidemics. ii.âĂŤthe problem of endemicity. *Proceedings of the Royal Society of London. Series A, containing papers of a mathematical and physical character*, 138(834):55–83.

Khalil, H. K. and Grizzle, J. W. (2002). *Nonlinear systems*, volume 3. Prentice hall Upper Saddle River, NJ.

Khan, M. A., Wahid, A., Islam, S., Khan, I., Shafie, S., and Gul, T. (2015). Stability analysis of an seir epidemic model with non-linear saturated incidence and temporary immunity. *Int. J. Adv. Appl. Math. and Mech*, 2(3):1–14.

Kinene, T., Luboobi, L. S., Nannyonga, B., and Mwanga, G. G. (2015). A mathematical model for the dynamics and cost effectiveness of the current controls of cassava brown streak disease in uganda. *J. Math. Comput. Sci.*, 5(4):567–600.

Kungaro, M., Massawe, E., and Makinde, O. (2013). Transmission dynamics of hiv/aids with screening and non-linear incidence. *African Journal of Science and Technology*, 12(2):31–43.

La Salle, J. P. (1976). *The stability of dynamical systems*. SIAM.

Lenhart, S. and Workman, J. T. (2007). *Optimal control applied to biological models*. CRC press.

Manuel, L., Talhinhas, P., Varzea, V., and Neves-Martins, J. (2010). Characterization of colletotrichum kahawae isolates causing coffee berry disease in angola. *Journal of phytopathology*, 158(4):310–313.

Martcheva, M. (2015). *An introduction to mathematical epidemiology*, volume 61. Springer.

Martin, J. H., Mifsud, D., and Rapisarda, C. (2000). The whiteflies (hemiptera: Aleyrodidae) of europe and the mediterranean basin. *Bulletin of entomological research*, 90(5):407–448.

Masaba and Van Der Vossen, H. (1982). Evidence of cork barrier formation as a resistance mechanism to berry disease (colletotrichum coffeanum) in arabica coffee. *Netherlands Journal of Plant Pathology*, 88(1):19–32.

Mbogne, D. J. F. and Thron, C. (2015). Optimal control of anthracnose using mixed strategies. *Mathematical Biosciences*, 269:186–198.

McDonald, J. et al. (1926). A preliminary account of a disease of green coffee berries in kenya colony. *Transactions of the British mycological Society*, 11(1-2).

Mikkelsen, L., Elphinstone, J., and Jensen, D. F. (2006). Literature review on detection and eradication of plant pathogens in sludge, soils and treated biowaste. *Desk study on bulk density. Bruxelles: The European Commission DG RTD under the Framework*, 6.

Mouen Bedimo, J., Bieysse, D., Cilas, C., and Nottéghem, J. (2007). Spatio-temporal dynamics of arabica coffee berry disease caused by colletotrichum kahawae on a plot scale. *Plant Disease*, 91(10):1229–1236.

Mouen Bedimo, J., Bieysse, D., Nyassé, S., Nottéghem, J., and Cilas, C. (2010). Role of rainfall in the development of coffee berry disease in coffea arabica caused by colletotrichum kahawae, in cameroon. *Plant pathology*, 59(2):324–329.

Mulinge, S. K. (1973). Outbreaks and new records, ethiopia, coffee berry disease. *FAO Plant Protection Bulletin*, 21(4):85–86.

Murray, J. D. (2002). *MathematicalBiology I. An Introduction*. Springer.

Murwayi, A., Onyango, T., and Owour, B. (2017). Mathematical analysis of plant disease dispersion model that incorporates wind strength and insect vector at equilibrium. *Journal of Advances in Mathematics and Computer Science*, pages 1–17.

Nicholls, N., Gruza, G., Jouzel, J., Karl, T., Ogallo, L., Parker, D., et al. (1996). *Observed climate variability and change*. Cambridge University Press Cambridge.

Oerke, E.-C. (2006). Crop losses to pests. *The Journal of Agricultural Science*, 144(1):31–43.

Opatowski, L., Guillemot, D., Boëlle, P.-Y., and Temime, L. (2011). Contribution of mathematical modeling to the fight against bacterial antibiotic resistance. *Current opinion in infectious diseases*, 24(3):279–287.

Pal, K. and Gardener, M. (2006). Biological control of plant pathogens. *The Plant Health Instructor DOI*, 10.

Pang, L., Ruan, S., Liu, S., Zhao, Z., and Zhang, X. (2015). Transmission dynamics and optimal control of measles epidemics. *Applied Mathematics and Computation*, 256:131–147.

Pests, F. K. P. (2015). Diseases at bay: Experts focus on global measures.

Peyser, G. (1958). On the cauchy-lipschitz theorem. *The American Mathematical Monthly*, 65(10):760–762.

Phiri, N., Hillocks, R., and Jeffries, P. (2001). Incidence and severity of coffee diseases in smallholder plantations in northern malawi. *Crop Protection*, 20(4):325–332.

Pontryagin, L. S. (1987). *Mathematical theory of optimal processes*. CRC press.

Pontryagin, L. S. (2018). *Mathematical theory of optimal processes*. Routledge.

Pontryagin, L. S., Boltyanskii, V., Gamkrelidze, R., Mishchenko, E., Trirogoff, K., and Neustadt, L. (2018). *LS Pontryagin Selected Works: The Mathematical Theory of Optimal Processes*. Routledge.

Purcell, A. H. and Almeida, R. P. (2005). Insects as vectors of disease agents. *Encyclopedia of plant and crop science*, 10:1–5.

Robinson, R. (1974). Terminal report of the fao coffee pathologist to the government of ethiopia, fao rome. Technical report, AGO/74/443.

Rutherford, M. A. (2006). Current knowledge of coffee wilt disease, a major constraint to coffee production in africa. *Phytopathology*, 96(6):663–666.

Schaechter, M. (2009). *Encyclopedia of microbiology*. Academic Press.

Siettos, C. I. and Russo, L. (2013). Mathematical modeling of infectious disease dynamics. *Virulence*, 4(4):295–306.

Silva, Varzea, V., Guerra-Guimaraes, L., Azinheira, H. G., Fernandez, D., Petitot, A.-S., Bertrand, B., Lashermes, P., and Nicole, M. (2006). Coffee resistance to the main diseases: leaf rust and coffee berry disease. *Brazilian journal of plant physiology*, 18(1):119–147.

Silva, M., Rijo, L., Geiger, J., and Rodrigues, Jr, C. (1999). Cytochemical aspects of the plant–rust fungus interface during the compatible interaction coffea arabica (cv. caturra)–hemileia vastatrix (race iii). *International Journal of Plant Sciences*, 160(1):79–91.

Takaidza, I., Makinde, O., and Okosun, O. (2017). Computational modelling and optimal control of ebola virus disease with non-linear incidence rate. In *Journal of Physics: Conference Series*, volume 818, page 012003. IOP Publishing.

Tesfaye, G. (2010). Predicting climate change impacts on the distributionn of coffea arabica l. *Ethiopia. Submitted to: Bale Eco-Region Sustainable Management Programme SOS Sahel/FARM-Africa*.

Tilahun, G. T., Makinde, O. D., and Malonza, D. (2017). Modelling and optimal control of pneumonia disease with cost-effective strategies. *Journal of Biological Dynamics*, 11(sup2):400–426.

Ullah, S. and Khan, M. A. (2020). Modeling the impact of non-pharmaceutical interventions on the dynamics of novel coronavirus with optimal control analysis with a case study. *Chaos, Solitons & Fractals*, 139:110075.

Van den Driessche, P. and Watmough, J. (2002). Reproduction numbers and sub-threshold endemic equilibria for compartmental models of disease transmission. *Mathematical biosciences*, 180(1-2):29–48.

Walkey, D. G. (2012). *Applied plant virology*. Springer Science & Business Media.

Waller (1972). Water-borne spore dispersal in coffee berry disease and its relation to control. *Annals of Applied Biology*, 71(1):1–18.

Waller, Bigger, M., and Hillocks, R. J. (2007). *Coffee pests, diseases and their management*. CABI.

Waller, Bridge, P., Black, R., and Hakiza, G. (1993). Characterization of the coffee berry disease pathogen, colletotrichum kahawae sp. nov. *Mycological Research*, 97(8):989–994.

Wiggins, S. (2003). *Introduction to applied nonlinear dynamical systems and chaos*, volume 2. Springer Science & Business Media.

Yemo, Y., Tsopmbeng, G., Keuete, E., and Nchongboh, C. (2017). Antifungal activities of plant extracts against coffee berry disease caused by colletotrichum kahawae l. *International Journal of Current Research in Biosciences and Plant Biology*, 4:60–66.

Zeru, A. (2006). Diversity of arabica coffee populations in afromontane rainforests of ethiopia in relation to colletotrichum kahawae and gibberella zylarioides.

Zeru, A., Assefa, F., Adugna, G., and Hindorf, H. (2012). Occurrence of fungal diseases of coffea arabica l. in montane rainforests of ethiopia. *Journal of applied Botany and food quality*, 82(2):148–151.

APPENDIX A

MATHEMATICAL PRELIMINARIES

In this Appendix, we described the basic tools in mathematical models. These basic tools come in the form of definitions, lemmas, propositions and theorems which are adapted from different literature. Since those are available in existing literature, we do not present any proof in most cases. We use those in our analysis as helping tools.

A.1 Stability Theory of Differential Equations

Mathematical models usually become so complex when higher degree of nonlinearity are employed in solving problem. Obtaining an explicit solution to these models might be impossible. However, numerical simulations are usually employed to obtain approximate solutions with fixed parameters but general solution might be still unknown. In situations where the general solution is difficult to be obtained, stability analysis are employed to get a general view of solution's behaviour. Stability analysis can be used to predict the long-term behavior of model solutions. Generally, stability can be grouped into two categories: Local stability and global stability. Local stability is basically concerned with behaviour of the model solution near an equilibrium point and global stability is concerned with the behaviour of the model solution in the entire domain (Boyce et al., 2017). Consider an autonomous system defined by

$$\frac{dx}{dt} = f(x),\ x \in U \subseteq \mathbb{R}^n, \tag{A.1}$$

where U is an open subset of $\mathbb{R}^n$ and $f : U \to \mathbb{R}$ satisfies the condition of existence and uniqueness of the solution to the initial value problem associated with equation (A.1).

Mathematical analysis of differential equations will be applied to derive conditions or threshold parameters that characterize the dynamics of disease. The study will involve qualitative study of the mathematical model. In this study, the following approaches and numbers will be used during the analysis.

A.1.1 Positivity of Model Variabilities

For a meaningful for epidemiological SIR model, we will need to prove that all the model variabilities and parameters are non-negative at all time since the SIR model deals with population (N) (Wiggins, 2003). Using the differential equation of the total population,

obtained by all the equations of the non-linear system with biological considerations, we will derive a region.

A.1.2 Reproductive Rate

The basic reproduction rate (R_0) is defined as the average number of secondary infections generated by one infectious individual introduced into a completely to susceptible population. It is obtained by computing the Jacobian of the system at the disease free equilibrium by posing the condition that all eigen values of the corresponding characteristic equation must have negative real parts.

A. 1.2.1 Basic Reproductive Rate

The basic reproductive rate is the number of secondary cases produced on average by one infected plant when all are susceptible. It combines the biology of infectious with the social and behaviour of the factors influencing contact rate. The basic reproduction rate (R_0) gives the number of secondary cases one infectious individual will produce in a population consisting only of susceptible individuals. The general method used to compute (R_0) in cases where one or more classes of infective are involved is called next generation matrix method (Van den Driessche and Watmough, 2002).

A. 1.2.2 Effective Reproductive Rate

The effective reproductive rate (R_e) is the number of secondary cases produced on average by one infected plant when a fraction of the population are susceptible. Simply, when S out of N are susceptible. Mathematically, R_e is given by

$$R_e = R_0 \left(\frac{S}{N} \right) \tag{A.2}$$

Assuming the population mix randomly. The disease persists for $R_e \geq 1$ and dies out for $R_e < 1$. The effective reproduction rate (R_e) is more realistic because in every population, not everyone is susceptible. There are those who are infected denoted by I and others who are immune denoted by R. The effective reproductive rate must always be less than unity to ensure that the disease dies out of the population. It is important to achieve $R_e < 1$. This can only be possible if a fraction of the population are treated or vaccinated large enough. As equation (A.2), the number of the susceptible must be reduce so that $R_e < 1$.

A. 1.2.3 Steady State

A disease is said to be in a steady state if $R_e = 1$. In this case, each infected plant is producing another infected plant before recovering or dying. From equation (A.2) and $R_e = 1$, we obtain

$R_0 = N/S$. In steady state, the number of population entering the susceptible is equal to the number of population leaving the susceptible population.

A.1.3 Routh-Hurwitz Criteria (Allen, 2007)

Definition A.1.1. *Let A be square matrix. The characteristic polynomial (P) of A is defined by* $P(\lambda) = det(A - \lambda I)$. *The zeros of P are the eigenvalues of the matrix A. If* λ *is an eigen value of A and* $x \neq 0$ *satisfies the relation* $(A - \lambda I)x = 0$, *then x is a characteristic vector or an eigenvector of the matrix A corresponding to the eigenvalue* (λ).

Considering the system of differential equation

$$x' = Ax, \tag{A.3}$$

where A is an $n \times n$ matrix. Then the characteristic polynomial (P) of the matrix A is given by

$$P(\lambda) = \lambda^n + a_{n-1}\lambda^{n-1} + a_{n-2}\lambda^{n-2} + a_{n-3}\lambda^{n-3} + ... + a_1\lambda + a_0. \tag{A.4}$$

Theorem A.1.1. *Given an n-dimensional linear system* (A.3) *with a characteristic polynomial in equation* (A.4). *Then all root of* $P(\lambda)$ *will have strictly negative real part provide* $det(M_k) > 0$, *for all* $k = 1, 2, 3, ..., n$. *Here the matrices* M_k, $k = 1, 2, 3, ..., n$, *are given by*

$$M_1 = a_{n-1},$$

$$M_2 = \begin{bmatrix} a_{n-1} & a_{n-3} \\ 1 & a_{n-2} \end{bmatrix},$$

$$M_3 = \begin{bmatrix} a_{n-1} & a_{n-3} & a_{n-5} \\ 1 & a_{n-2} & a_{n-4} \\ 0 & a_{n-1} & a_{n-3} \end{bmatrix},$$

$$M_4 = \begin{bmatrix} a_{n-1} & a_{n-3} & a_{n-5} & a_{n-7} \\ 1 & a_{n-2} & a_{n-4} & a_{n-6} \\ 0 & a_{n-1} & a_{n-3} & a_{n-5} \\ 0 & 1 & a_{n-2} & a_{n-4} \end{bmatrix},$$

$$M_n = \begin{bmatrix} a_{n-1} & a_{n-3} & . & . & . & a_{-n+1} \\ 1 & a_{n-2} & . & . & . & a_{-n+2} \\ 0 & a_{n-1} & . & . & . & a_{-n+3} \\ 0 & 1 & . & . & . & . \\ 0 & 0 & . & . & . & . \\ . & . & . & . & . & . \\ . & . & . & . & . & a_{-1} \\ 0 & 0 & . & . & . & a_0 \end{bmatrix}.$$

A.1.4 Descartes' Rule

Rene Descartes was a great French Mathematician and philosopher during the 17th century. Due to his vast contributions to the fields of mathematics and philosophy, he is often known as the 'Father of Modern Philosophy.'

Figure A.1: Rene Descartes (1596-1650).

R. Descartes invented analytical geometry and introduced skepticism as an essential part of the scientific method. His analytical geometry was a tremendous conceptual breakthrough, linking the previously separate fields of geometry and algebra. Some of his quetes are: "I think; therefore I am" and "It is not enough to have a good mind; the main thing is to use it well".

Theorem A.1.2. *(Descartes' Rule (Dickson, 1922)) The number of positive real roots of an equation with real coefficients is either equal to the number of its variations of sign or is less than that number by a positive even integer. A root of multiplicity m is here counted as m roots.*

Proof. Consider any real polynomial

$$f(x) = a_0x^n + a_1x^{n-1} + \cdots + a_lx^{n-l} \qquad (a_0 \neq 0,\ a_l \neq 0). \tag{A.5}$$

Let r be a positive real number. By actual multiplication,

$$F(x) = (x-r)f(x) = A_0x^{n+1} + A_1x^n + \cdots + A_{l+1}x^{n-l}, \tag{A.6}$$

where

$$A_0 = a_0, A_1 = a_1 - ra_0, A_2 = a_2 - ra_1, \cdots, A_l = a_l - ra_{l-1}, A_{l+1} = -ra_l.$$

In $f(x)$ let a_{k_1} be the first non-vanishing coefficient of different sign from a_0, let a_{k_2} be the first non-vanishing coefficient following a_{k_1} and of the same sign as a_0, etc., the last such

term, a_{k_v}, being either a_l or of the same sign as a_l. Evidently v is the number of variations of sign of $f(x)$.

The numbers $A_0, A_{k_1}, \cdots, A_{k_v}, A_{l+1}$ are all different from zero and have the same signs as $a_0, a_{k_1}, \cdots, a_{k_v}, -a_l$, respectively. This is obviously true for $A_0 = a_0$ and $A_{l+1} = -ra_l$. Next, A_{k_i} is the sum of the non-vanishing number A_{k_i} and the number $-ra_{k_{i-1}}$, which is either zero or else of the same sign as a_{k_i} since $a_{k_{i-1}}$ is either zero or of opposite sign to a_{k_i}. Hence the sum A_{k_i} is not zero and has the same sign as a_{k_i}.

By hypothesis, each of the numbers $a_0, a_{k_1}, \cdots, a_{k_v}$ after the first is of opposite sign to its predecessor, while $-a_l$ is of opposite sign to a_{k_v}. Hence each term after the first in the sequence $A_0, A_{k_1}, \cdots, A_{k_v}, A_{l+1}$ is of opposite sign to its predecessor. Thus these terms present $v+1$ variations of sign. We conclude that $F(x)$ has at least one more variation of sign than $f(x)$. □

For example, $x^4 + 3x^3 + x - 1 = 0$ has a single negative root due to a single sign variation in the equation.

A.1.5 Lyapunov Theory

The global analysis by Lyapunov function can possibly be extended beyond the small region near the equilibrium point. The idea in this technique is to seek for an appropriate function that continually decreases towards minimum values of the system. Consider

$$x'(t) = f(x(t)), \tag{A.7}$$

with equilibrium point x^* and suppose that $x(t)$ is a trajectory and $V(x(t))$ is a Lyapunov function that represents the corresponding value of $x(t)$ along the trajectory. The main idea of Lyapunov's theory is that if $V'(x(t))$ is negative along the trajectory of a given system, then $V(x(t))$ will definitely decrease with time.

Definition A.1.2. ***(Lyapunov functions** (Khalil and Grizzle, 2002)). A defined function $V(x(t))$ on a region Ω of the state space and containing x^* is a Lyapunov function if it satisfies the following three requirements:*

1. *$V(x(t))$ is continuous and should have continuous partial first derivatives.*
2. *$V(x(t))$ has unique minimum at x^* with respect to all other points in Ω.*
3. *The function $V'(x(t)) = \nabla V(x) \cdot f(x)$ satisfies $V'(x) \leq 0$ for all $x(t)$ in Ω,*

where "$\cdot$" is the dot product and ∇ is the gradient operator.

Theorem A.1.3. ***(Lyapunov Theorem)**. Let $V(x(t))$ be Lyapunov function and x^* is stable equilibrium point of given dynamical system, if the function $V'(x(t))$ is strictly negative for every point then the stability is asymptotic.*

A.1.6 Optimal Control Theory

Recently, optimal control theory has been found to have wide applications in many biological related complexities (Lenhart and Workman, 2007). In the late 1950's, Pontryagin and collaborators developed a control theory which was described as a basic principle that underlies analysis and the design of control systems. It influences the behaviour of the object in achieving the desired goals. In this work, the control technique to the population of chicken was introduced to protect them from ND. To achieve this goal, the mathematical concepts like the "optimal control theory" came into important play and is described as follows. Consider a dynamical system

$$X' = f(t, x(t), u(t)) \tag{A.8}$$

where $x(t)$ is a state variable at a time t and $u(t)$ represents control at time t, then the optimal control problem is to find a trajectory $\{x(t)\}$ by choosing a set $\{u(t)\}$ of controls so as to maximize or minimize the particular objective function. The model equations developed in this thesis are autonomous and are governed by a set of ordinary differential equations (ODEs). The objective function J of the particular problem follows the following form:

$$J = \min_{u} \int_{t_0}^{t_f} f(t, x(t), u(t))dt, \tag{A.9}$$

subject to:

$$\begin{aligned} x'(t) &= g(t, x(t), u(t)),\ t \in [t_0, t_f], \\ x(t_0) &= x_0,\ x(t_f) \text{ free} \end{aligned}$$

where the functions f and g are continuously differentiable in all variables. In this study, the optimal control problem with n states and m controls are expressed in a vector notation form:

$$\begin{aligned} \vec{x}(t) &= [x_1(t), ..., x_n(t)], \\ \vec{u}(t) &= [u_1(t), ..., u_m(t)], \\ \vec{x}_0 &= [x_{10}, ..., x_{n0}], \\ \vec{g}(t, \vec{x}, \vec{u}) &= [g_1(t, \vec{x}, \vec{u}), ..., g_n(t, \vec{x}, \vec{u})]. \end{aligned}$$

The optimisation problem can be written in vector notation as:

$$J = \min_{\vec{u}} \int_{t_0}^{t_f} f(t, \vec{x}(t), \vec{u}(t))dt, \tag{A.10}$$

subject to:

$$\begin{aligned} \vec{x}'(t) &= g(t, \vec{x}(t), \vec{u}(t)),\ t \in [t_0, t_f], \\ \vec{x}(t_0) &= \vec{x}_0,\ \vec{x}(t_f). \end{aligned}$$

The vectors $\vec{u}^*(t)$ and $\vec{x}^*(t)$ minimizes the objective functional of the optimal control and state variables, respectively.

A.1.7 Pontryagin's Minimum Principle (PMP)

In 1956, Lev Pontryagin and his collaborators developed and proved necessary conditions for optimal control theory which is now called Pontryagin's Minimum Principle (Boltyanskiy et al., 1961). A set of necessary conditions is obtained by introducing a piecewise differentiable vector-valued function $\vec{\lambda}(t) = [\lambda_1(t), ..., \lambda_n(t)]$, where each λ_i is the adjoint variable corresponding to x_i. We define the Hamiltonian function as

$$H(t, \vec{x}, \vec{u}, \vec{\lambda}) = f(t, \vec{x}, \vec{u}) + \vec{\lambda}(t) \cdot \vec{g}(t, \vec{x}, \vec{u}).$$

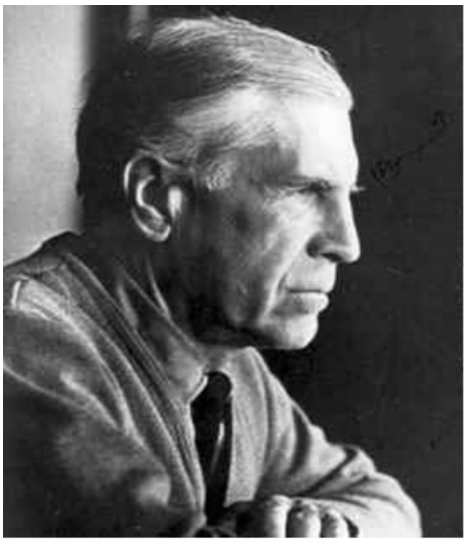

Figure A.2: Lev Semyonovich Pontryagin (1908-1988).

The PMP provides a set of necessary conditions such as optimality, adjoint, and transversality in each vector component that an optimal control and the corresponding states must satisfy. Namely, $\vec{u}^*$ minimizes $H(t, \vec{x}^*, \vec{u}, \vec{\lambda})$ with respect to $\vec{u}$ at each time t also $\vec{x}^*$, $\vec{u}^*$ and $\vec{\lambda}$ satisfy

$$\begin{aligned}
x_i'(t) &= \frac{\partial H}{\partial \lambda_i} = g_i(t, \vec{x}, \vec{u}, \vec{\lambda});\ x_{i0}(t_0) = x_{i0} \text{ for } i = 1, 2, ..., n, \\
\lambda_j'(t) &= -\frac{\partial H}{\partial \lambda_j};\ \lambda_j(t_f) = 0, \\
\frac{\partial H}{\partial u_k} &= 0 \text{ at } u^* \text{ for } k = 1, 2, ..., m,
\end{aligned}$$

where

$$H(t, \vec{x}, \vec{u}, \vec{\lambda}) = f(t, \vec{x}, \vec{u}) + \textstyle\sum_{i=1}^{n} \lambda_i(t) g_i(t, \vec{x}, \vec{u}).$$

Suppose that the control variables are bounds to $a_k \leq u_k \leq b_k$ then, the optimality condition is changed from:

$$\frac{\partial H}{\partial u_k} = 0 \text{ to } \begin{cases} u_k = a_k, & if \quad \dfrac{\partial H}{\partial u_k} < 0, \\ a_k \leq u_k \leq b_k, & if \quad \dfrac{\partial H}{\partial u_k} = 0, \\ u_k = b_k, & if \quad \dfrac{\partial H}{\partial u_k} > 0. \end{cases}$$

A.2 Applications of Fourth Order Runge-Kutta Methods

Runge-Kutta method is an effective and widely used method for solving the initial-value problems of differential equations. Numerical solution of the model problem under consideration will be solved completely using fourth order Runge-Kutta method of integration. Runge-Kutta methods is a numerical technique for solving an ODE of the form:

$$\frac{dy}{dx} = f(x,y),\ y(0) = y_0.$$

Let $h = x_{i+1} - x_i,\ i = 1,2,...,n$ so that the Taylor series of $y(x_{i+1}) = y_{i+1}$ about x_i is given by

$$y_{i+1} = y_i + hf(x_i,y_i) + \frac{1}{2!}h^2 f(x_i,y_i) + ... \tag{A.11}$$

In general, the Runge-Kutta fourth order is given by the relation:

$$y_{i+1} = y_n + \frac{1}{6}(k_1 + 2k_2 + 2k_3 + k_4), \tag{A.12}$$

where

$$\begin{aligned} k_1 &= hf(x_n,y_n), \\ k_2 &= hf(x_n + \frac{h}{2}, y_n + \frac{k_1}{2}), \\ k_3 &= hf(x_n + \frac{h}{2}, y_n + \frac{k_2}{2}), \\ k_4 &= hf(x_n + h, y_n + k_3). \end{aligned} \tag{A.13}$$

In general, forward-backward sweep is used to solve the state system and the adjoint system. The state system is solved using a forward method with the given initial data, while the adjoint system is solved using a backward method with the transversality condition. The value of each control variable is updated by taking the average of the previous value and new value arising from the control characterization. This process continues many times up to successive iterations that are close enough to each other (Lenhart and Workman, 2007). The Runge-Kutta method attempts to overcome the problem of the Euler's method, as far as

the choice of a sufficiently small step size is concerned, to reach a reasonable accuracy in the problem resolution.

APPENDIX B

MATLAB CODE

```
% Plant Pathogens Simulation Main program

%This function solves the plant pathogens model with control
x1 = hat(S)-susceptible population
x2 = hat(I)-Infected population
x3 = hat(R)-Removed population
x4 = hat(X)-Incolum Population

function y = Plant Pathogens control
test = -1;

mu = 0.001;
N = 1000;
t0=0;
tf=12;
t=linspace(0,12,N+1);
h = (tf-t0)/N;
h2 = h/2;

%Model Parameter Values
betap=1; betas=1; m=0.2; H=0.8; c=0.9;

% Objective functional parameter values
d=1000;
b1=3;
b2=3;

%Vectors for system state variable
u1= zeros(1,N+1);
u2= zeros(1,N+1);
x1= zeros(1,N+1);
x2= zeros(1,N+1);
x3= zeros(1,N+1);
```

```
x4= zeros(1,N+1);

%Vectors for system restrictions and control
lambda1 = zeros(1,N+1);
lambda2 = zeros(1,N+1);
lambda3 = zeros(1,N+1);
lambda4 = zeros(1,N+1);

%Initial conditions of the model
x1(1) = 0;
x2(1) = 2;
x3(1) = 4;
x4(1) = 1;

%Iterations of the method
while(test < 0)
oldu1 = u1;
oldu2 = u2;

oldx1 = x1;
oldx2 = x2;
oldx3 = x3;
oldx4 = x4;

oldlambda1 = lambda1;
oldlambda2 = lambda2;
oldlambda3 = lambda3;
oldlambda4 = lambda4;

%Forward Runge-Kutta iterations in state system
for i = 1:N
m11 = 1-x1(i)-(betap*x4(i)+(1-u1(i))*betas*x2(i))*x1(i);
m12 = (betap*x4(i)+(1-u1(i))*betas*x2(i))*x1(i)-(m + H)*x2(i);
m13 = x2(i)-H*x3(i);
m14 = x2(i)-(1+u2(i))*c*x4(i);

m21 = 1-x1(i)-h2*m11-(betap*(x4(i)+h2*m14)
+(1-0.5*(u1(i)+u1(i+1)))*betas*(x2(i)+h2*m12))*(x1(i)+h2*m11);
m22 = (betap*(x4(i)+h2*m14)+(1-0.5*(u1(i)+u1(i+1)))*betas*x2(i))*(x1(i)+h2*m11)-(m +
```

```
H)*(x2(i)+h2*m12);
m23 = x2(i)+h2*m12-H*(x3(i)+h2*m13);
m24 = x2(i)+h2*m12-(1+0.5*(u2(i)+u2(i+1)))*c*(x4(i)+h2*m14);

m31 = 1-x1(i)-h2*m21-(betap*(x4(i)+h2*m24)
+(1-0.5*(u1(i)+u1(i+1)))*betas*(x2(i)+h2*m22))*(x1(i)+h2*m21);
m32 = (betap*(x4(i)+h2*m24)+(1-0.5*(u1(i)+u1(i+1)))*betas*(x2(i)+h2*m22))*(x1(i)+h2*m21)-
(m + H)*(x2(i)+h2*m22);
m33 = x2(i)+h2*m22-H*(x3(i)+h2*m23);
m34 = x2(i)+h2*m22-(1+0.5*(u2(i)+u2(i+1)))*c*(x4(i)+h2*m24);

m41 = 1-x1(i)-h2*m31-(betap*(x4(i)+h2*m34)
+(1-u1(i)-u1(i+1))*betas*(x2(i)+h2*m32))*(x1(i)+h2*m31);
m42 = (betap*(x4(i)+h2*m34)+(1-u1(i)-u1(i+1))*betas*(x2(i)+h2*m32))*(x1(i)+h2*m31)-
(m + H)*(x2(i)+h2*m32);
m43 = x2(i)+h2*m32-H*(x3(i)+h2*m33);
m44 = x2(i)+h2*m32-(1+u2(i)+u2(i+1))*c*(x4(i)+h2*m34);

x1(i+1) = x1(i) + (h/6)*(m11 + 2*m21 + 2*m31 + m41);
x2(i+1) = x2(i) + (h/6)*(m12 + 2*m22 + 2*m32 + m42);
x3(i+1) = x3(i) + (h/6)*(m13 + 2*m23 + 2*m33 + m43);
x4(i+1) = x4(i) + (h/6)*(m14 + 2*m24 + 2*m34 + m44);

end

%Backward Runge-Kutta iterations in adjoint variables for i = 1:N
j = N + 2 - i;
n11 = lambda1(j)*(1+betap*x4(j)+(1-u1(j))*betas*x2(j));
n12 = -d+lambda1(j)*(1-u1(j))*betas*x1(j)-lambda2(j)*((1-u1(j))*betas*x1(j)-m-H)-lambda3(j)-
lambda4(j);
n13 = lambda3(j)*H ;
n14 =(lambda1(j)-lambda2(j))*betap*x1(j)+ lambda4(j)*(1+u2(j))*c;

n21 = (lambda1(j)-h2*n11)*(1+betap*0.5*(x4(j)+x4(j-1))
+(1-0.5*(u1(j)+u1(j-1)))*betas*0.5*(x2(j)+x2(j-1)));
n22 = -d+(lambda1(j)-h2*n11)*(1-0.5*(u1(j)+u1(j-1)))*betas*0.5*(x1(j)+x1(j-1))-(lambda2(j)-
h2*n12)* ((1-0.5*(u1(j)+u1(j-1)))*betas*0.5*(x1(j)+x1(j-1))-m-H)-(lambda3(j)-h2*n13)-(lambda4(j)-
h2*n14);
n23 = (lambda3(j)-h2*n13)*H ;
```

```
n24 = (lambda1(j)-h2*n11-(lambda2(j)-h2*n12))*betap*0.5*(x1(j)+x1(j-1))+(lambda1(j)-h2*n11-
(lambda2(j)-h2*n12))*betap*0.5*(x1(j)+x1(j-1))+(lambda4(j)-h2*n14)*(1+0.5*(u2(j)+u2(j-
1)))*c;

n31 = (lambda1(j)-h2*n21)*(1+betap*0.5*(x4(j)+x4(j-1))
+(1-0.5*(u1(j)+u1(j-1)))*betas*0.5*(x2(j)+x2(j-1)));
n32 = -d+(lambda1(j)-h2*n21)*(1-0.5*(u1(j)+u1(j-1)))*betas*0.5*(x1(j)+x1(j-1))-(lambda2(j)-
h2*n22)* ((1-0.5*(u1(j)+u1(j-1)))*betas*0.5*(x1(j)+x1(j-1))-m-H)-(lambda3(j)-h2*n23)-(lambda4(j)-
h2*n24);
n33 = (lambda3(j)-h2*n23)*H ;
n34 = (lambda1(j)-h2*n21-(lambda2(j)-h2*n22))*betap*0.5*(x1(j)+x1(j-1))
+(lambda4(j)-h2*n24)*(1+0.5*(u2(j)+u2(j-1)))*c;

n41 = (lambda1(j)-h2*n31)*(1+betap*(x4(j)+x4(j-1))+(1-(u1(j)+u1(j-1)))*betas*(x2(j)+x2(j-
1)));
n42 = -d+(lambda1(j)-h2*n31)*(1-(u1(j)+u1(j-1)))*betas*(x1(j)+x1(j-1))-(lambda2(j)-h2*n32)*
((1-(u1(j)+u1(j-1)))*betas*(x1(j)+x1(j-1))-m-H)-(lambda3(j)-h2*n33)-(lambda4(j)-h2*n34);
n43 = (lambda3(j)-h2*n33)*H ;
n44 = (lambda1(j)-h2*n31-(lambda2(j)-h2*n32))*betap*(x1(j)+x1(j-1))
+(lambda4(j)-h2*n34)*(1+u2(j)+u2(j-1))*c;

%Runge-Kutta new approximation in adjoint variables
lambda1(j-1) = lambda1(j) - h./6*(n11 + 2*n21 + 2*n31 +2* n41);
lambda2(j-1) = lambda2(j) - h./6*(n12 + 2*n22 + 2*n32 + 2*n42);
lambda3(j-1) = lambda3(j) - h./6*(n13 + 2*n23 + 2*n33 +2* n43);
lambda4(j-1) = lambda4(j) - h./6*(n14 + 2*n24 + 2*n34 +2* n44);

end
u1 = min(max(0,betas.*x1.*x2.*(lambda2-lambda1)./b1),1);
u1 = 0*(u1 + oldu1);
u2 = min(max(0,lambda4.*c.*x4./b2),1);
u2 = 0*(u2 + oldu2);
J = sum((d + b1 * u1.^2 + b2 * u2.^2) * (t(i+1) - t(i)));

%Absolute error for convergence

temp1 = mu*sum(abs(u1)) - sum(abs(oldu1 - u1));
temp2 = mu*sum(abs(u2)) - sum(abs(oldu2 - u2));
```

```
temp3 = mu*sum(abs(x1)) - sum(abs(oldx1 - x1));
temp4 = mu*sum(abs(x2)) - sum(abs(oldx2 - x2));
temp5 = mu*sum(abs(x3)) - sum(abs(oldx3 - x3));
temp6 = mu*sum(abs(x4)) - sum(abs(oldx4 - x4));

temp7 = mu*sum(abs(lambda1)) - ... sum(abs(oldlambda1 - lambda1));
temp8 = mu*sum(abs(lambda2)) - ... sum(abs(oldlambda2 - lambda2));
temp9 = mu*sum(abs(lambda3)) - ... sum(abs(oldlambda3 - lambda3));
temp10 = mu*sum(abs(lambda4)) - ... sum(abs(oldlambda4 - lambda4));

test = min(temp1, min(temp2, min(temp3, min(temp4, min(temp5, min(temp6, min(temp7,
min(temp8, min(temp9,temp10)))))))));
end
y(1,:) = t;
y(2,:) = u1;
y(3,:) = u2;
y(4,:) = x1;
y(5,:) = x2;
y(6,:) = x3;
y(7,:) = x4;
y(8,:) = lambda1;
y(9,:) = lambda2;
y(10,:) = lambda3;
y(11,:) = lambda4;
y(12,:)=J;
box on
hold on

%Ploting section
plot(y(1,:),y(4,:),'b','linewidth',2)
xlabel('Time (Months)','fontsize',12)
ylabel('Susceptible','fontsize',12)
legend('u_1 = 0, u_2 = 0','u_1 \neq 0, u_2 = 0')
hold on
```